USING PAMAM DENDRIMER FRAMEWORKS TO INVESTIGATE MULTIVALENT BINDING IN PROTEIN : CARBOHYDRATE INTERACTIONS

by

Mark Leroy Wolfenden

A dissertation submitted in partial fulfillment
of the requirements for the degree

of

Doctor of Philosophy

In

Chemistry

MONTANA STATE UNIVERSITY
Bozeman, Montana

August 2009

APPROVAL

of a dissertation submitted by

Mark Leroy Wolfenden

This dissertation has been read by each member of the dissertation committee and has been found to be satisfactory regarding content, English usage, format, citation, bibliographic style, and consistency, and is ready for submission to the Division of Graduate Education.

Dr. Mary J. Cloninger

Approved for the Department of Chemistry

Dr. David Singel

Approved for the Division of Graduate Education

Dr. Carl A. Fox

STATEMENT OF PERMISSION TO USE

In presenting this dissertation in partial fulfillment of the requirements for a doctoral degree at Montana State University, I agree that the Library shall make it available to borrowers under rules of the Library. I further agree that copying of this dissertation is allowable only for scholarly purposes, consistent with “fair use” as prescribed in the U.S. Copyright Law. Requests for extensive copying or reproduction of this dissertation should be referred to ProQuest Information and Learning, 300 North Zeeb Road, Ann Arbor, Michigan 48106, to whom I have granted “the exclusive right to reproduce and distribute my dissertation in and from microform along with the non-exclusive right to reproduce and distribute my abstract in any format in whole or in part.”

Mark Leroy Wolfenden

August, 2009

ACKNOWLEDGEMENTS

Firstly I must thank my wife Teresa for all her support, encouragement and being a truly wonderful partner. To my parents, along with my “big” sister, who have been a constant source of support, inspiration and invaluable assistance. A huge thank you must go to my advisor, Mary Cloninger, for the belief, support, funding, advice, guidance and all the interesting conversation about life the universe and everything…… and chemistry. The Cloninger research group has been a great help, from Eric Woller starting this projects wheels turning and creating a platform for me to work from, thanks Eric. To Jake, for being a great influence and playing unconventional cricket, golf and frisbee, along with a day or two teaching me what two planks on my feet can do for me. Nick, for the friendship and support through the trials and tribulations, it is greatly appreciated. Joel, Kristian, Natalie, Shannon, Julie, Anna, Amanda and all the undergrads involved, you all taught me something along the way. Thanks to Steve Holmgren for all the advice and conversation. Also to Eric, Greg, Lars and all the other grad students that have helped me in one way or another. Thanks to Bob and Walt, for the opening of doors and the all round entertainment in the late hours. And finally thank you to my committee members for being a part of my education, career and inspiration.

TABLE OF CONTENTS

TABLE OF CONTENTS CONTINUED

TABLE OF CONTENTS CONTINUED

LIST OF FIGURES

Figure Page

LIST OF FIGURES CONTINUED

Figure Page

LIST OF FIGURES CONTINUED

Figure Page

LIST OF FIGURES CONTINUED

Figure Page

LIST OF FIGURES CONTINUED

Figure Page

LIST OF FIGURES CONTINUED

Figure Page

LIST OF FIGURES CONTINUED

Figure Page

LIST OF FIGURES CONTINUED

Figure Page

LIST OF TABLES

Table Page

LIST OF TABLES CONTINUED

Table Page

LIST OF SCHEMES

Scheme Page

ABSTRACT

Polyvalent interactions in biological systems have been of great interest recently; how nature creates high affinity polyvalent binding with low monomeric affinity, is yet to be clearly understood. We have created a bivalent lectin-carbohydrate binding system using dendrimers as the carbohydrate mounted scaffold and Concanavalin A (Con A) as the mannose/glucose binding lectin to investigate this mode of interaction. The relative affinities of the utilized carbohydrates toward Con A are: mannose binds 4 times stronger than glucose, and galactose shows no affinity. With these relative affinities in hand and changing the ratios of mannose, glucose and galactose on the periphery of the PAMAM dendrimer scaffold, we have made a predictable and tuneable system with which to control the polyvalent binding relative affinity. By changing the carbohydrate presentation and varying the size of PAMAM dendrimer used, we can tune the affinity between two orders of magnitude. Although the relative affinities can be predictably altered, the clustering ability across the same generation dendrimer is not affected. In exploring more complex lectin : carbohydrate systems we have made a library of lactose, galactose and galNAc functionalized dendrimers to study binding to galectin-3. This lectin is implicated in numerous cancer related pathway, cellular proliferation and apoptosis. An ELISA based assay was developed to gain binding information of this intruiging interaction. The assay results suggest a reduced effect of binding association even with a large range of monomeric affinities, indicating a multivalent system. The monomer affinities did however affect the lectin recruitment to the dendrimers adsorbed onto a surface. The report here indicated a delicate interplay of modes of multivalent binding that dictate the biological behavior of this important galactose binding lectin.

CHAPTER 1

MULTIVALENCY IN CARBOHYDRATE BINDING

Introduction

Many biological pathways involving carbohydrates rely on multivalency to impart specificity and selectivity. Multivalency, broadly defined, is the use of more than one binding epitope to increase the binding efficacy or to cause an event such as clustering or aggregation. Multivalency plays a role in biological processes such as cellular adhesion, viral and bacterial infection, fertilization, and cancer progression (Figure 1).[1, 2] Elucidating multivalent effects is very challenging because the influences of the binding efficacy, clustering and aggregation are not consistent for different processes, and most likely a delicate interplay between these differing attributes is critically important. In other words, one overarching set of principles for how multivalency works is unlikely to emerge. Binding efficacy can be paramount in an inhibitory process, clustering is useful in an effector role such as concentrating receptor ligands, and aggregation is more important when concentrating larger bodies such as in cellular aggregation and tumor formation.[3] The delicate balance of these roles for multivalent biological recognition events make scaffolds with unique structural components very useful for a wide variety of biologically relevant interactions.

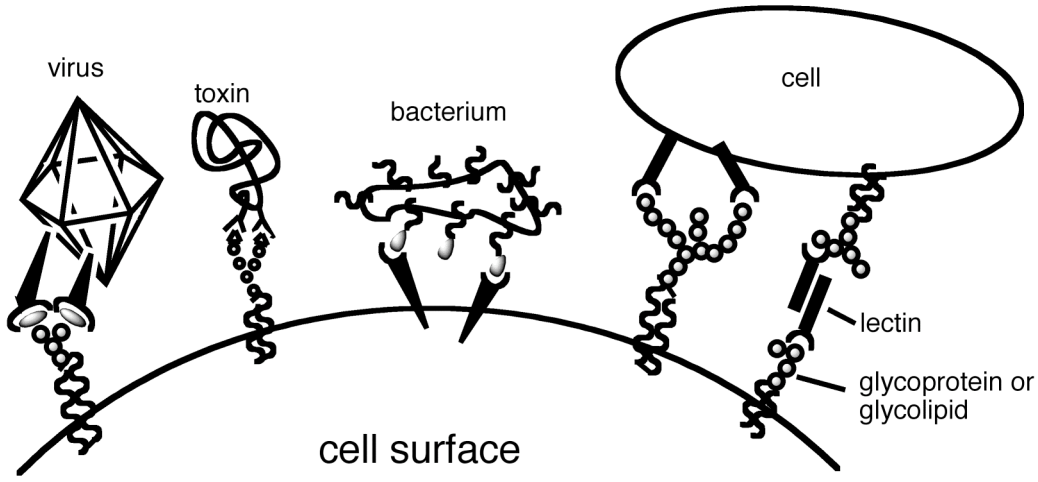

Figure 1 A schematic representation of biologically relevant multivalent carbohydrate recognition events.

The phenomenon of multivalency has been recognized for some time,[4] and Y.C. Lee used the term “cluster effect” in a pivotal article in 1983 in reference to carbohydrates.[5] Initially, multivalent enhancement was thought to be an additive effect and was considered to be a combination of binding constants.[6, 7] Since this discussion was introduced, attempts to quantify the multivalent effect have emerged. Different ways to consider multivalent effects are shown in Figure 2. The statistical or proximity effect causes an increase in the effective concentration of the ligand, and occurs when multiple ligands are clustered around the binding site of a receptor. Receptor clustering may occur subsequent to this. The chelate effect occurs because binding of a multidentate ligand to multiple binding sites on a multi-point receptor is more favorable than binding of multiple monodentate ligands to the same receptor. Bivalent (or higher)

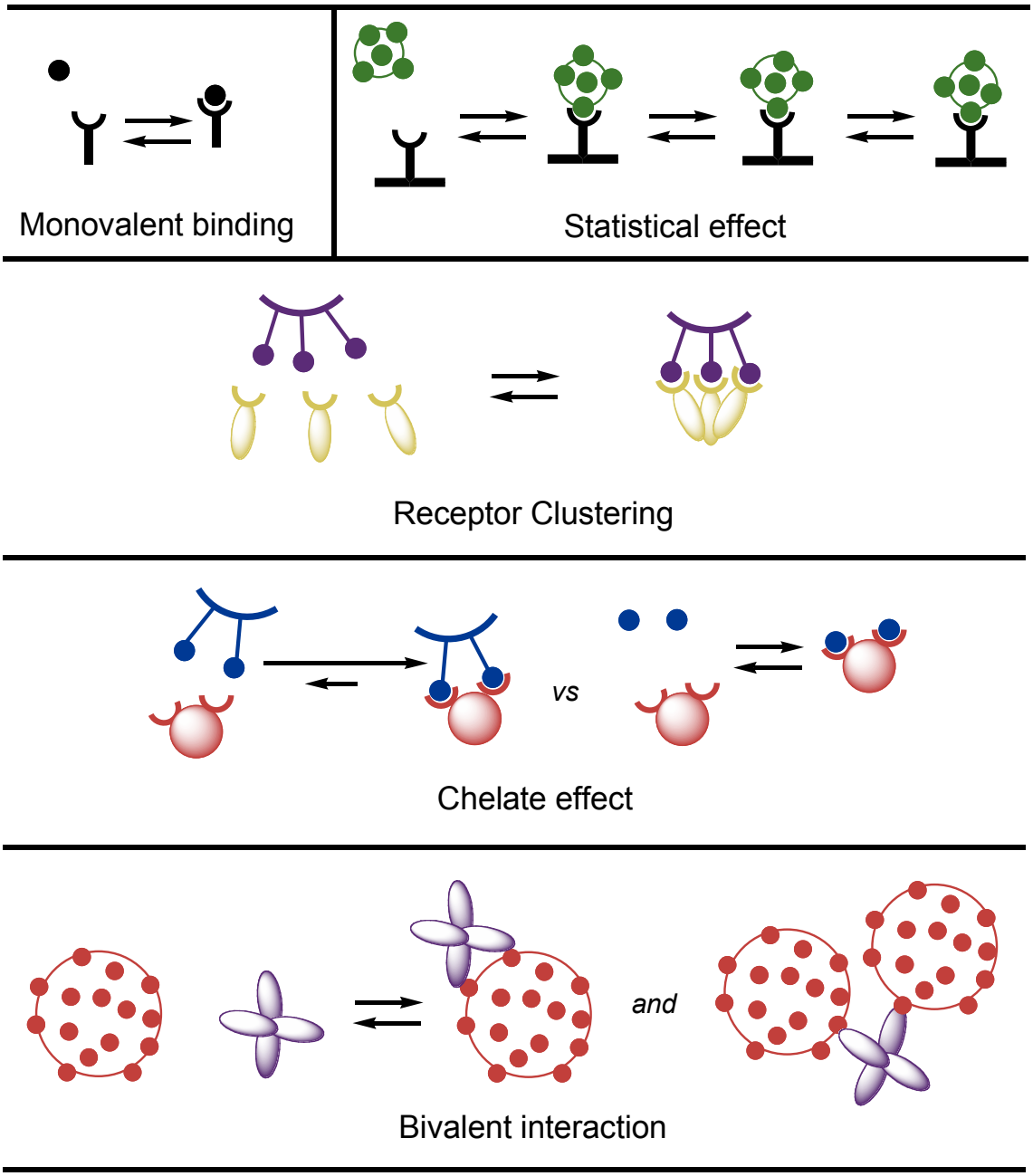

Figure 2 Schematic representations of various binding modes that are involved in multivalent interactions.

interactions occur when multiple binding sites on a multi-point receptor are simultaneously occupied, either by the same carbohydrate-functionalized

platform or by multiple glycosystems. All of these modes can proceed to higher order aggregates. Many factors including thermodynamic and kinetic effects, aggregation, clustering and effective concentration contribute to multivalent effects.

In this chapter, innovative approaches to using multivalent carbohydrate scaffolds in practical ways such as cell targeting, magnetic imaging and immune response manipulation are highlighted. Scaffold structure and design are also discussed.

Scaffolds

A large number of different scaffolds are being developed for multivalent presentation of carbohydrates. If the size of the system is of utmost importance, then frameworks ranging from small molecules to liposomes and viral capsids have been reported. When rigidity or flexibility is most important, systems spanning from fullerenes to polydisperse polymers to dendrimers are described. Self-assembling and disassembling natural and synthetic architectures are used when *in situ* formation or decomposition of the multivalent system is desired. This variety of scaffolds is required because of the wide variety of mechanisms of action with which biological multivalent carbohydrate interactions manifest themselves. For example, large polymers can bind very tightly and can cluster many targets, large spherical scaffolds can induce clustering and aggregation, small molecules can optimize statistical effects, self assembled molecules

(viruses, liposomes and synthetic vesicles) can form and then disassemble to reduce lifetime toxicity, and polyrotaxanes can optimize interactions based on movement along a backbone. The size of the scaffold and the presentation of the carbohydrate ligands often determine whether multivalent interactions with target receptors can occur or not. Key advances in the development of multivalent frameworks for the display of carbohydrates are described in this section of the chapter.

Polymers

Polymeric scaffolds have a major advantage for many applications in that they are very flexible structures that can be synthesized over a large range of sizes. Polymeric scaffolds enable the presentation of large numbers of carbohydrates and, accordingly, are able to induce strong binding interactions and to cause clustering/aggregating events. Although controlling the polydispersity of the glycopolymers is often challenging, improvements in polymer synthesis are allowing polymers to become a viable option for applications in multivalent research.

Some time ago, glycoproteins were shown to inhibit influenza virus agglutinin only when polymerized into polyvalent displays, suggesting that synthetic polymers would be very effective platforms for multivalent carbohydrate presentations.[8] An early example using a synthetic linear polymeric backbone was reported by Whitesides *et al*.; a polyacrylamide backbone conjugated with sialic acid derivatives was synthesized (Figure 3). These polydisperse

polymer:carbohydrate conjugates were shown to be up to a million times more effective than the monomer at binding influenza type A viruses.[9] Roy *et al*. reported a less toxic polymeric backbone, polylysine, onto which the carbohydrate was conjugated post polymerization.[10] Kiessling and co-workers synthesized a carbohydrate conjugated ROMP polymer, which provides a more rigid framework and has improved polydispersity (Figure 4).[11]

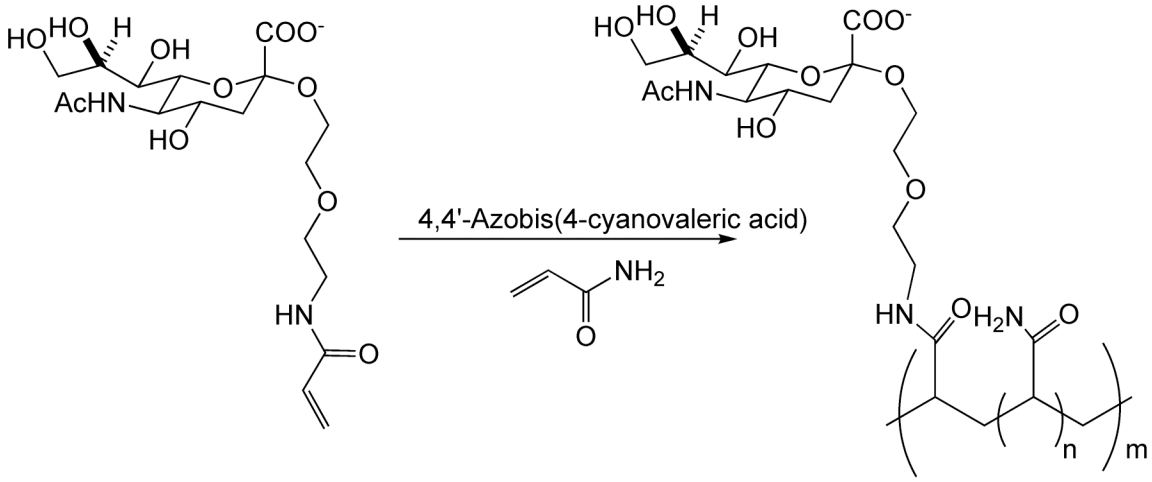

Figure 3 Synthesis of Whitesides' carbohydrate-conjugated acrylamide polymer.

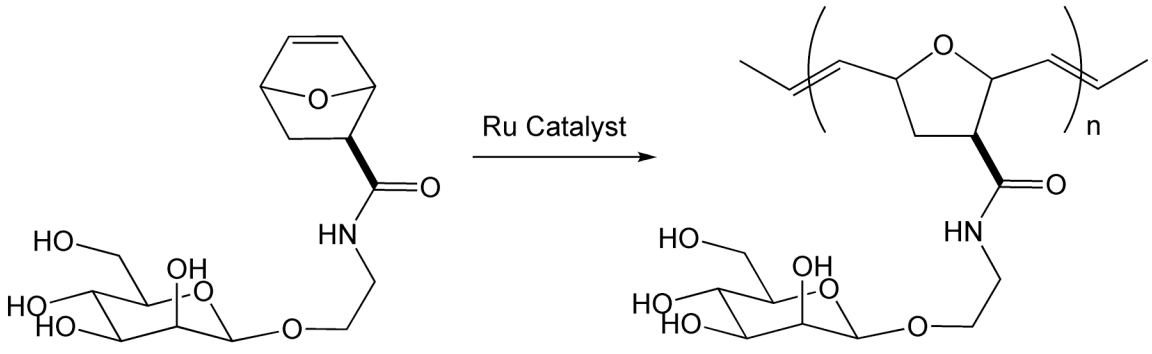

Figure 4 Synthesis of Kiessling's carbohydrate-conjugated linear ROMP polymer.

Polydisperse polymers are difficult to characterize for therapeutic use, and most linear polymers are unfortunately somewhat polydisperse. Further complicating matters, the 3-dimensional shape of the linear polymers is generally undefined. Biocompatibility of the linear polymers can also be problematic. However, the inherent flexibility and efficacy of linear polymers can be greatly advantageous for applications involving receptor clustering and a large number of binding interactions. As characterization methods and synthesis strategies are improving, linear polymers are becoming increasingly important glycosystems.

Gold Nanoparticles

Gold nanoparticles have a very desirable feature in that control of the particle size is readily achievable. Since gold nanoparticles are relatively inert, these compounds have high potential for use in biological applications. In most reported examples, the carbohydrate (or other) epitopes are attached to the gold nanoparticle using thiols.

With carbohydrate bearing gold nanoparticles, Penades *et al*. have reported influencing a “first recognition step” as potential inhibitors of an experimental lung metastasis. These lactose bearing GNPs were shown in mouse models to significantly reduce the progression of experimental metastasis.[12]

In a design that incorporates not only the carbohydrate but also the amino acid residues adjacent to the carbohydrate of a glycoprotein onto a GNP, Barchi and co-workers reported synthesis of a sixteen amino acid repeating unit in

mucin MUC4 (overexpressed in some cancers). To this backbone, Tf antigen carbohydrate epitopes were attached at the sixth and tenth amino acids; this whole structure was then attached via a thiol linker to a GNP (Figure 5). This is an excellent example of using the surrounding features of a carbohydrate antigen to enhance interactions.[13]

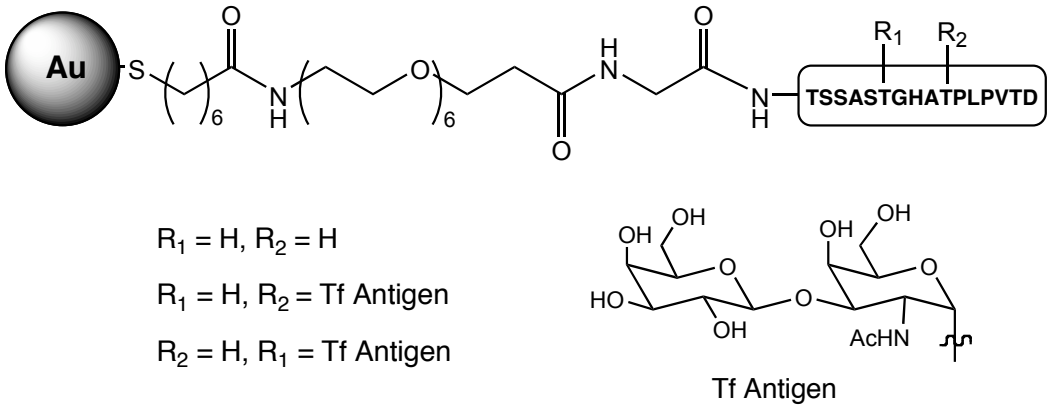

Figure 5 Gold nanoparticle prepared by Barchi with linker, mucin-based peptide, and Tf antigen

Gold nanoparticles are appealing scaffolds for multivalent carbohydrate recognition events for several reasons. They are inert, can be made in discreet sizes, and have excellent potential for imaging applications. The disadvantages for the GNP scaffold are that characterizing the amount of surface functionality that is present is difficult and that the GNP is very rigid (although tethers can be very variable and can impart some flexibility to the surface region of the particle).

Protein Based Scaffolds

Protein based scaffolds include everything from small synthetic peptides to existing proteins. On these protein-based frameworks, carbohydrate ligands can be conjugated. Since the conjugation of carbohydrates to peptides has been

thoroughly covered in a recent review, only a few important examples will be highlighted here.[14]

Kiick *et al*. reported polypeptide synthesis with defined spacing to complement the target receptors of the cholera toxin B5 (CT B5) subunit in a multivalent fashion.[15] Optimal spacing of the epitopes required them to be at least 35 Å apart, and the efficacy of CT B5 binding was found to correlate with increasing hydrodynamic volume (assessed via GPC).

Glycosylation of bovine serum albumin (BSA) is one of the most common approaches to formation of glycoproteins. For example, Gildersleeve and co-workers report the use of glycosylated BSA in glycan arrays. These arrays are an important addition to the available glycan array technology because they allow for clustered presentation of glycans into close proximity. Whereas other array platforms focus primarily on surface functionalization with monosaccharides, Gildersleeve's surface labeling with glycosylated BSA allows for extensive evaluation and screening of ligand specificity through multivalent interactions in an array protocol.[16, 17] Using a combination of scaffolds, Haddleton and co-workers report the synthesis of glycopolymers followed by the covalent linkage of these systems to BSA. This conjugation appeared to have little affect on the BSA structure, and functional aspects of the protein remained, indicating that glycopolymers are compatible with proteins.[18]

In a very innovative report, Davis *et al*. synthesized dendritic tethers which were then linked to a protein to mimic glycoproteins.[19] The protein scaffold that

was used was a protease, which via attachment through the glycan (galactose), cleaved its target receptor, part of the bacterium pathogen *Actinomyces naeslundii*. A K_D value of 1.4 x 10^{-7} M for the tetrameric galactose presenting synthetic glycoprotein was observed when tested against a galactose binding lectin in an ELLA assay (compared to ~10^{-3} M for dimeric ligands). When tested against the target receptor, *Actinomyces naeslundii's* ability to co-aggregate with co-pathogen *streptococcus oralis,* the dimeric ligand presentation was more effective, with an IC_{50} value of 20 nM (10^6 times more effective than monomer lactose, and 10^3 times more effective than the protease). Davis *et al*. reported that for optimal inhibition, essential properties are i) multiantennary carbohydrate display, ii) protein degrading activity and iii) galactose presentation.

Protein-based scaffolds are useful because they have the potential to be inert, as shown when BSA was used. Alternatively, protein-based scaffolds can provide added function if proteins with enzymatic activity are used, such as the protease described above. The very specific presentation of ligands that can be achieved via functionalization of protein side chains is also advantageous, although obtaining the appropriate spacings for the functional groups may require protein engineering.

Cyclodextrins, Polyrotaxanes, and Calixarenes

Pseudopolyrotaxanes were synthesized by Stoddart and co-workers, and the binding of these pseudopolyrotaxanes to Galectin-1 was investigated.[20] Galectin-1 is a member of the galectin family of lectins and plays an important role in cancer cellular processes. The reported pseudopolyrotaxanes are comprised of cyclodextrins that are tethered onto a polyviologen backbone, and migration of the cyclodextrins along the polymer chain can occur (Figure 6). The authors suggest that lower enthalpic penalties occur for this system than for other multivalent frameworks due to lack of strain; the carbohydrate ligands are able to adjust their position along the polymer in order to achieve optimal separation for multivalent binding.

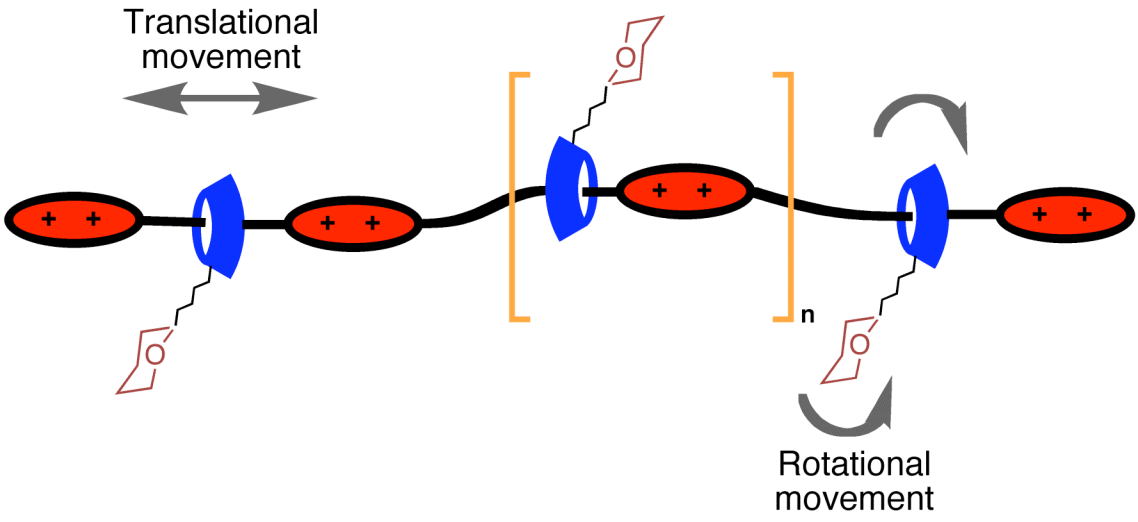

Figure 6 A schematic representation of Stoddart's pseudopolyrotaxanes.

The viologen backbone also has charged "speed bumps" that reduce translational motion of the cyclodextrins. In a T-cell agglutination assay, the

pseudopolyrotaxanes were able to prevent cellular aggregation caused by Galectin-1 more effectively than small dendritic structures and than the monomeric ligand were able to do.

Calixarenes have been functionalized with carbohydrate ligands and have been shown to increase efficacy, presumably through a proximity effect, relative to monomeric carbohydrates. For example, Ungaro *et al*. showed that calixarenes bearing carbohydrates can self aggregate into larger glycocluster nanoparticles (GNP's) of 4-6 units. These calixarenes also form larger 1:1 aggregates with guanosine 5'-monophosphate and adenosine mono, di and triphosphates suggesting that these multivalent carbohydrate calixarene conjugates may be able to serve as non-viral gene vectors.[15] As another example, Dondoni *et al*. studies reported a calix(4)arene with thiosialosides linked to both the upper and the lower rim of the oligophenol structure, making tetramers and octomers (Figure 7). These compounds showed almost two orders of magnitude binding enhancement over the monomeric sialoside in influenza A hemagglutination inhibition studies and also inhibited the "cytopathic effect" of the BK virus.[21]

Calixarenes have an inherent structural rigidity that creates a well-defined structure upon which carbohydrates can be precisely displayed and have been shown to have self assembly properties. When polyrotaxane and pseudopolyrotaxane scaffolds are used, they allow for the presentation of multiple calixarenes in a dynamic manner. Because the calixarene can move

along the backbone, studies with these compounds may lead to better understanding of requirements of ligand spacing, density, and other geometric factors for optimization of multivalent carbohydrate-mediated interactions.

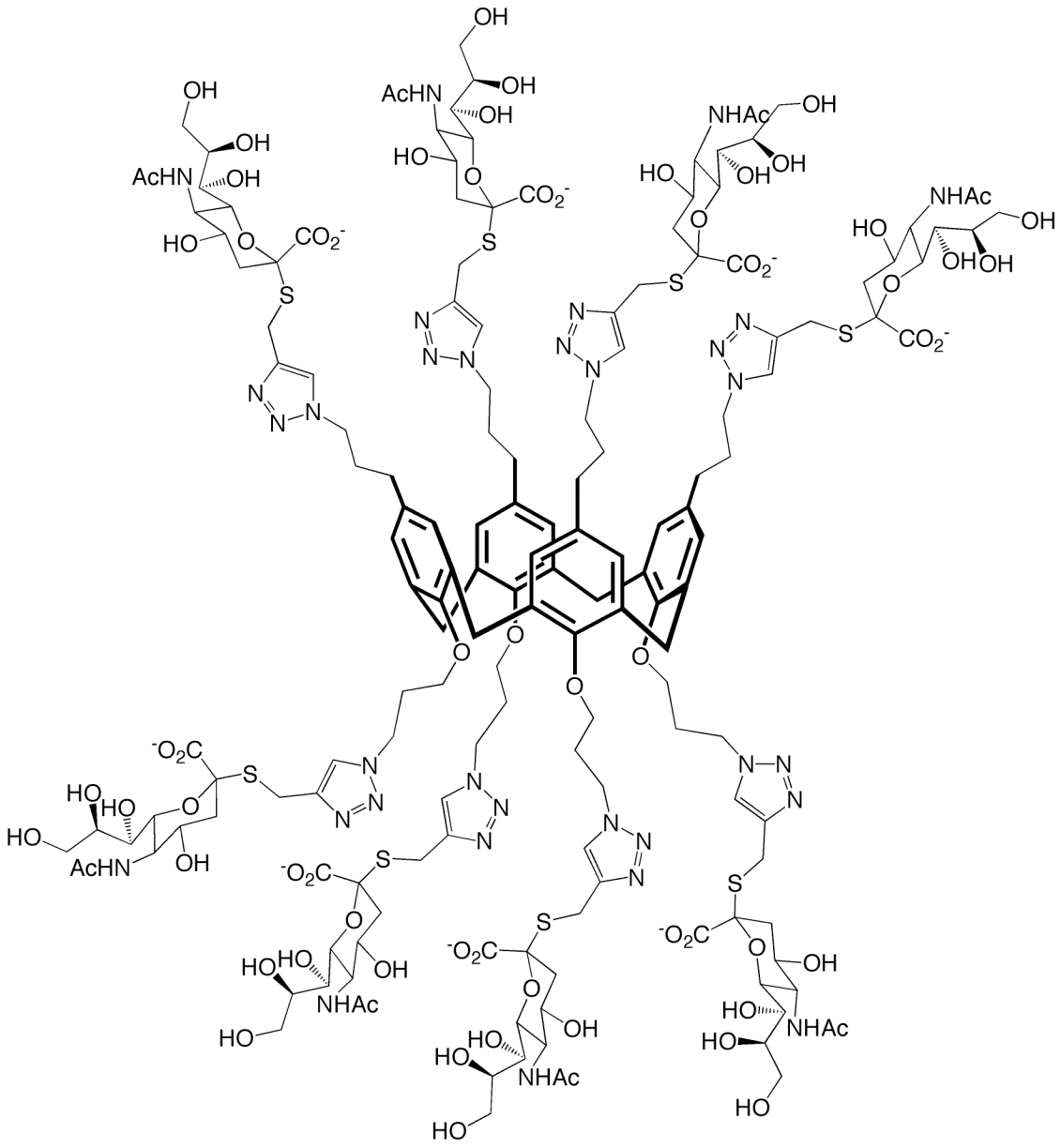

Figure 7 A carbohydrate-conjugated calix(4)arene; the ligands on the upper rim are farther apart than the ligands conjugated to the lower rim.

Dendritic and Large Spherical Structures

Dendrimers and dendritic structures are among the most studied systems for multivalent carbohydrate presentation. Two reviews of glycodendrimers by Roy and Chabre and by Bezouska have recently been published.[22, 23] An important focus of the former is the applications for which glycodendrimers are being developed, while a historical perspective is provided by the later.

(a)

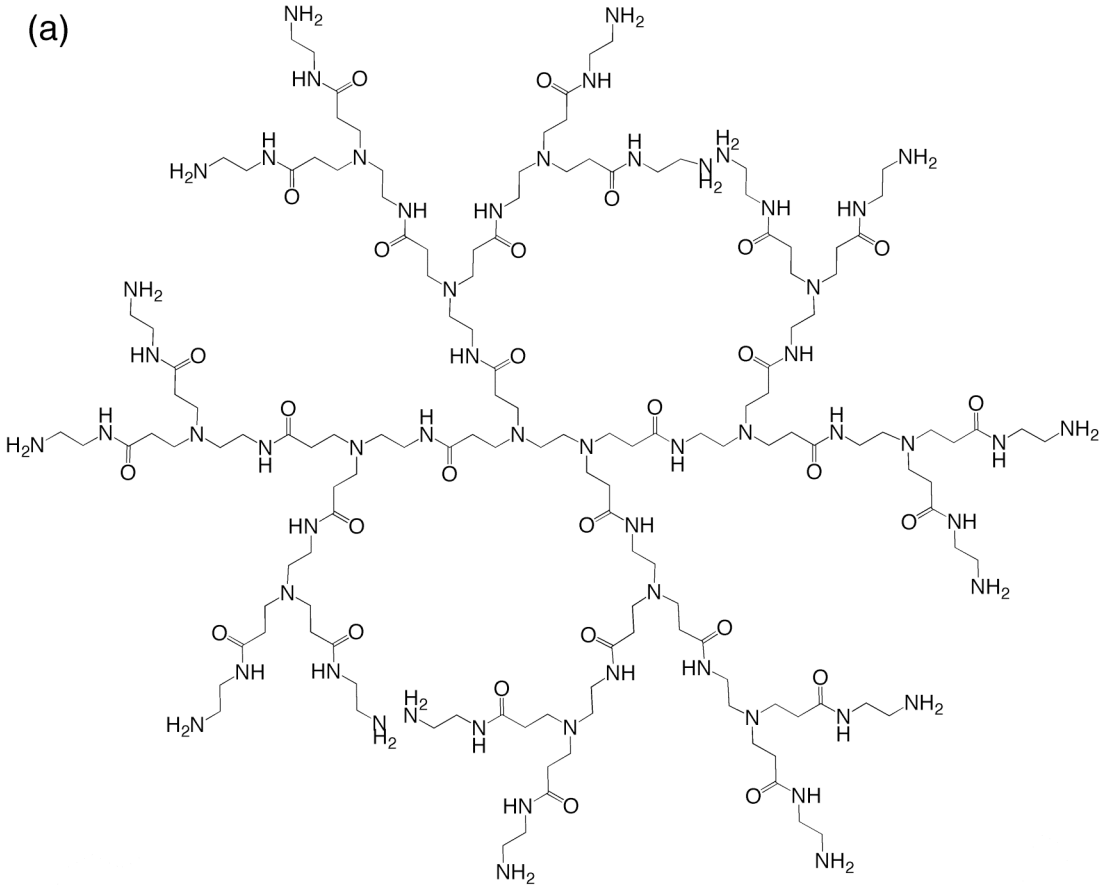

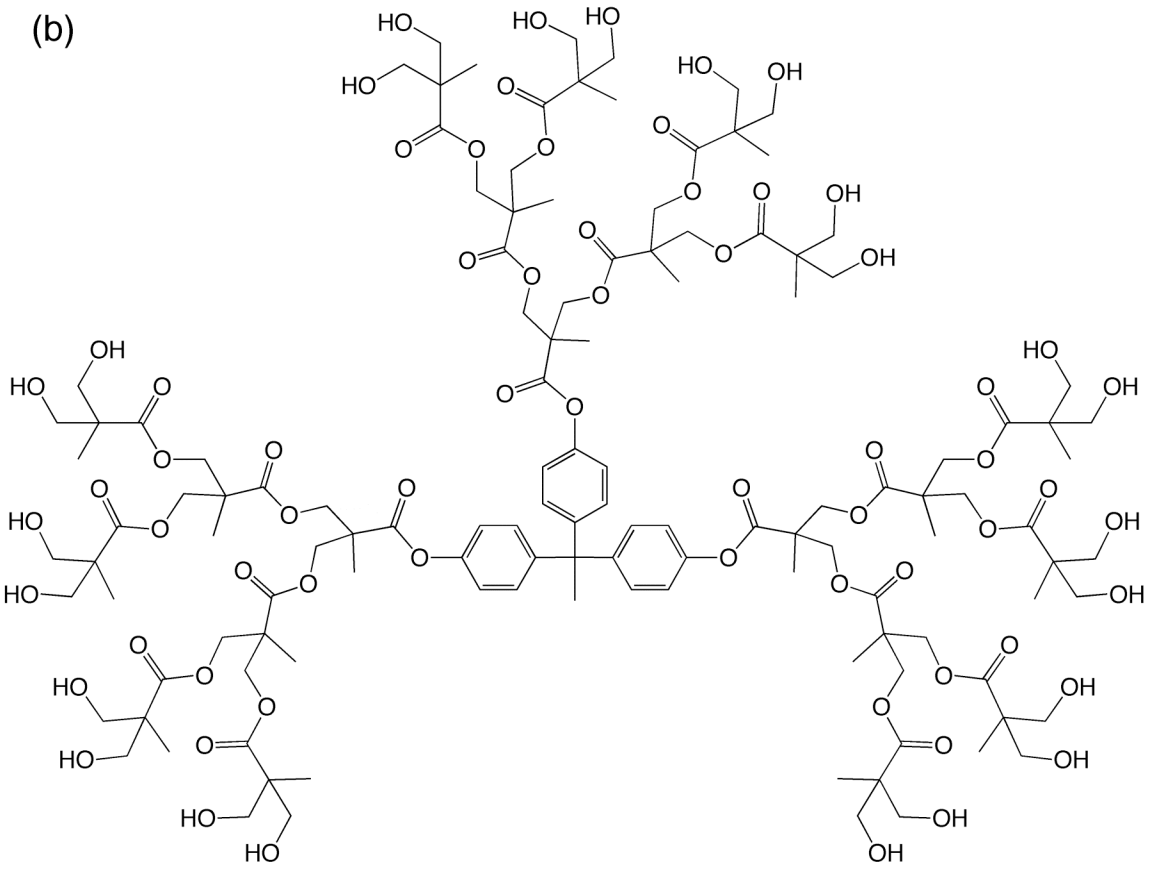

Figure 8 a) G(2)-PAMAM dendrimer, b) polyester dendrimer with 2,2-bis(hydroxymethyl)propionate repeating units.

Both convergent and divergent synthetic routes for glycodendrimer synthesis have been described. The smaller dendritic molecules have the advantage of being discrete structures but may be less effective if larger cross-linking agents are required for multivalent effects to be realized. The larger molecules have low polydispersities relative to other polymeric systems but are not as homogeneous as the smaller frameworks. Two popular dendrimers, the poly(amidoamine) (PAMAM) and the polyester dendrimer, are shown in Figure 8. Cloninger *et al*. reported optimization of carbohydrate density on the periphery of

PAMAM dendrimers in a mannose:Concanavalin A system. Functionalization of 50% of the possible PAMAM dendrimer endgroups was

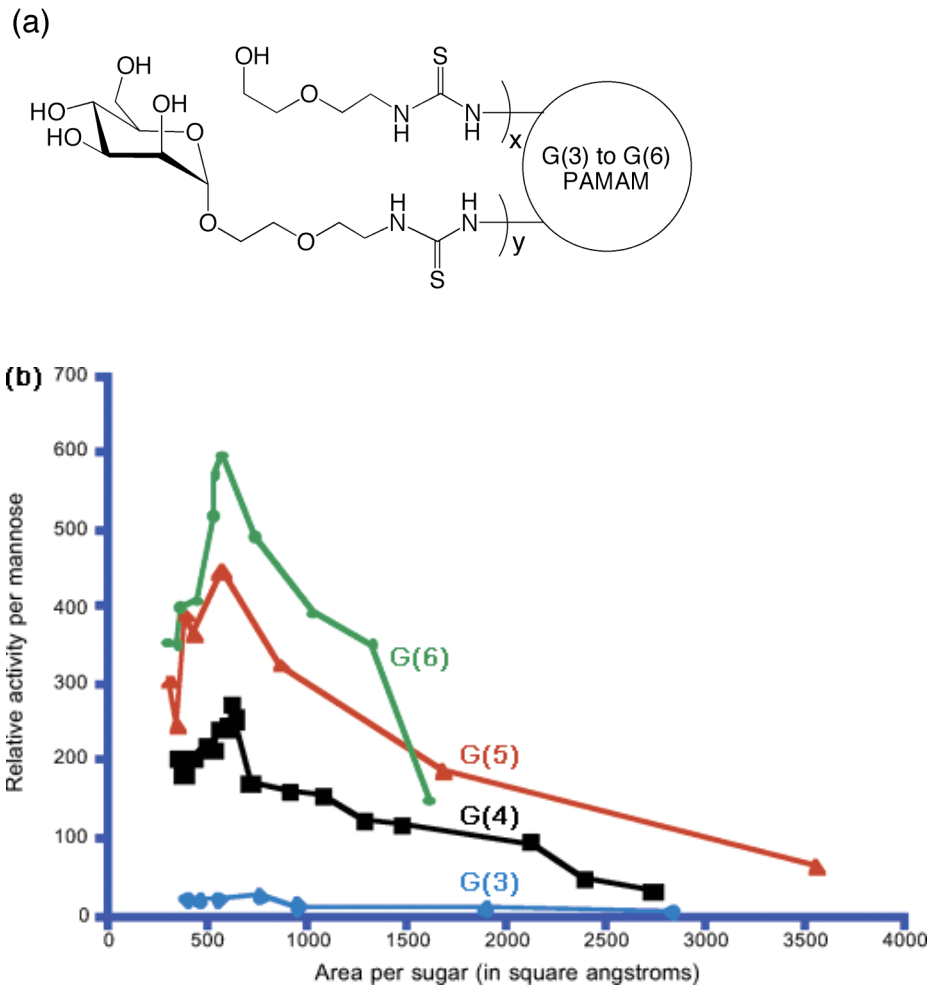

Figure 9 (a) Mannose/hydroxyl functionalized dendrimers, (b) mannose-functionalized G(4), G(5), and G(6)-PAMAM dendrimers with 50% loadings exhibited the highest activity in hemagglutination inhibition assays with Concanavalin A.

found to be most effective on a per sugar basis. This study also suggested that larger generation dendrimers are of sufficient size to span multiple binding sites on the Concanavalin A tetramer. Moving from a monovalent binding mode with small dendrimers to a bivalent binding mode with larger dendrimers increased

the interaction with Concanavalin A by 2-3 orders of magnitude. In addition, statistical effects were shown to effectively increase glycodendrimer activity by approximately one order of magnitude (Figure 9).[24]

Wong *et al*. synthesized mannose-functionalized dendrons to mimic the glycan of gp120, a glycoprotein HIV target, with the goal of developing anti-HIV vaccines.[25] The proposed target is the gp120:DC-SIGN (dendritic cell specific intercellular adhesion molecule-grabbing nonintegrin) interaction, thought to be a key step in the dissemintation of HIV-1 cells. The mannosylated dendrons exhibited increased affinity in a competition ELISA assay between DC-SIGN and glycan surface array, along with an immobilized gp120:2G12 (HIV antibody) competition assay. In the ELISA assay the glycoconjugate had an IC_{50} value up to 10^4 times better than the monomeric tether. The dendrons were evaluated for cellular surface DC-SIGN binding in a flow cytometry assay indicating the ability to bind to cell surface targets. The binding results suggest these mannosylated dendrons as candidates for carbohydrate vaccine formulation.

Dendrimers are highly promising scaffolds for biological applications in multivalent carbohydrate recognition because they can be very flexible, reducing the entropy cost associated with multivalent binding. In addition, the size of the framework is easy to systematically alter by using different generations of dendrimers. The degree of dendrimer functionalization can, in most cases, be readily evaluated using mass spectrometry. Although nonheterogeneity of

dendrimers can be an issue, dendrimers are excellent synthetic frameworks for the multivalent display of carbohydrates.

Self Assembled Scaffolds

Self assembled scaffolds, viral capsids, liposomes and synthetic vesicles that present carbohydrate motifs have all been reported. Finn and co-workers, for example, have used carbohydrate-functionalized virus capsids. These capsids are easily functionalized with carbohydrates and, as expected, show greatly increased binding to lectins. Inherently appealing in this strategy is the self assembly and disassembly that can occur with protein cages.[26]

The formation of both cylindrical and spherical vesicles along with micelles of discrete sizes have been reported by Myongsoon Lee *et al*. (Figure 10).[27] When presenting carbohydrates, these structures showed increased binding compared to the monomer unit. Thoma *et al*. reported synthesis of self assembled particles create larger units through aromatic stacking, forming up to 7100 kDa glycoconjugate nanoparticles. Binding assays suggested that aggregate particle size and efficacy are linked and can be controlled by the choice of size of the assembling subunit.[28] Kim *et al*. reported the synthesis of vesicles with a diameter of 170 ± 50 nm and with a thickness of 6 ± 1 nm that form stable host guest complexes with polyamines in aqueous solutions.

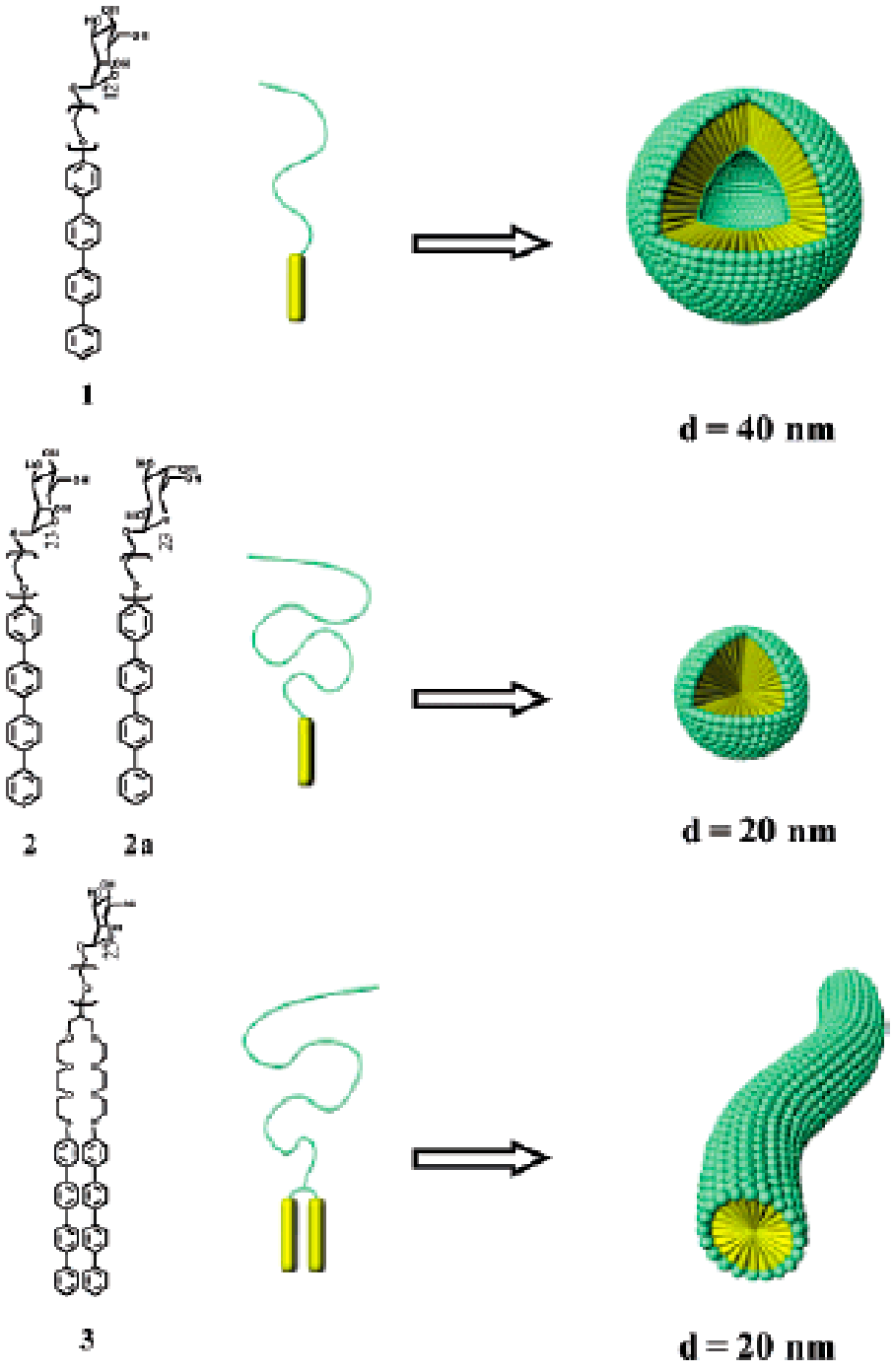

Figure 10 Lee's schematic representation of vesicles and spherical and cylindrical micelles.

These vesicles were evaluated using the mannose : Concanavalin A interaction using an SPR technique and showed binding enhancements of 3 orders of magnitude relative to the monomeric 1-*O*-methyl mannose.[27]

Liposomes were used as scaffolds by Nagy *et al*., who studied the effects of varying the carbohydrates that were presented by the liposomes. Using sLex like carbohydrates, different functional groups were inserted at the 3-position including NH_3^+, OH, COO^- and SO_3^{2-}. These liposomes were tested for binding to L, E and P selectins, and the sulfate was shown to be the most effective across all selectins. Evidence presented in this report suggests that the selectins may have a binding site that binds to both a carbohydrate and an ionic substrate.[29]

Self-assembled systems, regardless of whether they are liposomes, virus capsids, synthetic amphiphiles or vesicles, have the definite advantage that they can disassemble into smaller, discrete components. This may be highly desirable because their biological lifetimes and processing can benefit from disassembly.

Prominent Fundamental Examples

In 2002 Kiessling and co-workers published an intensive study of various architectures, low molecular weight molecules, PAMAM dendrimers, globular proteins, ROMP-derived linear polymers and polydisperse PEMA polymers to present multiple carbohydrate epitopes, and to understand how these different scaffolds may have varying utility.[3] A key aspect of this study was to broadly

determine which scaffolds would produce a better effector and which frameworks could serve as better scaffolds for creation of an inhibitor. Effectors were found to be ”influenced not only by apparent affinities but also by alternate factors, including the ability of a ligand to cluster receptors”. The best inhibitors, however, were found to have “high functional affinities of multivalent ligand-receptor interactions”. The results of solid phase binding, turbidity, fluorescence quenching and precipitation assays suggested that globular scaffolds, proteins and dendrimers make better inhibitors but do not have the relatively good clustering capacity that is necessary for effectors. Linear polymers performed well both in clustering and binding, and ROMP polymers exhibited good clustering properties that suggest that these polymers are potentially good effectors.[3]

In a remarkable example of binding efficacy and structural design optimization, Bundle and coworkers reported studies between a multivalent carbohydrate scaffold and shiga toxin.[30] A crystal structure of the toxin was used to design a distance-specific scaffold, and sub-nanomolar dissociation constants were reported. Enhancements in binding affinity to shiga toxin of 1-10 million fold relative to the monomeric carbohydrate were observed for this glycosystem. This is one of the few examples where a system showed positive cooperativity for binding.

In 1994, Whitesides *et al*. reported using a polyacrylamide scaffold bearing sialoside groups to target influenza virus.[9] A number of optimization

strategies were employed, including placing a strongly binding epitope alongside a weaker binder, altering the tether length to assess potential steric factors, and altering the polymer synthesis by using different molar ratios of the radical initiator and by using different types of copolymer. This study suggested that high molecular weight polymers bearing sialic acid moieties prevented virion infection by a steric stabilization of the virus, rather than occupying a high fraction of the sialic acid binding sites, and this is sensitive to the structural features of the polymeric scaffold.

In an innovative example of utilizing multiple components, Boons *et al*. synthesized a tumor associated T antigen and attached this to the C terminus of a synthesized T epitope lipopeptide. The lipopeptide enables the compound to be incorporated into liposomes, and the T-epitope peptide helps to induce a T cell dependent immune response that results in the production of IgG antibodies against the Tn antigen. The liposomes that were formed using this conjugate were used as an anti-cancer vaccine candidate and elicited a IgG and IgM Tn antigen immune response.[31]

For an example of creating a predictable and tuneable multivalent system using Whitesides model, see chapter 2 in this manuscript.

Carbohydrate-Carbohydrate Interactions

Although protein-carbohydrate interactions are the focus of most of the research that has been reported with multivalent glycosystems, multivalent

carbohydrate-carbohydrate interactions have also been investigated. A comprehensive review was published by Penades,[32] who with co workers reported the synthesis of carbohydrate (lactose and Lex) functionalized gold nanoparticles as mimics of cell surface glycan clusters that were formed in order to study further carbohydrate interactions.[33] Using TEM to monitor particle aggregation, a key component to these interactions was determined to be the presence of calcium ions. This binding interaction was tested using AFM and showed "that only specific binding events between Ca^{2+} ions and Lex molecules dictate the self aggregation", indicating Lex to be a homophilic adhesion molecule. Wang and co workers described the synthesis of carbon walled nanotube scaffolds that were coated with galactose and mannose and were used to capture anthrax spores. This capture process was proposed to be mediated by a carbohydrate-carbohydrate interaction and a divalent Ca^{2+} cation.[34] Basu *et al*. found that lactose functionalized PAMAM dendrimers underwent specific interactions with a GM3 functionalized monolayer. This carbohydrate-carbohydrate interaction was reported to be $CaCl_2$ dependent (experiments were done in 1 mM $CaCl_2$), showing that there was an electrostatic component to the interaction. The size of the glycodendrimer was also important: generation 4 was active but generations 1, 2 and 3 were inactive. This study indicated that multivalency is highly important for carbohydrate-carbohydrate interactions.[35]

The most prolific researcher in the area of carbohydrate-carbohydrate interactions is Hakomori, who has reported multivalent clustering effects in a

GlcNAc : GM3 interaction.[36] Glycosphingolipid mimics were synthesized, and glycans with five or six glcNAc residues showed enhanced binding and specificity to GM3 over other oligosaccharides.

Because of the inherent complexity and prevalence of carbohydrates, carbohydrate-carbohydrate interactions are currently difficult to monitor, and the degree of specificity that is achieved by these interactions is often unclear. However, with improving technologies and further insight, these interactions may well be shown to be influential.

Applications-Driven Examples

Roy and co-workers synthesized a multivalent, carbohydrate-based flu vaccine by attaching a Haemophilus influenzae type b carbohydrate epitope to human serum albumin (Figure 11).[37] This antigen had an average of eight repeating units of ribosylribitol phosphate, which was synthesized using a one pot condensation process that is scalable to >100 g batches. As a multivalent

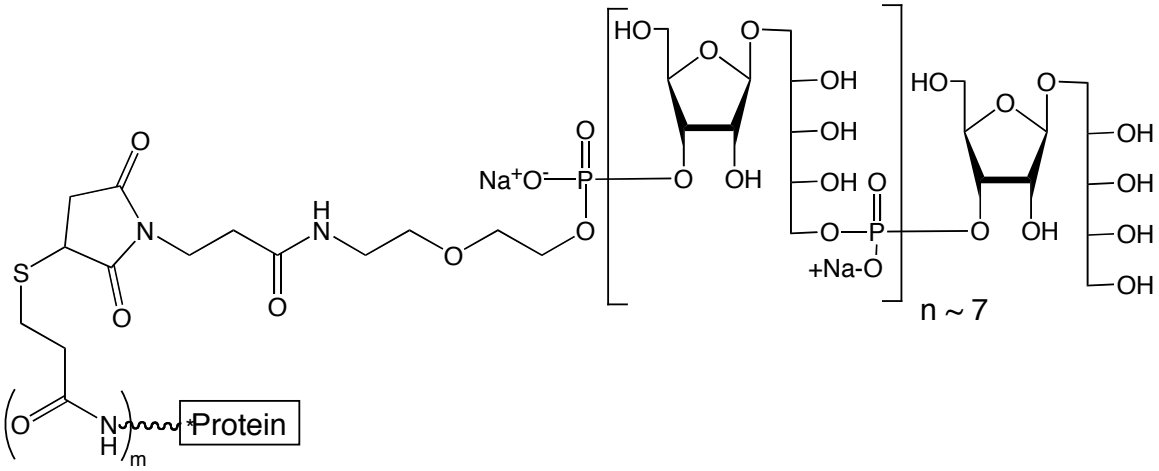

Figure 11 An influenza type b vaccine synthesized by Roy *et al*.

vaccine, this conjugate has been made available to developing countries where Haemophilus influenzae type b is partly responsible for high infant mortality.

In another study using human serum albumin as a scaffold, Kihlberg and coworkers synthesized a 3'-sialyllactose moiety covalently conjugated to HSA , designed to be an inhibitor of adenovirus AD37. [38] In a competitive cellular uptake assay, monitoring virion uptake relative to inhibitor concentration, these multivalent architectures provided binding enhancements of 100 fold relative to the 3'-sialyllactose monomer and demonstrated effectiveness as an inhibitor of the targeted virus. An advantage, shown in this study, of the HSA scaffold is the ease of biological utility.

For bacterial detection, Seeberger *et al*. used a fluorescent Poly(*p*-phenylene ethynylene) (PPE) backbone that was functionalized with carbohydrates after the synthesis of the polymer. The mannose-functionalized polymer was then added to *E. coli* cells that specifically bind mannose and due to the PPE backbone, fluoresce upon cellular aggregation of 30 to several thousand bacteria, indicating detection of a small bacterium.[39] Any sugar motif can be added to the reported polymer, and, since only aggregates fluoresce, multivalency is essential for detection. Moreover, the experiments were performed in 15 minutes with as little as 10,000 cells, making this an attractive system for detecting multivalent processes.

Kiessling and co workers reported a highly innovative approach for the activation of the immune response toward tumor cells using a multivalent

carbohydrate compound. [40] Taking advantage of a “pre-existing immune response that poses a major barrier to xenotransplantation”, Kiessling elicited an immune response by binding an RGD mimic to a cell surface integrin, $\alpha_v\beta_3$, for recognition (Figure 12). The RGD mimic was attached to a carbohydrate that causes an immune response resulting in cell lysis. This response appears to be mediated by the amount of carbohydrate presented on the cell surface; without a high enough integrin surface concentration, the multivalent interaction causing the immune response is inactive. The level of expression of $\alpha_v\beta_3$ integrin is elevated on invasive tumor cells and on the endothelium of the tumor vasculature. This work is a wonderful example of utilization of a strong

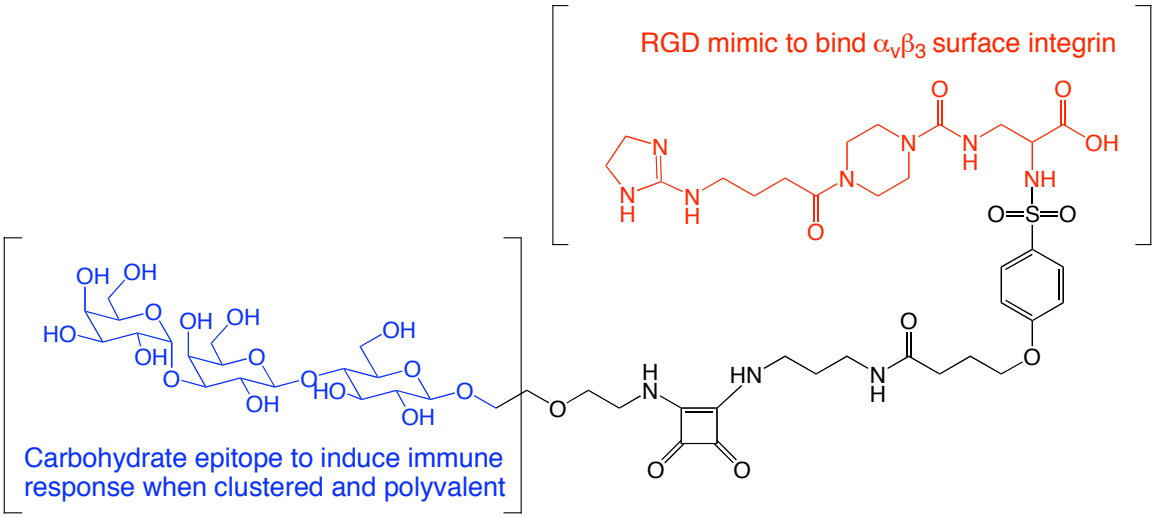

Figure 12 Kiessling *et al*.’s RGD mimic with an immune activating carbohydrate that responds only when clustered into a multivalent display.

monovalent interaction for initial recognition coupled to the exploitation of a multivalent cell surface interaction. The multivalent process requires an effective

concentration, which induces a very specific immune response to mediate cell death.

In 2009 Davis and co workers reported the synthesis of carbohydrate functionalized nanoparticles in which the nanoparticle is a “high iron content nanoparticular platform”.[41] This platform is highly sensitive in MRI imaging. A SeLx carbohydrate ligand was synthesized, mainly using various glycosyl transferase enzymes, and with a highly adaptable S-cyanomethyl functional group tether that can easily be modified for specific amine attachment. The SeLx ligand was present so that it could specifically target CD62 transmembrane proteins that are upregulated in response to injury or disease and utilized by the brain. Since the brain uses these proteins, the authors demonstrated that they could be used as a biomarker to identify brain disease. Through in vivo animal studies, these SeLx glyconanoparticles were shown to have high specificity to the targeted endothelial markers E-/P-selectin (CD62E/CD62P) when compared to other glycans, LacNAc and sialyl lacNAc. The multivalent component, with the particle being decorated with 10^6 glycans, was shown to be absolutely necessary. Cross species immune responses to the glycan were shown to be negligible, and the iron scaffold has low toxicity and is in clinical trials for other uses. Thus, these carbohydrate functionalized nanoparticles showed remarkable MRI imaging, great improvements on existing technologies and an ability to detect brain disease and inflammation.

Methods of Analysis

Good ways of monitoring the binding and activity of multivalent system are necessary if carbohydrate-driven multivalent effects are to be truly understood and mediated. Currently, several techniques are applied to the study of multivalent interactions including the hemagglutination inhibition assay (HIA),[42] surface plasmon resonance (SPR),[43] isothermal titration calorimetry (ITC),[44] the enzyme linked immunosorbent assay and the enzyme linked lectin assay (ELISA/ELLA),[45], the turbidity assay[46], the precipitation assay[47], fluorescence activated cell sorting (FACS),[48] atomic force microscopy (AFM),[49] back scattering interferometry,[50] and quartz crystal microbalance (QCM-D).[51] Toone *et al*. reviewed many of the available technologies and the inherent pros and cons associated with each process.[52] In Kiessling's article that compared various architectures, multiple assays were used to evaluate the differing physical attributes of each scaffold.[3] Here, Kiessling reported that "no single assay can elucidate the contributions of ligand structure to multivalent binding mechanisms", and we have observed this as well in our own experiments. Because so many techniques are used but each evaluates only some aspects of the multivalent binding interaction, a clear understanding of which scaffolds should be used for particular applications has not yet fully emerged. The understanding of how the nuances involved in multivalent interactions affect binding modes and influence biological processes is still evolving.

Summary and Discussion

Some key examples describing the creative ways that carbohydrates have been displayed in order to study and to tune multivalent processes have been described in this chapter. Carbohydrates contain a remarkable amount of information and complexity within their structure, and nature uses this information in very subtle yet powerful ways. Understanding the roles of carbohydrates in complex systems is paramount for the discernment of many biological pathways. Carbohydrates have already been shown to be very specific ligands in disease therapy, magnetic imaging, and immune response induction, and many more applications will undoubtedly emerge. Since multivalency is a key process by which nature uses carbohydrates and enhances weak binding interactions, a critical step in improving the treatment of many illnesses and diseases will involve increasing our ability to utilize multivalent interactions with carbohydrates.

CHAPTER 2

GLUCOSE, MANNOSE AND GALACTOSE FUNCTIONALIZED DENDRIMERS: CREATING A PREDICTABLE AND TUNABLE MULTIVALENT SYSTEM

Introduction

Multivalent carbohydrate displays are involved in a myriad of biological recognition processes. [1, 53-55] A variety of glycopolymers have been developed to decipher the mechanistic details of binding processes with lectins. [56] Glycoconjugates include linear polymers, virus cages, gold nanoparticles and dendrimers to name a few. [13, 20, 28, 31, 57-77] Multivalent compounds are now being tested for biological applications (see chapter 1).

Synthetic multivalent molecules are generally optimized for their particular application in an empirical fashion. However, model systems have been used to more generally evaluate the parameters governing multivalent protein-carbohydrate interactions. Concanavalin A (Con A) is the lectin that is used most commonly in model studies with glycopolymers. Con A is a plant lectin isolated from the jackbean, which exists as a homotetramer at pH 7. Each monomer unit has one sugar binding site. Con A has specificity for the α-pyranose forms of D-mannose and D-glucose, and the four sugar binding sites are 65 Å apart. [78] In work that inspired our choice of the Con A model system for this report, Kiessling and co-workers compared Con A binding by various scaffolds,[3] compared Con A binding by linear polymers bearing various glucose and mannose derivatives,[79]

and compared Con A binding by glucose-functionalized linear polymers of varying lengths. [80] In work that inspired our choice of the dendrimer framework, Roy and co-workers studied the binding of lactose-functionalized dendrimers to several lectins.[81]

Nature augments weak monovalent protein carbohydrate interactions by using multivalency. Multivalency can be broadly described as many interactions that have a more than additive effect, making low affinity interactions ($K_d \approx 10^{-3}$ M) into physiologically relevant affinities. [4, 52, 82] Glycoside clustering has been previously defined as "affinity enhancement achieved by multivalent ligands over monovalent ones that is greater than would be expected from a simple effect of concentration increase." [83, 84] For the discussion this definition of glycoside clustering is adopted, but applied more specifically than it is sometimes used in the carbohydrate literature. [7] Here, multivalent binding (the ability of one

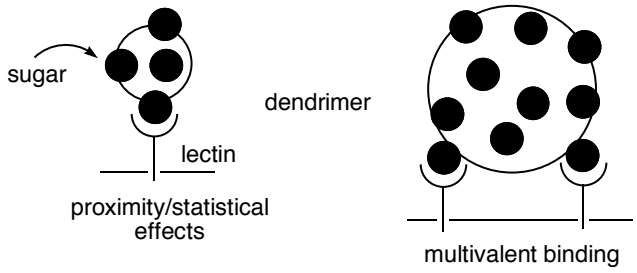

Figure 13 Proximity effects versus multivalent binding.

dendrimer to bind to multiple lectin binding sites) and proximity/statistical effects (a ligand concentration effect) are defined as two related but distinct terms. These definitions are shown pictorially in Figure 13.

Efforts to quantify the effects one would expect from the multivalent presentation of ligands have been reported. Page and Jencks' discussion of the chelate effect, [84] and Jencks' presentation of a "connection Gibbs energy" [7] serve as an important introduction to this area. Jencks proposed that binding of a protein to a bivalent molecule could be described as the sum of the "intrinsic binding energies" of the component parts plus a "connection Gibbs energy" arising primarily from changes in the translational and rotational entropy upon bivalent binding. [7] Two more recent examples of efforts to quantify components of multivalency have been presented by Lees *et al*. [85] and by Reinhoudt *et al*.. [86] Lees and co-workers describe a binding enhancement value for divalent, pentameric, and linear polymer systems, while Reinhoudt and co-workers relate the monovalent association constant to the multivalent association constant using an effective concentration value and a scaling factor. Both these methods progress the discussion of how monovalent association constants effect multivalent interactions, but both suffer from the difficulty of determining the appropriate value for the effective concentration.

In 1998, Whitesides *et al*. proposed a relationship between degree of multivalency and binding affinity with respect to the monomer (see equation 1 and the discussion section below).[4] In this equation N = number of interactions (bivalent = 2), and α represents cooperativity, when $\alpha > 1$ the system is positively cooperative, when $\alpha = 1$ the system is non-cooperative and when $\alpha < 1$ the system is negatively cooperative. In this chapter results can be described well by

this model; changes in activity could be predictably introduced into a multivalent dendritic system. [87]

$$K_N^{poly} = (K^{mono})^{\alpha N} \qquad \text{(eq. 1)}$$

Con A exists as a tetramer at neutral pH, with four carbohydrate binding sites located 6.5 nm apart. [88] Previously, our group has showed that mannose/hydroxyl functionalized G(4) to G(6)-PAMAM dendrimers with 50% mannose incorporation showed the highest activity in hemagglutination assays with Con A. [24] The G(4), G(5), and G(6) dendrimers are large enough to bind divalently to Con A, so these generations were chosen to study the tunability of affinity for this report. Described here are the synthesis of mannose/glucose dendrimers and the results of hemagglutination assays with these dendrimers and Con A.

Results

Synthesis of Mannose, Glucose and Galactose Functionalized PAMAM Dendrimers

To synthesize the carbohydrate tethers, a route was selected that maintains the anomeric integrity of the α sugar starting materials, as α-anomers have higher binding constants than β-anomers. Allylation of the anomeric hydroxyl of α sugar starting material, [89] peracetylation of the 2,3,4 and 6 hydroxyls, [90] and thiol radical addition of Boc-protected aminoethanethiol [42] afforded intermediate 1 (Scheme 1). Removal of the Boc group and addition of thiophosgene afforded the requisite mannose, glucose, and galactose

isothiocyanates 2a-c.Isothiocyanato carbohydrates 2a-c were sequentially added to the PAMAM dendrimers. MALDI-TOF analyses were performed 24 h after each addition to determine the degree of functionalization.

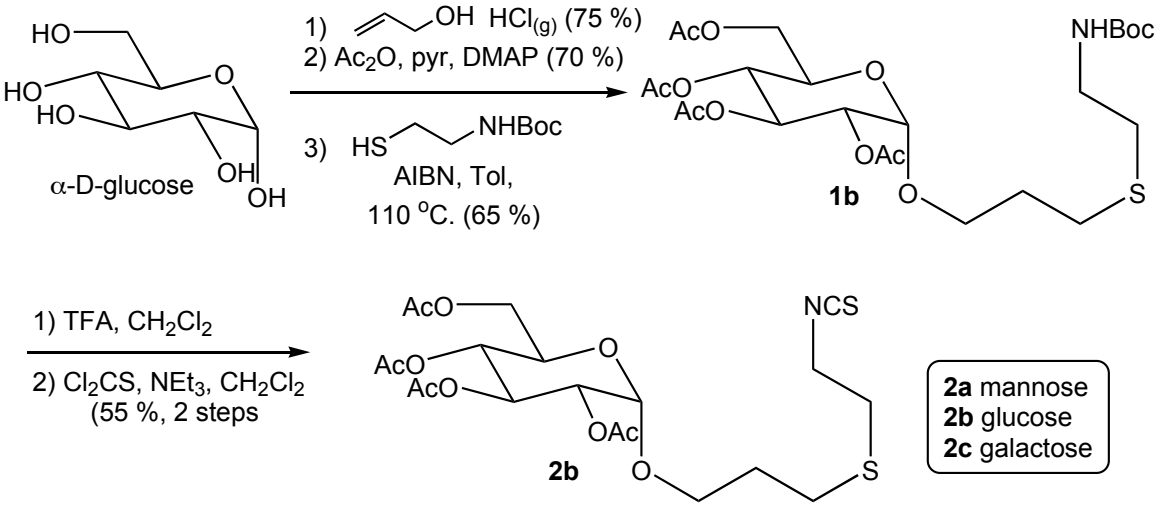

Scheme 1 Synthesis of isothiocyanato carbohydrates. Glucose is shown; mannose (1a and 2a) and galactose (1c and 2c) syntheses are analogous.

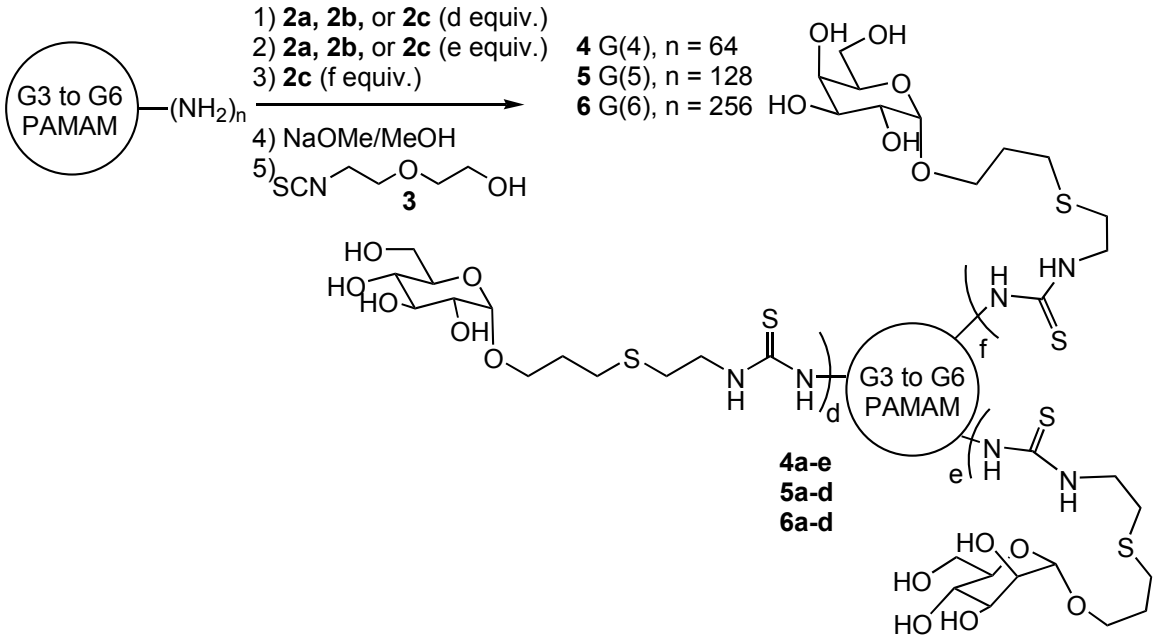

Scheme 2 Synthesis of mannose/glucose-functionalized dendrimers, galactose additions were low, see text for details. Amounts for x and y are provided in Table 1.

The acetyl protecting groups were removed under Zemplen conditions. Since our previous work indicated that 50% mannose functionalization caused the highest activity in the hemagglutination assay, 50% of the dendrimers' amino endgroups were functionalized with mannose and glucose,. [24]

After mixtures of mannose and glucose were added to the dendrimers in varying ratios to total 50% (as shown in Table 1), then galactose (which has no activity with Con A in the hemagglutination assay) was added. Although galactose additions of about 50% were intended, galactose addition was consistently low. Warming the galactose additions to 40 ^{o}C with both acetylated and deacetylated mannose/glucose-dendrimers and adding isothiocyanatoethoxyethanol 3 [24] failed to cause higher loadings.

Hemagglutination Inhibition Assay

Evaluation of Dendrimers.

Hemagglutination assays were performed to evaluate the relative activities of the carbohydrate-coated dendrimers 4–6 with Con A. [42] Control assays with PAMAM and galactose-functionalized dendrimers showed no non-specific dendrimer-lectin association. The relative activity numbers in Table 1 are on a per carbohydrate (glucose + mannose) basis and are relative to methyl mannose. As shown in Figure 14, the relative amounts of glucose and mannose induce a linear change in the relative activity in the hemagglutination assay for all three generations.

Table 1 Hemagglutination assay results.

Compound	# mannose residues[a]	# glucose residues[a]	Relative activity per active sugar[b]
4a	30	0	3820 ± 1650
4b	24	7	2660 ± 0
4c	18	13	2260 ± 780
4d	10	26	1090 ± 380
4e	0	29	260 ± 110
5a	44	0	4830 ± 2090
5b	38	13	3040 ± 0
5c	16	40	1270 ± 440
5d	0	45	310 ± 130
6a	53	0	5350 ± 0
6b	34	35	3510 ± 1220
6c	16	50	2150 ± 0
6d	0	77	470 ± 0

[a]# sugar residues was determined using MALDI-TOF MS data after deacetylation (M_W = 168 g/mol for 4 Ac) and after addition of tethered sugar (M_W = 507 g/mol per tethered sugar). [b]Active sugar = mannose + glucose. Standard deviation values are very large because of serial 2 fold dilutions. For standard deviation = 0, all inhibitory concentrations were equal. All values represent at least three trials.

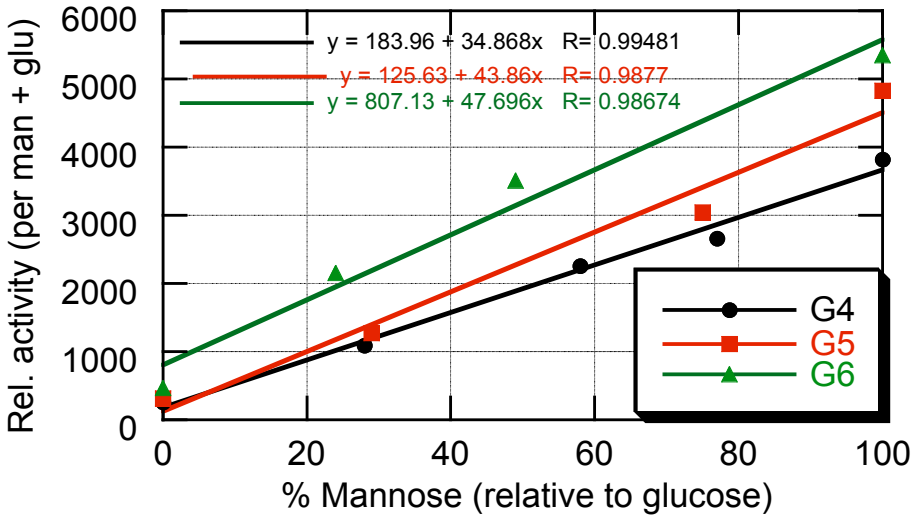

Figure 14 Percent mannose of the glucose/mannose mixture versus relative activity (per glucose + mannose).

The difference in relative activity between glucose-functionalized and mannose-functionalized dendrimers in the G(4) series is 14.7, the difference for G(5) dendrimers is 15.6 and the difference for G(6) dendrimers 11.4. Using equation 1, and assuming a cooperativity constant α of 1, one would predict that exchanging mannose for glucose would cause a 4^2 or 16-fold reduction in binding to Con A, since the dendrimer-Con A association is a divalent interaction. The G(4) and G(5) differences (14.7 and 15.6) are very near 16, while the G(6) value (11.4) is slightly lower. Perhaps the larger size of G(6) allows for a compensatory effect due to increased sugar clustering around the binding sites. [91] Alternatively, the curvature of the G(6) dendrimers may be different enough from G(4) and G(5) to change the shape complementarity between Con A and the dendrimer, which can significantly change the association motif. [92]

Conclusions

The results reported here with two ligands (mannose and glucose) that vary by a factor of 4 in the strength of their monovalent associations to Con A indicate that multivalency can be influenced in predictable–and therefore tunable–ways. Monovalent differences are amplified by multivalent associations, and mixtures of low and high affinity ligands can be used to attenuate multivalent affinities.

In summary, hemagglutination assays with Con A and mannose/glucose-functionalized dendrimers 4–6 indicate that multivalent affinities can be predicted

based on monovalent association constants. The glucose and mannose monomers differ in binding strength only by a factor of 4; multivalent association amplifies this difference. Transposition of the observed relationship between monovalent and multivalent association constants into more complex systems (for example, polyvalent rather than divalent complexes and non-dendritic frameworks) should reasonably follow and is currently being explored. Further evaluation of mannose/glucose dendrimer–Con A complexes using the hemagglutination and precipitation assays is also underway. That multivalent affinity can be attenuated by mixing ligands of varying binding strengths provides an new element of control and predictability to the design of synthetic multivalent molecules for biological applications.

Experimental Procedures

General Methods

General reagents were purchased from Acros and Aldrich Chemical Companies. PAMAM dendrimers were purchased from Dentritech. Concanavalin A (Con A) was purchased from Calbiochem. Methylene Chloride was purified on basic alumina, other solvents were used as received. 32-63μ “40 micron flash” silica gel for flash column chromatography purification was purchased from Scientific Adsorbants Incorperated.

Matrix Assisted Laser Desorption
Ionization MS (MALDI)

MALDI mass spectra were acquired using a Bruker Biflex-III time-of-flight mass spectrometer. Spectra of all functionalized dendrimers were obtained using a *trans*-3-indoleacrylic acid matrix with a matrix-analyte ratio of 3000:1 or 1000:1. Bovine serum albumin (MW 66,431 g/mol),Cytochrome C (MW 12,361 g/mol), and Trypsinogen (MW 23,982 g/mol) were used as external standards. An aliquot corresponding to 12-15 pmol of the analyte was deposited on the laser target. Positive ion mass spectra were acquired in linear mode and the ions were generated by using a nitrogen laser (337 nm) pulsed at 3 Hz with a pulse width of 3 nanoseconds. Ions were accelerated at 19-20,000 volts and amplified using a discrete dynode multiplier. Spectra (100 to 200) were summed into a LeCroy LSA1000 high-speed signal digitizer. All data processing was performed using Bruker XMass/XTOF V 5.0.2. Molecular mass data and polydispersities (PDI) of the broad peaks were calculated by using the Polymer Module included in the software package. The peaks were analyzed using the *continuous* mode.

To determine the number of carbohydrate residues of each type on the dendrimers, both the change in M_W after each sequential addition and after deacylation were used. Starting M_W for the PAMAM dendrimers was 13500 g/mol, 25500 g/mol and 50000g/mol for Generation 4,5 and 6 respectively. To calculate the number of different residues on each dendrimer, the MALDI-TOF MS M_w change upon each addition was divided by the M_w of the isothiocyanate tethered carbohydrate (507g/mol) (#A). The total number of loaded carbohydrate

residues was determined by dividing M_w change upon deacylation by 168 (the loss of 4 acetyl groups per sugar) (#B). The % of each carbohydrate residue was determined by (A/∑A)*B (#C). The values C and A were then averaged. An example, using 4c data: (22900-13500)/507 = 18.5 (A); (34200-13500)/507 = 40.8 (∑A); 18.5/40.8*100 = 45.4%; (34200-27700)/168 = 38.7 (B); 38.7*0.454 = 17.6 (C); (17.6+18.5)/2 = 18.0 (determined # of mannose residues).

NMR

^{1}H NMR spectra were recorded on Bruker DPX 300 (300MHz) and Bruker DPX-500 (500MHz) spectrometers. Chemical shifts are reported in ppm from tetramethylsilane with the residual protic solvent resonance as the internal standard (chloroform: δ 7.25 ppm; dimethyl sulfoxide: δ 2.50 ppm). Data are reported as follows: chemical shift, multiplicity (s = singlet, bs = broad singlet, d = doublet, t = triplet, q = quartet, p = pentet, m = multiplet, app = apparent), integration, coupling constants (in Hz) and assignments. ^{13}C NMR spectra were recorded on a Bruker DPX 500 (125 MHz) spectrometer with complete proton decoupling. Chemical shifts are reported in ppm from tetramethylsilane with the solvent as the internal standard ($CDCl_3$: δ 77.0 ppm)

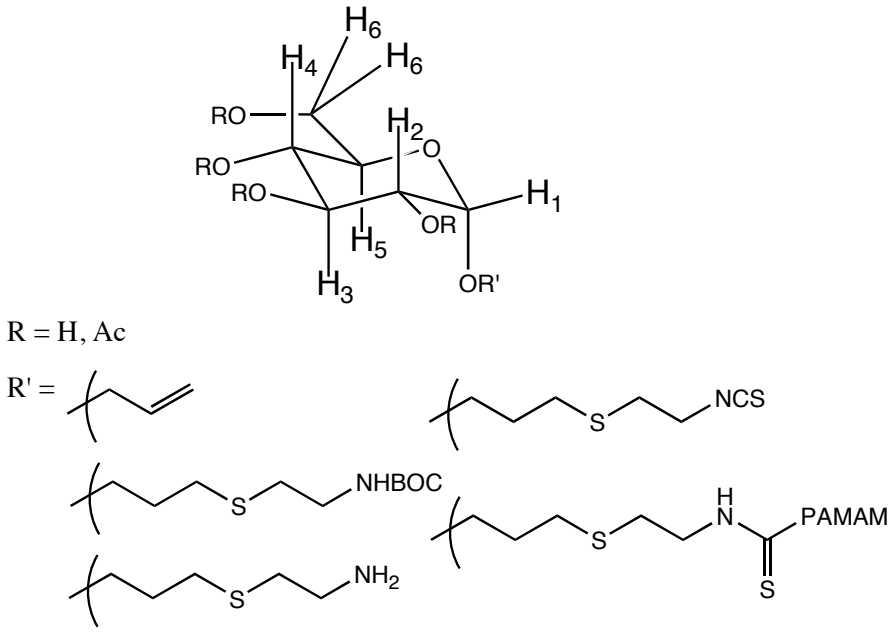

Figure 15 Numbering sequence for carbohydrate NMR data.

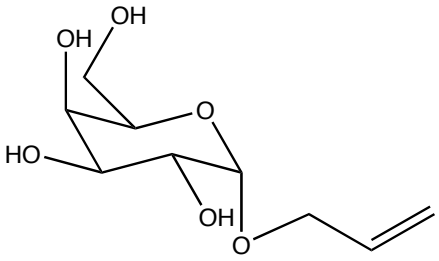

1-O-allyl-α-D-galactopyranoside. 1a. $HCl_{(g)}$ was bubbled through 100 mL of allyl alcohol at 0^{o} C for 20 minutes, then 14.7 g (81.6 mmol) α-D-galactopyranoside was added. The reaction was warmed to room temperature and let stir for 3 hours, or until the solution became clear. Solvent was removed *in vacuo* to afford 12.5 g of crude material, which was used without further purification. 1H NMR (300 MHz, D_2O) δ 5.98 (ddd, 1H, J = 17.1, 10.3, 6 Hz, OCH_2CH=CH_2), 5.26 (dd, 1H, J = 17.1, 1.4 Hz, OCH_2CH=CH_2), 5.13 (d, 1H, J = 10.3 Hz, OCH_2CH=CH_2),

4.78 (d, 1H, J = 3.0 Hz, *H1*), 4.72 (s, 1H), 4.11 (dd, 1H, J = 13.0, 6.2 Hz, OC*H*$_2$CH=CH$_2$), 3.97 (dd, 1H, J = 13.0, 6.2 Hz, OC*H*$_2$CH=CH$_2$), 3.60-3.82 (m, 5H, *H2, H3, H4, H5, H6*) ppm. As reported.[89]

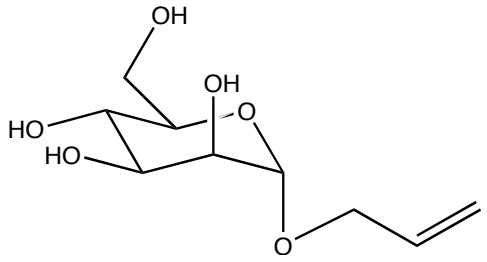

1-O-allyl-α-D-mannopyranoside. 1b. $HCl_{(g)}$ was bubbled through 300 mL of allyl alcohol at 0^{o}C for 20 minutes, then 14.7 g (81.6 mmol) α-D-mannopyranoside was added. The reaction was warmed to room temperature and was stirred for 3 hours. Solvent was removed *in vacuo* to afford 13.4 g of crude material which was used without further purification. 1H NMR (300 MHz, D_2O) δ 5.88 (app ddd 1H, J = 17.0, 10.1, 6.3 Hz, OCH_2CH=CH_2), 5.23 (dd, 1H, J = 17.0, 1.0 Hz, OCH_2CH=C*H*$_2$), 5.14 (app d, 1H, J = 10.1, OCH_2CH=C*H*$_2$), 4.78 (d, 1H, J= 1.5 Hz, *H*^{1}), 4.12 (dd, 1H, J = 13.1, 6.3 Hz OC*H*$_2$CH=CH$_2$), 3.96 (dd, 1H, J = 13.1, 6.3 Hz, OC*H*$_2$CH=CH$_2$), 3.51-3.82 (m, 5H) ppm. As reported.[89]

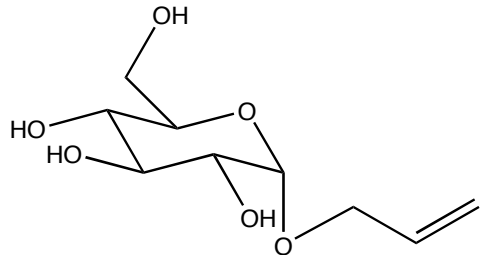

1-O-allyl-α-D-glucopyranoside. 1c. $HCl_{(g)}$ was bubbled through 100 mL of allyl alcohol at 0^o C for 20 minutes, then 14.7 g (81.6 mmol) α-D-glucopyranoside was added. The reaction was warmed to room temperature and let stir for 3 hours.

Solvent was removed *in vacuo* and the product taken on without purification. 1H NMR (250 MHz, D_2O) δ 5.85 (app ddd, 1H, J = 17.3, 10.4, 6.1 Hz, $OCH_2CH{=}CH_2$), 5.26 (app d, 1H, J = 17.3 Hz, $OCH_2CH{=}CH_2$), 5.15 (app d, 1H, J = 10.4 Hz, $OCH_2CH{=}CH_2$), 4.85 (d, 1H, J = 2.7 Hz, *H1*), 4.11 (dd, 1H, J = 12.8, 5.3 Hz, $OCH_2CH{=}CH_2$), 3.96 (dd, 1H, J = 12.8, 6.1Hz, $OCH_2CH{=}CH_2$), 3.30-3.68 (m, 5H, *H2, H3, H4, H5, H6*) ppm. As reported.[89]

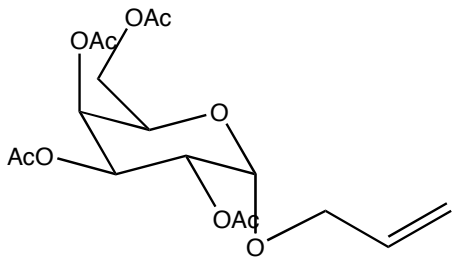

2,3,4,6-tetra-O-acetyl-1-O-allyl-α-D-galactopyranoside. 2a. 1a (6.8 g, 30 mmol) and acetic anhydride (16.2 g, 135 mmol) were combined in pyridine (200 mL) and cooled to 0^{o} C. Catalytic DMAP (0.5 g, 4.1 mol) was then added and the solution was stirred for 4 hrs and warmed to room temperature. The reaction was added to cold water (100 mL) and extracted with ethyl acetate (3 x 50 mL). The organic layer was then washed with 1N HCl solution (2 x 50 mL), brine (50 mL), and dried over magnesium sulfate. The solvent was then removed en vacuo leaving a yellowish oily liquid, a 7 g portion of which was purified by silica gel column chromatography (1:1 hexane:ethyl acetate)to yield 6.1 g (15.7 mmol). 1H NMR (300 MHz, CDCl3) δ 5.84 (app ddd, 1H, J = 17.0, 10.2, 6.3 Hz, $OCH_2CH{=}CH_2$), 5.45 (d, 1H, J = 3.0 Hz, *H4*), 5.38 (m, 1H, *H3*), 5.30 (dd, 1H, J = 10.2, 1.5 Hz, $OCH_2CH{=}CH_2$), 5.22 (d, 1H, J = 17.0 Hz, $OCH_2CH{=}CH_2$), 5.13 (m,

2H, *H2, H1*), 4.22 (app t, 1H. J = 6.2 Hz, *H5*), 4.18 (dd, 1H, J = 13.0, 6.3 Hz OC*H*$_2$CH=CH$_2$), 4.10 (d, 2H, J = 6.2 Hz, *H6*), 4.05 (dd, 1H, J = 13.0, 6.3 Hz OC*H*$_2$CH=CH$_2$), 2.16 (s, 3H), 2.14 (s, 3H), 2.13 (s, 3H), 2.11 (s, 3H) ppm. As reported.[89]

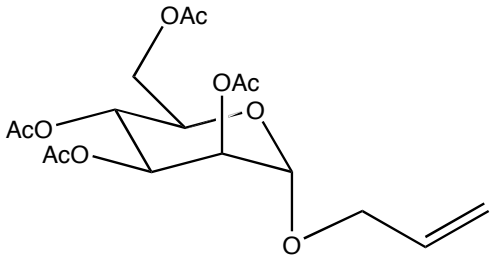

2,3,4,6-tetra-O-acetyl-1-O-allyl-α-D-mannopyranoside. 2b. 1b (12.2 g, 55.2 mmol) and acetic anhydride (32.4 g, 315.9 mmol) were combined in pyridine (300 mL) and cooled to 0 ^{o}C. Catalytic DMAP (0.1 g, 0.8 mmol) was then added and the solution was stirred for 4 hrs and warmed to room temperature. The reaction was added to cold water (300 mL) and extracted with ethyl acetate (3 x 50 mL). The organic layer was then washed with 1N HCl solution (2 x 50 mL), brine (1 x 50 mL), and dried over magnesium sulfate. The solvent was then removed *in vacuo* leaving a yellowish oily liquid. A 7.0 g portion of this was then purified by silica gel column chromatography (1:1 hexane:ethyl acetate) to yield 6.24 g (16.1 mmol) of pure product. 1H NMR (300 MHz, CDCl3) δ 5.87 (app ddd, 1H, J = 17.1, 10.3, 6.2 Hz, OCH$_2$C*H*=CH$_2$), 5.38 (dd, 1H, J = 10.3, 3.0 Hz, OCH$_2$CH=C*H*$_2$), 5.13-5.31 (m, 5H, *H2*, *H3*, *H4*, OCH$_2$CH=C*H*$_2$) 4.86 (d, 1H, J= 1.5 Hz, *H1*), 4.29 (dd, 1H, J = 11.9, 5.4 Hz, *H6a*), 4.19 (dd, 1H, J = 13.2, 6.2 Hz, OC*H*$_2$CH=CH$_2$), 4.10 (dd, 1H, J = 11.9, 2.0 Hz, *H6b*), 4.01 (m, 2H, *H5*,

OC*H*$_2$CH=CH$_2$), 2.16 (s, 3H), 2.14 (s, 3H), 2.13 (s, 3H), 2.11 (s, 3H) ppm. As reported.[89]

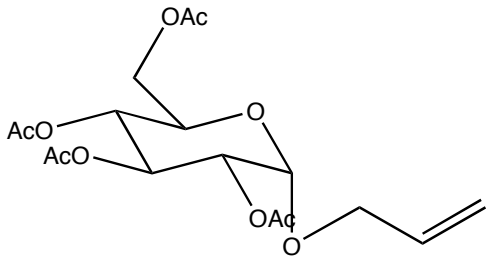

2,3,4,6-tetra-O-acetyl-1-O-allyl-α-D-glucopyranoside. 2c. 1c (12.2 g, 55.2 mmol) and acetic anhydride (32.4 g, 315.9 mmol) were combined in pyridine (300 mL) and cooled to 0^{o} C. Catalytic DMAP (0.1 g, 0.8 mmol) was then added and the solution was stirred for 4 hrs and warmed to room temperature. The reaction was added to cold water (300 mL) and extracted with ethyl acetate (3 x 50 mL). The organic layer was washed with 1N HCl solution (2 x 50 mL), brine (1 x 50 mL), and dried over magnesium sulfate. The solvent was then removed *in vacuo* leaving a yellowish oily liquid. A 7.0 g portion of this was then purified by silica gel column chromatography (1:1 hexane:ethyl acetate) to yield 6.24 g (16.1 mmol) of pure product. 1H NMR (500 MHz, CDCl3) δ 5.84 (ddd, 1H, J = 16.9, 10.8, 5.7 Hz, OCH$_2$C*H*=CH$_2$), 5.47 (ap t, 1H, J = 9.9 Hz, *H3*), 5.27 (dd, 1H, J = 16.9, 1.4 Hz, OCH$_2$CH=*CH$_2$*), 5.22 (dd, 1H, J = 10.8, 0.9 Hz, OCH$_2$CH=C*H$_2$*), 5.07 (d, 1H, J = 3.7 Hz, *H1*), 5.03 (ap t, 1H, J = 9.9 Hz, *H4*), 4.85 (dd, 1H, J = 9.9, 3.7 Hz, *H2*), 4.22 (dd, 1H. J = 12.8, 5.7 Hz, OC*H$_2$*CH=CH$_2$), 4.15 (dd, 1H, J = 12.8, 5.7 Hz OC*H$_2$*CH=CH$_2$), 4.05 (dd, 1H, J = 12.3, 2.3 Hz, *H6a*), 4.00 (m, 2H, *H5*, *H6b*), 2.16 (s, 3H), 2.14 (s, 3H), 2.13 (s, 3H), 2.11 (s, 3H) ppm. 13C NMR

(500 MHz, CDCl3) δ 170.56, 170.05, 170.00, 169.53, 133.07, 118.08, 94.85, 70.73, 70.15, 68.78, 68.57, 67.34, 61.87, 20.65, 20.62 (2), 20.55 ppm. As reported.[89]

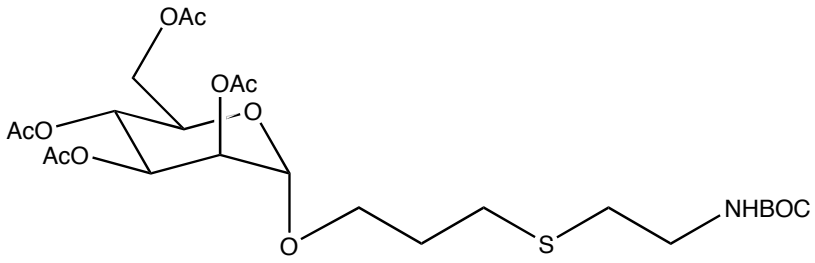

1-O-(6-t-Butylcarbamate-4-thiohexyl)- 2,3,4,6-tetra-O-acetyl-α-D-mannopyranoside. (1a) A solution of 4.80 g (12.4 mmol) 2,3,4,6-tetra-O-acetyl-1-O-allyl-α-D-mannopyranoside, 10.21 g (57.6 mmol) 2-t-Butylcarbamate-ethanethiol and 1.0 mL (0.5 g, 1.9 mmol) 1,1 Di(tert-butylperoxy)cyclohexane (50% w/v solution in mineral oil) in 100 mL of toluene was degassed with Argon and refluxed for 4 hrs. The solution was cooled and the solvent removed *in vacuo*. The remaining oily residue was then purified by silica gel column chromatography (1:1 hexanes:ethyl acetate) to give 4.41 g (7.81 mmol) of a yellow oil in 65% yield. ^{1}H NMR (300 MHz, $CDCl_3$) δ 5.21-5.30 (m, 3H, *H2*, *H3*, *H4*), 4.94 (bs, 1H, $CH_2NHCOOtBu$), 4.80 (s, 1H, *H1*), 4.28 (dd, 1H, J = 12.1, 5.2Hz, *H6a*), 4.11 (m, 1H, *H6b*), 3.98 (m, 1H, *H5*), 3.81 (dt, J = 9.5, 6.1 Hz, 1H, $OCH_2CH_2CH_2S$), 3.53 (dt, J = 9.5, 6.1 Hz, 1H, $OCH_2CH_2CH_2S$), 3.30 (m, 2H, $CH_2NHCOOtBu$), 2.63 (app q, J = 12.3, 6.1 Hz, 4H, $CH_2CH_2SCH_2CH_2$), 2.13 (s, 3H), 2.11 (s, 3H), 2.10 (s, 3H), 2.07 (s, 3H), 1.88 (m, 2H, $OCH_2CH_2CH_2SCH_2$), 1.45 (s, 9H) ppm. ^{13}C NMR (125 MHz, $CDCl_3$) δ 170.46, 169.90, 169.74, 169.58,

155.70, 97.49, 79.19, 69.52, 69.01, 68.53, 66.37, 66.14, 62.43, 39.77, 32.13, 29.00, 28.29, 28.22, 20.88, 20.73, 20.61, 20.55 ppm. HRMS (electrospray) *m/z* 588.2105 (M+Na, calc. 588.2091 for $C_{24}H_{39}NO_{12}SNa$)

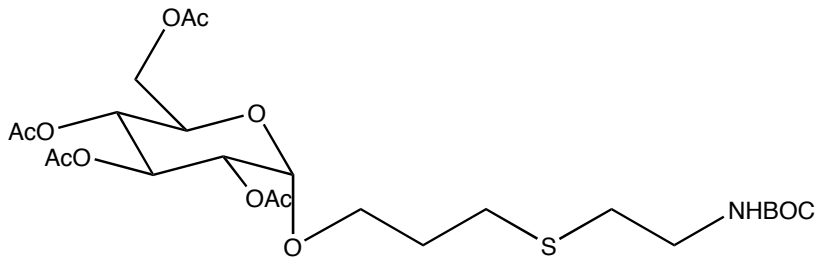

1-O-(6-t-Butylcarbamate-4-thiohexyl)- 2,3,4,6-tetra-O-acetyl-α-D-glucopyranoside. (1b) A solution of 0.4 g (1.0 mmol) 2,3,4,6-tetra-O-acetyl-1-O-allyl-α-D-glucopyranoside, 1.5 g (8.4 mmol) 2-t-Butylcarbamate-ethanethiol and 0.2 mL (0.1 g, 0.38 mmol) 1,1 Di(tert-butylperoxy)cyclohexane (50% w/v solution in mineral oil) in 20 mL of toluene was degassed with Argon and refluxed for 4 hrs. The solution was cooled and the solvent removed *in vacuo*. The remaining oily residue was then purified by silica gel column chromatography (1:1 hexanes:ethyl acetate) to give 0.42 g (0.74 mmol) of a yellow oil in 74% yield. ^{1}H NMR (500 MHz, $CDCl_3$) δ 5.39 (app t, 1H, J = 10.1 Hz, *H3*), 4.98 (m, 3H, *H4, H1,* $CH_2NHCOOtBu$), 4.80 (dd, 1H, J = 10.1, 3.7 Hz, *H2*), 4.19 (dd, 1H, J = 12.3, 3.9 Hz, *H6a*), 4.03 (dd, 1H, J = 12.3, 2.2 Hz, *H6b*), 3.95 (ddd, 1H, J = 2.2, 3.9, 10.2 Hz, *H5*), 3.74 (dt, 1H, J = 9.9, 6.1 Hz $OCH_2CH_2CH_2S$), 3.45 (dt, 1H, J = 9.9, 6.1 Hz, $OCH_2CH_2CH_2S$), 3.24 (m, 2H, $CH_2NHCOOtBu$), 2.57 (m, 4H, $CH_2CH_2SCH_2CH_2$), 2.03 (s, 3H), 2.00 (s, 3H), 1.96 (s, 3H), 1.94 (s, 3H), 1.83 (app p, 2H, J = 6.5 Hz, $OCH_2CH_2CH_2SCH_2$), 1.37 (s, 9H) ppm. ^{13}C NMR (125

MHz, $CDCl_3$) δ 170.53, 170.02 (2), 169.49, 155.72, 95.77, 79.33, 70.78, 70.13, 68.58, 67.28, 66.57, 61.89, 39.77, 32.08, 29.01, 28.32, 28.09, 20.64, 20.59, 20.52 ppm. HRMS (electrospray) *m/z* 588.2091 (M+Na, calc. 588.2091 for $C_{24}H_{39}NO_{12}SNa$).

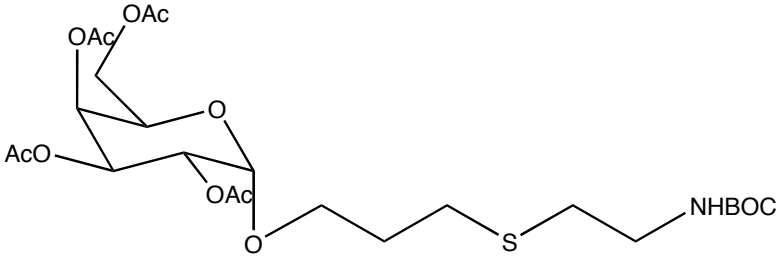

1-O-(6-t-Butylcarbamate-4-thiohexyl)- 2,3,4,6-tetra-O-acetyl-α-D-galactopyranoside. (1c) A solution of 3.90 g (10.1 mmol) 2,3,4,6-tetra-O-acetyl-1-O-allyl-α-D-galactopyranoside, 11.9 g (67.2 mmol) 2-t-Butylcarbamate-ethanethiol and 1.0 mL (0.5 g, 1.9 mmol) 1,1 Di(tert-butylperoxy)cyclohexane (50% w/v solution in mineral oil) in 100 mL of toluene was degassed with Argon and refluxed for 4 hrs. The solution was cooled and the solvent removed *in vacuo*. The remaining oily residue was then purified by silica gel column chromatography (1:1 hexanes:ethyl acetate) to give 4.3 g (7.61 mmol) of a yellow oil in 76% yield. ^{1}H NMR (300 MHz, $CDCl_3$) δ 5.44 (app d, 1H, J = 3.0 Hz, *H4*), 5.31 (dd, 1H, J = 3.0, 9.6 Hz, *H3*), 5.10 (m, 2H, *H1, H2*), 4.91 (bs, 1H, $CH_2NHCOOtBu$), 4.20 (ap t, 1H, J = 6.5 Hz, *H5*), 4.08 (d, 2H, J = 6.5 Hz, *H6*), 3.76 (dt, J = 6.0, 12.0 Hz, 1H, $OCH_2CH_2CH_2S$), 3.50 (dt, J = 6.0, 12.0 Hz, 1H, $OCH_2CH_2CH_2S$), 3.29 (m, 2H, $CH_2NHCOOtBu$), 2.60 (app q, J = 6.3, 12.3 Hz, 4H, $CH_2CH_2SCH_2CH_2$), 2.13 (s, 3H), 2.11 (s, 3H), 2.10 (s, 3H), 2.07 (s, 3H), 1.88

(app p, J = 6.6 Hz, 2H, $OCH_2CH_2CH_2SCH_2$), 1.45 (s, 9H) ppm. ^{13}C NMR (125 MHz, $CDCl_3$) δ 170.60, 170.54, 170.38, 170.19, 155.95, 96.52, 79.64, 68.42, 68.32, 67.83, 66.94, 66.58, 61.95, 40.01, 32.43, 29.36, 28.60, 28.46, 20.96, 20.90, 20.84, 20.82 ppm. HRMS (electrospray) *m/z* 588.2094 (M+Na, calc. 588.2091 for $C_{24}H_{39}NO_{12}SNa$).

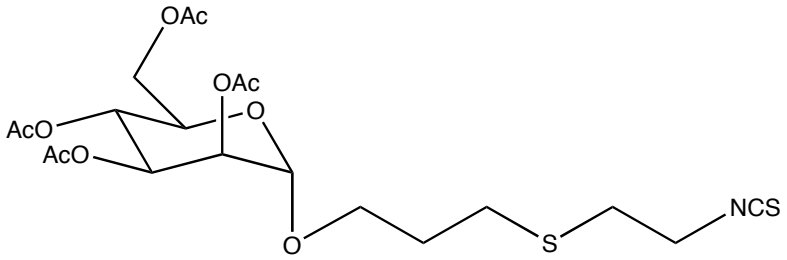

1-O-(6-isothiocyanato-4-thiohexyl)- 2,3,4,6-tetra-O-acetyl -α-D-mannopyranoside. (2a) 1.1 g (9.6 mmol) of trifluoroacetic acid was added to a solution of 1.0 g (1.8 mmol) of 1a in 10 mL of methylene chloride at 0^o C and let stir for 12 hrs. Solvent was removed *in vacuo* and 10 mL water added to the residue. The pH of the solution was then adjusted to ~12 with a solution of K_2CO_3 (sat.) and extracted with methylene chloride (3 x 10 mL). The organic layers where combined and washed with brine (10 mL) and dried with sodium sulfate. The extract was filtered and the solvent removed. The resulting oily material was then dissolved in dry methylene chloride (10 mL) with 0.45 g (4.5 mmol) of triethylamine. This was then added via syringe pump to a solution of 0.2 mL (0.3 g, 2.6 mmol) thiophosgene in 30 mL of dry methylene chloride at 0^o C over 1 hr and let stir for a further 2 hr. Water (30 mL) was added and extraction performed with methylene chloride (3 x 20 mL), the organic layers were then combined and dried over sodium sulfate. The extract was filtered and solvent removed *in vacuo*

to yield a reddish oily material. The product was purified via column chromatography on silica gel (2:1 ethyl acetate:hexanes) leaving 0.50 g (0.99 mmol) of a yellowish oil in a 55% yield. ^{1}H NMR (300 MHz, $CDCl_3$) δ 5.21-5.30 (m, 1H, *H2*, *H3*, *H4*), 4.80 (s, 1H, *H1*), 4.28 (dd, 1H, J = 12.3, 6.9Hz, *H6a*), 4.11 (app d, 1H, J = 12.3Hz, *H6b*), 3.98 (m, 1H, *H5*), 3.81 (dt, J = 6.1, 10.0 Hz, 1H, $OCH_2CH_2CH_2S$), 3.69 (t, 2H, J = 6.8 Hz, SCH_2CH_2NCS), 3.53 (dt, 1H, J = 6.1, 10.0 Hz, $OCH_2CH_2CH_2S$), 2.81 (t, 2H, J = 6.8 Hz, SCH_2CH_2NCS), 2.66 (t, 2H, J = 7.0 Hz, $OCH_2CH_2CH_2S$), 2.13 (s, 3H), 2.11 (s, 3H), 2.10 (s, 3H), 2.07 (s, 3H), 1.88 (m, 2H, $OCH_2CH_2CH_2SCH_2$) ppm. ^{13}C NMR (125 MHz, $CDCl_3$) δ 170.49, 169.95, 169.81, 169.61, 132.39, 97.53, 69.49, 69.01, 68.59, 66.25, 66.11, 62.45, 45.17, 32.25, 29.05, 28.88, 20.79, 20.69, 20.63, 20.60 ppm. HRMS (electrospray) *m/z* 530.1112 (M+Na, calc. 530.1131 for $C_{20}H_{29}NO_{10}S_2Na$).

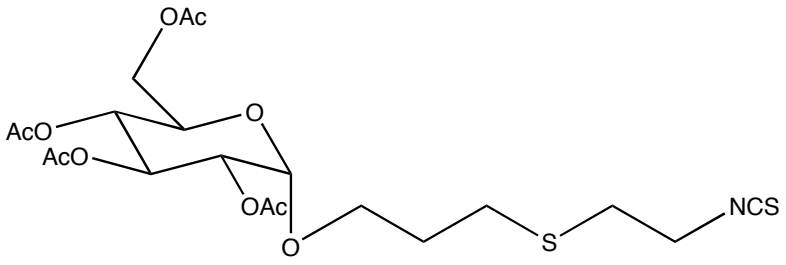

1-O-(6-isothiocyanato-4-thiohexyl)- 2,3,4,6-tetra-O-acetyl -α-D-glucopyranoside. (2b) 0.5 g (4 mmol) of trifluoroacetic acid was added to a solution of 0.42 g (0.74 mmol) of 1b in 5 mL of methylene chloride at 0^{o} C and let stir for 12 hrs. Solvent was removed *in vacuo* and 5 mL water added to the residue. The pH of the solution was then adjusted to ~12 with a solution of K_2CO_3 (sat.) and extracted with methylene chloride (3 x 10 mL). The organic layers where combined and

washed with brine (10 mL) and dried with sodium sulfate. The extract was filtered and the solvent removed *in vacuo*. The resulting oily material was then dissolved in dry methylene chloride (10 mL) with 0.2 g (2 mmol) of triethylamine. This was then added via syringe pump to a solution of 0.13 g (1 mmol) thiophosgene in 10 mL of dry methylene chloride at 0^{o} C over 1 hr. this was then let stir for 2 hr. Water (10 mL) was added and extracted with methylene chloride (3 x 10 mL), the organic layers were then combined and dried over sodium sulfate. The extract was filtered and solvent removed *in vacuo* to yield a reddish oily material. The product was purified via column chromatography on silica gel (2:1 ethyl acetate:hexanes) leaving 0.3 g (0.59 mmol) of a yellowish oil in an 80% yield. ^{1}H NMR (500 MHz, $CDCl_3$) δ 5.41 (app t, 1H, J = 10.0 Hz, *H3*), 5.01 (m, 2H, *H4, H1*), 4.82 (dd, 1H, J = 10.0, 3.7 Hz, *H2*), 4.21 (dd, 1H, J = 12.3, 4.5 Hz, *H6a*), 4.05 (dd, 1H, J = 12.3, 2.2 Hz, *H6b*), 3.95 (ddd, 1H, J = 10.2, 4.5, 2.2 Hz, *H5*), 3.77 (dt, 1H, J = 9.9, 6.0 Hz $OCH_2CH_2CH_2S$), 3.66 (t, 2H, J = 6.7 Hz, CH_2NCS), 3.48 (dt, 1H, J = 9.9, 6.0 Hz, $OCH_2CH_2CH_2S$), 2.78 (t, 2H, J = 6.7 Hz, SCH_2CH_2NCS), 2.65 (t, 2H, J = 7.0 Hz, CH_2CH_2S), 2.05 (s, 3H), 2.02 (s, 3H), 1.99 (s, 3H), 1.97 (s, 3H), 1.87 (app p, 2H, J = 6.5 Hz, $OCH_2CH_2CH_2SCH_2$), 1.37 (s, 9H) ppm. ^{13}C NMR (125 MHz, $CDCl_3$) δ 170.75, 170.27, 170.22, 169.71, 132.85, 96.02, 70.99, 70.28, 68.78, 67.81, 67.55, 66.64, 62.11, 45.79, 45.40, 32.39, 29.83, 29.30, 28.98, 20.89, 20.84, 20.77 ppm. HRMS (electrospray) *m/z* 530.1138 (M+Na, calc. 530.1131 for $C_{20}H_{29}NO_{10}S_2Na$).

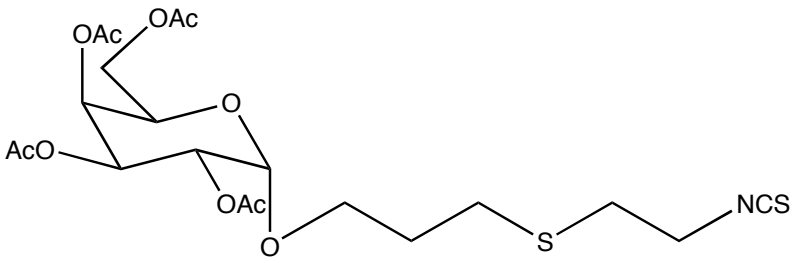

1-O-(6-isothiocyanato-4-thiohexyl)- 2,3,4,6-tetra-O-acetyl -α-D-galactopyranoside. (2c) 0.5 g (4 mmol) of trifluoroacetic acid was added to a solution of 0.42 g (0.74 mmol) of 1c in 10 mL of methylene chloride at 0^{o}C and let stir for 12 hrs. Solvent was removed *in vacuo* and 10 mL water added to the residue. The pH of the solution was then adjusted to ~12 with a solution of K_2CO_3 (sat.) and extracted with methylene chloride (3 x 10 mL). The organic layers where combined and washed with brine (10 mL) and dried with sodium sulfate. The extract was filtered and the solvent removed *in vacuo*. The resulting oily material was then dissolved in dry methylene chloride (10 mL) with 0.18 g (2 mmol) of triethylamine. This was then added via syringe pump to a solution of 0.12 g (1 mmol) thiophosgene in 20 mL of dry methylene chloride at 0^{o} C over 1 hr. The reaction was then let stir for 2hr. Water (30 mL) was added and extracted with methylene chloride (3 x 20mL), the organic layers were then combined and dried over sodium sulfate. The extract was filtered and solvent removed *in vacuo* to yield a reddish oily material. The product was purified via column chromatography on silica gel (2:1 ethyl acetate:hexanes) leaving 0.28 g (0.55 mmol) of a yellowish oil in a 75% yield. ^{1}H NMR (300 MHz, $CDCl_3$) δ 5.43 (d, 1H, J = 2.3 Hz, *H4*), 5.31 (dd, 1H, J = 10.1, 2.3 Hz, *H3*), 5.11 (m, 2H, *H1, H2*), 4.21 (t, 1H, J = 6.4 Hz, *H5*), 4.10 (m, 2H, *H6*), 3.79 (m, 1H, OC*H*$_2$CH$_2$CH$_2$S), 3.70 (t, 2H,

J = 6.8 Hz, SCH_2CH_2NCS), 3.52 (m, 1H $OCH_2CH_2CH_2S$), 2.80 (t, 2H, J = 6.8 Hz, SCH_2CH_2NCS), 2.66 (t, 2H, J = 6.7 Hz, $OCH_2CH_2CH_2S$), 2.11 (s, 3H), 2.06 (s, 3H), 2.03 (s, 3H), 1.98 (s, 3H), 1.88 (m, 2H, $OCH_2CH_2CH_2SCH_2$) ppm. ^{13}C NMR (125 MHz, $CDCl_3$) δ 170.47, 170.39, 170.27, 170.09, 132.71, 96.44, 68.27, 68.17, 67.67, 66.70, 66.48, 61.82, 45.36, 32.34, 29.33, 29.02, 20.89, 20.81, 20.74, 20.71 ppm. HRMS (electrospray) *m/z* 530.1130 (M+Na, calc. 530.1131 for $C_{20}H_{29}NO_{10}S_2Na$).

Representative procedure for the synthesis of heterogeneously functionalized PAMAM-based thiourea-linked 1-O-(6-thiourea-4-thiohexyl)- 2,3,4,6-tetra-O-acetyl -α-D-galactopyranoside, 1-O-(6- thiourea-4-thiohexyl)- 2,3,4,6-tetra-O-acetyl -α-D-glucopyranoside, 1-O-(6- thiourea-4-thiohexyl)- 2,3,4,6-tetra-O-acetyl -α-D-mannopyranoside. (4-6) An aqueous solution of amine terminated Starburst G(4)-PAMAM dendrimer (2.478 g of a 17% w/w solution in water, 421.2 mg, 31.2 μmol) was lyophilized to leave a foamy residue. 7.02 mL of DMSO was then added to this residue to give a 60 mg/mL solution. 0.047 mL of a 300 mM solution of 1-O-(6-isothiocyanato-4-thiohexyl)- 2,3,4,6-tetra-O-acetyl -α-D-mannopyranoside (2a, 14.1 μmol, 6.84 mg) in DMSO was added to 0.5 mL of a 60 mg/mL G(4) PAMAM dendrimer (30 mg, 4.40 μmol) solution. The reaction was stirred for 48 hrs at which point a 75 μL aliquot was removed for MALDI-TOF analysis. After MALI-TOF analysis indicated reaction completion 0.17 mL of a 300 mM solution of 1-O-(6-isothiocyanato-4-thiohexyl)- 2,3,4,6-tetra-O-acetyl -α-

D-glucopyranoside (2b, 49.4 μmol, 25.1 mg) was added. The solution was then stirred for 48 hrs. At this time a 75 μL aliquot was removed for analysis. After MALDI-TOF analysis indicated reaction completion, 0.19 mL of a 300 mM solution of 1-O-(6-isothiocyanato-4-thiohexyl)- 2,3,4,6-tetra-O-acetyl -α-D-galactopyranoside (2c, 56.9 μmol, 28.8 mg) was added and let stir for 48 hrs, when a 75 μL aliquot was removed for analysis. According to MALDI-TOF analysis the addition of 2c did not go to completion, so an additional spacer was added. 47.1 mg (30 μmol) of isothiocyanto-ethoxyethanol 3 in DMSO was added an let stir at room temperature for 2 days. Again MALDI-TOF analysis indicated no further addition. This step was repeated with mild warming (up to 40 ºC) and vigorous stirring. MALDI-TOF analysis again indicated no further addition, hence the product was taken forward.

Table 2 Amounts of compounds that were used for the experimental procedure above.

Compound #	PAMAM (μmol)	Mannose (μmol)	Glucose (μmol)	Galactose (μmol)	Ethoxy ethanol (μmol)
4a	2.2	71.1	0	57.0	30.0
4b	2.2	56.9	12.6	57.0	30.0
4c	2.2	35.6	32.4	57.0	30.0
4d	2.2	14.2	51.0	57.0	30.0
4e	1.5	0	47.3	49.3	30.0
5a	1.2	58.8	0	45.0	30.0
5b	1.2	47.1	10.5	45.0	30.0
5c	1.2	11.8	42.6	45.0	30.0
5d	0.7	0	39.5	49.3	30.0
6a	0.6	50.2	0	42.0	30.0
6b	0.6	25.1	22.5	42.0	30.0
6c	0.6	10.0	36.3	42.0	30.0
6d	0.4	0	33.5	49.3	30.0

4a: ^{1}H NMR (500 MHz, d_6-DMSO) δ 7.97 (bs, 1H, amide NH's), 7.90 (bs, 0.4H, amide NH's), 7.83 (bs, 0.5H, amide NH's), 7.77 (bs, 0.8H, amide NH's), 7.51 (bs, 1.8H, $CH_2NHC(S)NHCH_2$) 5.32(m, 0.7H), 5.17 (m, 0.8H), 5.07 (m, 1.6H), 5.02 (m, 0.8H), 4.92 (m, 1H), 4.84 (m, 0.5H), 4.21 (m, 0.7H), 4.10 (m, 0.9H), 4.00 (m, 2.3H), 3.90 (m, 0.7), 3.80 (t, 0.8H, J = 6.5 Hz), 3.68 (m, 1.8H), 3.50 (m, 3.2H), 3.14 (bs, 2.5H), 3.04 (bs, 3.9H), 2.81 (t, 0.5H J = 6.5 Hz), 2.56-2.64 (m, 11.4H), 2.17 (bs, 4.8H), 2.08 (s, 3.2H), 2.07 (s, 3H), 2.00 (m, 9H), 1.90 (s, 3.5H) 1.79 (m, 3.5H) ppm. MALDI-TOF (pos) m/z 34400.

4b: ^{1}H NMR (500 MHz, d_6-DMSO) δ 7.97 (bs, 1H, amide NH's), 7.90 (bs, 0.5H, amide NH's), 7.83 (bs, 0.5H, amide NH's), 7.77 (bs, 0.8H, amide NH's), 7.51 (bs, 1.8H, $CH_2NHC(S)NHCH_2$) 5.32(m, 0.8H), 5.17 (m, 0.8H), 5.07 (m, 1.1H), 5.02 (m, 0.8H), 4.99 (m, 0.17H), 4.93 (m, 0.9H), 4.84 (m, 0.5H), 4.21 (m, 0.8H), 4.10 (m, 0.8H), 4.00 (m, 2.4H), 3.80 (t, 1.1H, J = 6.5 Hz), 3.68 (m, 1.6H), 3.50 (m, 3.8H), 3.14 (bs, 2.5H), 3.04 (bs, 3.9H), 2.81 (t, 1H J = 6.5 Hz), 2.56-2.64 (m, 13H), 2.17 (bs, 5H), 2.08 (s, 4H), 2.07 (s, 2H), 2.00 (s, 3.5H), 1.99 (s, 3H) 1.98 (s, 3H), 1.97 (s, 3H), 1.90 (s, 3.5H) 1.79 (m, 4H) ppm. MALDI-TOF (pos) m/z 33800.

4c: ^{1}H NMR (500 MHz, d_6-DMSO) δ 7.97 (bs, 1H, amide NH's), 7.83 (bs, 1H, amide NH's), 7.77 (bs, 1H, amide NH's), 7.51 (bs, 1.8H, $CH_2NHC(S)NHCH_2$) 5.32(m, 0.8H), 5.25 (m, 0.5H), 5.17 (m, 0.8H), 5.07 (m, 0.5H), 5.02 (m, 0.8H),

4.99 (m, 0.5H), 4.92 (m, 1.3H), 4.84 (m, 0.3H), 4.75 (m, 0.7H), 4.21 (m, 0.8H), 4.09 (m, 0.8H), 4.00 (m, 2.6H), 3.80 (t, 1.1H, J = 6.5 Hz), 3.68 (m, 2H), 3.50 (m, 4H), 3.13 (bs, 2.5H), 3.04 (bs, 4.7H), 2.81 (t, 1H, J = 6.5 Hz), 2.56-2.64 (m, 17H), 2.17 (bs, 6.5H), 2.08 (s, 3.7H), 2.00 (s, 3H), 1.99 (s, 2H), 1.98 (s, 3H), 1.97 (s, 3H) 1.96 (s, 2H), 1.90 (s, 3H) 1.79 (m, 4.7H) ppm. MALDI-TOF (pos) m/z 34200.

4d: ^{1}H NMR (500 MHz, d_6-DMSO) δ 7.97 (bs, 1H, amide NH's), 7.78 (bs, 0.8H, amide NH's), 7.51 (bs, 2H, $CH_2N\mathit{H}C(S)N\mathit{H}CH_2$) 5.32(m, 0.9H), 5.26 (m, 1H), 5.17 (m, 1H), 5.02 (m, 0.8H), 4.99 (m, 0.8H) 4.92 (m, 1.6H), 4.76 (m, 1H), 4.21 (m, 1.1H), 4.10 (m, 1H), 4.00 (m, 2.9H), 3.95 (m, 1H), 3.81 (t, 1.6H, J = 6.5 Hz), 3.68 (m, 2.4H), 3.48 (m, 4.2H), 3.13 (bs, 3.2H), 3.04 (bs, 3.7H), 2.81 (t, 2.2H, J = 6.5 Hz), 2.56-2.65 (m, 10H), 2.17 (bs, 4.7H), 2.08 (s, 3H), 2.00 (s, 3H), 1.99 (s, 1H), 1.98 (s, 3H), 1.97 (s, 3H), 1.95 (s, 2H), 1.92 (s, 2H) 1.90 (s, 3H), 1.80 (m, 4.4H) ppm. MALDI-TOF (pos) m/z 36100.

4e: ^{1}H NMR (500 MHz, d_6-DMSO) δ 7.97 (bs, 1H, amide NH's), 7.90 (bs, 0.3H, amide NH's), 7.83 (bs, 0.3H, amide NH's), 7.77 (bs, 1H, amide NH's), 7.51 (bs, 1.9H, $CH_2N\mathit{H}C(S)N\mathit{H}CH_2$), 5.32 (s, 0.5H), 5.25 (m, 0.6H), 5.14 (m, 1H), 5.02 (m, 1H), 4.92 (m, 1H), 4.77 (m, 0.7H), 4.10-4.21 (m, 1.5H), 4.00 (m, 2.2H), 3.81 (t, 1.3H, J = 6.5 Hz), 3.68 (m, 1.4H), 3.50 (m, 4.1H), 3.13 (bs, 2.7H), 3.04 (bs, 3.4H), 2.81 (t, 1.3H J = 6.5 Hz), 2.56-2.64 (m, 10.5H), 2.37 (bs, 2.5H), 2.16 (bs,

4.8H), 2.07 (s, 2.7H), 2.00 (m, 9H), 1.90 (s, 2H) 1.79 (m, 3.6H) ppm. MALDI-TOF (pos) m/z 36300.

5a: ^{1}H NMR (500 MHz, d_6-DMSO) δ 7.97 (bs, 1H, amide NH's), 7.90 (bs, 0.4H, amide NH's), 7.83 (bs, 0.5H, amide NH's), 7.77 (bs, 0.8H, amide NH's), 7.51 (bs, 1.8H, $CH_2NHC(S)NHCH_2$) 5.32 (m, 0.7H), 5.17 (m, 0.8H), 5.07 (m, 1.6H), 5.02 (m, 0.8H), 4.92 (m, 1H), 4.84 (m, 0.5H), 4.21 (m, 0.7H), 4.10 (m, 0.9H), 4.00 (m, 2.3H), 3.90 (m, 0.7), 3.80 (t, 0.8H, J = 6.5 Hz), 3.68 (m, 1.8H), 3.50 (m, 3.2H), 3.14 (bs, 2.5H), 3.04 (bs, 3.9H), 2.81 (t, 0.5H J = 6.5 Hz), 2.56-2.64 (m, 11.4H), 2.17 (bs, 4.8H), 2.08 (s, 3.2H), 2.07 (s, 3H), 2.00 (m, 9H), 1.90 (s, 3.5H) 1.79 (m, 3.5H) ppm. MALDI-TOF (pos) m/z 63500.

5b: ^{1}H NMR (500 MHz, d_6-DMSO) δ 7.97 (bs, 1H, amide NH's), 7.90 (bs, 0.5H, amide NH's), 7.83 (bs, 0.5H, amide NH's), 7.77 (bs, 0.8H, amide NH's), 7.51 (bs, 1.8H, $CH_2NHC(S)NHCH_2$) 5.32(m, 0.8H), 5.17 (m, 0.8H), 5.07 (m, 1.1H), 5.02 (m, 0.8H), 4.99 (m, 0.17H), 4.93 (m, 0.9H), 4.84 (m, 0.5H), 4.21 (m, 0.8H), 4.10 (m, 0.8H), 4.00 (m, 2.4H), 3.80 (t, 1.1H, J = 6.5 Hz), 3.68 (m, 1.6H), 3.50 (m, 3.8H), 3.14 (bs, 2.5H), 3.04 (bs, 3.9H), 2.81 (t, 1H J = 6.5 Hz), 2.56-2.64 (m, 13H), 2.17 (bs, 5H), 2.08 (s, 4H), 2.07 (s, 2H), 2.00 (s, 3.5H), 1.99 (s, 3H) 1.98 (s, 3H), 1.97 (s, 3H), 1.90 (s, 3.5H) 1.79 (m, 4H) ppm. MALDI-TOF (pos) m/z 65500.

5c: ^{1}H NMR (500 MHz, d_6-DMSO) δ 7.97 (bs, 1H, amide NH's), 7.78 (bs, 0.8H, amide NH's), 7.51 (bs, 2H, $CH_2N\mathit{H}C(S)N\mathit{H}CH_2$) 5.32(m, 0.9H), 5.26 (m, 1H), 5.17 (m, 1H), 5.02 (m, 0.8H), 4.99 (m, 0.8H) 4.92 (m, 1.6H), 4.76 (m, 1H), 4.21 (m, 1H), 4.10 (m, 1H), 4.00 (m, 2.7H), 3.95 (m, 1H), 3.81 (t, 1.6H, J = 6.5 Hz), 3.68 (m, 2.4H), 3.48 (m, 4.2H), 3.13 (bs, 3.2H), 3.04 (bs, 3.7H), 2.81 (t, 2.2H, J = 6.5 Hz), 2.56-2.65 (m, 10H), 2.17 (bs, 4.7H), 2.08 (s, 3H), 2.00 (s, 3H), 1.99 (s, 1H), 1.98 (s, 3H), 1.97 (s, 3H), 1.95 (s, 2H), 1.92 (s, 2H) 1.90 (s, 3H), 1.80 (m, 4.4H) ppm. MALDI-TOF (pos) m/z 67000.

5d: ^{1}H NMR (500 MHz, d_6-DMSO) δ 7.97 (bs, 1H, amide NH's), 7.90 (bs, 0.3H, amide NH's), 7.83 (bs, 0.4H, amide NH's), 7.77 (bs, 1H, amide NH's), 7.51 (bs, 1.8H, $CH_2N\mathit{H}C(S)N\mathit{H}CH_2$), 5.31 (s, 0.4H), 5.25 (m, 0.4H), 5.16 (m, 1H), 5.02 (m, 1H), 4.92 (m, 1.1H), 4.77 (m, 0.6H), 4.10-4.21 (m, 0.9H), 4.00 (m, 1.7H), 3.80 (t, 0.5H, J = 6.5 Hz), 3.68 (m, 1.2H), 3.50 (m, 3.5H), 3.13 (bs, 2.6H), 3.04 (bs, 3.2H), 2.81 (t, 0.5H J = 6.5 Hz), 2.56-2.64 (m, 9.2H), 2.37 (bs, 2.4H), 2.16 (bs, 4.4H), 2.07 (s, 2.1H), 2.00 (m, 11H), 1.90 (s, 2H) 1.79 (m, 2.8H) ppm. MALDI-TOF (pos) m/z 66000.

6a: ^{1}H NMR (500 MHz, d_6-DMSO) δ 7.97 (bs, 1H, amide NH's), 7.90 (bs, 0.4H, amide NH's), 7.83 (bs, 0.5H, amide NH's), 7.77 (bs, 0.8H, amide NH's), 7.51 (bs, 1.8H, $CH_2N\mathit{H}C(S)N\mathit{H}CH_2$) 5.32(m, 0.7H), 5.17 (m, 0.8H), 5.07 (m, 1.6H), 5.02 (m, 0.8H), 4.92 (m, 1H), 4.84 (m, 0.5H), 4.21 (m, 0.7H), 4.10 (m, 0.9H), 4.00 (m,

2.3H), 3.90 (m, 0.7), 3.80 (t, 0.8H, J = 6.5 Hz), 3.68 (m, 1.8H), 3.50 (m, 3.2H), 3.14 (bs, 2.5H), 3.04 (bs, 3.9H), 2.81 (t, 0.5H J = 6.5 Hz), 2.56-2.64 (m, 11.4H), 2.17 (bs, 4.8H), 2.08 (s, 3.2H), 2.07 (s, 3H), 2.00 (m, 9H), 1.90 (s, 3.5H) 1.79 (m, 3.5H) ppm. MALDI-TOF (pos) m/z 113500.

6b: ^{1}H NMR (500 MHz, d_6-DMSO) δ 7.97 (bs, 1H, amide NH's), 7.83 (bs, 1H, amide NH's), 7.77 (bs, 1H, amide NH's), 7.51 (bs, 1.8H, $CH_2N\mathit{H}C(S)N\mathit{H}CH_2$) 5.32(m, 0.8H), 5.25 (m, 0.5H), 5.17 (m, 0.8H), 5.07 (m, 0.5H), 5.02 (m, 0.8H), 4.99 (m, 0.5H), 4.92 (m, 1.3H), 4.84 (m, 0.3H), 4.75 (m, 0.7H), 4.21 (m, 0.8H), 4.09 (m, 0.8H), 4.00 (m, 2.6H), 3.80 (t, 1.1H, J = 6.5 Hz), 3.68 (m, 2H), 3.50 (m, 4H), 3.13 (bs, 2.5H), 3.04 (bs, 4.7H), 2.81 (t, 1H, J = 6.5 Hz), 2.56-2.64 (m, 17H), 2.17 (bs, 6.5H), 2.08 (s, 3.7H), 2.00 (s, 3H), 1.99 (s, 2H), 1.98 (s, 3H), 1.97 (s, 3H) 1.96 (s, 2H), 1.90 (s, 3H) 1.79 (m, 4.7H) ppm. MALDI-TOF (pos) m/z 115500.

6c: ^{1}H NMR (500 MHz, d_6-DMSO) δ 7.97 (bs, 1H, amide NH's), 7.78 (bs, 0.8H, amide NH's), 7.51 (bs, 2H, $CH_2N\mathit{H}C(S)N\mathit{H}CH_2$) 5.32(m, 0.9H), 5.26 (m, 1H), 5.17 (m, 1H), 5.02 (m, 0.8H), 4.99 (m, 0.9H) 4.92 (m, 1.6H), 4.76 (m, 1H), 4.21 (m, 1H), 4.10 (m, 1H), 4.00 (m, 2.6H), 3.95 (m, 1H), 3.81 (t, 1.6H, J = 6.5 Hz), 3.68 (m, 2.4H), 3.48 (m, 4.2H), 3.13 (bs, 3.2H), 3.04 (bs, 3.7H), 2.81 (t, 2.2H, J = 6.5 Hz), 2.56-2.65 (m, 10H), 2.17 (bs, 4.7H), 2.08 (s, 3H), 2.00 (s, 3H), 1.99 (s, 1H),

1.98 (s, 3H), 1.97 (s, 3H), 1.95 (s, 2H), 1.92 (s, 2H) 1.90 (s, 3H), 1.80 (m, 4.4H) ppm. MALDI-TOF (pos) m/z 115000.

6d: ^{1}H NMR (500 MHz, d_6-DMSO) δ 7.97 (bs, 1H, amide NH's), 7.90 (bs, 0.4H, amide NH's), 7.83 (bs, 0.5H, amide NH's), 7.77 (bs, 1H, amide NH's), 7.51 (bs, 1.8H, $CH_2N\mathit{H}C(S)N\mathit{H}CH_2$), 5.32 (s, 1H), 5.25 (m, 1.1H), 5.14 (m, 0.5H), 5.02 (m, 1.1H), 4.92 (m, 1.4H), 4.77 (m, 0.8H), 4.10-4.21 (m, 2.4H), 4.00 (m, 3.3H), 3.81 (t, 2.5H, J = 6.5Hz), 3.68 (m, 2.1H), 3.50 (m, 4.6H), 3.13 (bs, 3.1H), 3.04 (bs, 3.8H), 2.81 (t, 2.5H J = 6.4Hz), 2.56-2.64 (m, 10.5H), 2.37 (bs, 2.5H), 2.16 (bs, 4.7H), 2.07 (s, 2.7H), 2.00 (m, 17H), 1.90 (s, 2H) 1.79 (m, 5.9H) ppm. MALDI-TOF (pos) m/z 116000.

General procedure for deacylation of dendrimers 4-6. To the lyophilized solid product of compounds 4-6 1 mL of 1:1 water:methanol was added, at which point the dendrimer would become a white precipitate solid. To this mixture was added 0.2 equivalents of NaOMe (0.8 M in MeOH) for each peripheral carbohydrate, and let stir for 3 hrs. If, at this time, the mixture had not become a clear solution a further 0.2 equivalents of NaOMe (0.8 M in MeOH) was added and this step was repeated until the mixture became a clear and colorless solution. $HCl_{(aq)}$ (0.1M) was then added slowly until the pH was ~ 7. This neutralized solution was placed in a centrifugal filter device, diluted with 3 mL 1:1 H_2O:MeOH and filtered at 3500rpm for 30 mins. The filtrate was then removed and 3 mL H_2O was added

and filtered for 30 mins at 3500rpm. This procedure was repeated 2 more times. At which point the remaining residue was taken up in Millipore water and lyophilized to give a white fluffy solid.

4a: ^{1}H NMR (500 MHz, d_6-DMSO) δ 7.96 (bs, 1H, amide NH's), 7.89 (bs, 0.4H, amide NH's), 7.83 (bs, 0.4H, amide NH's), 7.76 (bs, 1.1H, amide NH's), 7.52 (bs, 1.9H $CH_2N\mathit{H}C(S)N\mathit{H}CH_2$), 4.67 (bs, 1.4H), 4.58 (s, 0.5H), 4.54 (m, 1.9H), 4.41 (bs, 0.9H), 4.33 (bs, 0.3H), 3.65 (bs, 0.4), 3.59 (m, 2.2H), 3.54 (s, 1.6H), 3.39-3.51 (m, 5.7H), 3.12 (bs, 2.7H), 3.02 (bs, 4.0H), 2.48-2.63 (m, 10.1H), 2.38 (bs, 2.2H), 2.15 (bs, 5.1H), 1.73 (m, 2.9H) ppm; MALDI-TOF (pos) m/z 28000.

4b: ^{1}H NMR (500 MHz, d_6-DMSO) δ 7.99 (bs, 1H, amide NH's), 7.92 (bs, 0.5H, amide NH's), 7.85 (bs, 0.6H, amide NH's), 7.79 (bs, 1.2H, amide NH's), 7.54 (bs, 1.9H $CH_2N\mathit{H}C(S)N\mathit{H}CH_2$), 4.83 (s, 0.15H), 4.67 (s, 0.5H), 4.60 (s, 0.5H), 4.56 (m, 1.5H), 4.43 (bs, 0.9H), 4.35 (bs, 0.3), 3.60-3.67 (m, 2.5H), 3.56 (s, 1.4H), 3.48 (m, 2.7H), 3.34-3.44 (m, 6H), 3.13 (bs, 2.8H), 3.05 (bs, 5.1H), 2.60 (m, 10.9H), 2.40 (bs, 2.5H), 2.17 (bs, 6H), 1.77 (m, 3.5H) ppm. MALDI-TOF (pos) m/z 27600.

4c: ^{1}H NMR (500 MHz, d_6-DMSO) δ 7.97 (bs, 1H, amide NH's), 7.90 (bs, 0.5H, amide NH's), 7.83 (bs, 0.5H, amide NH's), 7.77 (bs, 1.2H, amide NH's), 7.52 (bs, 2H $CH_2N\mathit{H}C(S)N\mathit{H}CH_2$), 4.83 (s, 0.4H), 4.68 (m, 1.6H), 4.58 (m, 0.7), 4.55 (m, 1.2H), 4.41 (bs, 0.9H), 4.33 (bs, 0.2), 3.60 (m, 2.4H), 3.46-3.55 (m, 3.8H), 3.40

(m, 3.1H), 3.12 (bs, 3.2H), 3.03 (bs, 5.7H), 2.60 (m, 11.1H), 2.39 (bs, 2.8H), 2.16 (bs, 6.1H), 1.74 (m, 3.5H) ppm. MALDI-TOF (pos) m/z 27700.

4d: ^{1}H NMR (500 MHz, *d*$_6$-DMSO) δ 7.98 (bs, 1H, amide NH's), 7.91 (bs, 0.3H, amide NH's), 7.85 (bs, 0.3H, amide NH's), 7.78 (bs, 1H, amide NH's), 7.54 (bs, 1.9H $CH_2N\mathit{H}C(S)N\mathit{H}CH_2$), 4.98 (s, 0.14H), 4.92 (s, 0.14H), 4.84 (s, 0.8H), 4.57-4.75 (m, 2.8H), 4.43 (m, 1H), 4.43 (bs, 0.14), 3.48-3.77 (m, 5.2H), 3.36-3.48 (m, 5H), 3.14 (bs, 3.4H), 3.05 (bs, 4.6H), 2.60 (bs, 9.7H), 2.40 (bs, 2.3H), 2.17 (bs, 5.1H), 1.77 (m, 2.8H) ppm. MALDI-TOF (pos) m/z 30200.

4e: ^{1}H NMR (500 MHz, *d*$_6$-DMSO) δ 8.09 (bs, 0.8H, amide NH's), 7.92 (bs, 0.1H, amide NH's), 7.62 (bs, 0.8H $CH_2N\mathit{H}C(S)N\mathit{H}CH_2$), 4.87 (s, 0.14H), 4.76 (s, 0.14H), 4.66 (s, 0.8H), 4.57 (m, 2.8H), 4.45 (m, 1H), 3.36-3.77 (m, 12.6H), 3.14 (bs, 1.2H), 3.05 (bs, 0.9H), 2.90 (bs, 1.7H), 2.57 (m, 2.1H), 2.46 (s, 1H), 2.30 (bs, 1.6H), 1.77 (m, 1H) ppm. MALDI-TOF (pos) m/z 28900.

5a: ^{1}H NMR (500 MHz, *d*$_6$-DMSO) δ 7.98 (bs, 1H, amide NH's), 7.91 (bs, 0.6H, amide NH's), 7.85 (bs, 0.7H, amide NH's), 7.77 (bs, 1.2H, amide NH's), 7.52 (bs, 1.9H $CH_2N\mathit{H}C(S)N\mathit{H}CH_2$), 4.70 (bs, 1.4H), 4.60 (s, 0.6H), 4.56 (m, 1.9H), 4.41 (bs, 1H), 4.33 (bs, 0.4H), 3.65 (bs, 0.6), 3.59 (m, 2.2H), 3.35-3.55 (m, 10.6H), 3.12 (bs, 2.9H), 3.04 (bs, 5.1H), 2.48-2.63 (m, 11.1H), 2.38 (bs, 2.5H), 2.17 (bs, 6.2H), 1.73 (m, 3.6H) ppm; MALDI-TOF (pos) m/z 51500.

5b: ^{1}H NMR (500 MHz, d_6-DMSO) δ 7.99 (bs, 1H, amide NH's), 7.92 (bs, 0.5H, amide NH's), 7.85 (bs, 0.6H, amide NH's), 7.79 (bs, 1.2H, amide NH's), 7.54 (bs, 1.9H $CH_2N\mathit{H}C(S)N\mathit{H}CH_2$), 4.83 (s, 0.15H), 4.67 (s, 0.5H), 4.60 (s, 0.5H), 4.56 (m, 1.5H), 4.43 (bs, 0.9H), 4.35 (bs, 0.3), 3.60-3.67 (m, 2.5H), 3.56 (s, 1.4H), 3.48 (m, 2.7H), 3.34-3.44 (m, 6H), 3.13 (bs, 2.8H), 3.05 (bs, 5.1H), 2.60 (m, 10.9H), 2.40 (bs, 2.5H), 2.17 (bs, 6H), 1.77 (m, 3.5H) ppm. MALDI-TOF (pos) m/z 51500.

5c: ^{1}H NMR (500 MHz, d_6-DMSO) δ 7.98 (bs, 1H, amide NH's), 7.91 (bs, 0.3H, amide NH's), 7.85 (bs, 0.3H, amide NH's), 7.78 (bs, 1H, amide NH's), 7.54 (bs, 1.9H $CH_2N\mathit{H}C(S)N\mathit{H}CH_2$), 4.98 (s, 0.15H), 4.92 (s, 0.15H), 4.84 (s, 0.9H), 4.57-4.75 (m, 2.8H), 4.43 (m, 1H), 4.43 (bs, 0.15H), 3.48-3.77 (m, 5.5H), 3.36-3.48 (m, 5H), 3.14 (bs, 3.7H), 3.05 (bs, 4.9H), 2.60 (bs, 10H), 2.40 (bs, 2.5H), 2.17 (bs, 5H), 1.77 (m, 2.8H) ppm. MALDI-TOF (pos) m/z 56000.

5d: ^{1}H NMR (500 MHz, d_6-DMSO) δ 7.98 (bs, 1H, amide NH's), 7.91 (bs, 0.3H, amide NH's), 7.85 (bs, 0.3H, amide NH's), 7.78 (bs, 1H, amide NH's), 7.54 (bs, 1.9H $CH_2N\mathit{H}C(S)N\mathit{H}CH_2$), 4.86 (s, 0.7H), 4.76 (s, 0.6H), 4.66 (s, 0.5H), 4.60 (s, 0.9H), 4.55 (m, 0.9H), 4.44 (m, 0.8H), 4.37 (bs, 0.5H), 3.35-3.77 (m, 10.8H), 3.14 (bs, 3.4H), 3.05 (bs, 4.2H), 2.60 (bs, 9.7H), 2.40 (bs, 2.1H), 2.17 (bs, 5.1H), 1.77 (m, 3.0H) ppm. MALDI-TOF (pos) m/z 54000.

6a: ^{1}H NMR (500 MHz, d_6-DMSO) δ 7.96 (bs, 1H, amide NH's), 7.89 (bs, 0.4H, amide NH's), 7.83 (bs, 0.4H, amide NH's), 7.76 (bs, 1.1H, amide NH's), 7.52 (bs, 1.9H $CH_2N\mathit{H}C(S)N\mathit{H}CH_2$), 4.67 (bs, 1.4H), 4.58 (s, 0.5H), 4.54 (m, 1.9H), 4.41 (bs, 0.9H), 4.33 (bs, 0.3H), 3.65 (bs, 0.4), 3.59 (m, 2.2H), 3.54 (s, 1.6H), 3.39-3.51 (m, 5.7H), 3.12 (bs, 2.7H), 3.02 (bs, 4.0H), 2.48-2.63 (m, 10.1H), 2.38 (bs, 2.2H), 2.15 (bs, 5.1H), 1.73 (m, 2.9H) ppm; MALDI-TOF (pos) m/z 93000.

6b: ^{1}H NMR (500 MHz, d_6-DMSO) δ 7.97 (bs, 1H, amide NH's), 7.90 (bs, 0.5H, amide NH's), 7.83 (bs, 0.5H, amide NH's), 7.77 (bs, 1.2H, amide NH's), 7.52 (bs, 2H $CH_2N\mathit{H}C(S)N\mathit{H}CH_2$), 4.83 (s, 0.4H), 4.68 (m, 1.6H), 4.58 (m, 0.7), 4.55 (m, 1.2H), 4.41 (bs, 0.9H), 4.33 (bs, 0.2), 3.60 (m, 2.4H), 3.46-3.55 (m, 3.8H), 3.40 (m, 3.1H), 3.12 (bs, 3.2H), 3.03 (bs, 5.7H), 2.60 (m, 11.1H), 2.39 (bs, 2.8H), 2.16 (bs, 6.1H), 1.74 (m, 3.5H) ppm. MALDI-TOF (pos) m/z 95500.

6c: ^{1}H NMR (500 MHz, d_6-DMSO) δ 7.98 (bs, 1H, amide NH's), 7.91 (bs, 0.3H, amide NH's), 7.85 (bs, 0.3H, amide NH's), 7.78 (bs, 1H, amide NH's), 7.54 (bs, 1.9H $CH_2N\mathit{H}C(S)N\mathit{H}CH_2$), 4.98 (s, 0.14H), 4.92 (s, 0.14H), 4.84 (s, 0.8H), 4.57-4.75 (m, 2.8H), 4.43 (m, 1H), 4.43 (bs, 0.14), 3.48-3.77 (m, 5.2H), 3.36-3.48 (m, 5H), 3.14 (bs, 3.4H), 3.05 (bs, 4.6H), 2.60 (bs, 9.7H), 2.40 (bs, 2.3H), 2.17 (bs, 5.1H), 1.77 (m, 2.8H) ppm. MALDI-TOF (pos) m/z 95500.

6d: ^{1}H NMR (500 MHz, d_6-DMSO) δ 8.16 (bs, 1H, amide NH's), 7.96 (bs, 0.2H, amide NH's), 7.65 (bs, 0.8H $CH_2N\mathit{H}C(S)N\mathit{H}CH_2$), 4.90 (s, 0.4H), 4.80 (s, 0.3H), 4.69 (s, 0.4H), 4.60 (m, 0.9H), 4.48 (bs, 0.6H), 3.36-3.77 (m, 7H), 3.16 (bs, 2.4H), 3.05 (bs, 2.1H), 2.90 (bs, 1.7H), 2.57 (m, 2.9H), 2.30 (bs, 1.5H), 1.76 (m, 1.5H) ppm.. MALDI-TOF (pos) m/z 94500.

Table 3 Hemagglutination assay and M_W results (from MALDI-TOF MS) *for 4–6.*

Cmpd	M_W After Mannose Addition	# mannose residues[a]	M_W After Glucose Addition	# glucose residues[a]	M_w after Galactose addition	M_w after deacylation	Relative activity per active sugar[b]
4a	29200	30	n/a	0	34400	28000	3820 ± 1650
4b	26300	24	30200	7	33800	27600	2660 ± 0
4c	22900	18	29700	13	34200	27700	2260 ± 780
4d	18700	10	33500	26	36100	30200	1090 ± 380
4e	n/a	0	28300	29	36300	28900	260 ± 110
5a	48000	44	n/a	0	63500	51500	4830 ± 2090
5b	44500	38	51000	13	65500	51500	3040 ± 0
5c	34700	16	57000	40	67000	56000	1270 ± 440
5d	n/a	0	49500	45	66000	54000	310 ± 130
6a	77000	53	n/a	0	113500	93000	5350 ± 0
6b	68000	34	86500	35	115500	95500	3510 ± 1220
6c	58500	16	85500	50	115000	95500	2150 ± 0
6d	n/a	0	90000	77	116000	94500	470 ± 0

[a]# sugar residues was determined using MALDI-TOF MS data after deacetylation (M_W = 168 g/mol for 4 Ac) and after addition of tethered sugar (M_W = 507 g/mol per tethered sugar). [b]Active sugar = mannose + glucose. Standard deviation values are very large because of serial 2 fold dilutions. For standard deviation = 0, all inhibitory concentrations were equal. All values represent at least three trials.

General Hemagglutination Inhibition Assay Procedures

Concanavalin A preparation: In a 10 mL centrifuge tube, approximately 5 mg of Concanavalin A (Con A) was dissolved without agitation in 10 mL of HEPES buffer with 100μM $CaCl_2$ (pH = 8.5). The tube was stored at 4 ºC for 8 hours to allow the Con A to dissolve. Afterwards, the solution was placed in a dialysis tube and dialyzed against 1 L of tris buffered saline (TBS) for 4 hours. This was repeated with fresh TBS solution, followed by dialysis against 1 L of phosphate-buffered saline (PBS) for 8 hours. The dialysis was done to remove any excess Ca^{2+} from the lectin solution. The Con A solution was removed from the tube and stored at 4 ºC until needed.

Blood preparation: Fresh whole rabbit blood was obtained from the MSU animal care center in 4mL vials. Alsever's solution was added to the blood to make up a 60:40 v/v solution. The blood was separated into 2 mL aliquots in 15 mL centrifuge tubes. These were then diluted to 12 mL with Alsevers solution. The cells were pelleted by centrifugation (1100rpm x 10 min), and the layer of white blood cells and plasma proteins was removed by pipet. This process was repeated 2 more times using PBS instead of Alsever's solution. The blood was then made up in the assay buffer solution, PBS w/ 0.5%BSA.

Concanavalin A Titration: Decreasing amounts of Con A were incubated with red blood cells to determine the lectin concentration needed to agglutinate cells.

Serial two fold dilutions were made by adding 50 μL of Con A solution to the first well, then 50 μL of buffer solution to all 24 wells. 50 μL was then transferred from the first well to the second. The second well was mixed and 50 μL was transferred to the third well. This procedure was repeated until the 24th was ll two fold serial dilutions. To each well 50 μL of the blood solution was added and incubated for 2 hours at 22-25 ^{o}C. After this time the wells were examined and the amount of Con A required to agglutinate was determined. This was then considered to be 1 unit. For the inhibition assay an 8 unit Con A solution was made up and the concentration of Con A determined by spectrophotometric analysis.

Inhibiting Dose Determination: Starting with a concentration of 5 mg/mL, serial two-fold dilutions of the inhibitors were made as described above. the inhibitor solutions were incubated with 50 μL of the 8 unit Con A solution for 2-3 hours at 22-25^{o}C. the minimum concentration causing inhibition was determined and this was the inhibiting dose. The HI assays of all compounds that are directly compared in Tables 1-4 were preformed simultaneously to provide the exact same conditions, enabling an accurate comparison of relative activity. The values given are the average of three or more independent measurements.

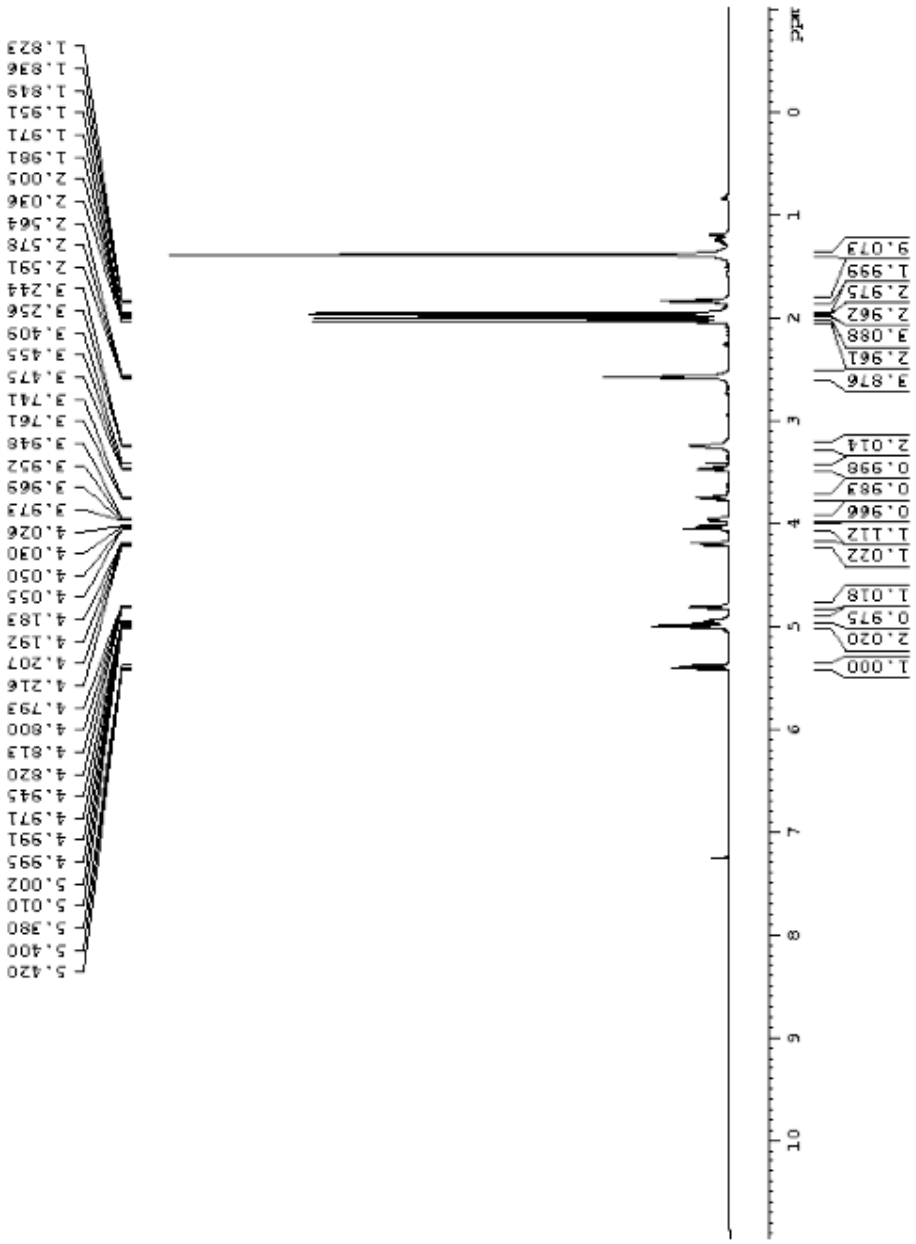

Figure 16 ^{1}H NMR spectrum (500 MHz, $CDCl_3$) of 1b.

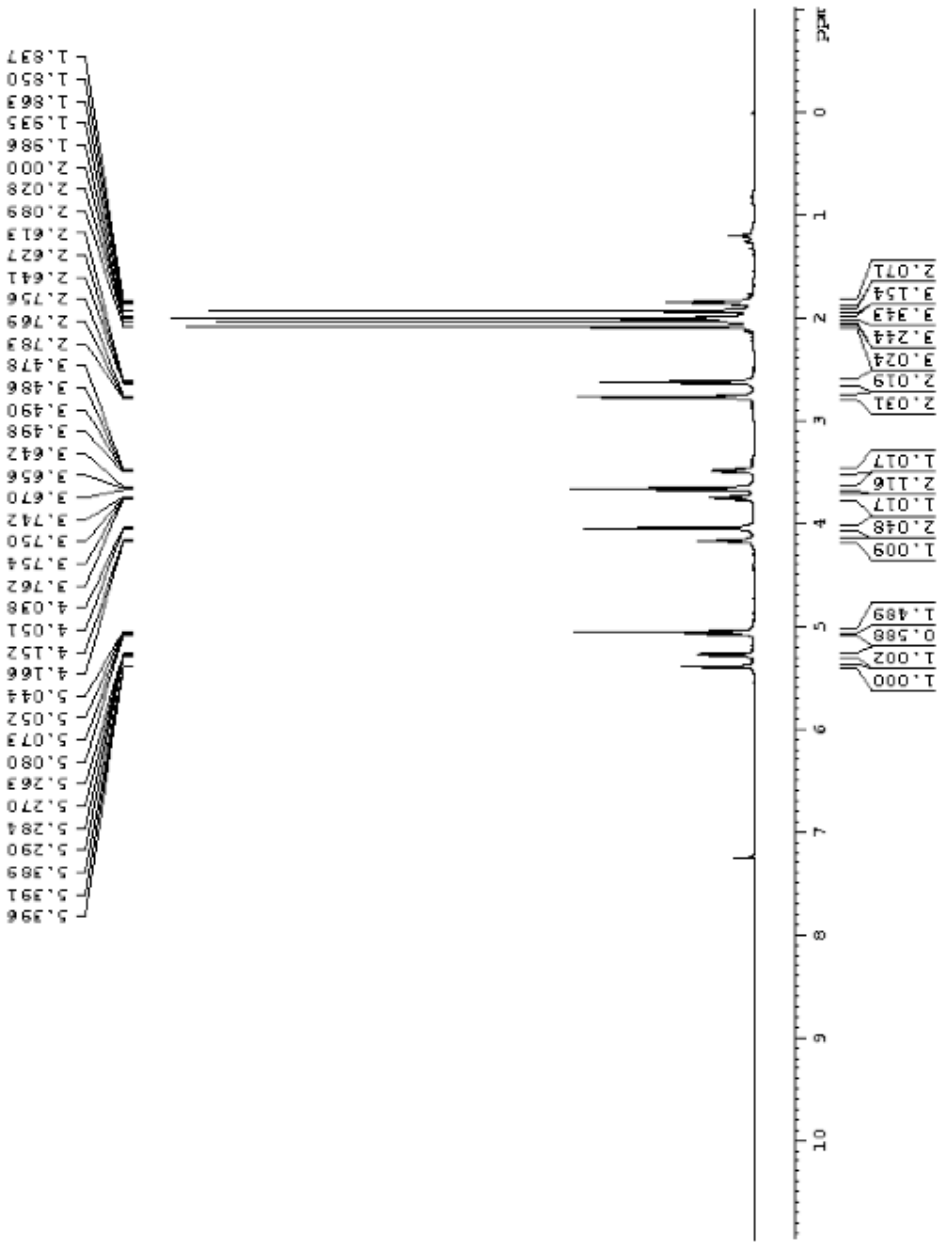

Figure 17 ^{1}H NMR spectrum (500 MHz, $CDCl_3$) of 2c.

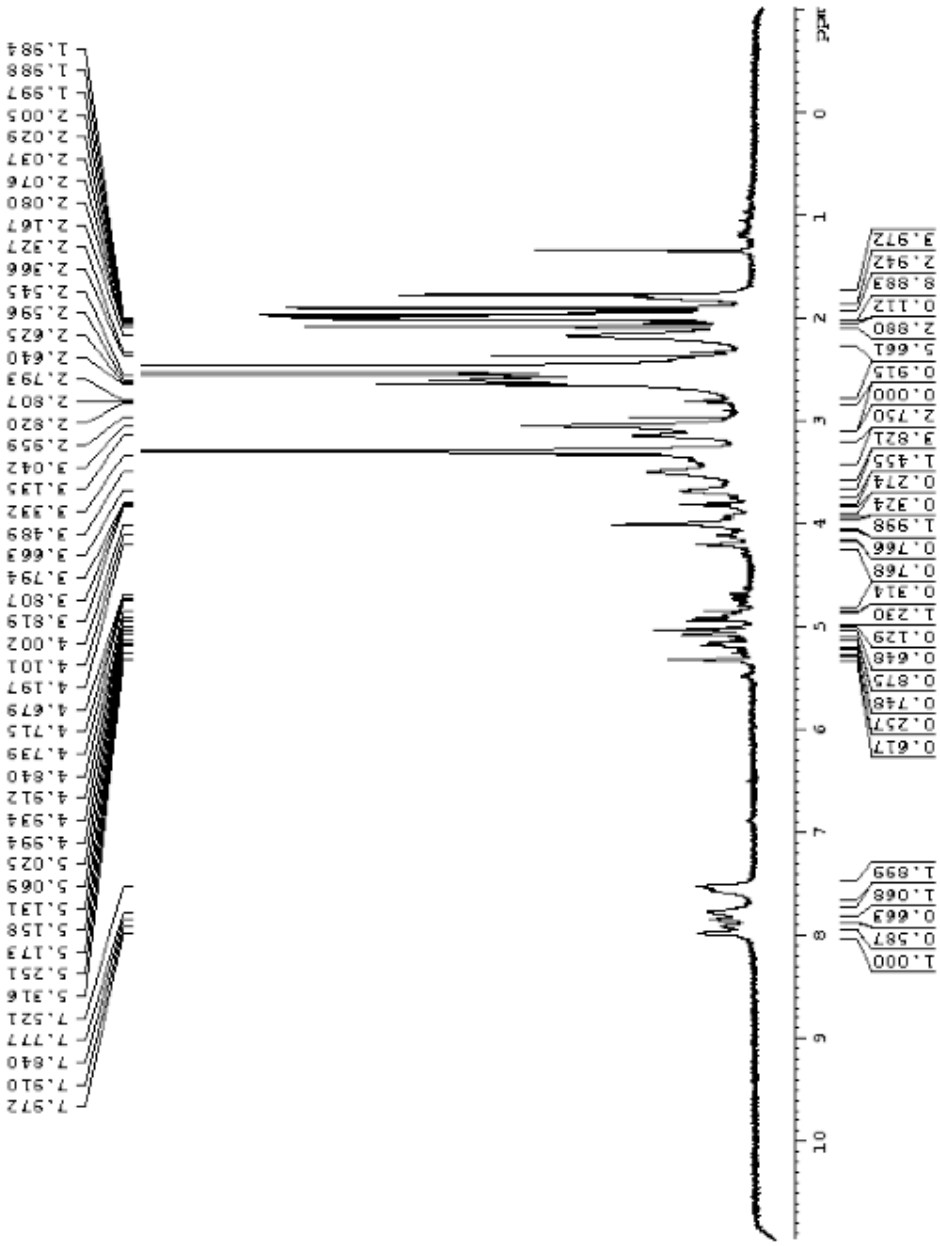

Figure 18 ^{1}H NMR spectrum (500 MHz, d_6-DMSO) of 4c (peracetylated).

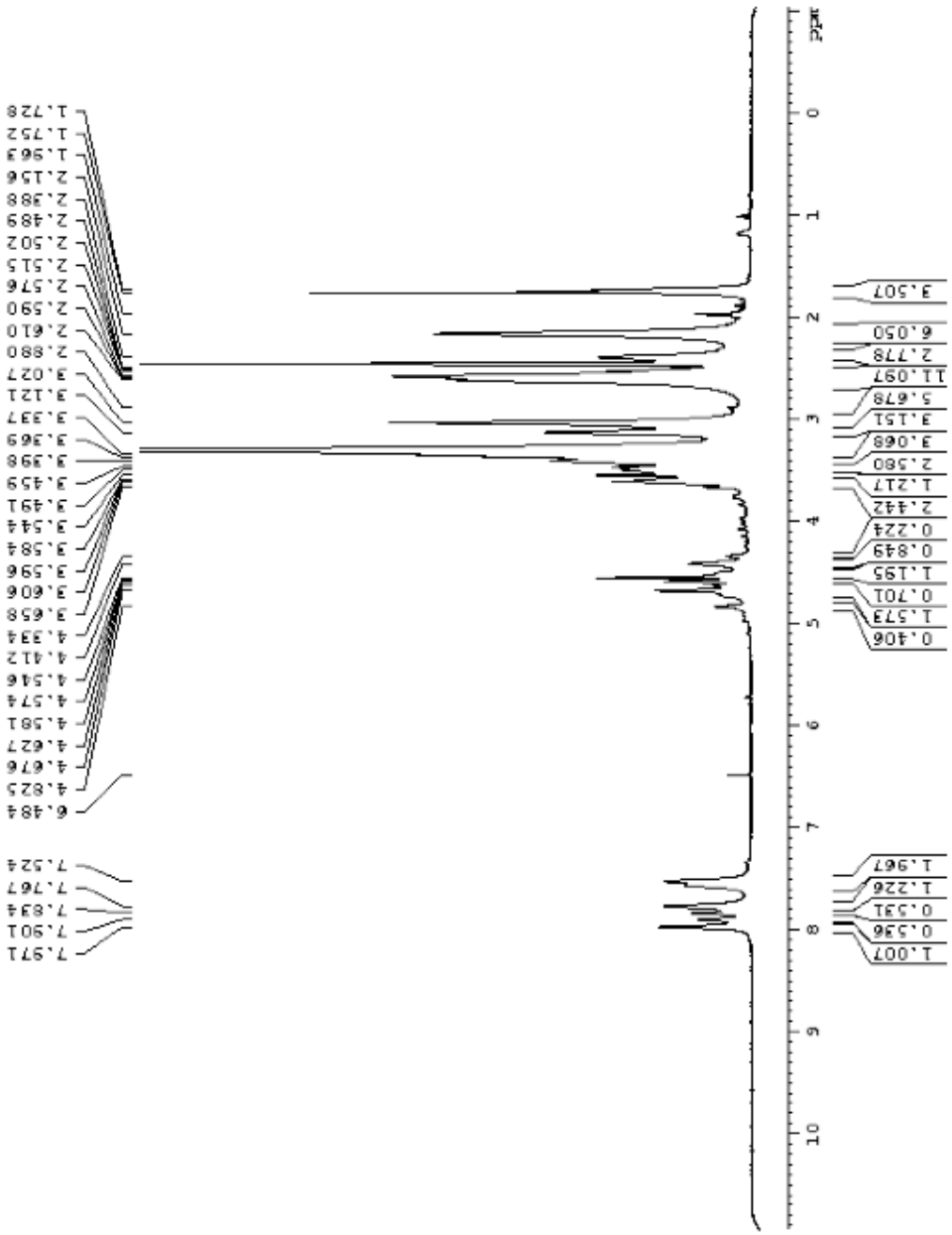

Figure 19 ^{1}H NMR spectrum (500 MHz, d_6-DMSO) of 4c (deacetylated).

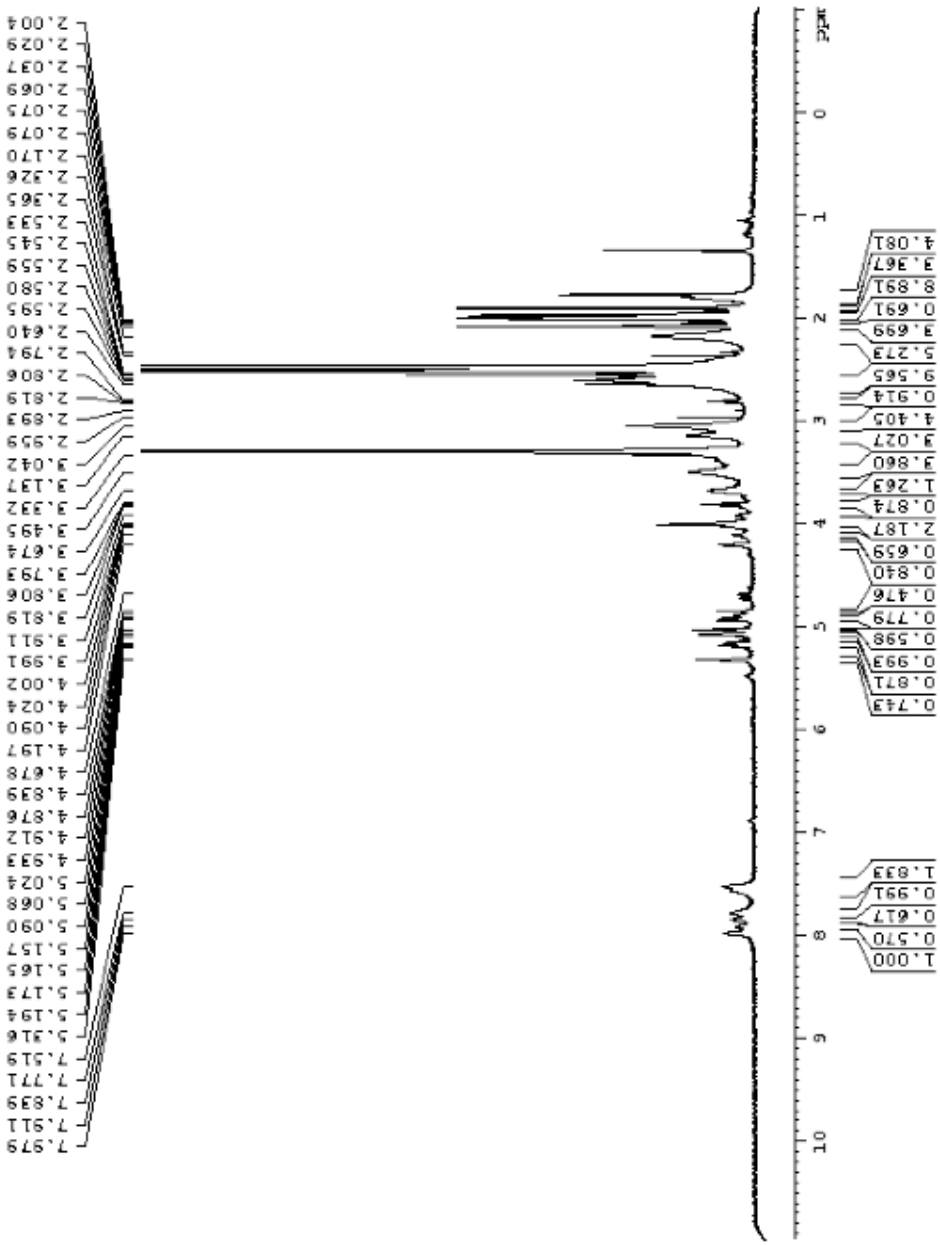

Figure 20 ^{1}H NMR spectrum (500 MHz, d_6-DMSO) of 5e (peracetylated).

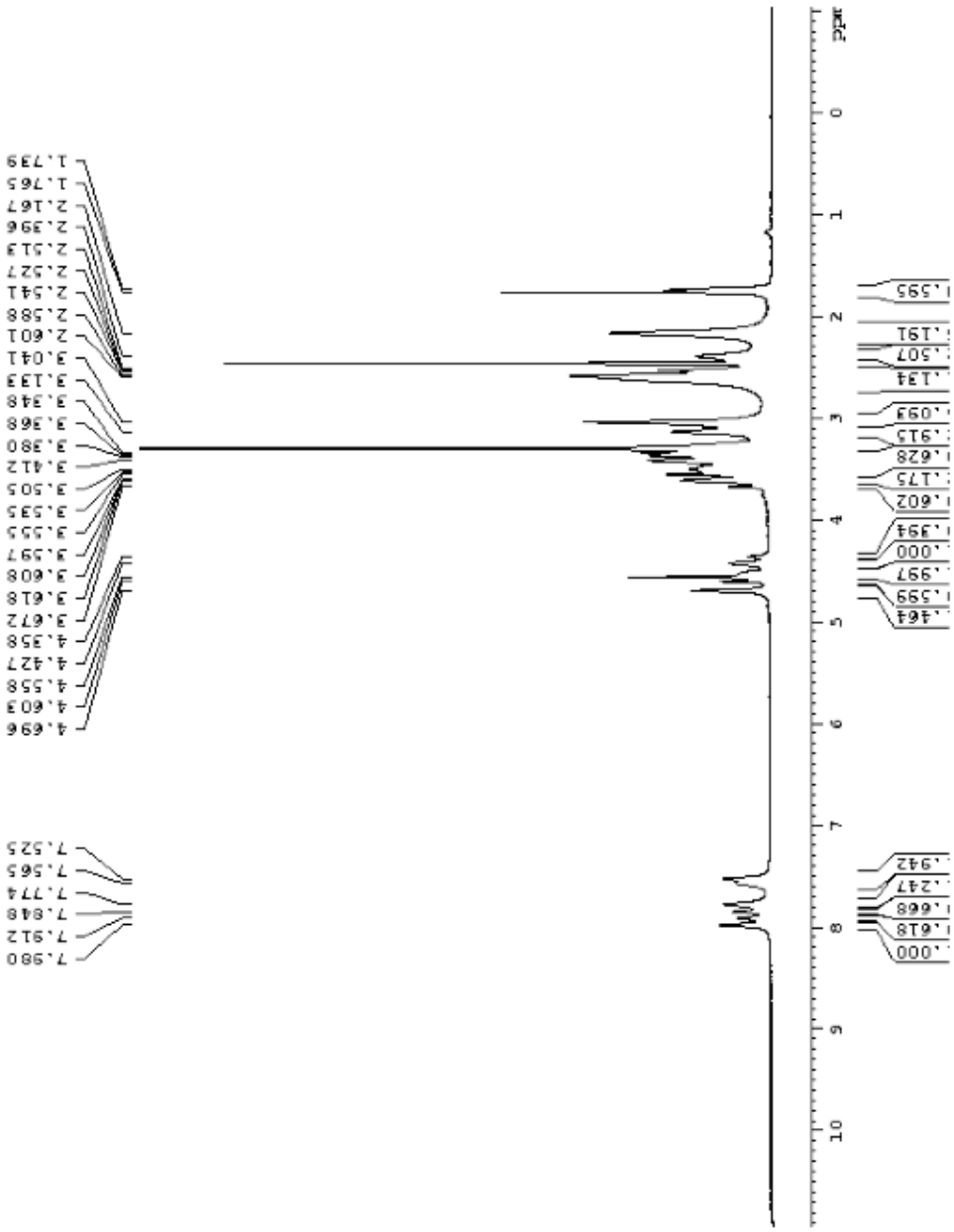

Figure 21 ^{1}H NMR spectrum (500 MHz, d_6-DMSO) of 5e (deacetylated).

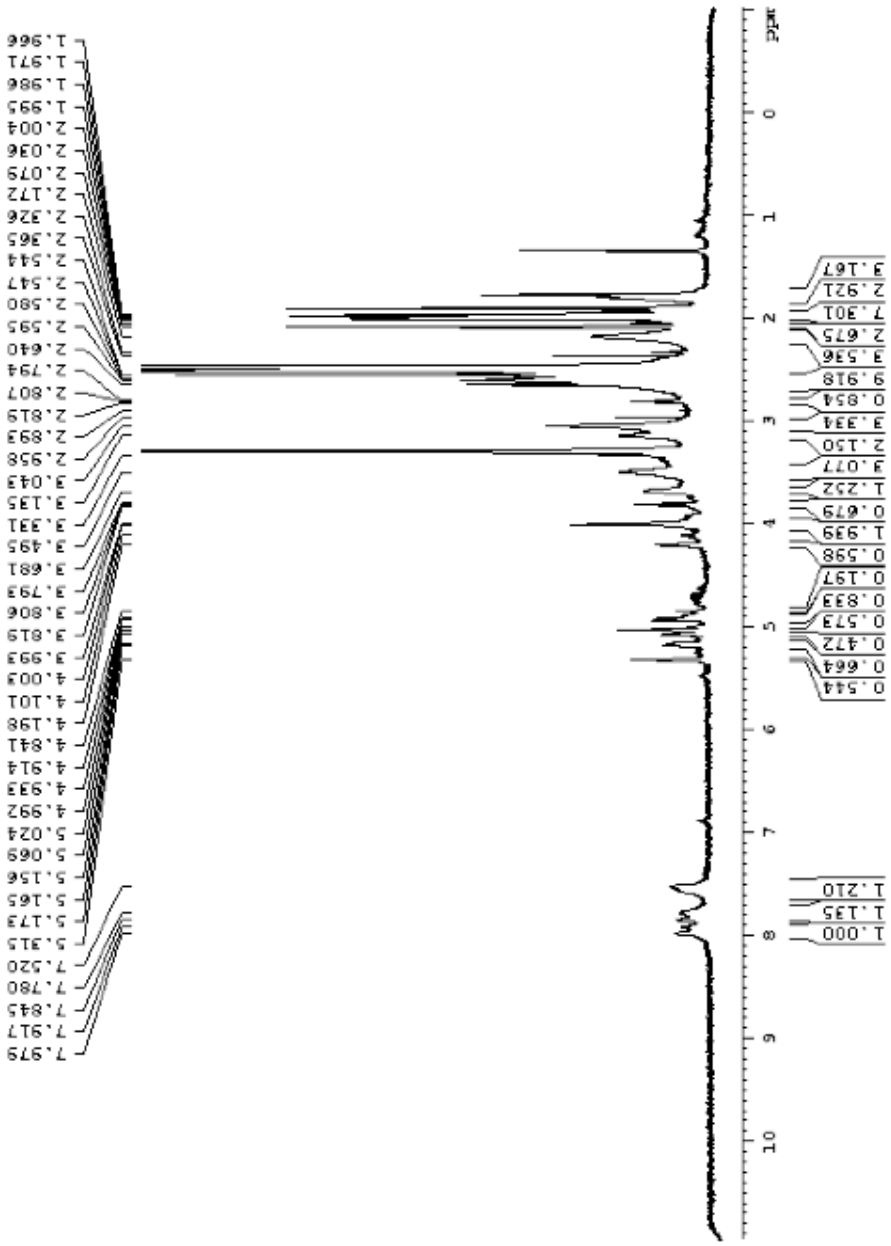

Figure 22 ^{1}H NMR spectrum (500 MHz, d_6-DMSO) of 6d (peracetylated).

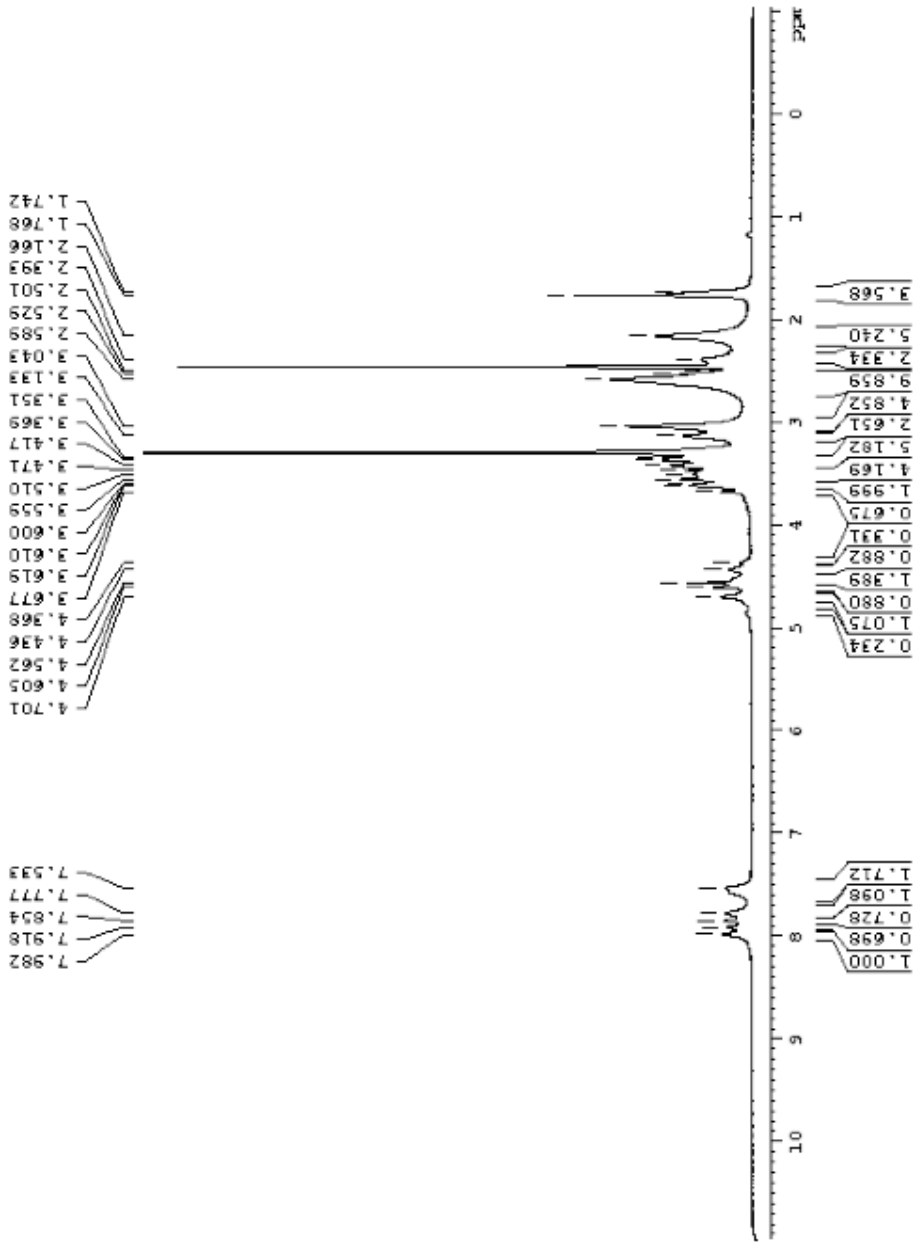

Figure 23 ^{1}H NMR spectrum (500 MHz, d_6-DMSO) of 6d (deacetylated).

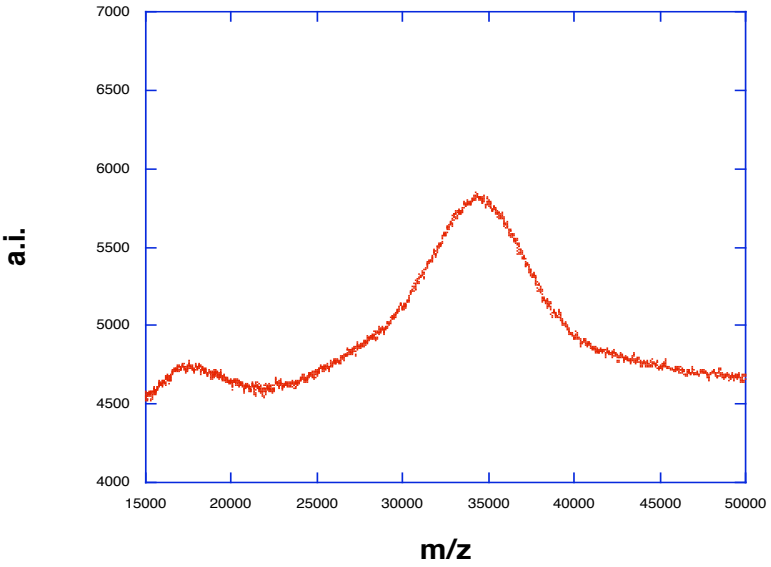

Figure 24 MALDI-TOF spectra of 4c peracylated. M_W = 34200 g/mol, PDI = 1.02

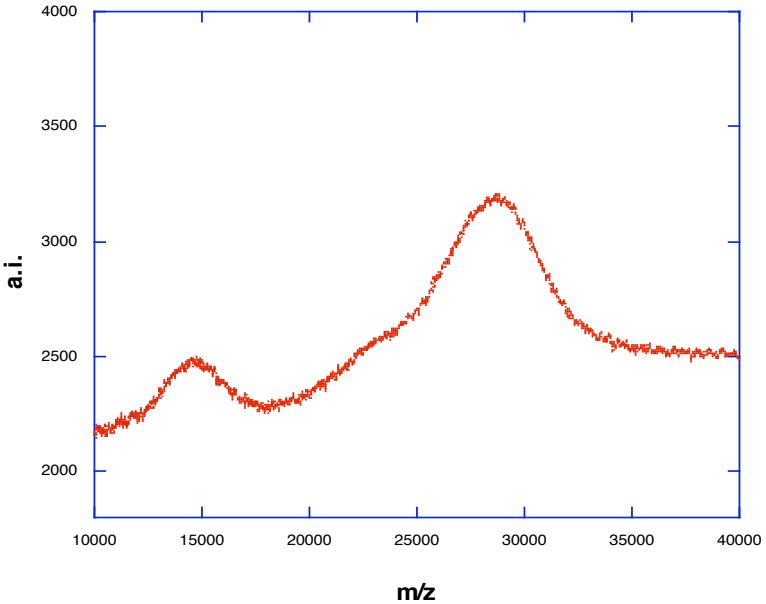

Figure 25 MALDI-TOF spectra of 4c deacylated, M_W = 27700 g/mol, PDI = 1.01.

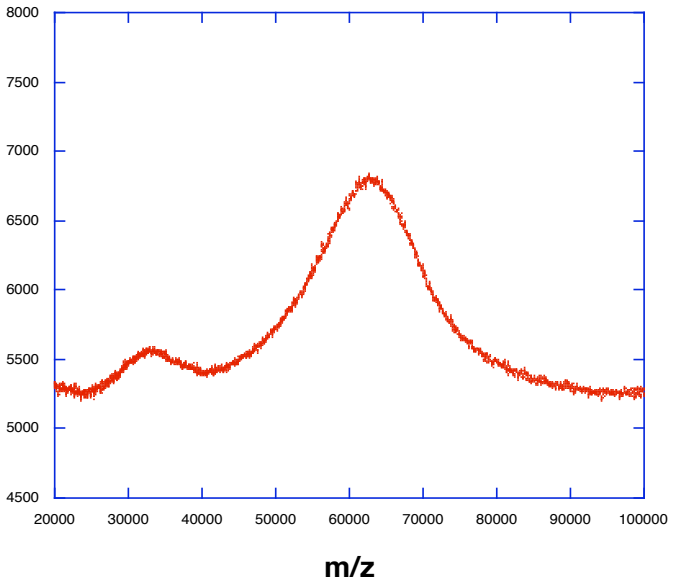

Figure 26 MALDI-TOF spectra of 5d peracylated. M_W = 63500 g/mol, PDI = 1.02.

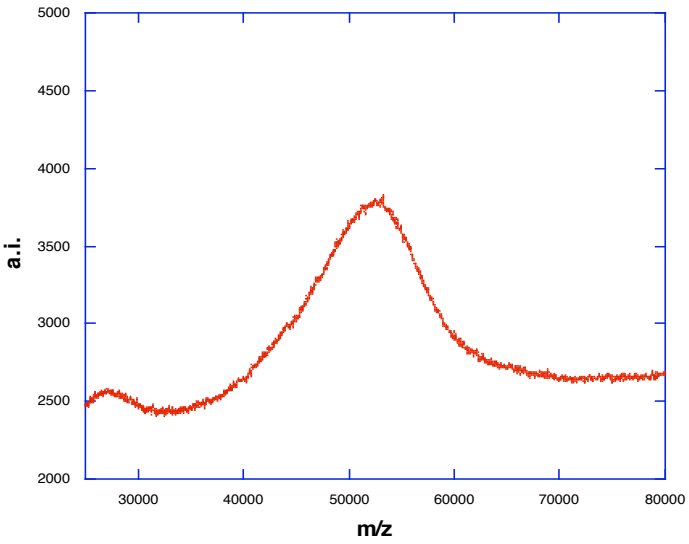

Figure 27 MALDI-TOF spectra of 5d deacylated, M_W = 54000 g/mol, PDI = 1.01

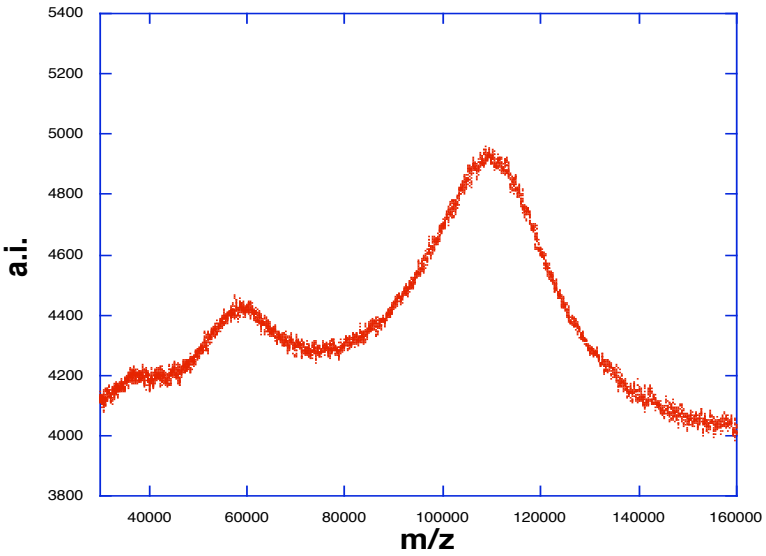

Figure 28 MALDI-TOF spectra of 6c peracylated. M_W = 115000, PDI = 1.02

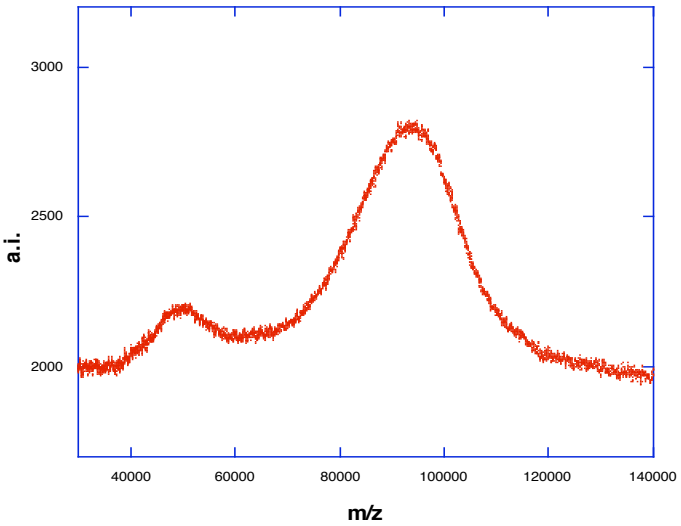

Figure 29 MALDI-TOF spectra of 6c deacylated, M_W = 94500 g/mol, PDI = 1.01

CHAPTER 3

SYNTHESIS AND EVALUATION OF MANNOSE:GLUCOSE FUNCTIONALIZED DENDRIMERS

Introduction

In the previous chapter a model that Whitesides *et al*. proposed a relationship between degree of multivalency and binding affinity with respect to the monomer (see equation 1 and the discussion section below) was investigated, and the results can be described well by this model; changes in activity could be predictably introduced into a multivalent dendritic system. [87]

$$K_N^{poly} = (K^{mono})^{\alpha N} \qquad \text{(eq. 1)}$$

Here, the full study is described, with a larger library of dendrimers bearing varying amounts of mannose, glucose, and galactose residues, and with additional assays to evaluate the protein-carbohydrate interaction. Binding trends are reported for dendrimers of different generations bearing presentations of ligands with varying affinities for Con A. Hemagglutination assay results to show changes in activity with Con A are presented, and precipitation assay results to show how protein activity and protein clustering can be independently attenuated are described.

Results

Synthesis and Characterization of Carbohydrate Functionalized PAMAM Dendrimers.

A general procedure for functionalization of the dendrimers with two or three carbohydrates is shown in Scheme 3. Mannose/glucose/galactose, mannose/glucose, glucose/galactose, and mannose/galactose functionalized dendrimers were synthesized as shown for mannose in Scheme 3. To retain the α-anomeric integrity of the carbohydrates, allylation of the anomeric position and thiol addition to the olefin was performed. [89] The subsequently formed peracylated isothiocyanto sugars 2 were added sequentially to a solution of PAMAM dendrimer in DMSO. [93] When adding more than one sugar to the PAMAM dendrimer, incomplete loading was observed. The addition of excess isothiocyanato sugar with mild warming did not induce further loading to any significant extent. A third isothiocyanato sugar or isothiocyanato alcohol 3 also failed to give full loading (steps 3 and 5 in Scheme 3, step 3 was omitted when only two carbohydrates were added to the dendrimer), indicating that any remaining primary amines on the dendrimer were inaccessible for reaction with the desired isothiocyanates. Global deprotection via Zemplen conditions in 1:1 MeOH : H_2O and purification by centrifugal filtration in water and lyophilization afforded compounds 4a–n, 5a–n, 6a–l and 7a–l. The compound numbers 4–7 indicate the generation of the dendrimer that was used (G(3) = 4, G(4) = 5, G(5) = 6, G(6) = 7), and the letters indicate the number and nature of the sugars that

are added to the dendrimers. The sugar composition of each dendrimer is given in Tables 4-7. Although not shown in Scheme 3, addition of 3 to protected carbohydrate-functionalized dendrimers (reversal of steps 4 and 5 in Scheme 3) also failed to increase the carbohydrate loadings of the dendrimers.

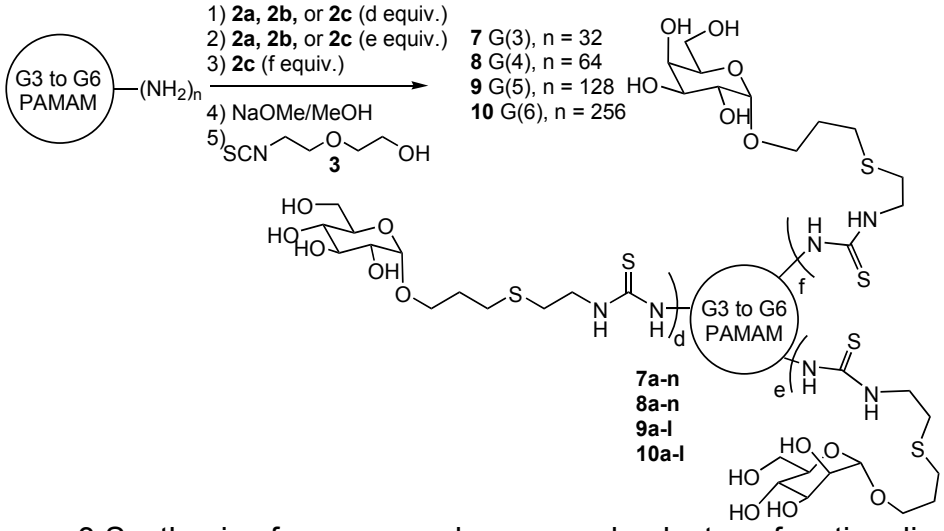

Scheme 3 Synthesis of mannose, glucose, and galactose functionalized dendrimers. Letters after 7–10 correlate the number of mannose, glucose, and galactose residues present on each dendrimer (see Tables 4-7). The amount of 2 added in each reaction is provided in the experimental section.

Characterization of Carbohydrate Functionalized PAMAM Dendrimers

MALDI-TOF MS was used to determine the number of carbohydrate residues of each type on the dendrimers. Both the change in M_W after each sequential addition and the change in M_W after deacylation were used. Details of the calculations are provided in the supporting information. The MALDI-TOF MS-derived number of sugars tethered to each dendrimer is shown in Tables 4-7. Data for man/glc/gal functionalized dendrimers is reported in Table 4, data for man/glc functionalized dendrimers is reported in Table 5, data for glc/gal

functionalized dendrimers is reported in Table 6, and data for man/gal functionalized dendrimers is reported in Table 7. Although NMR spectra revealed that the carbohydrates had been successfully added to the dendrimers (downfield thiourea peaks appear in the ^{1}H NMR spectra, for example), the spectra were broadened and overlapped such that the integration ratios could not be used to quantify carbohydrate loadings. The ^{1}H NMR spectra did reveal the level of deprotection of the acetyl groups, since these methyl groups caused sharp distinctive peaks at ~ 2 ppm.

Table 4 Summary of characterization data for 50% man/glc functionalized dendrimers.

Dendrimer generation	Compound	Mannose residues[a]	Glucose residues[a]	Galactose residues[a]	Rel. activity/active sugar[b]	Con A/dendrimer[c]
3	7a	15	0	11	120	7
3	7b	10	4	9	112	7
3	7c	6	7	8	111	7
3	7d	3	12	7	116	6
3	7e	0	14	7	65	4
4	8a (4a)[d]	30	0	10	3820	12
4	8b (4b)[d]	24	7	7	2660	13
4	8c (4c)[d]	18	13	9	2260	12
4	8d (4d)[d]	10	26	5	1090	12
4	8e (4e)[d]	0	29	16	260	8
5	9a (5a)[d]	44	0	31	4830	15
5	9b (5b)[d]	38	13	29	3040	14
5	9c (5c)[d]	16	40	18	1270	14
5	9d (5d)[d]	0	45	31	310	13
6	10a (6a)[d]	53	0	73	5350	25
6	10b (6b)[d]	34	35	55	3510	23
6	10c (6c)[d]	16	50	55	2150	23
6	10d (6d)[d]	0	77	51	470	18

a. Average number of sugar residues was determined using MALDI-TOF MS data. See experimental procedures for details.
b. Active sugar = man + glc. Standard deviation values were no more than 46%. All values represent at least three trials. Relative activity of methyl mannose = 1.
c. All values represent at least three trials.
d. Compounds from chapter 2, for continuity and clarity these compounds are numbered in order with the other series compounds for this chapter.

Table 5 Summary of characterization data for man/glc functionalized dendrimers.

Dendrimer generation	Compound	Mannose residues[a]	Glucose residues[a]	Galactose residues[a]	Rel. activity/active sugar[b]	Con A/dendrimer[c]
3	7f	0	28	0	60	5
3	7g	5	19	0	190	6
3	7h	13	11	0	480	ND[d]
3	7i	11	12	0	311	7
3	7l	28	0	0	490	7
4	8f	0	60	0	370	8
4	8g	4	45	0	280	12
4	8h	12	27	0	390	12
4	8i	19	21	0	830	12
4	8l	60	0	0	1030	13
5	9e	0	104	0	380	14
5	9f	13	57	0	760	17
5	9g	33	40	0	980	ND[d]
5	9h	39	34	0	1350	16
5	9i	104	0	0	1780	17
6	10e	0	172	0	690	18
6	10f	33	72	0	960	25
6	10g	48	61	0	1540	26
6	10h	176	0	0	2460	25

a. Average number of sugar residues was determined using MALDI-TOF MS data. See experimental procedures for details.
b. Active sugar = man + glc. Standard deviation values were no more than 46%. All values represent at least three trials. Relative activity of methyl mannose = 1.
c. All values represent at least three trials.
d. ND = not determined.

Table 6 Summary of characterization data for glc/gal functionalized dendrimers.

Dendrimer generation	Compound	Mannose residues[a]	Glucose residues[a]	Galactose residues[a]	Rel. activity/active sugar[b]	Con A/dendrimer[c]
3	7k	0	10	10	NR[d]	5
3	7e	0	14	11	65	ND[e]
3	7l	0	18	6	75	8
3	7f	0	28	0	55	7
4	8k	0	20	17	10	8
4	8e	0	29	15	240	8
4	8l	0	43	4	4450	12
4	8f	0	60	0	370	13
5	9j	0	32	35	40	14
5	9d	0	45	31	320	13
5	9k	0	62	14	580	15

Table 6 Continued

Dendrimer generation	Compound	Mannose residues[a]	Glucose residues[a]	Galactose residues[a]	Rel. activity/active sugar[b]	Con A/dendrimer[c]
5	9e	0	104	0	380	16
6	10i	0	47	79	80	20
6	10d	0	77	51	470	18
6	10j	0	80	38	860	21
6	10e	0	172	0	690	22

a. Average number of sugar residues was determined using MALDI-TOF MS data. See experimental procedures for details.
b. Active sugar = man + glc. Standard deviation values were no more than 46%. All values represent at least three trials. Relative activity of methyl mannose = 1.
c. All values represent at least three trials.
d. NR = no response recorded.
e. ND = not determined.

Table 7 Summary of characterization data for man/gal functionalized dendrimers.

Dendrimer generation	Compound	Mannose residues[a]	Glucose residues[a]	Galactose residues[a]	Rel. activity/active sugar[b]	Con A/dendrimer[c]
3	7m	8	0	12	30	6
3	7a	12	0	7	120	7
3	7n	19	0	5	310	7
3	7j	28	0	0	490	7
4	8m	18	0	31	360	12
4	8a	30	0	10	1140	12
4	8n	38	0	9	1150	12
4	8j	60	0	0	1030	13
5	9l	26	0	43	750	17
5	9a	43	0	30	1440	15
5	9i	104	0	0	1780	16
6	10k	30	0	87	2300	17
6	10a	53	0	73	3370	25
6	10l	87	0	33	3170	26
6	10h	176	0	0	2460	25

a. Average number of sugar residues was determined using MALDI-TOF MS data. See experimental procedures for details.
b. Active sugar = man + glc. Standard deviation values were no more than 46%. All values represent at least three trials. Relative activity of methyl mannose = 1.
c. All values represent at least three trials.

Hemagglutination Inhibition Assays.

Hemagglutination inhibition assays were performed by adding erythrocytes to preincubated solutions of Con A (~1 μM) with varying concentrations of dendrimer. [42] The synthesis and analysis of G(4) to G(6) PAMAM dendrimers with fifty percent mannose and glucose incorporation is reported in chapter 2. [24] These dendrimers showed a linear trend for relative activity in the hemagglutination assay (on a per active sugar basis) versus percent mannose of the mannose/glucose mixture and were consistent with a divalent interaction in the model set out by Whitesides *et al*. (see the discussion section below for full details). [4] Here, the G(3) series of 50% mannose/glucose functionalized dendrimers have been added. Mannose/galactose, glucose/galactose and mannose/glucose dendrimers with higher carbohydrate loadings in generations 3 through 6 are also reported. Results of the hemagglutination assays are shown in Tables 4-7. The relative activity numbers in the tables are on a per carbohydrate (glc + man) basis and are relative to methyl mannose. Some of the compounds appear in multiple tables, since assays were performed simultaneously for compounds when their results were to be compared. Different samples of rabbit erythrocytes, and even the relative freshness of erythrocytes from the same blood sample, can affect the absolute (but not the relative) values that are obtained from the hemagglutination assay.

Precipitation Assays

To determine the lectin clustering ability of these dendrimers, precipitation assays were performed. As described by Brewer *et al*., the dendrimer was incubated at varying concentrations with a constant concentration of Con A. [47] When the Con A concentration is sufficiently high, the mannose functionalized dendrimer forms a precipitate with the Con A. The supernatant is removed, and the precipitate is washed with cold buffer and subsequently redissolved with a solution of 0.1 M methyl mannopyranoside solution. The Con A concentration in the remaining solution is then determined by measuring the UV absorbance at 280 nm. At the point that maximum precipitation of Con A is observed, the maximum Con A to dendrimer ratio can be determined. The precipitation assay results are provided in Tables 4-7. As with the hemagglutination assay results, some compounds are listed in more than one table so that trends across a series of carbohydrate loadings are easier to evaluate.

Discussion

Synthesis and Characterization of Carbohydrate-Functionalized Dendrimers.

Dendrimers, macromolecules that are comprised of a series of branches emanating from a central core, [94] are ideal frameworks for the study of how systematic structural changes alter the way that a glycopolymer interacts with a protein. Higher generation dendrimers (PAMAM generations 4-6) are large enough to span multiple binding sites on a lectin, while lower generation

dendrimers (generations 1-3) are too small to bind to multiple binding sites on Con A. In addition to changing the dendrimer generation, the degree of carbohydrate loading on a dendrimer can also be readily changed by controlling the number of equivalents of isothiocyanate that are added to the dendrimer solution. Because systematic changes can readily be made and because the three-dimensional (roughly spherical) structure of the dendrimer lends itself well to data interpretation, dendrimers were chosen as the structural frameworks for our synthetic multivalent systems. Mannose, glucose, and galactose were chosen as ligands because of their known differences in affinity when binding to Con A. Mannose has a fourfold higher affinity for Con A than glucose does, and galactose has no affinity for Con A. [95] Because of the tetrahedral arrangements of the Con A binding sites, even the largest dendrimers used in this study (G(6)) cannot simultaneously bind to more than two of the four binding sites. Thus, for the dendrimer-Con A system, monovalent and divalent (as in Figure 13) associations can be expected to occur.

Reported in chapter 2 is the binding by Con A of mannose/hydroxyl functionalized dendrimers. Optimal activity in the hemagglutination assay was observed when the dendrimers had fifty percent mannose incorporation. Dendrimers with higher mannose loadings had reduced activities with Con A (on a per sugar basis), suggesting that unfavorable steric interactions precluded optimal binding at high carbohydrate functionalization. [96] For the research reported here, the goal was to quantify the effect that functionalization of the

dendrimer with monomers of varying affinities would have on the multivalent activity of the dendrimer with lectins. Because of the previously optimized mannose/hydroxyl functionalized dendritic system, dendrimers with fifty percent functionalization by mannose and glucose were synthesized. The preliminary results with these compounds were reported in chapter 2. Full studies with mannose/glucose functionalized dendrimers at 50% percent combined loading of mannose and glucose are the subject of this chapter, Including complete studies with mannose/glucose, mannose/galactose, and glucose/galactose functionalized dendrimers are reported.

The synthesis scheme for dendrimer functionalization is shown in Scheme 3. When multiple sugars were added to the PAMAM dendrimers, incomplete addition of the final carbohydrate was observed. The excess isothiocyanate could be monitored by ^{1}H NMR, with the methylene group alpha to the isothiocyanato group giving rise to a triplet at 3.8 ppm. To cap any remaining accessible terminal amines, reactions with excess isothiocyanato sugars and with isothiocyanato ethoxyethanol 3 were heated to 40 ºC. When neither of these additions was successful, it was concluded that no primary amines were accessible on the periphery of the carbohydrate functionalized dendrimers. Unfunctionalized primary amines near the dendrimer surface could be protonated at physiological pH and could cause nonspecific interactions with Con A during assays. However, control hemagglutination assay and precipitation assay experiments with unfunctionalized PAMAMs and Con A indicated no interaction between the

amine-functionalized PAMAM dendrimers and the protein. The degree of carbohydrate functionalization was in all cases determined by MALDI-TOF MS. Details of the MALDI-TOF MS characterization procedure are provided in the experimental procedures section, and the resultant number of sugars is reported in Tables 4 through 7.

Hemagglutination Inhibition Assays Using Dendrimers with 50% Mannose/Glucose Incorporation.

In Figure 30, the activity with Con A of dendrimers with 50% combined functionalization by mannose and glucose (4a–e, 5a–e, 6a–d, 7a–d) is shown. When dendrimers are fifty percent functionalized with man/glc mixtures, the relative amounts of glucose and mannose induce a linear change in the relative activity for generation 4, 5, and 6 dendrimers. The difference in relative activity between glucose-functionalized and mannose-functionalized dendrimers in the G(4) series (5a vs. 5e) is 14.7, the difference for G(5) dendrimers (6a vs. 6d) is 15.6 and the difference for G(6) dendrimers (7a vs. 7d) is 11.4. Dendrimers with partial mannose and partial glucose incorporation fall linearly between the all mannose and all glucose-functionalized dendrimers. In the G(3) series, all of the dendrimers have comparable activities toward Con A. This is as expected, since carbohydrate functionalized G(3) PAMAMs are too small to bind divalently to Con A, and only monovalent associations are likely.

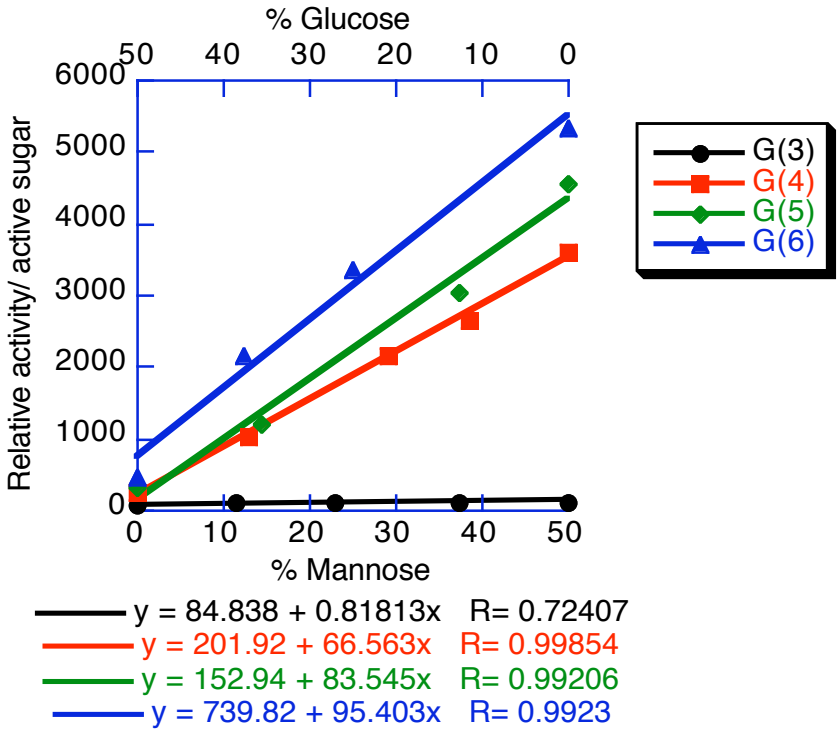

Figure 30 Relative activity per active sugar (man + glc) for dendrimers with 50% man/glc functionalization (see Table 3.1 for compound numbers and values).

Equation 1 was used to evaluate the hemagglutination assay data for compounds 5a–e, 6a–d, and 7a–d. In equation one, K^{mono} is the monovalent association constant, K_N^{poly} is the multivalent association constant, N is the number of receptor-ligand interactions, and α is the cooperativity factor. Here, a cooperativity constant α of 1 was used. Negatively cooperative, positively cooperative, and non-cooperative systems are all theoretically possible. However, only one or two examples of protein-carbohydrate interactions with thermodynamic parameters suggestive of positive cooperativity have been reported. [4] Negatively cooperative and non-cooperative systems are much more common. Due to precedent where non-cooperative associations were assumed

for Con A[96], α is left as 1 and because a Con A-dendrimer interaction where the first binding event at one binding site is thermodynamically significantly different from the second binding event at a second binding site is not expected. Although the appropriate value of N for this system cannot be assigned with absolute certainty (because precipitation occurs under conditions appropriate for ITC), N must surely be equal to one or two. The shape of tetrameric Con A and the relative locations of the mannose binding sites on tetrameric Con A preclude trivalent or tetravalent binding by a roughly spherical, dendritic system. Although a value of N = 1 is possible, N = 2 is suggested for 5–7 by the results of precipitation assay experiments, transmission electron micrographs, and hemagglutination assays.[24, 87, 97]

Using equation 1, and assuming α = 1 and N = 2, one would predict that exchanging mannose for glucose would cause a 4^2 or 16-fold reduction in binding to Con A, since the relative activities of monomeric methyl mannose and methyl glucose vary by a factor of four. This is very close to the values observed for G(4) (14.6), G(5) (15.6), and G(6) (11.4). Perhaps the larger deviation from 16 for G(6) is due to the larger size of G(6), which could allow for a compensatory effect due to increased sugar clustering around the binding sites. [82] Alternatively, the curvature of the G(6) dendrimers may be different enough from G(4) and G(5) to change the shape complementarity between Con A and the dendrimer, which can significantly change the association motif. [97]

Hemagglutination Inhibition Assays using
Mannose/Glucose Functionalized Dendrimers

The activity with Con A of man/glc functionalized dendrimers 7f–7j, 8f–8j, 9e–9i, 10e–10h is shown in Figure 30. Increasing the number of mannose residues while decreasing the number of glucose residues causes an increase in the relative activity with Con A. As with the dendrimers bearing 50% mannose/glucose loading, a linear relationship between man/glc loading and assay activity is observed. However, the difference between fully mannose functionalized dendrimers and fully glucose functionalized dendrimers never approaches 16. For generation three compounds 7f–7j, mannose functionalized compounds 7j have an eight-fold higher relative activity with Con A than do the glucose functionalized compounds 7f. For generations four, five, and six, the differences between mannose and glucose-functionalized compounds are 2.8 (8f vs. 8j), 4.7 (9e vs. 9i), and 3.7 (10e vs. 10h), respectively. Also, having more than 50% loading by the active sugars decreases the assay activity (for example, 9b is about twice as active as 9h).

Previously lower affinity of dendrimers above 50% sugar loading has been attributed to unfavorable steric interactions between the dendrimer and the protein. [24] The deviation from the 16-fold affinity difference predicted by equation 1 and the reduced activity for compounds with higher than 50% loading suggest that the degree of clustering of the sugars may be more important for some compounds than for others. Dendrimers with higher glucose content have lower intrinsic binding affinities for Con A (than highly mannose functionalized

dendrimers) and may rely more on statistical binding effects. Differences in how the dendrimers overcome unfavorable steric crowding coupled to differences in how important clustering of carbohydrates is could cause the cooperativity constant α to change from one and could account for the fact that the difference between mannose and glucose functionalized dendrimers is significantly lower than 16.

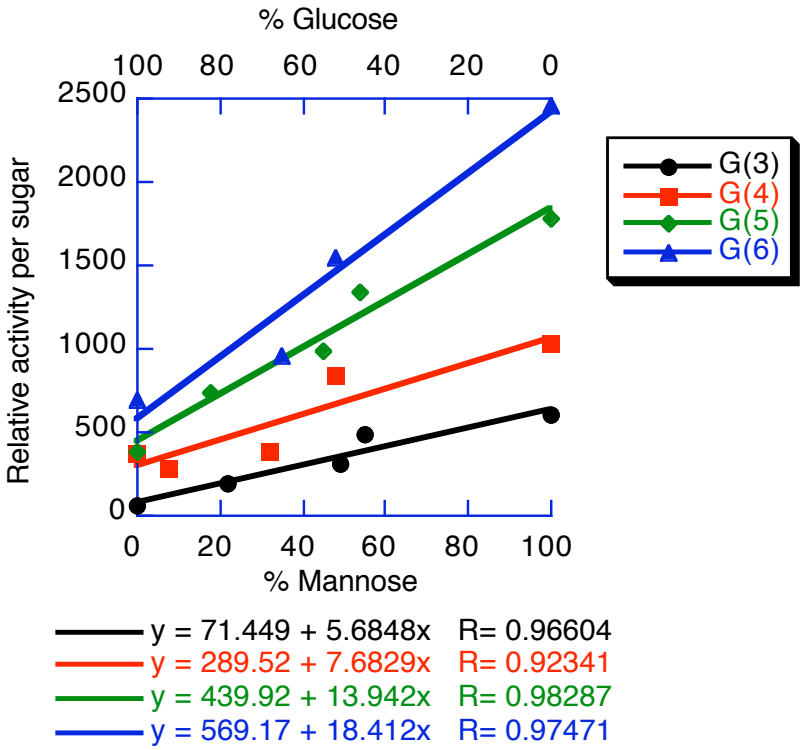

Figure 31 Relative activity per active sugar (man + glc) for man/glc functionalized dendrimers (see Table 3.2 for compound numbers and values).

Hemagglutination Inhibition Assays with
Mannose/Galactose and Glucose/Galactose Functionalized Dendrimers.

The activities with Con A of glc/gal and man/gal functionalized dendrimers (7e,f,k–n, 8e,f,j–n, 9d–f,j–l, 10d,e,i–l) are shown in Figures 31 and 32. All of the glc/gal dendrimers have lower activities than their analogous man/gal dendrimers. In the G(3) series, the glc/gal dendrimers with the highest activity are 6.5 times less active than the highest activity man/gal dendrimers (7j vs. 7l). In generations 4-6, the glc/gal dendrimers with the highest activity are 2.6 times (8n vs. 8l), 2.5-3.1 times (9a or 9i vs. 9k), and 3.7-3.9 times (10a or 10l vs. 10j) less active. These differences are considerably lower than those observed for the 50% functionalized mannose/glucose series (Figure 31), where nearly 16-fold differences in activity were observed.

Following trends that were previously observed for mannose/hydroxyl functionalized dendrimers, [81] the fully carbohydrate functionalized dendrimers have lower relative activities (on a per sugar basis) than the partially carbohydrate functionalized dendrimers do. Man/gal functionalized dendrimers have optimum activity with Con A at 50-60% mannose incorporation (G(4)), 40-50% mannose incorporation (G(5)), and 30-40% mannose incorporation (G(6)). Higher glucose loadings are required to achieve optimal activity with glc/gal dendrimers; roughly 70%, 60%, and 50% glucose functionalization produced the highest activity with Con A for generations 4, 5, and 6, respectively. This is of interest as it may indicate that, with a weaker interaction, proximity/statistical effects are more important to binding. Both the man/gal and the glc/gal G(3)

dendrimers have relatively low activity toward Con A in the assay, as would be expected for small dendrimers where statistical enhancements on binding affinity (and not multivalency) are observed.

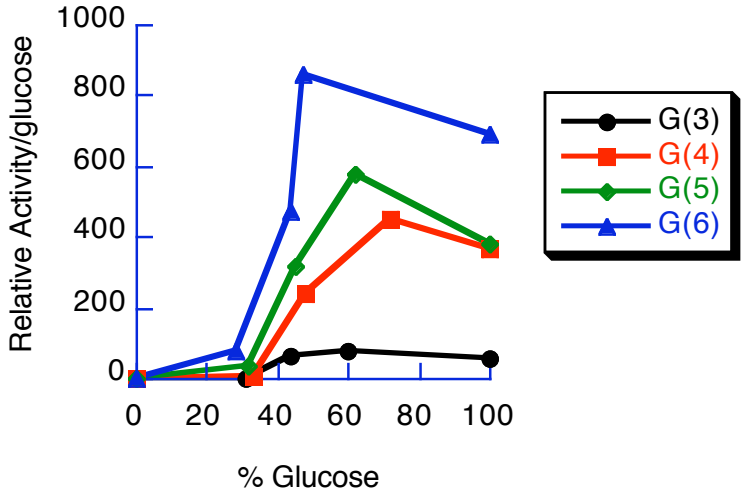

Figure 32 Relative activity per glucose for glc/gal functionalized dendrimers (see Table 6 for compound numbers and values).

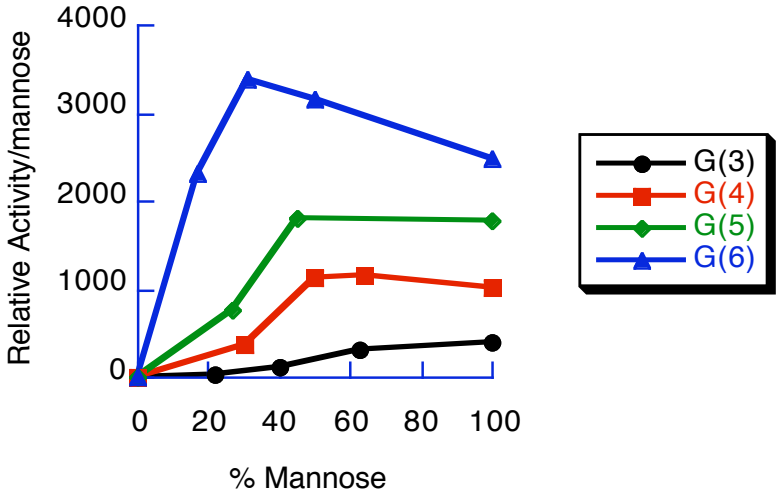

Figure 33 Relative activity per mannose for man/gal functionalized dendrimers (see Table 7 for compound numbers and values).

Hemagglutination inhibition assays in general. Taken together, the data from the four series of compounds above suggests that, for optimized systems, equation 1 works well to predict how monovalent ligands displayed on a multivalent framework attenuate binding activity. However, the system must be optimized, or affinity differences much lower than those predicted by equation 1 will be obtained. When low affinity ligands (such as glucose) are present in significant quantities, proximity effects may become more important than they are when higher affinity ligands (such as mannose) are present as the major functionality.

Precipitation Assays

Graphs showing the maximum number of Con A lectins recruited by each dendrimer are shown in Figure 34. Figure 34a shows the Con A : dendrimer ratio for 50% mannose/glucose functionalized dendrimers, Figure 34b shows the Con A : dendrimer ratio for mannose/glucose functionalized dendrimers, Figure 34c shows the Con A : dendrimer ratio for mannose/galactose functionalized dendrimers, and Figure 34d shows the Con A : dendrimer ratio for glucose/galactose functionalized dendrimers. The maximum average number of Con A's that can fit around carbohydrate functionalized dendrimers was previously determined to be 9-10, 12-13, 15-16 and 22-23 for G(3) through G(6), respectively. [24] For all of the series shown here, the G(3) dendrimers recruit less than the optimal number of Con A lectins. This suggests that Con A binds monovalently to all of the G(3)-PAMAMs, reducing the strength of the association and causing unoptimized binding to occur. [98] All carbohydrate-functionalized G(4)

and G(5) PAMAMs recruit the optimal number of Con A lectins, while the carbohydrate-functionalized G(6)-PAMAMs typically bind to slightly more than the theoretically determined number of proteins. [99] The 50% man/glc functionalized compounds 8a-e, 9a-d and 10a-d show no change in clustering until all the active sugar is glucose, then the ratio's drop from 12-13 to 8, 14-15 to 13 and 23-25 to 18 respectively (Figure 34a). Comparable trends are observed for man/glc functionalized dendrimers with higher ligand loadings (Figure 34b). Similarly, in the man/gal series (Figure 34c) and the glc/gal series (Figure 34d), the maximum number of Con A lectins that can be recruited are clustered around the dendrimers when at least 25% of the carbohydrates are Con A binding ligands. Glc/gal dendrimers appear to show small increases in Con A recruitment with increased glucose functionalization, but man/gal dendrimers level off after 25% mannose incorporation. The number of Con A lectins recruited is the same for generations 3-5. For generation 6, man/gal functionalized dendrimers cluster consistently more Con A lectins (25-26 lectins) than glc/gal functionalized dendrimers do (18-22 lectins). Control dendrimers with only galactose functionalization fail to precipitate Con A. The precipitation assay results indicate that the number of Con A lectins that can be recruited by a dendrimer is not greatly affected when the relative activity (as determined in the hemagglutination assays) is altered by an order of magnitude.

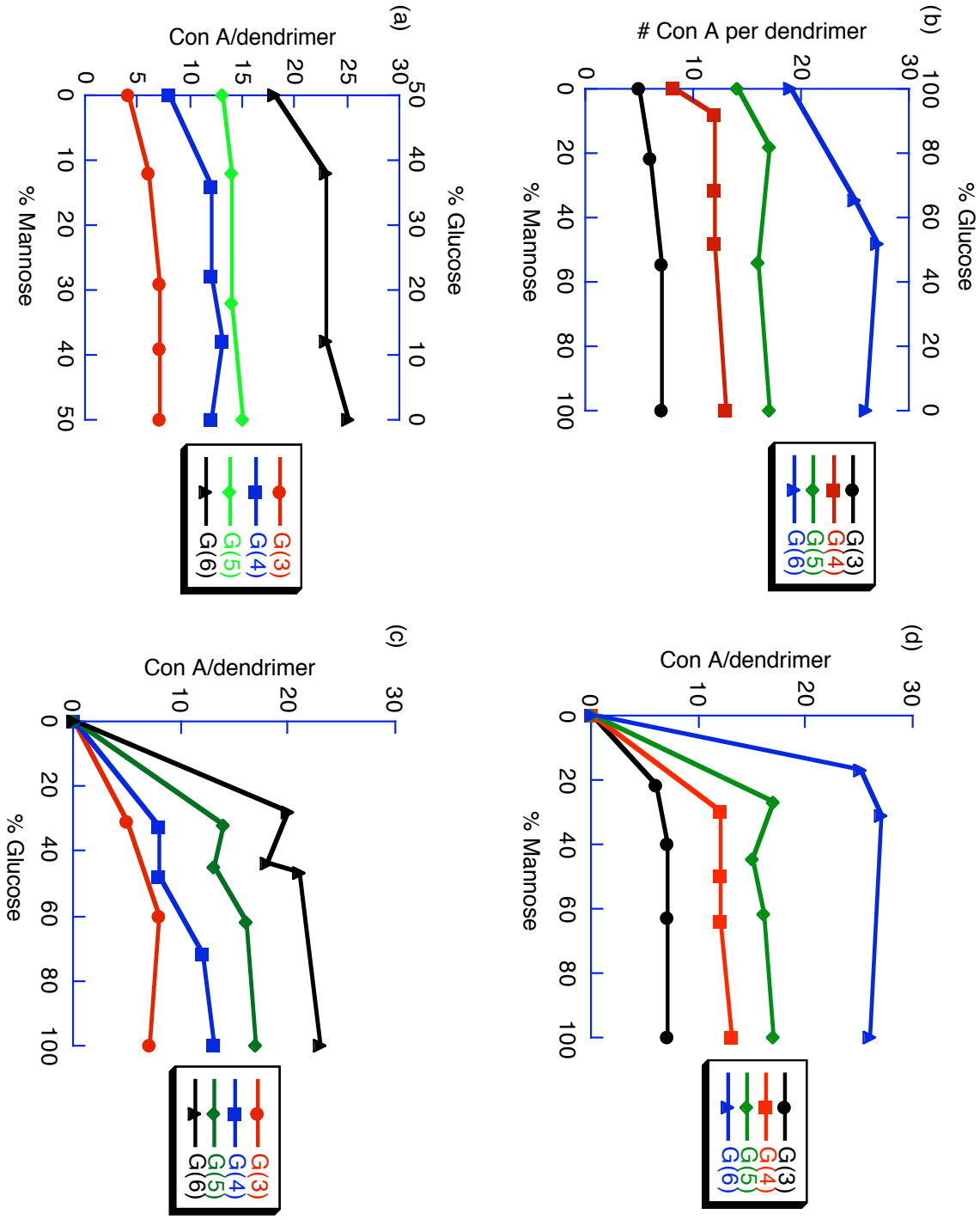

Figure 34 Number of Con A lectins per dendrimer (a) dendrimers with 50% man/glc functionalization, (b) man/glc functionalized dendrimers (c) glc/gal functionalized dendrimers (d) man/gal functionalized dendrimers. Values are given in Tables 4-7.

Conclusion

Multivalent binding between proteins and carbohydrates mediates many biological events. The goal of the research reported here was to determine whether monovalent differences in affinity affect multivalent association constants in predictable ways. For optimized systems such as the dendrimers with 50% loading of mannose and glucose, the equation described by Whitesides and co-workers (equation one) works well to predict how monovalent ligands displayed on a multivalent framework will attenuate binding activity. For more highly functionalized man/glc, man/gal, and glc/gal dendrimers, activity differences for hemagglutination assays with Con A that were much lower than those predicted by equation one were obtained. For this system, dendrimers with more glucose residues appear to compensate for the steric downfall of full functionalization by relying more on proximity enhancements than mannose functionalized dendrimers do. Although varying the ligands on the dendrimer can cause up to sixteen-fold differences in relative activity in the hemagglutination assay, only small differences in the maximum number of Con A lectins recruited by the dendrimers were observed.

The results reported here suggest that multivalency can be influenced in predictable–and therefore tunable–ways. Monovalent differences are amplified by multivalent associations, and mixtures of low and high affinity ligands can be used to attenuate multivalent binding activities. Attenuation of the binding activity

(as studied in the hemagglutination assay) is largely independent of the degree of protein clustering (as measured in the precipitation assay). Natural systems likely use modulation of properties such as avidity and protein clustering to control physiological processes. Because of their ready tunability, the carbohydrate functionalized dendrimers described here should provide guidelines for the development of synthetic multivalent frameworks for many applications in chemical biology. Studies are currently underway to investigate how these results will transpose into more complex biological systems.

Experimental Procedures

General methods. General reagents were purchased from Acros and Aldrich Chemical Companies. PAMAM dendrimers were purchased from Dendritech. Concanavalin A (Con A) was purchased from Calbiochem. Methylene Chloride was purified on basic alumina; other solvents were used as received. 32-63μ “40 micron flash” silica gel for flash column chromatography purification was purchased from Scientific Adsorbants Incorporated. Centrifugal devices used were Millipore amicon ultra 4 mL 5000 M_w and 10000 M_w cutoff filters. For dialysis, spectrum laboratories membranes, diameter 11.5 mm, 1000 M_w and 3500 M_w cutoff, in 0.1% sodium azide solution were used.

Matrix Assisted Laser Desorption
Ionization MS (MALDI)

Matrix assisted laser desorption ionization mass spectra were acquired using a Bruker Biflex-III time-of-flight mass spectrometer. Spectra of all functionalized dendrimers were obtained using a *trans*-3-indoleacrylic acid matrix with a matrix-analyte ratio of 3000:1 or 1000:1. Bovine serum albumin (MW 66,431 g/mol), Cytochrome C (MW 12,361 g/mol), and Trypsinogen (MW 23,982 g/mol) were used as external standards. An aliquot corresponding to 12-15 pmol of the analyte was deposited on the laser target. Positive ion mass spectra were acquired in linear mode, and the ions were generated by using a nitrogen laser (337 nm) pulsed at 3 Hz with a pulse width of 3 nanoseconds. Ions were accelerated at 19,000-20,000 volts and amplified using a discrete dynode multiplier. Spectra (100 to 200) were summed into a LeCroy LSA1000 high-speed signal digitizer. All data processing was performed using Bruker XMass/XTOF V 5.0.2. Molecular mass data and polydispersities (PDI) of the broad peaks were calculated by using the Polymer Module included in the software package. The peaks were analyzed using the *continuous* mode. The M_W for unfunctionalized generation 3, 4, 5, and 6 PAMAM dendrimers was determined to be 6,800 g/mol, 13,500 g/mol, 25,500 g/mol and 50,000 g/mol, respectively. MALDI-TOF MS spectra were obtained after each addition of isothiocyanate, and the change in M_w upon the first addition was divided by the M_w of the isothiocyanato carbohydrate (507 g/mol) to give a quantity that is denoted here as A (equation 2). The total number of carbohydrate residues (B in

equation 3) was determined by subtracting M_w for unfunctionalized PAMAM from the M_w after all the sequential additions of isothiocyanates and then dividing by 507 g/mol. The total number of carbohydrate residues was also determined by dividing the change in M_w upon deacylation by 168 (the loss of 4 acetyl groups per sugar), and this number is denoted as B' (equation 4). The percentage of the first carbohydrate that makes up the total carbohydrate addition (C, equation 5) was determined by taking A over B (and then multiplying by 100). The number of residues of the first sugar was also obtained by multiplying C times B' to give A' as shown in equation 6. The values of A and A' were then averaged (equation 7) to obtain the most accurate value for how many residues of the first isothiocyanato sugar (and also by difference for how many residues of the second isothiocyanato sugar) were added to the dendrimer. Sample numbers using data from compound 5c are provided in the equations below.

$$A = \frac{M_w \text{ (one RNCS addition)} - M_w \text{ (PAMAM)}}{507} = \frac{22{,}900 - 13{,}500}{507} = 18.5 \qquad \text{(eq. 2)}$$

$$B = \frac{M_w \text{ (all RNCS additions)} - M_w \text{ (PAMAM)}}{507} = \frac{34{,}200 - 13{,}500}{507} = 40.8 \qquad \text{(eq. 3)}$$

$$B' = \frac{M_w \text{ (all RNCS added)} - M_w \text{ (deacetylated)}}{168} = \frac{34,\ 200 - 27,\ 700}{168} = 38.7 \qquad \text{(eq. 4)}$$

$$C = A/B = 18.5/40.8 = 0.454 \qquad \text{(eq. 5)}$$

$$A' = B' \times C = 38.7 \times 0.454 = 17.6 \qquad \text{(eq. 6)}$$

$$\frac{A + A'}{2} = \frac{18.5 + 17.6}{2} = 18 \qquad \text{(eq. 7)}$$

NMR

^{1}H NMR spectra were recorded on Bruker DPX 300 (300 MHz) and Bruker DPX-500 (500 MHz) spectrometers. Chemical shifts are reported in ppm from tetramethylsilane with the residual protic solvent resonance as the internal standard (chloroform: δ 7.25 ppm; dimethyl sulfoxide: δ 2.50 ppm). Data are reported as follows: chemical shift, multiplicity (s = singlet, bs = broad singlet, d = doublet, t = triplet, q = quartet, p = pentet, m = multiplet, app = apparent), integration, coupling constants (in Hz) and assignments. ^{13}C NMR spectra were recorded on a Bruker DPX 500 (125 MHz) spectrometer with complete proton decoupling. Chemical shifts are reported in ppm from tetramethylsilane with the solvent as the internal standard ($CDCl_3$: δ 77.0 ppm).

General Hemagglutination Inhibition
Assay Procedures

Concanavalin A Preparation: In a 10 mL centrifuge tube, approximately 5 mg of Concanavalin A (Con A) was dissolved without agitation in 10 mL of HEPES buffer with 100 μM $CaCl_2$ (pH = 8.5). The tube was stored at 4 ºC for 8 hours to allow the Con A to dissolve. Afterwards, the solution was placed in a dialysis tube and dialyzed against 1 L of tris buffered saline (TBS) for 4 hours. This was repeated with fresh TBS solution and followed by dialysis against 1 L of phosphate-buffered saline (PBS) for 8 hours. The dialysis was done to remove any excess Ca^{2+} from the lectin solution. The Con A solution was removed from the tube and stored at 4 ºC until needed.

Blood Preparation*:* Fresh whole rabbit blood was obtained from the MSU animal care center in 4 mL vials. Alsever's solution was added to the blood to make up a 60:40 v/v solution. The blood was separated into 2 mL aliquots in 15 mL centrifuge tubes. These were then diluted to 12 mL with Alsevers solution. The cells were pelleted by centrifugation (1100 rpm x 10 min), and the layer of white blood cells and plasma proteins was removed by pipette. This process was repeated 2 more times using PBS instead of Alsever's solution. The blood was then made up in the assay buffer solution, PBS with 0.5% BSA.

Concanavalin A Titration: Decreasing amounts of Con A were incubated with red blood cells to determine the lectin concentration needed to agglutinate cells. Serial two fold dilutions were made by adding 50 μL of Con A solution to the first well, then 50 μL of buffer solution to all 24 wells. 50 μL was then transferred from the first well to the second. The second well was mixed and 50 μL was transferred to the third well. This procedure was repeated until the 24th was ll two fold serial dilutions. To each well 50 μL of the blood solution was added and incubated for 2 hours at 22-25 ^{o}C. After this time the wells were examined and the amount of Con A required to agglutinate was determined. This was then considered to be 1 unit. For the inhibition assay an 8 unit Con A solution was made up and the concentration of Con A determined by spectrophotometric analysis.

Inhibiting Dose Determination: Starting with a concentration of 5 mg/mL, serial two-fold dilutions of the inhibitors were made as described above. the inhibitor

solutions were incubated with 50 μL of the 8 unit Con A solution for 2-3 hours at 22-25^{o}C. the minimum concentration causing inhibition was determined and this was the inhibiting dose. The HI assays of all compounds that are directly compared in Tables 4-7 were preformed simultaneously to provide the exact same conditions, enabling an accurate comparison of relative activity. The values given are the average of three or more independent measurements.

General Precipitation Assay Procedure

The assay was performed at 22 ºC in 0.1 M Tris/HCl buffer, pH 7.2, containing 0.15 M NaCl, 1 mM $CaCl_2$ and 1 mM $MnCl_2$. Con A (500 μL, 66 μM) was added to 500 μL of a two-fold serial dilution of carbohydrate-functionalized dendrimers. The mixtures were allowed to sit for 20 h. The solutions were centrifuged (3000 rpm for 5 minutes) to pellet the precipitate. The pellets were washed with 500 μL of cold buffer three times. The precipitates were dissolved in 500 μL of 0.1 M methyl mannoside solution and diluted with 1000 μL of buffer. The concentration of Con A in each solution was determined by UV at 280 nm using an extinction coefficient at 280 nm of 1.37 for a 1 mg/mL solution. The values given are the average of three independent measurements.

Experimental procedures and ^{1}H NMR, ^{13}C NMR and MS data for compounds 1a-c, 2a-c and 3; ^{1}H NMR spectra for 8c (4c), 9e (5e) and 10d (6d), and MALDI-TOF spectra for 8c (4c), 9d (5d) and 10c (6c) can be found in Chapter 2.

^{1}H NMR data for 8a-e, 9a-d and 10a-d can be found in the experimental procedures section of chapter 2.

4a-n. Representative procedure for the synthesis of heterogeneously functionalized generation 3.0 PAMAM-based thiourea-linked 1-O-(6-thiourea-4-thiohexyl)- 2,3,4,6-tetra-O-acetyl -α-D-galactopyranoside, 1-O-(6- thiourea-4-thiohexyl)- 2,3,4,6-tetra-O-acetyl -α-D-glucopyranoside, 1-O-(6- thiourea-4-thiohexyl)- 2,3,4,6-tetra-O-acetyl -α-D-mannopyranoside. An aqueous solution of amine terminated Starburst G(3)-PAMAM dendrimer (1.925 g of a 18% w/w solution in water, 346.4 mg, 50.9 μmol) was lyophilized to leave a foamy residue. 5.78 mL of DMSO was then added to this residue to give a 60 mg/mL solution. 0.047 mL of a 300 mM solution of 2a (14.1 μmol, 6.84 mg) in DMSO was added to 0.5 mL of a 60 mg/mL G(3) PAMAM dendrimer (30 mg, 4.40 μmol) solution. The reaction was stirred for 48 hrs at which point a 75 μL aliquot was removed for MALDI-TOF analysis. After MALDI-TOF indicated reaction completion, 0.17 mL of a 300 mg/mL solution of 2b (49.4 μmol, 20.14 mg) was added. The solution was then stirred for 48 hrs. At this time a 75 μL aliquot was removed for analysis. After MALDI-TOF indicated reaction completion, 0.19 mL of a 300 mg/mL solution of 2c (58.3 μmol, 23.43 mg) was added and let stir for 48 hrs, when a 75 μL aliquot was removed for analysis. According to MALDI-TOF analysis the final addition proved to be unsuccessful at fully functionalizing all terminal amine groups so an additional spacer was added. 47.1 mg (30 μmol) of 3 in DMSO was added and let stir at room temperature for 2 days. Again MALDI-

TOF analysis indicated no further addition. This step was repeated with mild warming (up to 40 ºC) and vigorous stirring. MALDI-TOF analysis again indicated no addition, hence the product was taken forward.

Table 8 Amounts of compounds that were used for the experimental procedure above for the synthesis of 7a-7n.

G3	Pamam (μmol)	mannose (μmol)	Glucose (μmol)	Galactose (μmol)	Ethoxy ethanol (μmol)
7a	4.4	70.6	0	57.0	30
7b	4.4	56.5	12.6	57.0	30
7c	4.4	35.3	32.2	57.0	30
7d	4.4	14.1	51.0	57.0	30
7e	4.4	0	70.6	57.0	30
7f	4.4	0	150.0	0	0
7g	4.4	17.0*	106.2*	0	30
7h	2.9	45.0	48.0	0	30
7i	4.4	51.0*	35.4*	0	30
7j	4.4	150.0	0	0	0
7k	4.4	0	35.4*	51.0*	30
7l	4.4	0	106.2*	17.0*	30
7m	4.4	35.4	0	90.0	30
7n	4.4	106.2	0	30.0	30

**Solution was equally split and mannose was added to one half and galactose added to the other.*

7a: ^{1}H NMR (500 MHz, DMSO) δ 7.97 (bs, 1H, amide NH's), 7.90 (bs, 0.4H, amide NH's), 7.83 (bs, 0.5H, amide NH's), 7.77 (bs, 0.8H, amide NH's), 7.51 (bs, 1.8H, $CH_2N\mathit{H}C(S)N\mathit{H}CH_2$) 5.32(m, 0.7H), 5.17 (m, 0.8H), 5.07 (m, 1.6H), 5.02 (m, 0.8H), 4.92 (m, 1H), 4.84 (m, 0.5H), 4.21 (m, 0.7H), 4.10 (m, 0.9H), 4.00 (m, 2.3H), 3.90 (m, 0.7), 3.80 (t, 0.8H, J = 6.5Hz), 3.68 (m, 1.8H), 3.50 (m, 3.2H), 3.14 (bs, 2.5H), 3.04 (bs, 3.9H), 2.81 (t, 0.5H J = 6.4Hz), 2.56-2.64 (m, 11.4H),

2.17 (bs, 4.8H), 2.08 (s, 3.2H), 2.07 (s, 3H), 2.00 (m, 9H), 1.90 (s, 3.5H) 1.79 (m, 3.5H) ppm. MALDI-TOF (pos) m/z 17500 g/mol.

7b: ^{1}H NMR (500 MHz, DMSO) δ 7.97 (bs, 1H, amide NH's), 7.90 (bs, 0.5H, amide NH's), 7.83 (bs, 0.5H, amide NH's), 7.77 (bs, 0.8H, amide NH's), 7.51 (bs, 1.8H, $CH_2N\mathit{H}C(S)N\mathit{H}CH_2$) 5.32(m, 0.8H), 5.17 (m, 0.8H), 5.07 (m, 1.1H), 5.02 (m, 0.8H), 4.99 (m, 0.17H), 4.93 (m, 0.9H), 4.84 (m, 0.5H), 4.21 (m, 0.8H), 4.10 (m, 0.8H), 4.00 (m, 2.4H), 3.80 (t, 1.1H, J = 6.5Hz), 3.68 (m, 1.6H), 3.50 (m, 3.8H), 3.14 (bs, 2.5H), 3.04 (bs, 3.9H), 2.81 (t, 1H J = 6.5Hz), 2.56-2.64 (m, 13H), 2.17 (bs, 5H), 2.08 (s, 4H), 2.07 (s, 2H), 2.00 (s, 3.5H), 1.99 (s, 3H) 1.98 (s, 3H), 1.97 (s, 3H), 1.90 (s, 3.5H) 1.79 (m, 4H) ppm. MALDI-TOF (pos) m/z 18200 g/mol.

7c: ^{1}H NMR (500 MHz, DMSO) δ 7.97 (bs, 1H, amide NH's), 7.78 (bs, 0.9H, amide NH's), 7.51 (bs, 1.8H, $CH_2N\mathit{H}C(S)N\mathit{H}CH_2$) 5.32(m, 0.8H), 5.25 (m, 0.8H), 5.17 (m, 0.8H), 5.07 (m, 0.6H), 5.02 (m, 0.7H), 4.99 (m, 0.6H), 4.92 (m, 1.3H), 4.75 (m, 0.8H), 4.21 (m, 0.8H), 4.09 (m, 0.8H), 4.00 (m, 2.4H), 3.81 (t, 1.1H, J = 6.5Hz), 3.68 (m, 2H), 3.50 (m, 4H), 3.13 (bs, 2.7H), 3.04 (bs, 4.6H), 2.81 (t, 1.2H, J = 6.4Hz), 2.56-2.64 (m, 17H), 2.17 (bs, 6.5H), 2.08 (s, 3.7H), 2.00 (s, 3H), 1.99 (s, 2H), 1.98 (s, 3H), 1.97 (s, 3H) 1.96 (s, 2H), 1.90 (s, 3H) 1.79 (m, 4.7H) ppm. MALDI-TOF (pos) m/z 18100 g/mol.

7d: ^{1}H NMR (500 MHz, DMSO) δ 7.97 (bs, 1H, amide NH's), 7.78 (bs, 0.8H, amide NH's), 7.51 (bs, 2H, $CH_2N\mathit{H}C(S)N\mathit{H}CH_2$) 5.32(m, 0.9H), 5.26 (m, 1H), 5.17 (dd, 1H, J = 10.7, 3.6Hz), 5.02 (d, 0.8H, J = 3.3Hz), 4.99 (d, 0.8H, J = 3.3Hz) 4.92 (m, 1.6H), 4.76 (m, 1H), 4.21 (m, 1H), 4.10 (d, 1H, J = 11.9Hz), 4.00 (d, 2.7H, J = 6.5Hz), 3.95 (m, 1H), 3.81 (t, 1.6H, J = 6.5Hz), 3.68 (m, 2.4H), 3.48 (m, 4.2H), 3.13 (bs, 3.2H), 3.04 (bs, 3.7H), 2.81 (t, 2.2H, J = 6.4Hz), 2.56-2.65 (m, 10H), 2.17 (bs, 4.7H), 2.08 (s, 3H), 2.00 (s, 3H), 1.99 (s, 1H), 1.98 (s, 3H), 1.97 (s, 3H), 1.95 (s, 2H), 1.92 (s, 2H) 1.90 (s, 3H), 1.80 (m, 4.4H) ppm. MALDI-TOF (pos) m/z 17500 g/mol.

7e: ^{1}H NMR (500 MHz, DMSO) δ 7.99 (bs, 1H, amide NH's), 7.84 (bs, 0.9H, amide NH's), 7.54(bs, 1.8H, $CH_2N\mathit{H}C(S)N\mathit{H}CH_2$), 5.31(s, 0.6H), 5.25 (t, 0.7H, J = 9.8Hz), 5.16 (m, 0.6H), 5.02 (s, 0.7H), 4.99 (d, 0.6H, J = 3.4 Hz), 4.91 (m, 1.3H), 4.76 (m, 0.9H), 4.62 (m, 1.4H), 4.20 (m, 0.7H), 4.10 (m, 0.9H), 3.99 (m, 2.3H), 3.94 (m, 0.9H), 3.78 (m, 3.8H), 3.68 (m, 2H), 3.58 (m, 4H), 3.48 (m, 7H), 3.13 (m, 6H), 2.54-70 (m, 10H), 2.20 (bs, 4.0H), 2.07 (s, 2H), 1.89-2.00 (m, 17H), 1.78 (m, 3H) ppm. MALDI-TOF (pos) m/z 19300 g/mol.

7f: ^{1}H NMR (500 MHz, DMSO) δ 7.96 (bs, 1H, amide NH's), 7.75 (bs, 0.6H, amide NH's), 7.51 (bs, 1.5H $CH_2N\mathit{H}C(S)N\mathit{H}CH_2$), 5.24 (t, 0.8H, 9.7 Hz), 4.98 (m, 0.9H), 4.91 (t, 0.9H, 9.7 Hz), 4.77 (m, 0.9H), 4.11 (m, 0.9H), 4.01 (m, 1H), 3.92 (m, 1H), 3.71 (m, 1.2H), 3.49 (m, 3H), 3.37 (m, 1.4H), 3.13 (m, 3H), 2.47-2.63 (m,

9H), 2.36 (m, 2.3H), 2.19 (bs, 3.3H), 2.01 (s, 5.8H), 1.97 (s, 3H), 1.93 (s, 2.8H), 1.78 (m, 1.9H). MALDI-TOF (pos) m/z 21000 g/mol.

7g: ^{1}H NMR (500 MHz, DMSO) δ 8.02 (bs, 1H, amide NH's), 7.86 (bs, 1H, amide NH's), 7.57 (bs, 2H, $CH_2N\mathit{H}C(S)N\mathit{H}CH_2$) 5.25(m, 1H), 5.07 (m, 7H), 4.99 (d, 0.3H, J = 3.4Hz), 4.92 (t, 0.6H, J = 9.8Hz), 4.84 (s, 2H), 4.75 (m, 0.7H), 4.61 (s, 3H), 4.11 (dd, 3H, J = 12.2, 5.3Hz), 4.02 (d, 3H, J = 12.2Hz), 3.90 (m, 3H), 3.78 (m, 8H), 3.67 (m, 3H), 3.56 (m, 7H), 3.45 (m, 16H), 3.30 (bs, 9H), 3.13 (bs, 4H), 3.04 (s, 2H), 2.81 (t, 2H, J = 6.5Hz), 2.58 (m, 10H), 2.22 (bs, 5H), 2.07 (s, 7H), 2.03 (s, 7H), 1.99 (s, 7H), 1.98 (m, 18H), 1.94 (m, 2H) 1.90 (s, 7H), 1.82 (m, 4H) ppm. MALDI-TOF (pos) m/z 18300 g/mol.

7h: ^{1}H NMR (500 MHz, DMSO) δ 8.00 (bs, 1H, amide NH's), 7.85 (bs, 0.8H, amide NH's), 7.57 (bs, 1.9H, $CH_2N\mathit{H}C(S)N\mathit{H}CH_2$), 5.25(m, 1H), 5.07 (m, 0.8H), 4.99 (d, 0.3H, J = 3.4Hz), 4.92 (t, 0.5H, J = 9.8Hz), 4.83 (s, 1.8H), 4.74 (m, 0.7H), 4.62 (s, 3H), 4.11 (dd, 2.8H, J = 12.2, 5.3Hz), 4.02 (d, 2.9H, J = 12.2Hz), 3.91 (m, 2.7H), 3.78 (m, 6.8H), 3.65 (m, 3H), 3.45-3.58 (m 14H), 3.30 (bs, 8H), 3.13 (bs, 3.6H), 3.04 (bs, 2H), 2.81 (t, 2H, J = 6.5 Hz), 2.58 (m, 9H), 2.22 (bs, 4.8H), 2.07 (s, 6.4H), 2.03 (s, 6.7H), 1.99 (s, 6.2H), 1.98 (m, 2.8H), 1.94 (m, 2H) 1.90 (s, 2H), 1.82 (m, 4H) ppm. MALDI-TOF (pos) m/z 18300 g/mol.

7i: ^{1}H NMR (500 MHz, DMSO) δ 7.98 (bs, 1H, amide NH's), 7.90 (bs, 0.4H, amide NH's), 7.76-7.84 (bs, 1.2H, amide NH's), 7.54(bs, 1.8H, $CH_2NHC(S)NHCH_2$), 5.25 (m, 0.35H), 5.07 (m, 3.6H), 4.85 (s, 1H), 4.77 (m, 0.35H), 4.11 (dd, 1.5H, J = 12.0, 5.0Hz), 4.01 (d, 1.5H, J = 12.0Hz), 3.92 (m, 1.5H), 3.81 (t, 0.5H, J = 6.5Hz), 3.68 (m, 1.8H), 3.51 (m, 3.7H), 3.13 (bs, 2.8H), 3.04 (m 3.4H), 2.54-70 (m, 10.7H), 2.17 (bs, 4.0H), 2.07 (s, 3.5H), 1.99 (m, 8H), 1.90 (s, 3.5H), 1.81 (m, 3.3H) ppm. MALDI-TOF (pos) m/z 19200 g/mol.

7j: ^{1}H NMR (500 MHz, DMSO) δ 7.96 (bs, 1H, amide N*H*'s), 7.74 (bs, 1H, amide N*H*'s), 7.51 (bs, 2H, $CH_2NHC(S)NHCH_2$), 5.08 (m, 3H, *H2, H3, H4*), 4.84 (s, 1H, *H1*), 4.12 (dd, 1H, J = 11.5, 5.2 Hz, *H6*), 4.02 (app d, 1H, J = 11.5 Hz, *H6*), 3.91 (bs, 1H), 3.69 (m, 1H, *H5*), 3.48 (m, 3H), 3.32 (m, 1H), 3.13 (bs, 2H), 3.04 (bs, 2H), 2.53-2.65 (m, 9H), 2.39 (bs, 2H), 2.16 (bs, 4H), 2.07 (s, 3H), 1.98 (s, 6H), 1.89 (s, 3H), 1.81 (m, 2H, $OCH_2CH_2CH_2SCH_2$) ppm MALDI-TOF (pos) m/z 21300 g/mol.

7k: ^{1}H NMR (500 MHz, DMSO) δ 7.99 (bs, 1H, amide NH's), 7.92 (bs, 0.6H, amide NH's), 7.85 (2bs, 1.3H, amide NH's), 7.54(2bs, 1.8H, $CH_2NHC(S)NHCH_2$), 5.31(s, 1.3H), 5.16 (dd, 1.3H, J = 10.8, 3.2 Hz), 5.02 (m, 1.3H), 4.91 (dd, 1.3H, J = 10.9, 3.2 Hz), 4.76 (m, 0.3H), 4.63 (m, 1.3H), 4.19 (m, 1.3H), 3.99 (m, 3H), 3.76 (m, 4H), 3.68 (m, 2H), 3.57 (m, 4H), 3.44 (m, 6H), 3.12 (bs, 3H), 3.04 (bs,

3H), 2.60 (m, 10H), 2.18 (bs, 4.5H), 2.07 (s, 4H), 1.99 (s, 5H), 1.96 (s, 5H), 1.89 (s, 4H), 1.78 (m, 4H) ppm. MALDI-TOF (pos) m/z 17700 g/mol.

7l: ^{1}H NMR (500 MHz, DMSO) δ 7.99 (bs, 1H, amide NH's), 7.92 (bs, 0.5H, amide NH's), 7.84 (bs, 1H, amide NH's), 7.54(bs, 2H, $CH_2N\mathit{H}C(S)N\mathit{H}CH_2$), 5.31(s, 1H), 5.17 (d, 1H, J = 7.1Hz), 5.07 (m, 0.4H), 5.02 (d, 1H, J = 10.8Hz), 4.84 (m, 1.4H), 4.62 (m, 0.8H), 4.19 (m, 1H), 3.99 (m, 3H), 3.97 (m, 2H), 3.67 (m, 2H), 3.58 (m, 2H), 3.44 (m, 4H), 3.13 (bs, 3H), 2.95 (bs, 5H), 2.64 (m, 8H), 2.18 (bs, 5H), 2.07 (s, 4H), 2.00 (s, 1H), 1.99 (s, 4H), 1.96 (s, 4H), 1.89 (s, 4H), 1.78 (m, 3H) ppm. MALDI-TOF (pos) m/z 19400 g/mol.

7m: ^{1}H NMR (500 MHz, DMSO) δ 7.99 (bs, 1H, amide NH's), 7.63 (bs, 0.8H, amide NH's), 7.84 (bs, 1H, amide NH's), 7.54(bs, 2H, $CH_2N\mathit{H}C(S)N\mathit{H}CH_2$), 5.31(s, 0.35H), 5.17 (d, 0.35H, J = 10.9), 5.07 (m, 3H), 4.93 (d, 0.35H, J = 10.7Hz), 4.84 (m, 1H), 4.62 (m, 0.7H), 4.19 (m, 0.35H), 4.12 (m, 1H), 4.00 (m, 2H), 3.91 (m, 1H), 3.78 (m, 2H), 3.68 (m, 2H), 3.58 (m, 2H), 3.48 (m, 4H), 3.12 (bs, 3H), 3.04 (bs, 3H), 2.55 (bs and m, 10H), 2.18 (bs, 4H), 2.06 (s, 3.9H), 1.99 (m, 9H), 1.89 (s, 3.9H), 1.78 (m, 2.8H) ppm. MALDI-TOF (pos) m/z 17500 g/mol.

7n: ^{1}H NMR (500 MHz, DMSO) δ 7.98 (bs, 1H, amide NH's), 7.90 (bs, 0.3H, amide NH's), 7.76-7.83 (bs, 1H, amide NH's), 7.54(bs, 1.8H, $CH_2N\mathit{H}C(S)N\mathit{H}CH_2$), 5.25 (t, 0.88H, J = 10.9 Hz), 5.07 (m, 1.2H), 4.99 (m, 0.5H),

4.91 (t, 0.8H, J = 9.9 Hz), 4.84 (m, 0.5H), 4.76 (dd, 0.9H, J = 10.3, 3.6Hz), 4.11 (dd, 1.3H, J = 12.3, 4.5Hz), 4.01 (m, 1.3H), 3.92 (m, 1.3H), 3.69 (m, 1.6H), 3.48 (m, 4H), 3.14 (bs 2.4H), 3.04 (bs, 2.7H), 2.54-2.70 (m, 10H), 2.17 (bs, 3.9H), 2.07 (s, 1.3H), 1.98 (s, 6.5H), 1.95 (s, 2.6H), 1.92 (s, 2.4H), 1.90 (s, 1.6H), 1.81 (m, 2H) ppm. MALDI-TOF (pos) m/z 19200 g/mol.

8a-n. Representative procedure for the synthesis of heterogeneously functionalized generation 4.0 PAMAM-based thiourea-linked 1-O-(6-thiourea-4-thiohexyl)- 2,3,4,6-tetra-O-acetyl -α-D-galactopyranoside, 1-O-(6- thiourea-4-thiohexyl)- 2,3,4,6-tetra-O-acetyl -α-D-glucopyranoside, 1-O-(6- thiourea-4-thiohexyl)- 2,3,4,6-tetra-O-acetyl -α-D-mannopyranoside. An aqueous solution of amine terminated Starburst G(4)-PAMAM dendrimer (2.478 g of a 17% w/w solution in water, 421.2 mg, 31.2 μmol) was lyophilized to leave a foamy residue. 7.02 mL of DMSO was then added to this residue to give a 60 mg/mL solution. 0.047 mL of a 300 mM solution of 2a (14.1 μmol, 6.84 mg) in DMSO was added to 0.5 mL of a 60 mg/mL G(4) PAMAM dendrimer (30 mg, 4.40 μmol) solution. The reaction was stirred for 48 hrs at which point a 75 μL aliquot was removed for MALDI-TOF analysis. After MALI-TOF analysis indicated reaction completion 0.17 mL of a 300 mM solution of 2b (49.4 μmol, 25.1 mg) was added. The solution was then stirred for 48 hrs. At this time a 75 μL aliquot was removed for analysis. After MALDI-TOF analysis indicated reaction completion, 0.19 mL of a 300 mM solution of 2c (56.9 μmol, 28.8 mg) was added and let stir for 48 hrs, when a 75 μL aliquot was removed for analysis. According to MALDI-TOF

analysis the final addition proved to be unsuccessful at fully functionalizing all terminal amine groups so an additional spacer was added. 47.1 mg (30 μmol) of 3 in DMSO was added an let stir at room temperature for 2 days. Again MALDI-TOF analysis indicated no further addition. This step was repeated with mild warming (up to 40 ºC) and vigorous stirring. MALDI-TOF analysis again indicated no further addition, hence the product was taken forward.

Table 9 Amounts of compounds that were used for the experimental procedure above for the synthesis of 8f-8n.

G4	Pamam (μmol)	Mannose (μmol)	Glucose (μmol)	Galactose (μmol)	Ethoxy ethanol (μmol)
8f	2.2	0	150	0	0
8g	2.2	17.0	107.1*	0	30
8h	1.5	45	48*	0	30
8i	2.2	51.0	35.7	0	30
8j	2.2	150	0	0	0
8k	2.2	0	35.7*	51.0	30
8l	2.2	0	107.1*	17.0	30
8m	2.2	35.7	0	90.0	30
8n	2.2	107.1	0	30.0	30

**Solution was equally split and mannose was added to one half and galactose added to the other.*

8f: ^{1}H NMR (500 MHz, DMSO) δ 7.96 (bs, 1H, amide NH's), 7.75 (bs, 0.8H, amide NH's), 7.51 (bs, 1.6H $CH_2N\mathit{H}C(S)N\mathit{H}CH_2$), 5.24 (t, 0.9H, 9.7 Hz), 4.98 (m, 0.8H), 4.91 (t, 0.9H, 9.7 Hz), 4.77 (m, 0.9H), 4.11 (m, 1H), 4.01 (m, 0.9H), 3.92 (m, 1.1H), 3.69 (m, 1.3H), 3.48 (m, 4H), 3.37 (m, 1.6H), 3.19 (m, 3H), 2.47-2.63 (m, 9H), 2.36 (m, 3H), 2.19 (bs, 3.2H), 2.01 (s, 5.6H), 1.97 (s, 2.8H), 1.93 (s, 2.6H), 1.78 (m, 1.8H). MALDI-TOF (pos) m/z 41900 g/mol.

8g: ^{1}H NMR (500 MHz, DMSO) δ 7.98 (bs, 1H, amide NH's), 7.90 (bs, 0.3H, amide NH's), 7.76-7.83 (bs, 1H, amide NH's), 7.54(bs, 1.8H, $CH_2NHC(S)NHCH_2$), 5.25 (t, 0.88H, J = 10.9 Hz), 5.07 (m, 1.2H), 4.99 (m, 0.5H), 4.91 (t, 0.8H, J = 9.9 Hz), 4.84 (m, 0.5H), 4.76 (dd, 0.9H, J = 10.3, 3.6Hz), 4.11 (dd, 1.3H, J = 12.3, 4.5Hz), 4.01 (m, 1.3H), 3.92 (m, 1.3H), 3.69 (m, 1.6H), 3.48 (m, 4H), 3.14 (bs 2.4H), 3.04 (bs, 2.7H), 2.54-2.70 (m, 10H), 2.17 (bs, 3.9H), 2.07 (s, 1.3H), 1.98 (s, 6.5H), 1.95 (s, 2.6H), 1.92 (s, 2.4H), 1.90 (s, 1.6H), 1.81 (m, 2H) ppm. MALDI-TOF (pos) m/z 34300 g/mol.

8h: ^{1}H NMR (500 MHz, DMSO) δ 8.02 (bs, 1H, amide NH's), 7.86 (bs, 1H, amide NH's), 7.57 (bs, 2H, $CH_2NHC(S)NHCH_2$) 5.25(m, 1H), 5.07 (m, 7H), 4.99 (d, 0.3H, J = 3.4Hz), 4.92 (t, 0.6H, J = 9.8Hz), 4.84 (s, 2H), 4.75 (m, 0.7H), 4.61 (s, 3H), 4.11 (dd, 3H, J = 12.2, 5.3Hz), 4.02 (d, 3H, J = 12.2Hz), 3.90 (m, 3H), 3.78 (m, 8H), 3.67 (m, 3H), 3.56 (m, 7H), 3.45 (m, 16H), 3.30 (bs, 9H), 3.13 (bs, 4H), 3.04 (s, 2H), 2.81 (t, 2H, J = 6.5Hz), 2.58 (m, 10H), 2.22 (bs, 5H), 2.07 (s, 7H), 2.03 (s, 7H), 1.99 (s, 7H), 1.98 (m, 18H), 1.94 (m, 2H) 1.90 (s, 7H), 1.82 (m, 4H) ppm. MALDI-TOF (pos) m/z 32400 g/mol.

8i: ^{1}H NMR (500 MHz, DMSO) δ 7.98 (bs, 1H, amide NH's), 7.90 (bs, 0.4H, amide NH's), 7.76-7.84 (bs, 1.2H, amide NH's), 7.54(bs, 1.8H, $CH_2NHC(S)NHCH_2$), 5.25 (m, 0.35H), 5.07 (m, 3.6H), 4.85 (s, 1H), 4.77 (m, 0.35H), 4.11 (dd, 1.5H, J = 12.0, 5.0Hz), 4.01 (d, 1.5H, J = 12.0Hz), 3.92 (m,

1.5H), 3.81 (t, 0.5H, J = 6.5Hz), 3.68 (m, 1.8H), 3.51 (m, 3.7H), 3.13 (bs, 2.8H), 3.04 (m 3.4H), 2.54-70 (m, 10.7H), 2.17 (bs, 4.0H), 2.07 (s, 3.5H), 1.99 (m, 8H), 1.90 (s, 3.5H), 1.81 (m, 3.3H) ppm. MALDI-TOF (pos) m/z 36700 g/mol.

8j: ^{1}H NMR (500 MHz, DMSO) δ 7.96 (bs, 1H, amide N*H*'s), 7.74 (bs, 1H, amide N*H*'s), 7.51 (bs, 2H, CH_2N*H*C(S)N*H*CH_2), 5.08 (m, 3H), 4.84 (s, 1H), 4.12 (dd, 1H, J = 11.5, 5.2 Hz), 4.02 (app d, 1H, J = 11.5 Hz), 3.91 (bs, 1H), 3.69 (m, 1H), 3.48 (m, 3H), 3.32 (m, 1H), 3.13 (bs, 2H), 3.04 (bs, 2H), 2.53-2.65 (m, 9H), 2.39 (bs, 2H), 2.16 (bs, 4H), 2.07 (s, 3H), 1.98 (s, 6H), 1.89 (s, 3H), 1.81 (p, 2H) ppm; MALDI-TOF (pos) m/z 42500 g/mol.

8k: ^{1}H NMR (500 MHz, DMSO) δ 7.99 (bs, 1H, amide NH's), 7.92 (bs, 0.6H, amide NH's), 7.85 (2bs, 1.3H, amide NH's), 7.54(2bs, 1.8H, CH_2N*H*C(S)N*H*CH_2), 5.31(s, 1.3H), 5.16 (dd, 1.3H, J = 10.8, 3.2Hz), 5.02 (m, 1.3H), 4.91 (dd, 1.3H, J = 10.9, 3.2Hz), 4.76 (m, 0.3H), 4.63 (m, 1.3H), 4.19 (m, 1.3H), 3.99 (m, 3H), 3.76 (m, 4H), 3.68 (m, 2H), 3.57 (m, 4H), 3.44 (m, 6H), 3.12 (bs, 3H), 3.04 (bs, 3H), 2.60 (m, 10H), 2.18 (bs, 4.5H), 2.07 (s, 4H), 1.99 (s, 5H), 1.96 (s, 5H), 1.89 (s, 4H), 1.78 (m, 4H) ppm. MALDI-TOF (pos) m/z 33000 g/mol.

8l: ^{1}H NMR (500 MHz, DMSO) δ 7.99 (bs, 1H, amide NH's), 7.84 (bs, 0.9H, amide NH's), 7.54(bs, 1.8H, CH_2N*H*C(S)N*H*CH_2), 5.31(s, 0.6H), 5.25 (t, 0.7H, J = 9.8Hz), 5.16 (m, 0.6H), 5.02 (s, 0.7H), 4.99 (d, 0.6H, J = 3.4Hz), 4.91 (m, 1.3H),

4.76 (m, 0.9H), 4.62 (m, 1.4H), 4.20 (m, 0.7H), 4.10 (m, 0.9H), 3.99 (m, 2.3H), 3.94 (m, 0.9H), 3.78 (m, 3.8H), 3.68 (m, 2H), 3.58 (m, 4H), 3.48 (m, 7H), 3.13 (m, 6H), 2.54-70 (m, 10H), 2.20 (bs, 4.0H), 2.07 (s, 2H), 1.89-2.00 (m, 17H), 1.78 (m, 3H) ppm. MALDI-TOF (pos) m/z 37200 g/mol.

8m: ^{1}H NMR (500 MHz, DMSO) δ 7.99 (bs, 1H, amide NH's), 7.92 (bs, 0.5H, amide NH's), 7.84 (bs, 1H, amide NH's), 7.54(bs, 2H, $CH_2N\mathit{H}C(S)N\mathit{H}CH_2$), 5.31(s, 1H), 5.17 (d, 1H, J = 7.1Hz), 5.07 (m, 0.4H), 5.02 (d, 1H, J = 10.8Hz), 4.84 (m, 1.4H), 4.62 (m, 0.8H), 4.19 (m, 1H), 3.99 (m, 3H), 3.97 (m, 2H), 3.67 (m, 2H), 3.58 (m, 2H), 3.44 (m, 4H), 3.13 (bs, 3H), 2.95 (bs, 5H), 2.64 (m, 8H), 2.18 (bs, 5H), 2.07 (s, 4H), 2.00 (s, 1H), 1.99 (s, 4H), 1.96 (s, 4H), 1.89 (s, 4H), 1.78 (m, 3H) ppm. MALDI-TOF (pos) m/z 36100 g/mol.

8n: ^{1}H NMR (500 MHz, DMSO) δ 7.99 (bs, 1H, amide NH's), 7.63 (bs, 0.8H, amide NH's), 7.84 (bs, 1H, amide NH's), 7.54(bs, 2H, $CH_2N\mathit{H}C(S)N\mathit{H}CH_2$), 5.31(s, 0.35H), 5.17 (d, 0.35H, J = 10.9), 5.07 (m, 3H), 4.93 (d, 0.35H, J = 10.7Hz), 4.84 (m, 1H), 4.62 (m, 0.7H), 4.19 (m, 0.35H), 4.12 (m, 1H), 4.00 (m, 2H), 3.91 (m, 1H), 3.78 (m, 2H), 3.68 (m, 2H), 3.58 (m, 2H), 3.48 (m, 4H), 3.12 (bs, 3H), 3.04 (bs, 3H), 2.55 (bs and m, 10H), 2.18 (bs, 4H), 2.06 (s, 3.9H), 1.99 (m, 9H), 1.89 (s, 3.9H), 1.78 (m, 2.8H) ppm. MALDI-TOF (pos) m/z 37100 g/mol.

9a-l. Representative procedure for the synthesis of heterogeneously functionalized generation 5.0 PAMAM-based thiourea-linked 1-O-(6-thiourea-4-thiohexyl)- 2,3,4,6-tetra-O-acetyl -α-D-galactopyranoside, 1-O-(6- thiourea-4-thiohexyl)- 2,3,4,6-tetra-O-acetyl -α-D-glucopyranoside, 1-O-(6- thiourea-4-thiohexyl)- 2,3,4,6-tetra-O-acetyl -α-D-mannopyranoside. An aqueous solution of amine terminated Starburst G(5)-PAMAM dendrimer (1.938 g of a 23% w/w solution in water, 445.8 mg, 17.5 μmol) was lyophilized to leave a foamy residue. 7.43 mL of DMSO was then added to this residue to give a 60 mg/mL solution. 0.039 mL of a 300 mM solution of 2a (11.8 μmol, 5.96 mg) in DMSO was added to 0.5 mL of a 60 mg/mL G(5) PAMAM dendrimer (30 mg, 1.18 μmol) solution. The reaction was stirred for 48 hrs at which point a 75 μL aliquot was removed for MALDI-TOF analysis. After MALDI-TOF analysis indicated reaction completion 0.14 mL of a 300 mM solution of 2b (42.4 μmol, 22.1 mg) was added. The solution was then stirred for 48 hrs. At this time a 75 μL aliquot was removed for analysis. After MALDI-TOF indicated reaction completion, 0.15 mL of a 300 mM solution of 2c (45 μmol, 23.2 mg) was added and let stir for 48 hrs, when a 75 μL aliquot was removed for analysis. According to MALDI-TOF analysis the final addition proved to be unsuccessful at fully functionalizing all terminal amine groups so an additional spacer was added. 47.1 mg (30 μmol) of 3 in DMSO was added an let stir at room temperature for 2 days. Again MALDI-TOF analysis indicated no further addition. This step was repeated with mild warming (up to 40

ºC) and vigorous stirring. MALDI-TOF analysis again indicated no addition, hence the product was taken forward.

Table 10 Amounts of compounds that were used for the experimental procedure above for the synthesis of 9e-9n.

G5	PAMAM (μmol)	Mannose (μmol)	Glucose (μmol)	Galactose (μmol)	Ethoxy ethanol (μmol)
9e	1.18	0	150	0	0
9f	1.18	15.0	88.2*	0	30
9g	0.77	45.0	48.0	0	30
9h	1.18	45.0	29.4*	0	30
9i	1.18	150	0	0	0
9j	1.18	0	29.4*	45.0	30
9k	1.18	0	88.2*	15.0	30
9l	1.18	29.4	0	90.0	30

**Solution was equally split and mannose was added to one half and galactose added to the other.*

9e: ^{1}H NMR (500 MHz, DMSO) δ 7.96 (bs, 1H, amide NH's), 7.73 (bs, 0.6H, amide NH's), 7.51 (bs, 1.8H $CH_2N\mathit{H}C(S)N\mathit{H}CH_2$), 5.24 (t, 1H, 9.7 Hz), 4.98 (m, 1H), 4.91 (t, 0.8H, J = 9.7 Hz), 4.77 (m, 0.9H), 4.11 (m, 0.8H), 4.01 (m, 1H), 3.92 (m, 1H), 3.71 (m, 1.3H), 3.49 (m, 3.5H), 3.37 (m, 1.7H), 3.13 (bs, 2.7H), 2.50-2.65 (m, 10H), 2.36 (m, 2.1H), 2.19 (bs, 3.5H), 2.01 (s, 6H), 1.97 (s, 3.0H), 1.93 (s, 2.6H), 1.79 (m, 2H). MALDI-TOF (pos) m/z 76000 g/mol.

9f: ^{1}H NMR (500 MHz, DMSO) δ 7.98 (bs, 1H, amide NH's), 7.90 (bs, 0.3H, amide NH's), 7.76-7.83 (bs, 1H, amide NH's), 7.54(bs, 1.8H, $CH_2N\mathit{H}C(S)N\mathit{H}CH_2$), 5.25 (t, 0.88H, J = 10.9 Hz), 5.07 (m, 1.2H), 4.99 (m, 0.5H), 4.91 (t, 0.8H, J = 9.9 Hz), 4.84 (m, 0.5H), 4.76 (dd, 0.9H, J = 10.3, 3.6Hz), 4.11

(dd, 1.3H, J = 12.3, 4.5Hz), 4.01 (m, 1.3H), 3.92 (m, 1.3H), 3.69 (m, 1.6H), 3.48 (m, 4H), 3.14 (bs 2.4H), 3.04 (bs, 2.7H), 2.54-2.70 (m, 10H), 2.17 (bs, 3.9H), 2.07 (s, 1.3H), 1.98 (s, 6.5H), 1.95 (s, 2.6H), 1.92 (s, 2.4H), 1.90 (s, 1.6H), 1.81 (m, 2H) ppm. MALDI-TOF (pos) m/z 63000 g/mol.

9g: ^{1}H NMR (500 MHz, DMSO) δ 8.02 (bs, 1H, amide NH's), 7.86 (bs, 1H, amide NH's), 7.57 (bs, 2H, $CH_2N\mathit{H}C(S)N\mathit{H}CH_2$) 5.25(m, 1H), 5.07 (m, 7H), 4.99 (d, 0.3H, J = 3.4Hz), 4.92 (t, 0.6H, J = 9.8Hz), 4.84 (s, 2H), 4.75 (m, 0.7H), 4.61 (s, 3H), 4.11 (dd, 3H, J = 12.2, 5.3Hz), 4.02 (d, 3H, J = 12.2Hz), 3.90 (m, 3H), 3.78 (m, 8H), 3.67 (m, 3H), 3.56 (m, 7H), 3.45 (m, 16H), 3.30 (bs, 9H), 3.13 (bs, 4H), 3.04 (s, 2H), 2.81 (t, 2H, J = 6.5Hz), 2.58 (m, 10H), 2.22 (bs, 5H), 2.07 (s, 7H), 2.03 (s, 7H), 1.99 (s, 7H), 1.98 (m, 18H), 1.94 (m, 2H) 1.90 (s, 7H), 1.82 (m, 4H) ppm. MALDI-TOF (pos) m/z 60500 g/mol.

9h: ^{1}H NMR (500 MHz, DMSO) δ 7.98 (bs, 1H, amide NH's), 7.90 (bs, 0.4H, amide NH's), 7.76-7.84 (bs, 1.2H, amide NH's), 7.54(bs, 1.8H, $CH_2N\mathit{H}C(S)N\mathit{H}CH_2$), 5.25 (m, 0.35H), 5.07 (m, 3.6H), 4.85 (s, 1H), 4.77 (m, 0.35H), 4.11 (dd, 1.5H, J = 12.0, 5.0Hz), 4.01 (d, 1.5H, J = 12.0Hz), 3.92 (m, 1.5H), 3.81 (t, 0.5H, J = 6.5Hz), 3.68 (m, 1.8H), 3.51 (m, 3.7H), 3.13 (bs, 2.8H), 3.04 (m 3.4H), 2.54-70 (m, 10.7H), 2.17 (bs, 4.0H), 2.07 (s, 3.5H), 1.99 (m, 8H), 1.90 (s, 3.5H), 1.81 (m, 3.3H) ppm. MALDI-TOF (pos) m/z 64500 g/mol.

9i: ^{1}H NMR (500 MHz, DMSO) δ 7.96 (bs, 1H, amide N*H*'s), 7.74 (bs, 1H, amide N*H*'s), 7.51 (bs, 2H, CH_2N*H*C(S)N*H*CH_2), 5.08 (m, 3H), 4.84 (s, 1H), 4.12 (dd, 1H, J = 11.5, 5.2 Hz), 4.02 (d, 1H, J = 11.5 Hz), 3.91 (bs, 1H), 3.69 (m, 1H), 3.48 (m, 3H), 3.32 (m, 1H), 3.13 (bs, 2H), 3.04 (bs, 2H), 2.53-2.65 (m, 7H), 2.39 (bs, 2H), 2.16 (bs, 4H), 2.07 (s, 3H), 1.98 (s, 6H), 1.89 (s, 3H), 1.81 (p, 2H) ppm; MALDI-TOF (pos) m/z 78500 g/mol.

9j: ^{1}H NMR (500 MHz, DMSO) δ 7.99 (bs, 1H, amide NH's), 7.92 (bs, 0.6H, amide NH's), 7.85 (2bs, 1.3H, amide NH's), 7.54(2bs, 1.8H, CH_2N*H*C(S)N*H*CH_2), 5.31(s, 1.3H), 5.16 (dd, 1.3H, J = 10.8, 3.2Hz), 5.02 (m, 1.3H), 4.91 (dd, 1.3H, J = 10.9, 3.2Hz), 4.76 (m, 0.3H), 4.63 (m, 1.3H), 4.19 (m, 1.3H), 3.99 (m, 3H), 3.76 (m, 4H), 3.68 (m, 2H), 3.57 (m, 4H), 3.44 (m, 6H), 3.12 (bs, 3H), 3.04 (bs, 3H), 2.60 (m, 10H), 2.18 (bs, 4.5H), 2.07 (s, 4H), 1.99 (s, 5H), 1.96 (s, 5H), 1.89 (s, 4H), 1.78 (m, 4H) ppm. MALDI-TOF (pos) m/z 61500 g/mol.

9k: ^{1}H NMR (500 MHz, DMSO) δ 7.99 (bs, 1H, amide NH's), 7.84 (bs, 0.9H, amide NH's), 7.54(bs, 1.8H, CH_2N*H*C(S)N*H*CH_2), 5.31(s, 0.6H), 5.25 (t, 0.7H, J = 9.8Hz), 5.16 (m, 0.6H), 5.02 (s, 0.7H), 4.99 (d, 0.6H, J = 3.4Hz), 4.91 (m, 1.3H), 4.76 (m, 0.9H), 4.62 (m, 1.4H), 4.20 (m, 0.7H), 4.10 (m, 0.9H), 3.99 (m, 2.3H), 3.94 (m, 0.9H), 3.78 (m, 3.8H), 3.68 (m, 2H), 3.58 (m, 4H), 3.48 (m, 7H), 3.13 (m, 6H), 2.54-70 (m, 10H), 2.20 (bs, 4.0H), 2.07 (s, 2H), 1.89-2.00 (m, 17H), 1.78 (m, 3H) ppm. MALDI-TOF (pos) m/z 65500 g/mol.

9l: ^{1}H NMR (500 MHz, DMSO) δ 7.99 (bs, 1H, amide NH's), 7.92 (bs, 0.5H, amide NH's), 7.84 (bs, 1H, amide NH's), 7.54(bs, 2H, $CH_2N\mathit{H}C(S)N\mathit{H}CH_2$), 5.31(s, 1H), 5.17 (d, 1H, J = 7.1Hz), 5.07 (m, 0.4H), 5.02 (d, 1H, J = 10.8Hz), 4.84 (m, 1.4H), 4.62 (m, 0.8H), 4.19 (m, 1H), 3.99 (m, 3H), 3.97 (m, 2H), 3.67 (m, 2H), 3.58 (m, 2H), 3.44 (m, 4H), 3.13 (bs, 3H), 2.95 (bs, 5H), 2.64 (m, 8H), 2.18 (bs, 5H), 2.07 (s, 4H), 2.00 (s, 1H), 1.99 (s, 4H), 1.96 (s, 4H), 1.89 (s, 4H), 1.78 (m, 3H) ppm. MALDI-TOF (pos) m/z 61500 g/mol.

10a-l. Representative procedure for the synthesis of heterogeneously functionalized generation 6.0 PAMAM-based thiourea-linked 1-O-(6-thiourea-4-thiohexyl)- 2,3,4,6-tetra-O-acetyl -α-D-galactopyranoside, 1-O-(6- thiourea-4-thiohexyl)- 2,3,4,6-tetra-O-acetyl -α-D-glucopyranoside, 1-O-(6- thiourea-4-thiohexyl)- 2,3,4,6-tetra-O-acetyl -α-D-mannopyranoside. An aqueous solution of amine terminated Starburst G(6)-PAMAM dendrimer (2,777 g of a 17% w/w solution in water, 472.1 mg, 9.3 μmol) was lyophilized to leave a foamy residue. 7.87 mL of DMSO was then added to this residue to give a 60 mg/mL solution. 0.033mL of a 300mM solution of 2a (9.9 μmol, 5.1 mg) in DMSO was added to 0.5 mL of a 60 mg/mL G(6) PAMAM dendrimer (30 mg, 4.40 μmol) solution. The reaction was stirred for 48 hrs at which point a 75 μL aliquot was removed for MALDI-TOF analysis. After MALSI-TOF analysis indicated reaction completion 0.12 mL of a 300 mM solution of 2b (36 μmol, 18.2 mg) was added. The solution was then stirred for 48 hrs. At this time a 75 μL aliquot was removed for analysis.

After MALDI-TOF analysis indicated reaction completion, 0.14 mL of a 300 mM solution of 2c (42 μmol, 21.6 mg) was added and let stir for 48 hrs, when a 75 μL aliquot was removed for analysis. According to MALDI-TOF analysis the final addition proved to be unsuccessful at fully functionalizing all terminal amine groups so an additional spacer was added. 47.1 mg (30 μmol) of 3 in DMSO was added an let stir at room temperature for 2 days. Again MALDI-TOF analysis indicated no further addition. This step was repeated with mild warming (up to 40 ºC) and vigorous stirring. MALDI-TOF analysis again indicated no addition, hence the product was taken forward without further purification.

Table 11 Amounts of compounds that were used for the experimental procedure above for the synthesis of 10e-10n.

G6	Pamam (μmol)	Mannose (μmol)	Glucose (μmol)	Galactose (μmol)	Ethoxy ethanol (μmol)
10e	0.59	0	150	0	0
10f	0.59	13.0	75.0*	0	30
10g	0.38	45.0	48.0	0	30
10h	0.59	150	0	0	0
10i	0.59	0	24.9*	39.0	30
10j	0.59	0	75.0*	13.0	30
10k	0.59	24.9	0	90	30
10l	0.59	75.0	0	30	30

**Solution was equally split and mannose was added to one half and galactose added to the other.*

10e: ^{1}H NMR (500 MHz, DMSO) δ 7.96 (bs, 1H, amide NH's), 7.75 (bs, 0.8H, amide NH's), 7.51 (bs, 1.7H $CH_2N\mathit{H}C(S)N\mathit{H}CH_2$), 5.24 (t, 1H, 9.7 Hz), 4.98 (m, 1H), 4.91 (t, 1H, 9.7 Hz), 4.77 (m, 1H), 4.11 (m, 1H), 4.01 (m, 1H), 3.92 (m, 1H),

3.71 (m, 1.3H), 3.49 (m, 3.5H), 3.37 (m, 1.6H), 3.13 (m, 2.7H), 2.47-2.63 (m, 10H), 2.36 (m, 2.1H), 2.19 (bs, 3.6H), 2.01 (s, 6.6H), 1.97 (s, 3.4H), 1.93 (s, 3.0H), 1.78 (m, 2H). MALDI-TOF (pos) m/z 139000 g/mol.

10f: ^{1}H NMR (500 MHz, DMSO) δ 8.02 (bs, 1H, amide NH's), 7.86 (bs, 1H, amide NH's), 7.57 (bs, 2H, $CH_2N\mathit{H}C(S)N\mathit{H}CH_2$) 5.25(m, 1H), 5.07 (m, 7H), 4.99 (d, 0.3H, J = 3.4Hz), 4.92 (t, 0.6H, J = 9.8Hz), 4.84 (s, 2H), 4.75 (m, 0.7H), 4.61 (s, 3H), 4.11 (dd, 3H, J = 12.2, 5.3Hz), 4.02 (d, 3H, J = 12.2Hz), 3.90 (m, 3H), 3.78 (m, 8H), 3.67 (m, 3H), 3.56 (m, 7H), 3.45 (m, 16H), 3.30 (bs, 9H), 3.13 (bs, 4H), 3.04 (s, 2H), 2.81 (t, 2H, J = 6.5Hz), 2.58 (m, 10H), 2.22 (bs, 5H), 2.07 (s, 7H), 2.03 (s, 7H), 1.99 (s, 7H), 1.98 (m, 18H), 1.94 (m, 2H) 1.90 (s, 7H), 1.82 (m, 4H) ppm. MALDI-TOF (pos) m/z 109000 g/mol.

10g: ^{1}H NMR (500 MHz, DMSO) δ 7.98 (bs, 1H, amide NH's), 7.90 (bs, 0.3H, amide NH's), 7.76-7.83 (bs, 1H, amide NH's), 7.54(bs, 1.8H, $CH_2N\mathit{H}C(S)N\mathit{H}CH_2$), 5.25 (t, 0.88H, J = 10.9 Hz), 5.07 (m, 1.2H), 4.99 (m, 0.5H), 4.91 (t, 0.8H, J = 9.9 Hz), 4.84 (m, 0.5H), 4.76 (dd, 0.9H, J = 10.3, 3.6Hz), 4.11 (dd, 1.3H, J = 12.3, 4.5Hz), 4.01 (m, 1.3H), 3.92 (m, 1.3H), 3.69 (m, 1.6H), 3.48 (m, 4H), 3.14 (bs 2.4H), 3.04 (bs, 2.7H), 2.54-2.70 (m, 10H), 2.17 (bs, 3.9H), 2.07 (s, 1.3H), 1.98 (s, 6.5H), 1.95 (s, 2.6H), 1.92 (s, 2.4H), 1.90 (s, 1.6H), 1.81 (m, 2H) ppm. MALDI-TOF (pos) m/z 106500 g/mol.

10h: ^{1}H NMR (500 MHz, DMSO) δ 7.96 (bs, 1H, amide N*H*'s), 7.74 (bs, 1H, amide N*H*'s), 7.51 (bs, 2H, CH_2N*H*C(S)N*H*CH_2), 5.08 (m, 3H), 4.84 (s, 1H), 4.12 (dd, 1H, J = 11.5, 5.2 Hz), 4.02 (d, 1H, J = 11.5 Hz), 3.91 (bs, 1H), 3.69 (m, 1H), 3.48 (m, 3H), 3.32 (m, 1H), 3.13 (bs, 2H), 3.04 (bs, 2H), 2.53-2.65 (m, 7H), 2.39 (bs, 2H), 2.16 (bs, 4H), 2.07 (s, 3H), 1.98 (s, 6H), 1.89 (s, 3H), 1.81 (p, 2H) ppm; MALDI-TOF (pos) m/z 142000 g/mol.

10i: ^{1}H NMR (500 MHz, DMSO) δ 7.99 (bs, 1H, amide NH's), 7.92 (bs, 0.6H, amide NH's), 7.85 (2bs, 1.3H, amide NH's), 7.54(2bs, 1.8H, CH_2N*H*C(S)N*H*CH_2), 5.31(s, 1.3H), 5.16 (dd, 1.3H, J = 10.8, 3.2Hz), 5.02 (m, 1.3H), 4.91 (dd, 1.3H, J = 10.9, 3.2Hz), 4.76 (m, 0.3H), 4.63 (m, 1.3H), 4.19 (m, 1.3H), 3.99 (m, 3H), 3.76 (m, 4H), 3.68 (m, 2H), 3.57 (m, 4H), 3.44 (m, 6H), 3.12 (bs, 3H), 3.04 (bs, 3H), 2.60 (m, 10H), 2.18 (bs, 4.5H), 2.07 (s, 4H), 1.99 (s, 5H), 1.96 (s, 5H), 1.89 (s, 4H), 1.78 (m, 4H) ppm. MALDI-TOF (pos) m/z 114500 g/mol.

10j: ^{1}H NMR (500 MHz, DMSO) δ 7.99 (bs, 1H, amide NH's), 7.84 (bs, 0.9H, amide NH's), 7.54(bs, 1.8H, CH_2N*H*C(S)N*H*CH_2), 5.31(s, 0.6H), 5.25 (t, 0.7H, J = 9.8Hz), 5.16 (m, 0.6H), 5.02 (s, 0.7H), 4.99 (d, 0.6H, J = 3.4Hz), 4.91 (m, 1.3H), 4.76 (m, 0.9H), 4.62 (m, 1.4H), 4.20 (m, 0.7H), 4.10 (m, 0.9H), 3.99 (m, 2.3H), 3.94 (m, 0.9H), 3.78 (m, 3.8H), 3.68 (m, 2H), 3.58 (m, 4H), 3.48 (m, 7H), 3.13 (m, 6H), 2.54-70 (m, 10H), 2.20 (bs, 4.0H), 2.07 (s, 2H), 1.89-2.00 (m, 17H), 1.78 (m, 3H) ppm. MALDI-TOF (pos) m/z 110000 g/mol.

10k: ^{1}H NMR (500 MHz, DMSO) δ 8.00 (bs, 1H, amide NH's), 7.93 (bs, 0.6H, amide NH's), 7.86 (bs, 1H, amide NH's), 7.54 (bs, 2H, $CH_2N\mathit{H}C(S)N\mathit{H}CH_2$), 5.31(s, 1H), 5.17 (d, 1H, J = 7.1Hz), 5.07 (m, 0.4H), 5.02 (d, 1H, J = 10.8Hz), 4.84 (m, 1.4H), 4.62 (m, 0.8H), 4.19 (m, 1H), 3.99 (m, 3H), 3.97 (m, 2H), 3.67 (m, 2H), 3.58 (m, 2H), 3.44 (m, 4H), 3.13 (bs, 3H), 2.95 (bs, 5H), 2.64 (m, 8H), 2.18 (bs, 5H), 2.07 (s, 4H), 2.00 (s, 1H), 1.99 (s, 4H), 1.96 (s, 4H), 1.89 (s, 4H), 1.78 (m, 3H) ppm. MALDI-TOF (pos) m/z 111000 g/mol.

10l: ^{1}H NMR (500 MHz, DMSO) δ 7.99 (bs, 1H, amide NH's), 7.63 (bs, 0.8H, amide NH's), 7.84 (bs, 1H, amide NH's), 7.54(bs, 2H, $CH_2N\mathit{H}C(S)N\mathit{H}CH_2$), 5.31(s, 0.35H), 5.17 (d, 0.35H, J = 10.9), 5.07 (m, 3H), 4.93 (d, 0.35H, J = 10.7Hz), 4.84 (m, 1H), 4.62 (m, 0.7H), 4.19 (m, 0.35H), 4.12 (m, 1H), 4.00 (m, 2H), 3.91 (m, 1H), 3.78 (m, 2H), 3.68 (m, 2H), 3.58 (m, 2H), 3.48 (m, 4H), 3.12 (bs, 3H), 3.04 (bs, 3H), 2.55 (bs and m, 10H), 2.18 (bs, 4H), 2.06 (s, 3.9H), 1.99 (m, 9H), 1.89 (s, 3.9H), 1.78 (m, 2.8H) ppm. MALDI-TOF (pos) m/z 111000 g/mol.

General procedure for deacylation of dendrimers 7a-n, 8a-n, 9a-l, 10a-l. To the lyophilized solid product of compounds 7a-n, 8a-n, 9a-l, 10a-l 1 mL of 1:1 water:methanol was added, at which point the dendrimer would become a white precipitate solid. To this mixture was added 0.2 equivalents of Na OMe (0.8 M in MeOH) for each peripheral carbohydrate, and let stir for 3 hrs. If, at this time, the

mixture had not become a clear solution a further 0.2 equivalents of NaOMe (0.8 M in MeOH) was added and this step was repeated until the mixture became a clear and colorless solution. $HCl_{(aq)}$ (0.1M) was then added slowly until the pH was ~ 7. This neutralized solution was placed in a centrifugal filter device, diluted with 3 mL 1:1 H_2O:MeOH and filtered at 3500 rpm for 30 mins. The filtrate was then removed and 3 mL H_2O was added and filtered for 30 mins at 3500 rpm. This procedure was repeated 2 more times. At which point the remaining residue was taken up in Millipore water and lyophilized to give a white fluffy solid.

7a: ^{1}H NMR (500 MHz, DMSO) δ 7.96 (bs, 1H, amide NH's), 7.89 (bs, 0.4H, amide NH's), 7.83 (bs, 0.4H, amide NH's), 7.76 (bs, 1.1H, amide NH's), 7.52 (bs, 1.9H $CH_2N\mathit{H}C(S)N\mathit{H}CH_2$), 4.67 (bs, 1.4H), 4.58 (s, 0.5H), 4.54 (m, 1.9H), 4.41 (bs, 0.9H), 4.33 (bs, 0.3H), 3.65 (bs, 0.4), 3.59 (m, 2.2H), 3.54 (s, 1.6H), 3.39-3.51 (m, 5.7H), 3.12 (bs, 2.7H), 3.02 (bs, 4.0H), 2.48-2.63 (m, 10.1H), 2.38 (bs, 2.2H), 2.15 (bs, 5.1H), 1.73 (m, 2.9H) ppm; MALDI-TOF (pos) m/z 14000 g/mol.

7b: ^{1}H NMR (500 MHz, DMSO) δ 7.99 (bs, 1H, amide NH's), 7.92 (bs, 0.5H, amide NH's), 7.85 (bs, 0.6H, amide NH's), 7.79 (bs, 1.2H, amide NH's), 7.54 (bs, 1.9H $CH_2N\mathit{H}C(S)N\mathit{H}CH_2$), 4.83 (s, 0.15H), 4.67 (s, 0.5H), 4.60 (s, 0.5H), 4.56 (m, 1.5H), 4.43 (bs, 0.9H), 4.35 (bs, 0.3), 3.60-3.67 (m, 2.5H), 3.56 (s, 1.4H), 3.48 (m, 2.7H), 3.34-3.44 (m, 6H), 3.13 (bs, 2.8H), 3.05 (bs, 5.1H), 2.60 (m, 10.9H),

2.40 (bs, 2.5H), 2.17 (bs, 6H), 1.77 (m, 3.5H) ppm. MALDI-TOF (pos) m/z 14900 g/mol.

7d: ^{1}H NMR (500 MHz, DMSO) δ 7.98 (bs, 1H, amide NH's), 7.91 (bs, 0.3H, amide NH's), 7.85 (bs, 0.3H, amide NH's), 7.78 (bs, 1H, amide NH's), 7.54 (bs, 1.9H $CH_2N\mathit{H}C(S)N\mathit{H}CH_2$), 4.98 (s, 0.14H), 4.92 (s, 0.14H), 4.84 (s, 0.8H), 4.57-4.75 (m, 2.8H), 4.43 (m, 1H), 4.43 (bs, 0.14), 3.48-3.77 (m, 5.2H), 3.36-3.48 (m, 5H), 3.14 (bs, 3.4H), 3.05 (bs, 4.6H), 2.60 (bs, 9.7H), 2.40 (bs, 2.3H), 2.17 (bs, 5.1H), 1.77 (m, 2.8H) ppm. MALDI-TOF (pos) m/z 15000 g/mol.

7e: ^{1}H NMR (500 MHz, DMSO) δ 8.02 (bs, 1H, amide NH's), 7.85 (bs, 0.9H, amide NH's), 7.56 (bs, 1.8H $CH_2N\mathit{H}C(S)N\mathit{H}CH_2$), 4.97 (bs, 0.2H), 4.85 (bs, 0.9H), 4.75 (bs, 0.6H), 4.65 (m, 0.6H),4.59 (s, 0.9H), 4.43 (bs, 0.8H), 4.35 (bs, 0.2), 3.68 (m, 1.6H), 3.47-3.59 (m, 3.8H), 3.34-3.43 (m, 4.3H), 3.13 (bs, 4.5H), 3.04 (bs, 2.6H), 2.69 (bs, 3.8H), 2.57 (m, 4.7H), 2.22 (bs, 3.9H), 1.76 (m, 2.4H) ppm. MALDI-TOF (pos) m/z 15000 g/mol.

7f: ^{1}H NMR (500 MHz, DMSO) δ 8.00 (bs, 1H, amide NH's), 7.78 (bs, 0.8H, amide NH's), 7.65 (bs, 1.7H $CH_2N\mathit{H}C(S)N\mathit{H}CH_2$), 4.90 (s, 1H), 4.80 (s, 1H), 4.69 (s, 0.9H), 4.58 (s, 0.9H), 4.44 (bs, 1H), 3.60 (m, 3H), 3.35 (m, 4.1H), 3.14 (bs, 3.3H), 3.04 (bs, 2.9H), 2.57 (m, 6H), 2.36 (bs, 1.8H), 2.15 (bs, 3.5H), 1.76 (m, 1.9H) ppm MALDI-TOF (pos) m/z 16400 g/mol.

7g: ^{1}H NMR (500 MHz, DMSO) δ 8.03 (bs, 1H, amide NH's), 7.97 (bs, 0.7H, amide NH's), 7.89 (bs, 0.3H, amide NH's), 7.59 (bs, 0.7H $CH_2N\mathit{H}C(S)N\mathit{H}CH_2$), 4.84 (bs, 0.6H), 4.69 (m, 1.9H), 4.59 (s, 0.7H), 4.58 (s, 0.7H), 4.42 (m, 0.8H), 3.54-3.64 (m, 4H), 3.42-3.51 (m, 8.9H), 3.13 (bs, 5.7H) 3.04 (bs, 3.6H), 2.70 (bs, 6.1H), 2.58 (m, 6.1H), 2.22 (bs, 5.7H), 1.78 (m, 3.7H) ppm. MALDI-TOF (pos) m/z 15000 g/mol.

7i: ^{1}H NMR (500 MHz, DMSO) δ 7.99 (bs, 1H, amide NH's), 7.92 (bs, 0.4H, amide NH's), 7.85 (bs, 0.5H, amide NH's), 7.80 (bs, 1H, amide NH's), 7.54 (bs, 1.8H $CH_2N\mathit{H}C(S)N\mathit{H}CH_2$), 4.84 (bs, 0.3H), 4.69 (m, 1.8H), 4.59 (m, 0.4H), 4.56 (s, 1.1H), 4.42 (bs, 0.9H), 3.60 (m, 2.4), 3.56 (s, 1.2H), 3.48 (bs, 3.1H), 3.41 (m, 3.3H), 3.13 (bs, 3.1H), 3.04 (bs, 4.4H), 2.51-2.64 (m, 10.1H), 2.50 (bs, 2.1H), 2.18 (bs, 5.1H), 1.75 (m, 3H) ppm. MALDI-TOF (pos) m/z 15200 g/mol.

7j: ^{1}H NMR (500 MHz, DMSO) δ 7.96 (bs, 1H, amide NH's), 7.74 (bs, 1H, amide NH's), 7.51 (bs, 2H, $CH_2N\mathit{H}C(S)N\mathit{H}CH_2$), 4.53 (m, 3H), 3.73 (s, 1H), 3.25-3.65 (m, 10H), 3.01-3.14 (m, 5H), 2.58 (m, 9H), 2.18 (bs, 4H), 1.79 (m, 2H) ppm; MALDI-TOF (pos) m/z 16600 g/mol.

7k: ^{1}H NMR (500 MHz, DMSO) δ 8.02 (bs, 1H, amide NH's), 7.96 (bs, 0.5H, amide NH's), 7.87 (bs, 1.5H, amide NH's), 7.56 (bs, 1.9H $CH_2N\mathit{H}C(S)N\mathit{H}CH_2$), 4.85 (bs, 0.3H), 4.69 (m, 0.2H), 4.60 (s, 1.1H), 4.52 (m, 1.1H), 4.44 (m, 0.7H),

4.36 (bs, 0.6), 3.67 (s, 0.7H), 3.59 (m, 1.6H), 3.47-3.55 (m, 5.4H), 3.34-3.41 (m, 3.6H), 3.04-3.14 (m, 8.4H), 2.69 (bs, 5.1H), 2.57 (m, 5.3H), 2.21 (bs, 5.6H), 1.77 (m, 3.4H) ppm. MALDI-TOF (pos) m/z14800 g/mol.

7l: ^{1}H NMR (500 MHz, DMSO) δ 8.00 (bs, 1H, amide NH's), 7.93 (bs, 0.6H, amide NH's), 7.86 (bs, 0.6H, amide NH's), 7.80 (bs, 1.1H, amide NH's), 7.57 (bs, 2H $CH_2N\mathit{H}C(S)N\mathit{H}CH_2$), 4.69 (bs, 0.9H), 4.60 (s, 1H), 4.56 (s, 2.2H), 4.43 (bs, 1.3H), 4.35 (bs, 1.5), 3.68 (s, 1H), 3.62 (m, 2.3H), 3.48-3.56 (m, 6.7H), 3.34-3.41 (m, 5H), 3.14 (bs, 3.2H) 3.04 (bs, 4.7H), 2.53-2.64 (m, 10.1H), 2.42 (bs, 2.7H), 2.18 (bs, 5.2H), 1.76 (m, 3.7H) ppm. MALDI-TOF (pos) m/z 15200 g/mol.

7m: ^{1}H NMR (500 MHz, DMSO) δ 7.98 (bs, 1H, amide NH's), 7.91 (bs, 0.2H, amide NH's), 7.78 (bs, 1.2H, amide NH's), 7.53 (bs, 2.0H $CH_2N\mathit{H}C(S)N\mathit{H}CH_2$), 4.68 (bs, 1.9H), 4.60 (s, 0.3H), 4.56 (s, 2H), 4.41 (bs, 1H), 4.35 (bs, 0.2H), 3.67 (bs, 0.3), 3.60 (m, 2.5H), 3.55 (s, 1.6H), 3.48 (m, 2.2H), 3.41 (m, 3.3H), 3.13 (bs, 2.8H), 3.04 (bs, 3.2H), 2.51-2.64 (m, 10.2H), 2.41 (bs, 2.1H), 2.17 (bs, 4.9H), 1.77 (m, 2.7H) ppm. MALDI-TOF (pos) m/z 14100 g/mol.

7n: ^{1}H NMR (500 MHz, DMSO) δ 7.99 (bs, 1H, amide NH's), 7.92 (bs, 0.3H, amide NH's), 7.85 (bs, 0.3H, amide NH's), 7.79 (bs, 0.9H, amide NH's), 7.54 (bs, 1.9H $CH_2N\mathit{H}C(S)N\mathit{H}CH_2$), 4.85 (bs, 0.8H), 4.75 (bs, 0.6H), 4.70 (bs, 0.6H), 4.65 (bs, 0.6H), 4.60 (s, 0.7H), 4.56 (m, 0.7H), 4.43 (bs, 1H) 3.56-3.62 (m, 3.1),

3.36-3.49 (m, 8.9H), 3.13 (bs, 3.6H), 3.04 (bs, 4.3H), 2.51-2.64 (m, 9.8H), 2.41 (bs, 2.1H), 2.17 (bs, 5H), 1.75 (m, 2.7H) ppm. MALDI-TOF (pos) m/z 15200 g/mol.

G(4)

8f: ^{1}H NMR (500 MHz, DMSO) δ 8.00 (bs, 1H, amide NH's), 7.78 (bs, 1H, amide NH's), 7.65 (bs, 1.7H $CH_2N\mathit{H}C(S)N\mathit{H}CH_2$), 4.89 (s, 1H), 4.80 (s, 0.9H), 4.69 (s, 0.8H), 4.58 (s, 0.9H), 4.45 (bs, 1H), 3.60 (m, 3.8H), 3.35 (m, 4.7H), 3.14 (bs, 3.6H), 3.04 (bs, 3.0H), 2.57 (m, 7.6H), 2.38 (bs, 1.8H), 2.15 (bs, 3.7H), 1.74 (m, 2H) ppm. MALDI-TOF (pos) m/z 31500 g/mol.

8g: ^{1}H NMR (500 MHz, DMSO) δ 7.99 (bs, 1H, amide NH's), 7.92 (bs, 0.3H, amide NH's), 7.85 (bs, 0.3H, amide NH's), 7.79 (bs, 0.9H, amide NH's), 7.54 (bs, 1.9H $CH_2N\mathit{H}C(S)N\mathit{H}CH_2$), 4.85 (bs, 0.8H), 4.75 (bs, 0.6H), 4.70 (bs, 0.6H), 4.65 (bs, 0.6H), 4.60 (s, 0.7H), 4.56 (m, 0.7H), 4.43 (bs, 1H) 3.56-3.62 (m, 3.1), 3.36-3.49 (m, 8.9H), 3.13 (bs, 3.6H), 3.04 (bs, 4.3H), 2.51-2.64 (m, 9.8H), 2.41 (bs, 2.1H), 2.17 (bs, 5H), 1.75 (m, 2.7H) ppm. MALDI-TOF (pos) m/z 27700 g/mol.

8h: ^{1}H NMR (500 MHz, DMSO) δ 8.07 (bs, 1H, amide NH's), 7.89 (bs, 0.3H, amide NH's), 7.59 (bs, 0.7H $CH_2N\mathit{H}C(S)N\mathit{H}CH_2$), 4.86 (bs, 0.3H), 4.70 (bs, 0.7H), 4.59 (s, 0.3H), 4.57 (s, 0.2H), 4.44 (m, 0.3H), 3.56-3.63 (m, 1.2H), 3.42-

3.51 (m, 2.6H), 3.15 (bs, 2.7H) 3.06 (bs, 2H), 2.79 (bs, 2.9H), 2.58 (m, 3.2H), 2.28 (m, 2.5H), 1.78 (m, 1.7H) ppm. MALDI-TOF (pos) m/z 25500 g/mol.

8i: ^{1}H NMR (500 MHz, DMSO) δ 7.99 (bs, 1H, amide NH's), 7.92 (bs, 0.4H, amide NH's), 7.85 (bs, 0.5H, amide NH's), 7.80 (bs, 1H, amide NH's), 7.54 (bs, 1.8H $CH_2N\mathit{H}C(S)N\mathit{H}CH_2$), 4.84 (bs, 0.3H), 4.69 (m, 1.8H), 4.59 (m, 0.4H), 4.56 (s, 1.1H), 4.42 (bs, 0.9H), 3.60 (m, 2.4), 3.56 (s, 1.2H), 3.48 (bs, 3.1H), 3.41 (m, 3.3H), 3.13 (bs, 3.1H), 3.04 (bs, 4.4H), 2.51-2.64 (m, 10.1H), 2.50 (bs, 2.1H), 2.18 (bs, 5.1H), 1.75 (m, 3H) ppm. MALDI-TOF (pos) m/z 28000 g/mol.

8j: ^{1}H NMR (500 MHz, DMSO) δ 7.96 (bs, 1H, amide NH's), 7.74 (bs, 1H, amide NH's), 7.51 (bs, 2H, $CH_2N\mathit{H}C(S)N\mathit{H}CH_2$), 4.53 (m, 3H), 3.73 (s, 1H), 3.25-3.65 (m, 10H), 3.01-3.14 (m, 5H), 2.58 (m, 9H), 2.18 (bs, 4H), 1.79 (m, 2H) ppm; MALDI-TOF (pos) m/z 33200 g/mol.

8k: ^{1}H NMR (500 MHz, DMSO) δ 8.02 (bs, 1H, amide NH's), 7.96 (bs, 0.5H, amide NH's), 7.87 (bs, 1.5H, amide NH's), 7.56 (bs, 1.9H $CH_2N\mathit{H}C(S)N\mathit{H}CH_2$), 4.85 (bs, 0.3H), 4.69 (m, 0.2H), 4.60 (s, 1.1H), 4.52 (m, 1.1H), 4.44 (m, 0.7H), 4.36 (bs, 0.6), 3.67 (s, 0.7H), 3.59 (m, 1.6H), 3.47-3.55 (m, 5.4H), 3.34-3.41 (m, 3.6H), 3.04-3.14 (m, 8.4H), 2.69 (bs, 5.1H), 2.57 (m, 5.3H), 2.21 (bs, 5.6H), 1.77 (m, 3.4H) ppm. MALDI-TOF (pos) m/z 27500 g/mol.

8l: ^{1}H NMR (500 MHz, DMSO) δ 8.02 (bs, 1H, amide NH's), 7.85 (bs, 0.9H, amide NH's), 7.56 (bs, 1.8H $CH_2N\mathit{H}C(S)N\mathit{H}CH_2$), 4.97 (bs, 0.2H), 4.85 (bs, 0.9H), 4.75 (bs, 0.6H), 4.65 (m, 0.6H),4.59 (s, 0.9H), 4.43 (bs, 0.8H), 4.35 (bs, 0.2), 3.68 (m, 1.6H), 3.47-3.59 (m, 3.8H), 3.34-3.43 (m, 4.3H), 3.13 (bs, 4.5H), 3.04 (bs, 2.6H), 2.69 (bs, 3.8H), 2.57 (m, 4.7H), 2.22 (bs, 3.9H), 1.76 (m, 2.4H) ppm. MALDI-TOF (pos) m/z 29000 g/mol.

8m: ^{1}H NMR (500 MHz, DMSO) δ 7.99 (bs, 1H, amide NH's), 7.93 (bs, 0.5H, amide NH's), 7.85 (bs, 0.7H, amide NH's), 7.80 (bs, 1.2H, amide NH's), 7.55 (bs, 1.9H $CH_2N\mathit{H}C(S)N\mathit{H}CH_2$), 4.69 (bs, 0.9H), 4.60 (s, 0.8H), 4.56 (s, 0.7H), 4.52 (m, 1.1H), 4.43 (m, 0.9H), 4.35 (bs, 0.6), 3.68 (s, 0.8H), 3.62 (m, 2H), 3.48-3.56 (m, 5.7H), 3.34-3.41 (m, 5.4H), 3.14 (bs, 2.8H) 3.05 (bs, 5.3H), 2.53-2.64 (m, 11.1H), 2.42 (bs, 2.5H), 2.18 (bs, 5.6H), 1.76 (m, 3.7H) ppm. MALDI-TOF (pos) m/z 27000 g/mol.

8n: ^{1}H NMR (500 MHz, DMSO) δ 7.98 (bs, 1H, amide NH's), 7.91 (bs, 0.2H, amide NH's), 7.78 (bs, 1.2H, amide NH's), 7.53 (bs, 2.0H $CH_2N\mathit{H}C(S)N\mathit{H}CH_2$), 4.68 (bs, 1.9H), 4.60 (s, 0.3H), 4.56 (s, 2H), 4.41 (bs, 1H), 4.35 (bs, 0.2H), 3.67 (bs, 0.3), 3.60 (m, 2.5H), 3.55 (s, 1.6H), 3.48 (m, 2.2H), 3.41 (m, 3.3H), 3.13 (bs, 2.8H), 3.04 (bs, 3.2H), 2.51-2.64 (m, 10.2H), 2.41 (bs, 2.1H), 2.17 (bs, 4.9H), 1.77 (m, 2.7H) ppm. MALDI-TOF (pos) m/z 29000 g/mol.

G(5)

9e: ^{1}H NMR (500 MHz, DMSO) δ 8.01 (bs, 1H, amide NH's), 7.79 (bs, 1H, amide NH's), 7.69 (bs, 1.6H $CH_2N\mathit{H}C(S)N\mathit{H}CH_2$), 4.92 (bs, 0.9H), 4.84 (s, 0.8H) 4.73 (s, 0.8H), 4.59 (s, 0.8H), 4.49 (bs, 1H), 3.57 (m, 2.9H), 3.35 (m, 6H), 3.14 (bs, 3.4H), 3.04 (bs, 3.1H), 2.57 (m, 7.8H), 2.36 (bs, 1.8H), 2.16 (bs, 3.7H), 1.77 (m, 2H) ppm. MALDI-TOF (pos) m/z 59000 g/mol.

9f: ^{1}H NMR (500 MHz, DMSO) δ 7.99 (bs, 1H, amide NH's), 7.92 (bs, 0.3H, amide NH's), 7.85 (bs, 0.3H, amide NH's), 7.79 (bs, 0.9H, amide NH's), 7.54 (bs, 1.9H $CH_2N\mathit{H}C(S)N\mathit{H}CH_2$), 4.85 (bs, 0.8H), 4.75 (bs, 0.6H), 4.70 (bs, 0.6H), 4.65 (bs, 0.6H), 4.60 (s, 0.7H), 4.56 (m, 0.7H), 4.43 (bs, 1H) 3.56-3.62 (m, 3.1), 3.36-3.49 (m, 8.9H), 3.13 (bs, 3.6H), 3.04 (bs, 4.3H), 2.51-2.64 (m, 9.8H), 2.41 (bs, 2.1H), 2.17 (bs, 5H), 1.75 (m, 2.7H) ppm. MALDI-TOF (pos) m/z 51000 g/mol.

9g: ^{1}H NMR (500 MHz, DMSO) δ 8.07 (bs, 1H, amide NH's), 7.89 (bs, 0.3H, amide NH's), 7.59 (bs, 0.7H $CH_2N\mathit{H}C(S)N\mathit{H}CH_2$), 4.86 (bs, 0.3H), 4.70 (bs, 0.7H), 4.59 (s, 0.3H), 4.57 (s, 0.2H), 4.44 (m, 0.3H), 3.56-3.63 (m, 1.2H), 3.42-3.51 (m, 2.6H), 3.15 (bs, 2.7H) 3.06 (bs, 2H), 2.79 (bs, 2.9H), 2.58 (m, 3.2H), 2.28 (m, 2.5H), 1.78 (m, 1.7H) ppm. MALDI-TOF (pos) m/z 47500 g/mol.

9h: ^{1}H NMR (500 MHz, DMSO) δ 8.00 (bs, 1H, amide NH's), 7.94 (bs, 0.5H, amide NH's), 7.86 (bs, 0.6H, amide NH's), 7.81 (bs, 1H, amide NH's), 7.55 (bs, 2H $CH_2N\mathit{H}C(S)N\mathit{H}CH_2$), 4.85 (bs, 0.4H), 4.70 (m, 2.1H), 4.59 (m, 0.6H), 4.56 (s, 1.1H), 4.42 (bs, 1H), 3.60 (m, 4H), 3.36-3.47 (m, 8.8H), 3.13 (bs, 3.4H), 3.04 (bs, 4.4H), 2.51-2.64 (m, 10.9H), 2.18 (bs, 5.4H), 1.75 (m, 3.2H) ppm. MALDI-TOF (pos) m/z 54000 g/mol.

9i: ^{1}H NMR (500 MHz, DMSO) δ 7.96 (bs, 1H, amide NH's), 7.74 (bs, 1H, amide NH's), 7.51 (bs, 2H, $CH_2N\mathit{H}C(S)N\mathit{H}CH_2$), 4.53 (m, 3H), 3.73 (s, 1H), 3.25-3.65 (m, 10H), 3.01-3.14 (m, 5H), 2.58 (m, 9H), 2.18 (bs, 4H), 1.79 (m, 2H) ppm; MALDI-TOF (pos) m/z 61000 g/mol.

9j: ^{1}H NMR (500 MHz, DMSO) δ 8.02 (bs, 1H, amide NH's), 7.96 (bs, 0.5H, amide NH's), 7.87 (bs, 1.5H, amide NH's), 7.56 (bs, 1.9H $CH_2N\mathit{H}C(S)N\mathit{H}CH_2$), 4.85 (bs, 0.3H), 4.69 (m, 0.2H), 4.60 (s, 1.1H), 4.52 (m, 1.1H), 4.44 (m, 0.7H), 4.36 (bs, 0.6), 3.67 (s, 0.7H), 3.59 (m, 1.6H), 3.47-3.55 (m, 5.4H), 3.34-3.41 (m, 3.6H), 3.04-3.14 (m, 8.4H), 2.69 (bs, 5.1H), 2.57 (m, 5.3H), 2.21 (bs, 5.6H), 1.77 (m, 3.4H) ppm. MALDI-TOF (pos) m/z 50500 g/mol.

9k: ^{1}H NMR (500 MHz, DMSO) δ 8.02 (bs, 1H, amide NH's), 7.85 (bs, 0.9H, amide NH's), 7.56 (bs, 1.8H $CH_2N\mathit{H}C(S)N\mathit{H}CH_2$), 4.97 (bs, 0.2H), 4.85 (bs, 0.9H), 4.75 (bs, 0.6H), 4.65 (m, 0.6H),4.59 (s, 0.9H), 4.43 (bs, 0.8H), 4.35 (bs,

0.2), 3.68 (m, 1.6H), 3.47-3.59 (m, 3.8H), 3.34-3.43 (m, 4.3H), 3.13 (bs, 4.5H), 3.04 (bs, 2.6H), 2.69 (bs, 3.8H), 2.57 (m, 4.7H), 2.22 (bs, 3.9H), 1.76 (m, 2.4H) ppm. MALDI-TOF (pos) m/z 52500 g/mol.

9l: ^{1}H NMR (500 MHz, DMSO) δ 7.99 (bs, 1H, amide NH's), 7.93 (bs, 0.5H, amide NH's), 7.85 (bs, 0.7H, amide NH's), 7.80 (bs, 1.2H, amide NH's), 7.55 (bs, 1.9H $CH_2N\mathit{H}C(S)N\mathit{H}CH_2$), 4.69 (bs, 0.9H), 4.60 (s, 0.8H), 4.56 (s, 0.7H), 4.52 (m, 1.1H), 4.43 (m, 0.9H), 4.35 (bs, 0.6), 3.68 (s, 0.8H), 3.62 (m, 2H), 3.48-3.56 (m, 5.7H), 3.34-3.41 (m, 5.4H), 3.14 (bs, 2.8H) 3.05 (bs, 5.3H), 2.53-2.64 (m, 11.1H), 2.42 (bs, 2.5H), 2.18 (bs, 5.6H), 1.76 (m, 3.7H) ppm. MALDI-TOF (pos) m/z 50500 g/mol.

G(6)

10e: ^{1}H NMR (500 MHz, DMSO) δ 8.02 (bs, 1H, amide NH's), 7.79 (bs, 1.1H, amide NH's), 7.69 (bs, 1.2H $CH_2N\mathit{H}C(S)N\mathit{H}CH_2$), 4.92 (bs, 1.8H), 4.73 (bs, 0.8H), 4.59 (s, 0.9H), 4.49 (bs, 1H), 3.57 (m, 2.9H), 3.35 (m, 6H), 3.14 (bs3.4H), 3.04 (bs, 3.1H), 2.57 (m, 7.8H), 2.16 (bs, 4H), 1.76 (m, 2.1H) ppm. MALDI-TOF (pos) m/z 110500 g/mol.

10f: ^{1}H NMR (500 MHz, DMSO) δ 7.99 (bs, 1H, amide NH's), 7.92 (bs, 0.3H, amide NH's), 7.85 (bs, 0.3H, amide NH's), 7.79 (bs, 0.9H, amide NH's), 7.54 (bs, 1.9H $CH_2N\mathit{H}C(S)N\mathit{H}CH_2$), 4.85 (bs, 0.8H), 4.75 (bs, 0.6H), 4.70 (bs, 0.6H),

4.65 (bs, 0.6H), 4.60 (s, 0.7H), 4.56 (m, 0.7H), 4.43 (bs, 1H) 3.56-3.62 (m, 3.1), 3.36-3.49 (m, 8.9H), 3.13 (bs, 3.6H), 3.04 (bs, 4.3H), 2.51-2.64 (m, 9.8H), 2.41 (bs, 2.1H), 2.17 (bs, 5H), 1.75 (m, 2.7H) ppm. MALDI-TOF (pos) m/z 93000 g/mol.

10g: ^{1}H NMR (500 MHz, DMSO) δ 8.07 (bs, 1H, amide NH's), 7.89 (bs, 0.3H, amide NH's), 7.59 (bs, 0.7H $CH_2N\mathit{H}C(S)N\mathit{H}CH_2$), 4.86 (bs, 0.3H), 4.70 (bs, 0.7H), 4.59 (s, 0.3H), 4.57 (s, 0.2H), 4.44 (m, 0.3H), 3.56-3.63 (m, 1.2H), 3.42-3.51 (m, 2.6H), 3.15 (bs, 2.7H) 3.06 (bs, 2H), 2.79 (bs, 2.9H), 2.58 (m, 3.2H), 2.28 (m, 2.5H), 1.78 (m, 1.7H) ppm. MALDI-TOF (pos) m/z 88000 g/mol.

10h: ^{1}H NMR (500 MHz, DMSO) δ 7.96 (bs, 1H, amide NH's), 7.74 (bs, 1H, amide NH's), 7.51 (bs, 2H, $CH_2N\mathit{H}C(S)N\mathit{H}CH_2$), 4.53 (m, 3H), 3.73 (s, 1H), 3.25-3.65 (m, 10H), 3.01-3.14 (m, 5H), 2.58 (m, 9H), 2.18 (bs, 4H), 1.79 (m, 2H) ppm; MALDI-TOF (pos) m/z 113000 g/mol.

10i: ^{1}H NMR (500 MHz, DMSO) δ 8.03 (bs, 1H, amide NH's), 7.96 (bs, 0.5H, amide NH's), 7.88 (bs, 1.5H, amide NH's), 7.56 (bs, 1.8H $CH_2N\mathit{H}C(S)N\mathit{H}CH_2$), 4.85 (bs, 0.3H), 4.61 (s, 1.3H), 4.52 (m, 1.2H), 4.44 (m, 0.9H), 4.38 (bs, 0.7H), 3.67 (s, 1H), 3.59 (m, 1.8H), 3.37-3.55 (m, 10.4H), 3.04-3.14 (m, 8H), 2.57-67 (m, 10.7H), 2.21 (bs, 5.6H), 1.77 (m, 3.6H) ppm. MALDI-TOF (pos) m/z. 93000 g/mol.

10j: ^{1}H NMR (500 MHz, DMSO) δ 8.02 (bs, 1H, amide NH's), 7.85 (bs, 0.9H, amide NH's), 7.56 (bs, 1.8H $CH_2N\mathit{H}C(S)N\mathit{H}CH_2$), 4.97 (bs, 0.2H), 4.85 (bs, 0.9H), 4.75 (bs, 0.6H), 4.65 (m, 0.6H),4.59 (s, 0.9H), 4.43 (bs, 0.8H), 4.35 (bs, 0.2), 3.68 (m, 1.6H), 3.47-3.59 (m, 3.8H), 3.34-3.43 (m, 4.3H), 3.13 (bs, 4.5H), 3.04 (bs, 2.6H), 2.69 (bs, 3.8H), 2.57 (m, 4.7H), 2.22 (bs, 3.9H), 1.76 (m, 2.4H) ppm. MALDI-TOF (pos) m/z 90000 g/mol.

10k: ^{1}H NMR (500 MHz, DMSO) δ 7.99 (bs, 1H, amide NH's), 7.93 (bs, 0.5H, amide NH's), 7.85 (bs, 0.7H, amide NH's), 7.80 (bs, 1.2H, amide NH's), 7.55 (bs, 1.9H $CH_2N\mathit{H}C(S)N\mathit{H}CH_2$), 4.69 (bs, 0.9H), 4.60 (s, 0.8H), 4.56 (s, 0.7H), 4.52 (m, 1.1H), 4.43 (m, 0.9H), 4.35 (bs, 0.6), 3.68 (s, 0.8H), 3.62 (m, 2H), 3.48-3.56 (m, 5.7H), 3.34-3.41 (m, 5.4H), 3.14 (bs, 2.8H) 3.05 (bs, 5.3H), 2.53-2.64 (m, 11.1H), 2.42 (bs, 2.5H), 2.18 (bs, 5.6H), 1.76 (m, 3.7H) ppm. MALDI-TOF (pos) m/z 91500 g/mol.

10l: ^{1}H NMR (500 MHz, DMSO) δ 7.98 (bs, 1H, amide NH's), 7.91 (bs, 0.2H, amide NH's), 7.78 (bs, 1.2H, amide NH's), 7.53 (bs, 2.0H $CH_2N\mathit{H}C(S)N\mathit{H}CH_2$), 4.68 (bs, 1.9H), 4.60 (s, 0.3H), 4.56 (s, 2H), 4.41 (bs, 1H), 4.35 (bs, 0.2H), 3.67 (bs, 0.3), 3.60 (m, 2.5H), 3.55 (s, 1.6H), 3.48 (m, 2.2H), 3.41 (m, 3.3H), 3.13 (bs, 2.8H), 3.04 (bs, 3.2H), 2.51-2.64 (m, 10.2H), 2.41 (bs, 2.1H), 2.17 (bs, 4.9H), 1.77 (m, 2.7H) ppm. MALDI-TOF (pos) m/z 90500 g/mol.

The Following is ^{1}H NMR and MALDI-TOF data for Galactose functionalized dendrimers. These compounds were used as controls for assays and are not reported in the main text of this chapter.

Generation 3.0 PAMAM-based thiourea-linked 1-O-(6-thiourea-4-thiohexyl)-2,3,4,6-tetra-O-acetyl-α-D-galactopyranoside dendrimer. ^{1}H NMR (500 MHz, DMSO) δ 7.98 (bs, 1H, amide N*H*'s), 7.77 (bs, 0.8H, amide N*H*'s), 7.57 (bs, 1.8H, $CH_2NHC(S)NHCH_2$), 5.30(s, 1H), 5.16 (dd, 1H, J = 10.0, 2.9 Hz), 5.02 (d, 1H, J = 3.0 Hz), 4.92 (dd, 1H, J = 10.0, 3.0Hz), 4.20 (t, 1H, J = 6.8 Hz), 4.00 (m, 2H), 3.68 (m, 1H), 3.49 (m, 3.2H), 3.29 (bs, 6.2H), 3.13 (bs, 2.3H), 3.03 (bs, 2.1H), 2.40-2.67 (m, 8H), 2.18 (bs, 3.1H),2.08 (s, 3H), 1.99 (s, 3H), 1.96 (s, 3H), 1.90 (s, 3H), 1.77 (m, 2H) ppm. MALDI-TOF (pos) m/z 21200.

Generation 4.0 PAMAM-based thiourea-linked 1-O-(6-thiourea-4-thiohexyl)-2,3,4,6-tetra-O-acetyl-α-D-galactopyranoside dendrimer. ^{1}H NMR (500 MHz, DMSO) δ 7.99 (bs, 1H, amide N*H*'s), 7.77 (bs, 0.8H, amide N*H*'s), 7.58 (bs, 1.7H, $CH_2NHC(S)NHCH_2$), 5.31(s, 1H), 5.16 (dd, 1H, J = 10.0, 2.9Hz), 5.02 (d, 1H, J = 2.9Hz), 4.92 (dd, 1H, J = 10, 2.9Hz), 4.20 (t, 1H, J = 6.8Hz), 3.99 (m, 2H), 3.68 (m, 1H), 3.49 (m, 3H), 3.30 (bs, 6H), 3.13 (bs, 2H), 3.03 (bs, 2H), 2.40-2.70 (m, 9H), 2.18 (bs, 4H), 2.07 (s, 3H), 1.99 (s, 3H), 1.96 (s, 3H), 1.90 (s, 3H), 1.78 (m, 2H) ppm. MALDI-TOF (pos) m/z 41900.

Generation 5.0 PAMAM-based thiourea-linked 1-O-(6-thiourea-4-thiohexyl)-2,3,4,6-tetra-O-acetyl-α-D-galactopyranoside dendrimer. ^{1}H NMR (500 MHz, DMSO) δ 7.98 (bs, 1H, amide N*H*'s), 7.77 (bs, 1H, amide N*H*'s), 7.58 (bs, 2H, CH_2N*H*C(S)N*H*CH_2) 5.31(s, 1H), 5.16 (dd, 1H, J = 10.0, 3.0Hz), 5.02 (d, 1H, J = 3.0Hz), 4.92 (dd, 1H, J = 10.0, 3.0Hz), 4.20 (t, 1H, J = 6.8Hz), 4.00 (m, 2H), 3.68 (m, 1H), 3.49 (m, 3H), 3.29 (bs, 6H), 3.13 (bs, 2H), 3.03 (bs, 2H), 2.39-2.68 (m, 10H), 2.18 (bs, 4.2H), 2.08 (s, 3H), 2.00 (s, 3H), 1.97 (s, 3H), 1.91 (s, 3H), 1.78 (m, 2H) ppm. MALDI-TOF (pos) m/z 78000

Generation 6.0 PAMAM-based thiourea-linked 1-O-(6-thiourea-4-thiohexyl)-2,3,4,6-tetra-O-acetyl-α-D-galactopyranoside dendrimer. ^{1}H NMR (500 MHz, DMSO) δ 7.98 (bs, 1H, amide N*H*'s), 7.77 (bs, 1H, amide N*H*'s), 7.58 (bs, 2H, CH_2N*H*C(S)N*H*CH_2) 5.31(s, 1H), 5.16 (dd, 1H, J = 10.1, 2.7 Hz), 5.02 (d, 1H, J = 2.7 Hz), 4.92 (dd, 1H, J = 10.1, 2.7 Hz), 4.20 (t, 1H, J = 6.7 Hz), 4.00 (m, 2H), 3.68 (m, 1H), 3.48 (m, 3H), 3.29 (bs, 5.5H), 3.13 (bs, 3H), 3.03 (bs, 2H), 2.40-2.70 (m, 10.4H), 2.18 (bs, 4.6H),2.08 (s, 3H), 1.99 (s, 3H), 1.96 (s, 3H), 1.90 (s, 3H), 1.77 (m, 2H). MALDI-TOF (pos) m/z 140500

Generation 3.0 PAMAM-based thiourea-linked 1-O-(6-thiourea-4-thiohexyl) -α-D-galactopyranoside dendrimer. ^{1}H NMR (500 MHz, DMSO) δ 7.98 (bs, 1H, amide NH's), 7.77 (bs, 0.7H, amide NH's), 7.57 (bs, 1.8H, CH_2N*H*C(S)N*H*CH_2), 4.61 (s,

1H), 4.45 (m, 3H), 3.68 (s, 1H), 3.30-3.60 (m, 10H), 3.01-3.16 (m, 5.3H), 2.58 (m, 9H), 2.18 (bs, 4.2H), 1.78 (m, 2H) ppm. MALDI-TOF (pos) m/z 15400.

Generation 4.0 PAMAM-based thiourea-linked 1-O-(6-thiourea-4-thiohexyl) -α-D-galactopyranoside dendrimer. ^{1}H NMR (500 MHz, DMSO) δ 7.99 (bs, 1H, amide NH's), 7.79 (bs, 1H, amide NH's), 7.57 (bs, 2H, $CH_2N\mathit{H}C(S)N\mathit{H}CH_2$) 4.61 (s, 1H), 4.45 (m, 3H), 3.68 (s, 1H), 3.30-3.60 (m, 11H), 3.01-3.14 (m, 5H), 2.58 (m, 9H), 2.18 (bs, 4H), 1.78 (m, 2.1H) ppm. MALDI-TOF (pos) m/z 30300.

Generation 5.0 PAMAM-based thiourea-linked 1-O-(6-thiourea-4-thiohexyl) -α-D-galactopyranoside dendrimer. ^{1}H NMR (500 MHz, DMSO) δ 8.00 (bs, 1H, amide NH's), 7.77 (bs, 0.8H, amide NH's), 7.57 (bs, 1.8H, $CH_2N\mathit{H}C(S)N\mathit{H}CH_2$) 4.61 (s, 1H), 4.45 (m, 3H), 3.68 (s, 1H), 3.30-3.60 (m, 11H), 3.01-3.14 (m, 5H), 2.58 (m, 8.4H), 2.18 (bs, 4H), 1.77 (m, 2.1H) ppm. MALDI-TOF (pos) m/z 53000.

Generation 6.0 PAMAM-based thiourea-linked 1-O-(6-thiourea-4-thiohexyl) -α-D-galactopyranoside dendrimer. ^{1}H NMR (500 MHz, DMSO) δ 7.99 (bs, 1H, amide NH's), 7.77 (bs, 0.7H, amide NH's), 7.57 (bs, 1.7H, $CH_2N\mathit{H}C(S)N\mathit{H}CH_2$) 4.61 (s, 1H), 4.45 (m, 3H), 3.68 (s, 1H), 3.30-3.60 (m, 10H), 3.01-3.14 (m, 6H), 2.58 (m, 7.9H), 2.18 (bs, 3.8H), 1.77 (m, 2H) ppm. MALDI-TOF (pos) m/z 107500.

Table 12 MALDI-TOF data for heterogeneously functionalized dendrimers.[a]

Compound #	M_w after Mannose addition	M_w after Glucose addition	M_w after Galactose addition	M_w after deacylation
7a (4a)	14200	n/a[b]	17500	14000
7b (4b)	11700	13500	18200	14800
7c (4c)	10000	14000	18100	14900
7d (4d)	8300	14100	17500	15000
7e (4e)	n/a	13700	19300	15000
7f	n/a	21000	n/a	16400
7g	18700	12300	n/a	14800
7h	18300	12600	n/a	15000
7i	19200	16500	n/a	15200
7j	21300	n/a	n/a	16600
7k	n/a	12300	17700	14800
7l	n/a	16500	19400	15200
7m	11200	n/a	17500	14100
7n	16400	n/a	19200	15200
8a (5a)	29200	n/a	34400	28000
8b (5b)	26300	30200	33800	27600
8c (5c)	22900	29700	34200	27700
8d (5d)	18700	33500	36100	30200
8e (5e)	n/a	28300	36200	28900
8f	n/a	41900	n/a	31500
8g	34300	24500	n/a	27700
8h	32400	26500	n/a	25500
8i	36700	35000	n/a	28000
8j	42500	n/a	n/a	33200
8k	n/a	24500	33000	27500
8l	n/a	35000	37200	29000
8m	21800	n/a	36100	27000
8n	32600	n/a	37100	29000
9a (5a)	48000	n/a	63500	51500
9b (5b)	44500	51000	65500	51500
9c (5c)	34800	57000	67000	56000
9d (5d)	n/a	49500	66000	54000
9e	n/a	76000	n/a	59000
9f	63000	43000	n/a	51000
9g	60500	44500	n/a	47500
9h	64500	57500	n/a	54000
9i	78500	n/a	n/a	61000

Table 12 Continued

Compound #	M_w after Mannose addition	M_w after Glucose addition	M_w after Galactose addition	M_w after deacylation
9j	n/a	43000	61500	50500
9k	n/a	57500	65500	52500
9l	39000	n/a	61500	50500
10a (7a)	77000	n/a	114000	93000
10b (7b)	71000	83000	112500	94500
10c (7c)	68000	86500	115500	95500
10d (7d)	n/a	90000	116000	94500
10e	n/a	139000	n/a	110500
10f	109000	91000	n/a	93000
10g	106500	82000	n/a	88000
10h	142000	n/a	n/a	113000
10i	n/a	75000	114500	93000
10j	n/a	91000	110000	90000
10k	66500	n/a	111000	91500
10l	94500	n/a	111000	90500

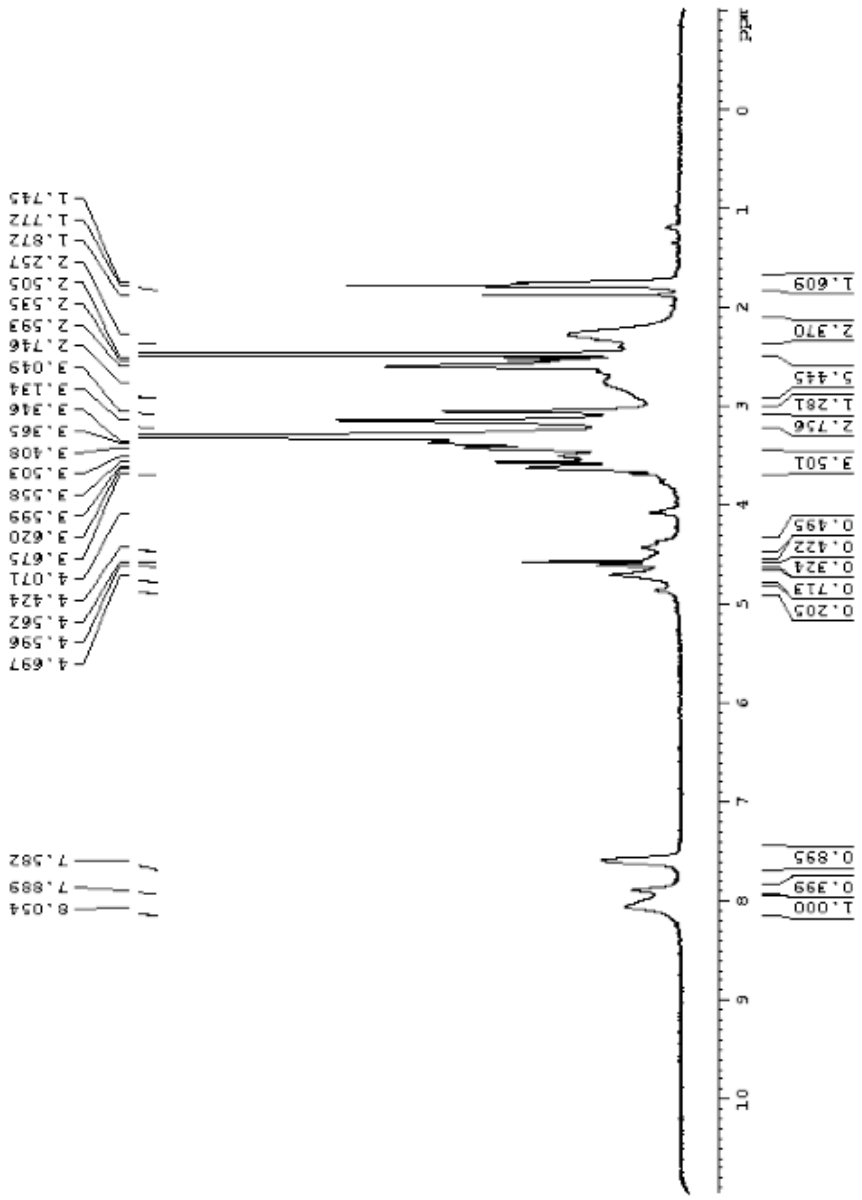

Figure 35 ^{1}H NMR spectrum (500 MHz, d_6-DMSO) of 7b (4b) (peracetylated).

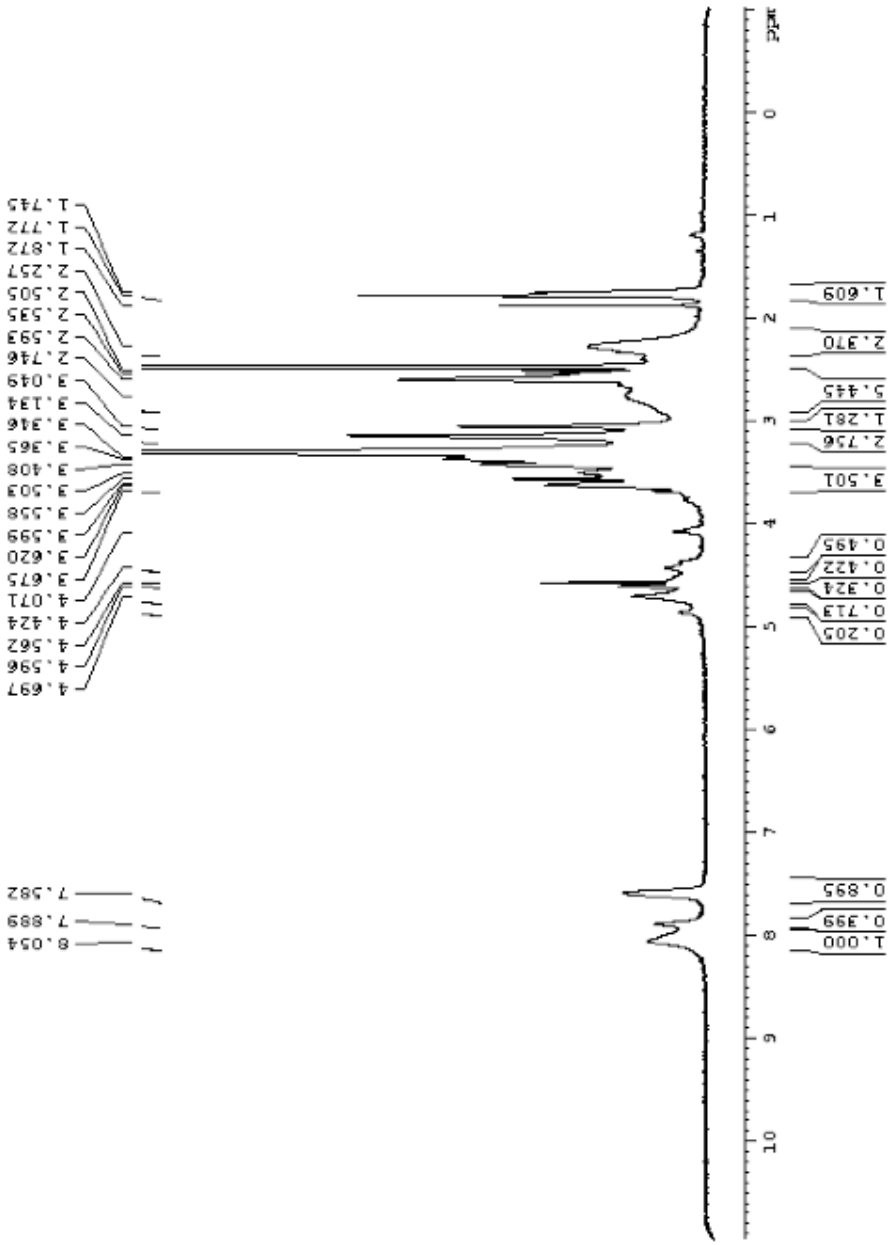

Figure 36 ^{1}H NMR spectrum (500 MHz, d_6-DMSO) of 7b (4b) (deacetylated).

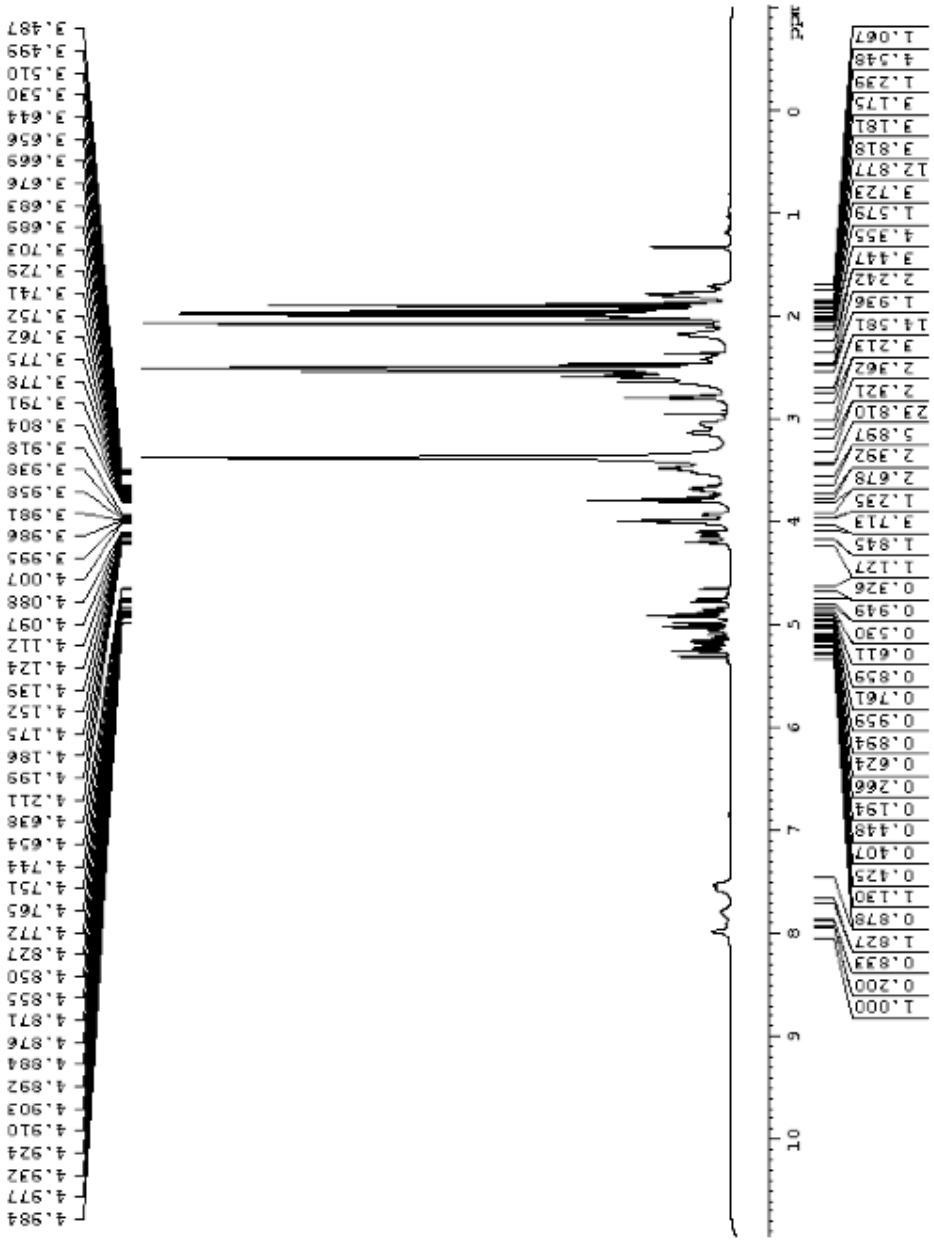

Figure 37 ^{1}H NMR spectrum (500 MHz, d_6-DMSO) of 7d (4d) (peracetylated).

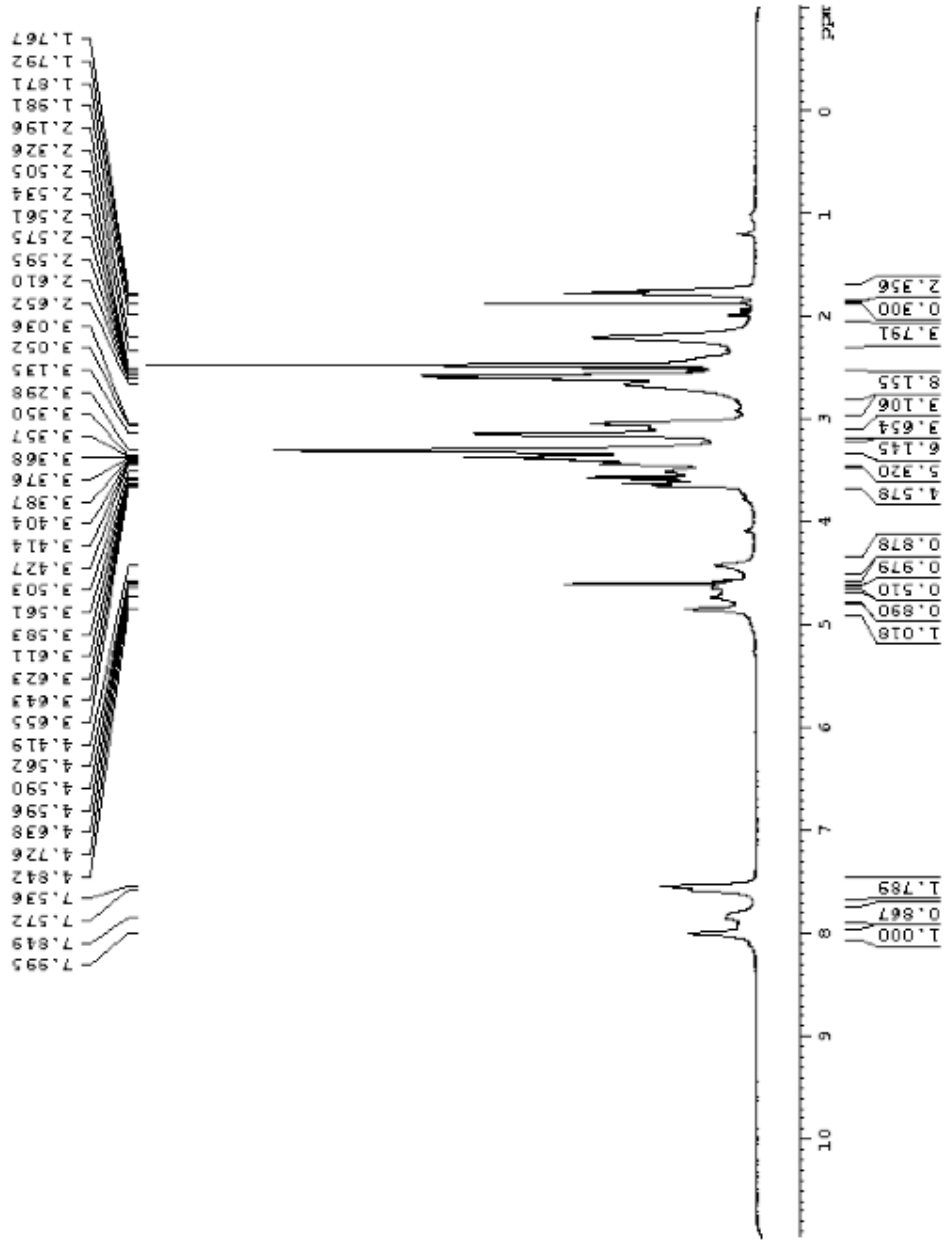

Figure 38 ^{1}H NMR spectrum (500 MHz, d_6-DMSO) of 7d (4d) (deacetylated).

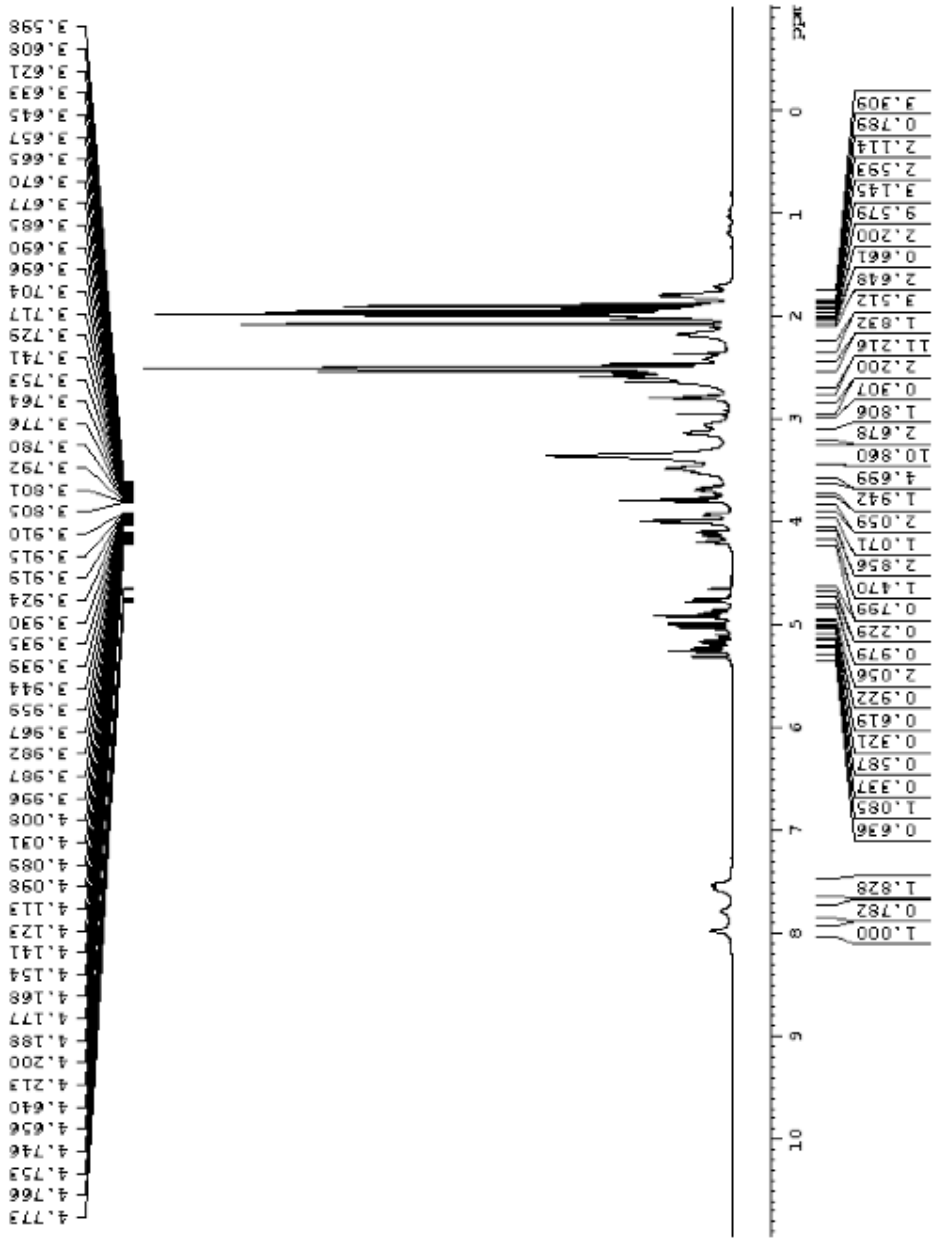

Figure 39 ^{1}H NMR spectrum (500 MHz, d_6-DMSO) of 7e (4e) (peracetylated).

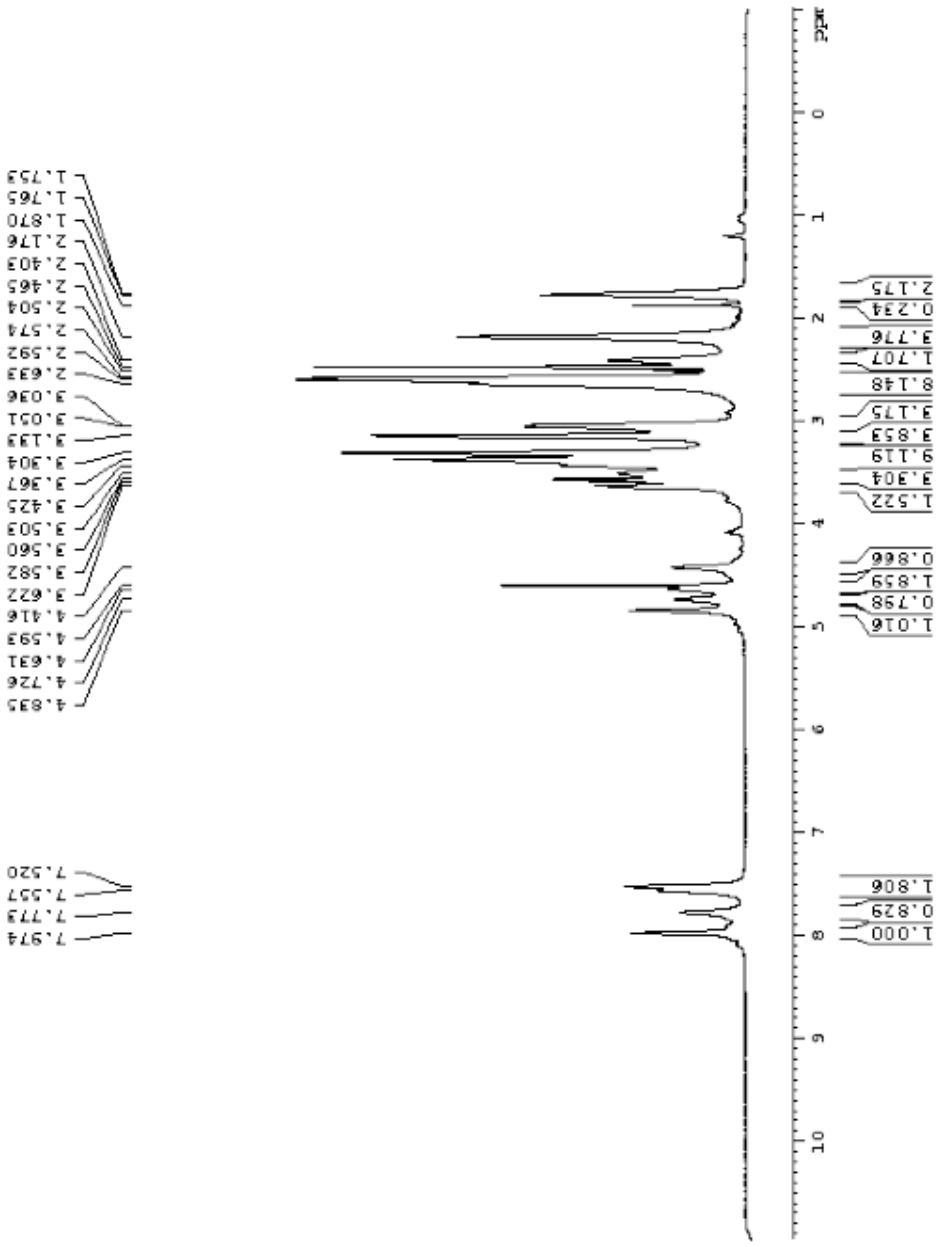

Figure 40 ^{1}H NMR spectrum (500 MHz, d_6-DMSO) of 7e (4e) (deacetylated).

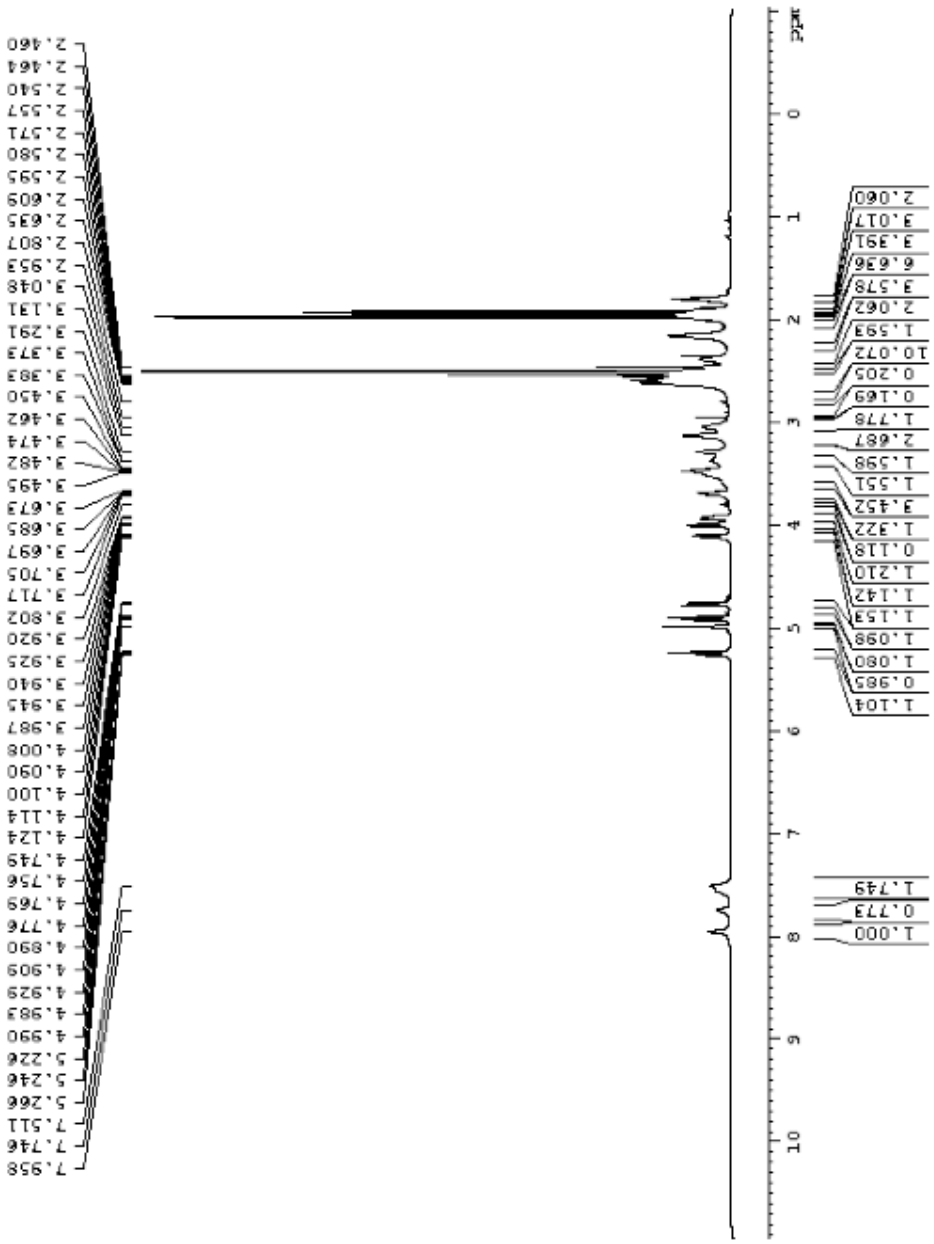

Figure 41 ^{1}H NMR spectrum (500 MHz, d_6-DMSO) of 8f (peracetylated).

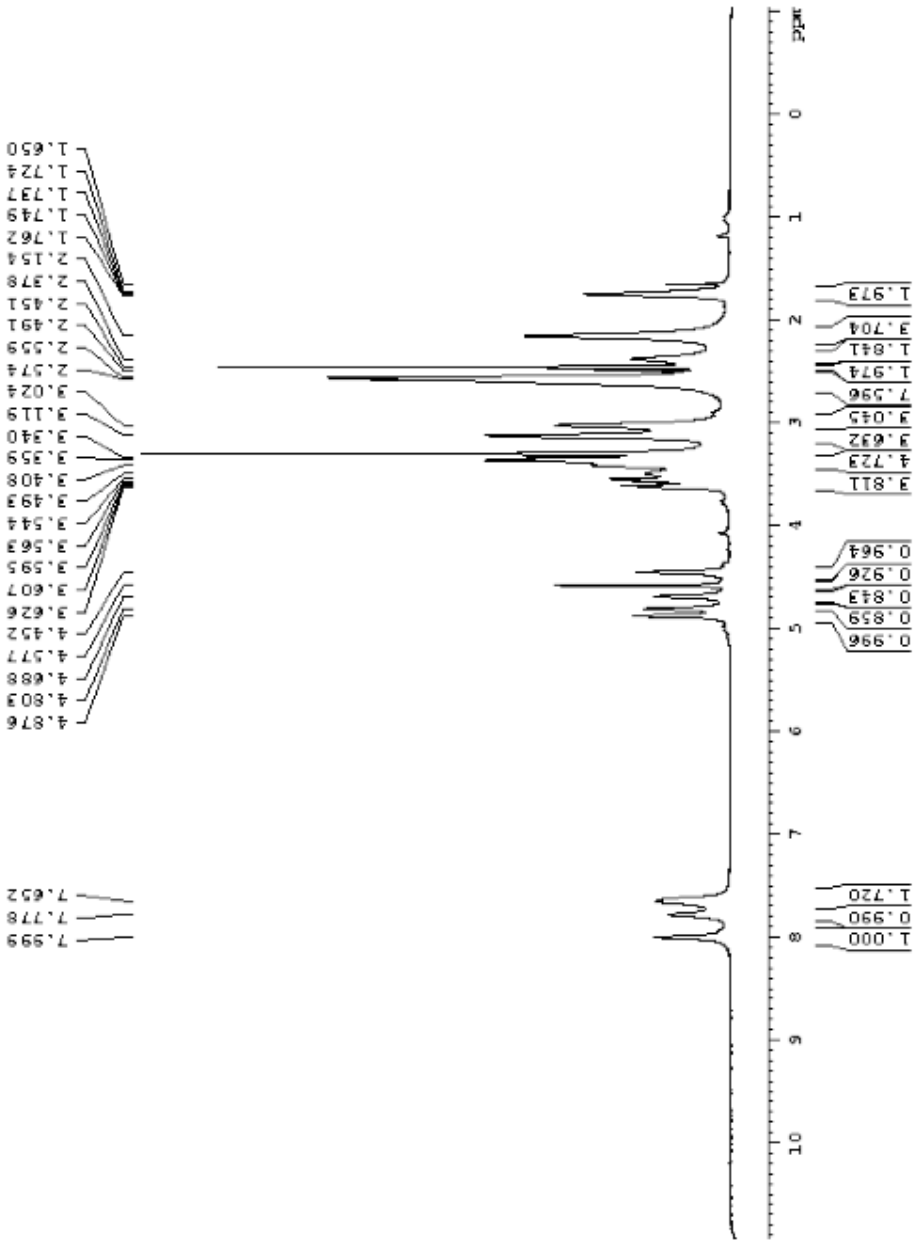

Figure 42 ^{1}H NMR spectrum (500 MHz, d_6-DMSO) of 8f (deacetylated).

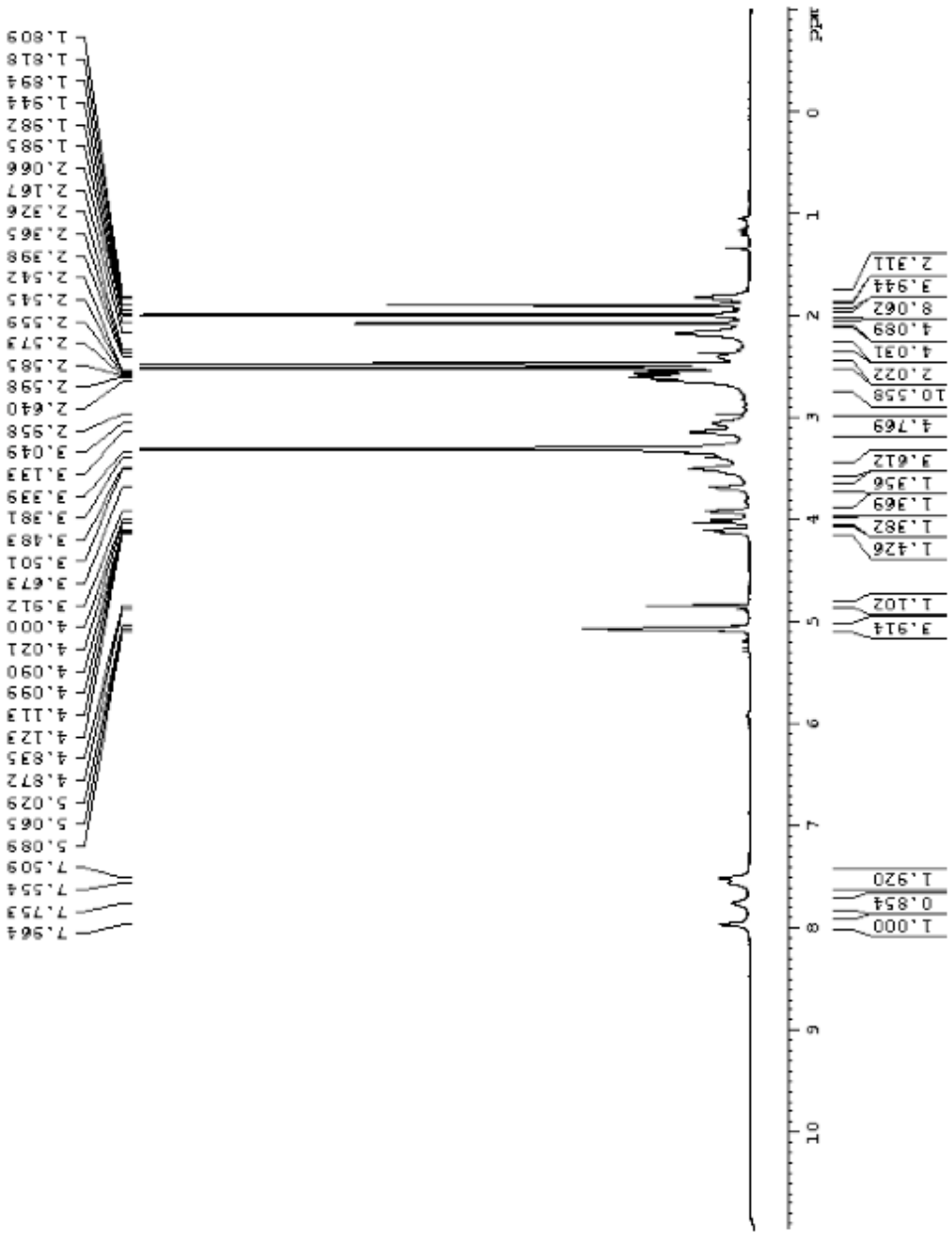

Figure 43 ^{1}H NMR spectrum (500 MHz, d_6-DMSO) of 8j (peracetylated).

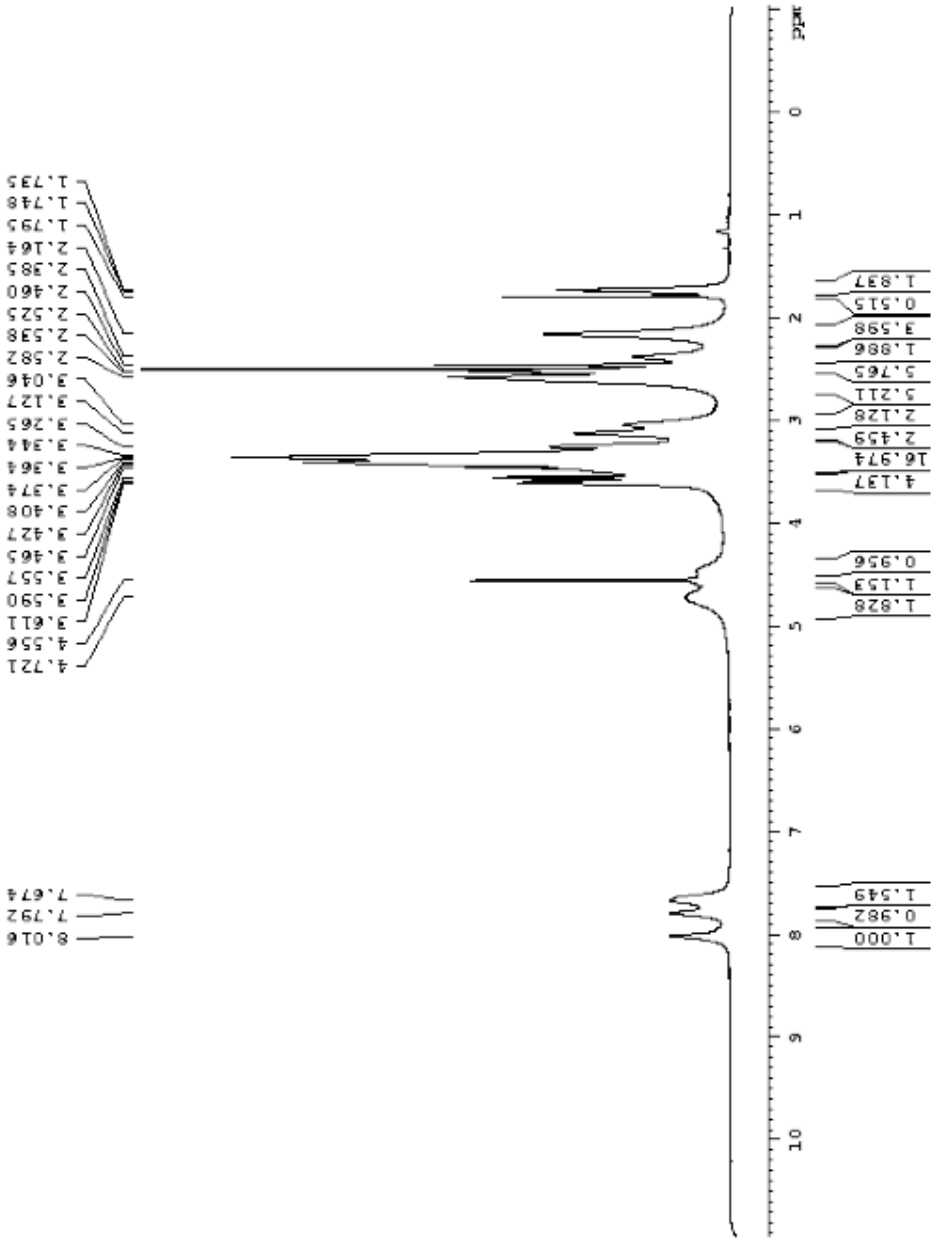

Figure 44 ^{1}H NMR spectrum (500 MHz, d_6-DMSO) of 8j (deacetylated).

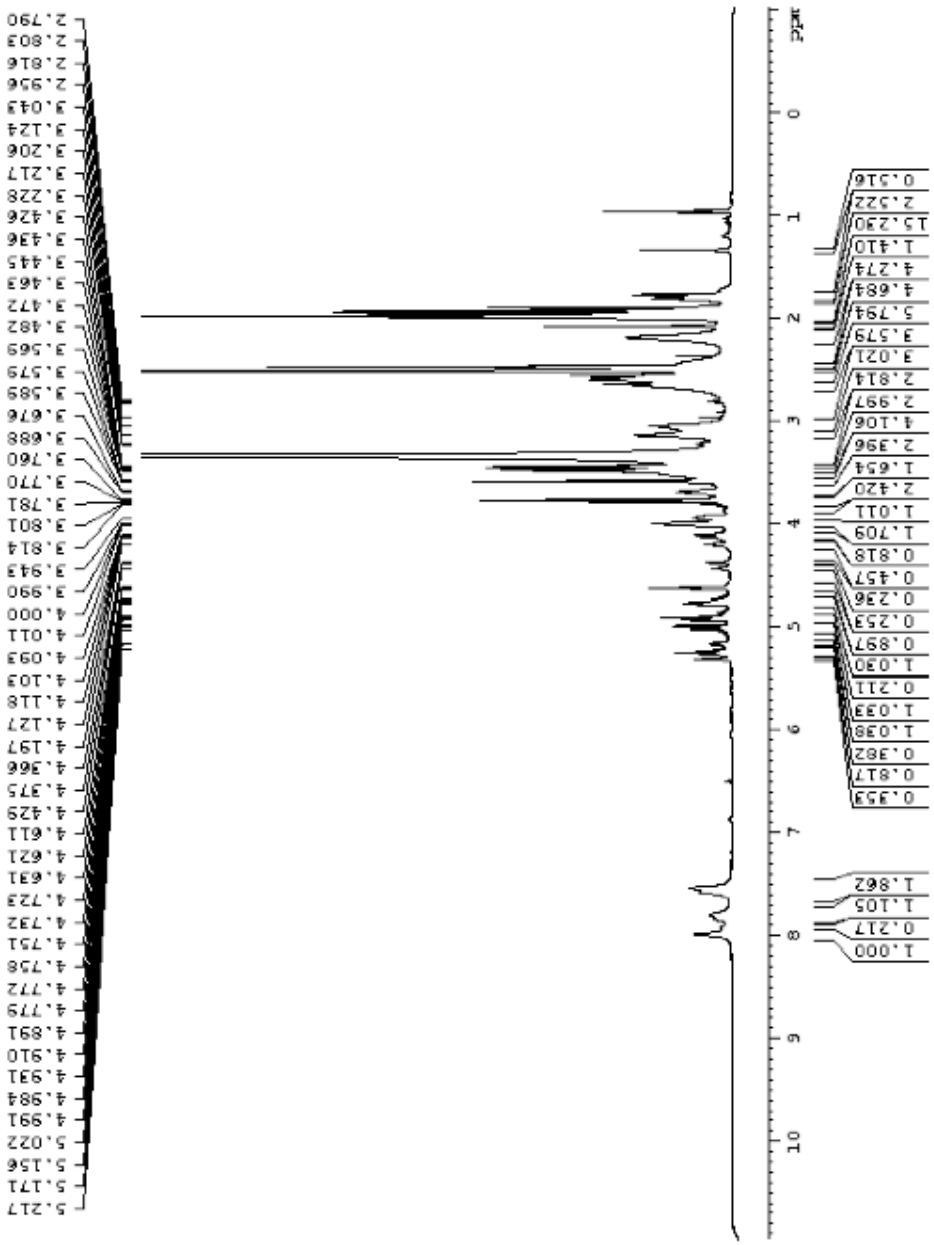

Figure 45 ^{1}H NMR spectrum (500 MHz, d_6-DMSO) of 8l (peracetylated).

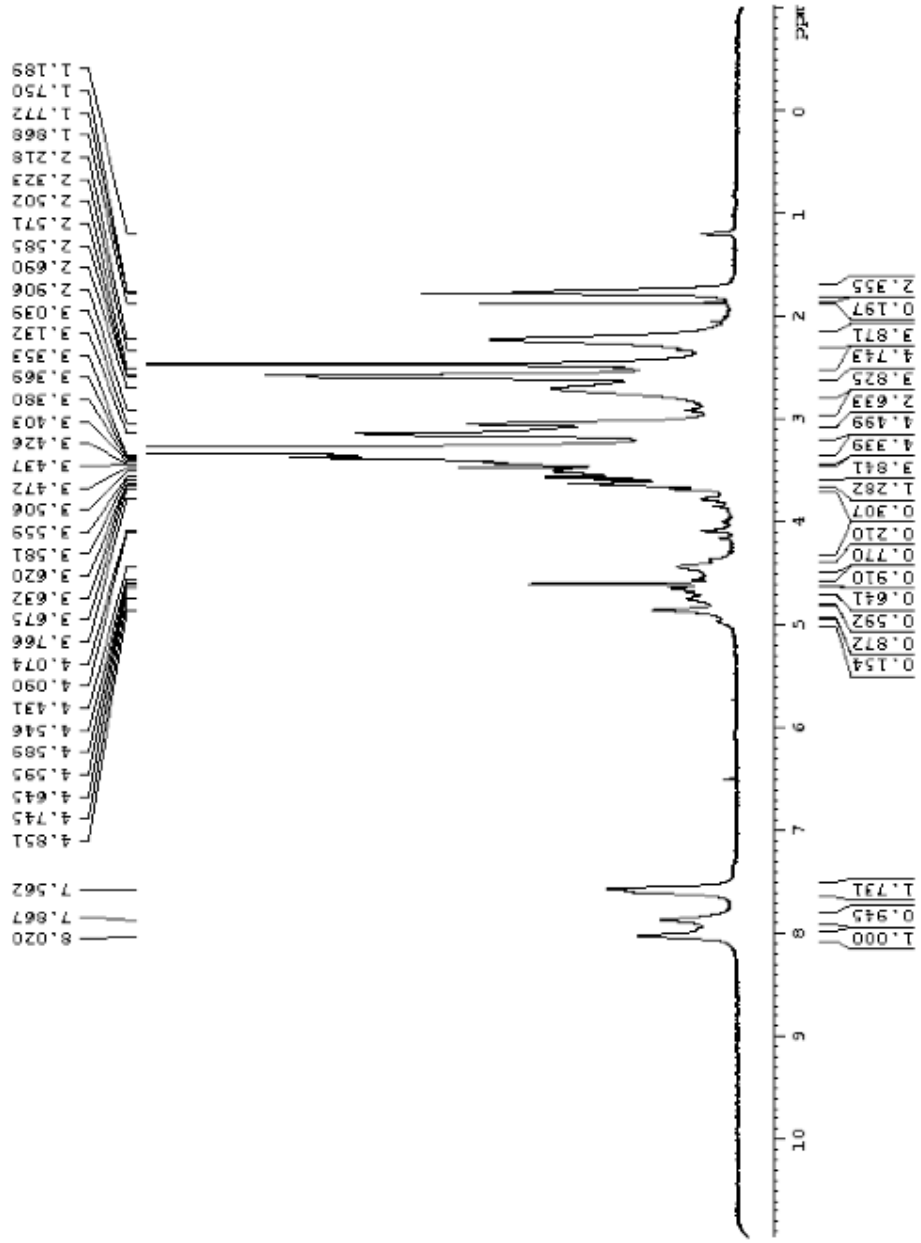

Figure 46 ^{1}H NMR spectrum (500 MHz, d_6-DMSO) of 8l (deacetylated).

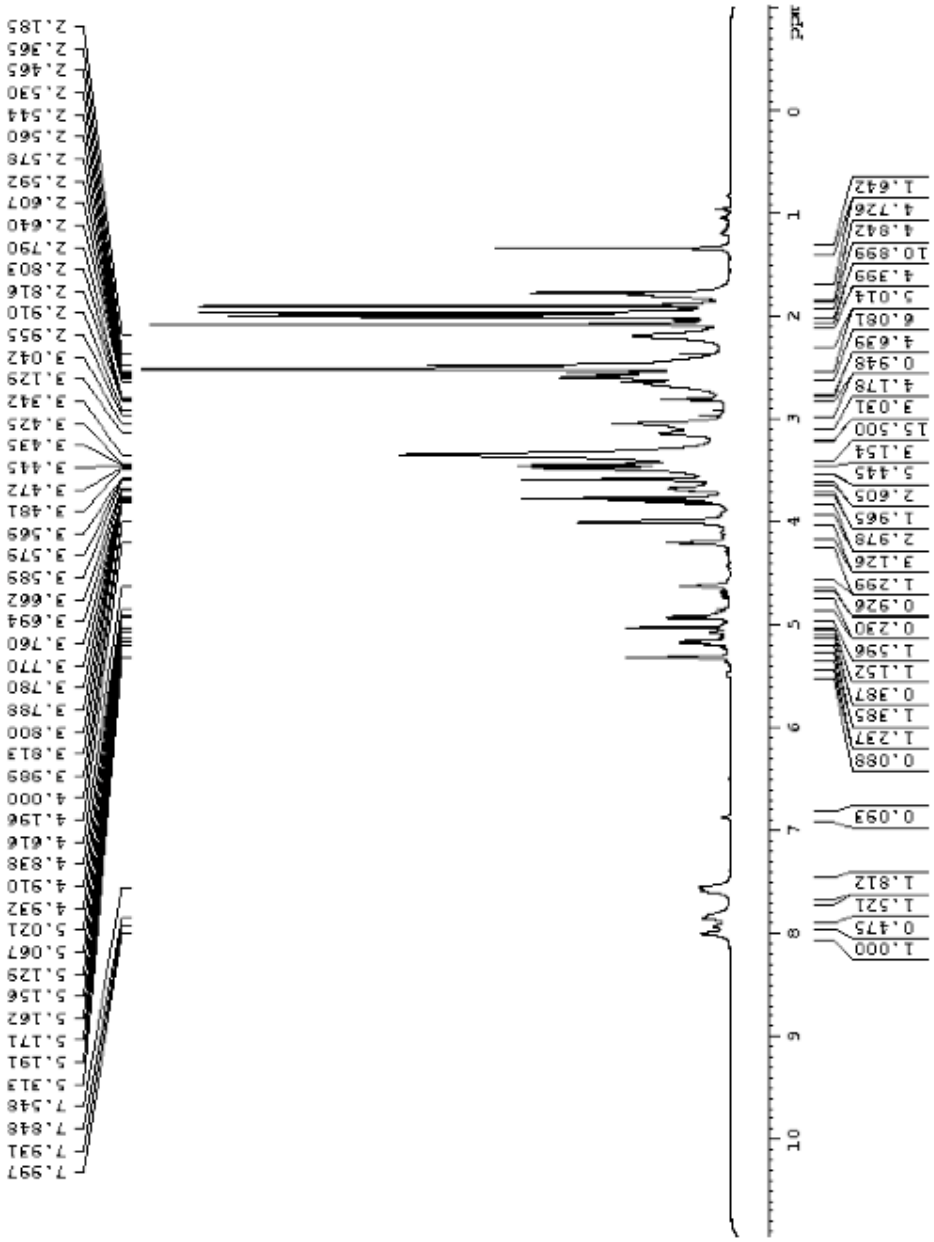

Figure 47 ^{1}H NMR spectrum (500 MHz, d_6-DMSO) of 9m (peracetylated).

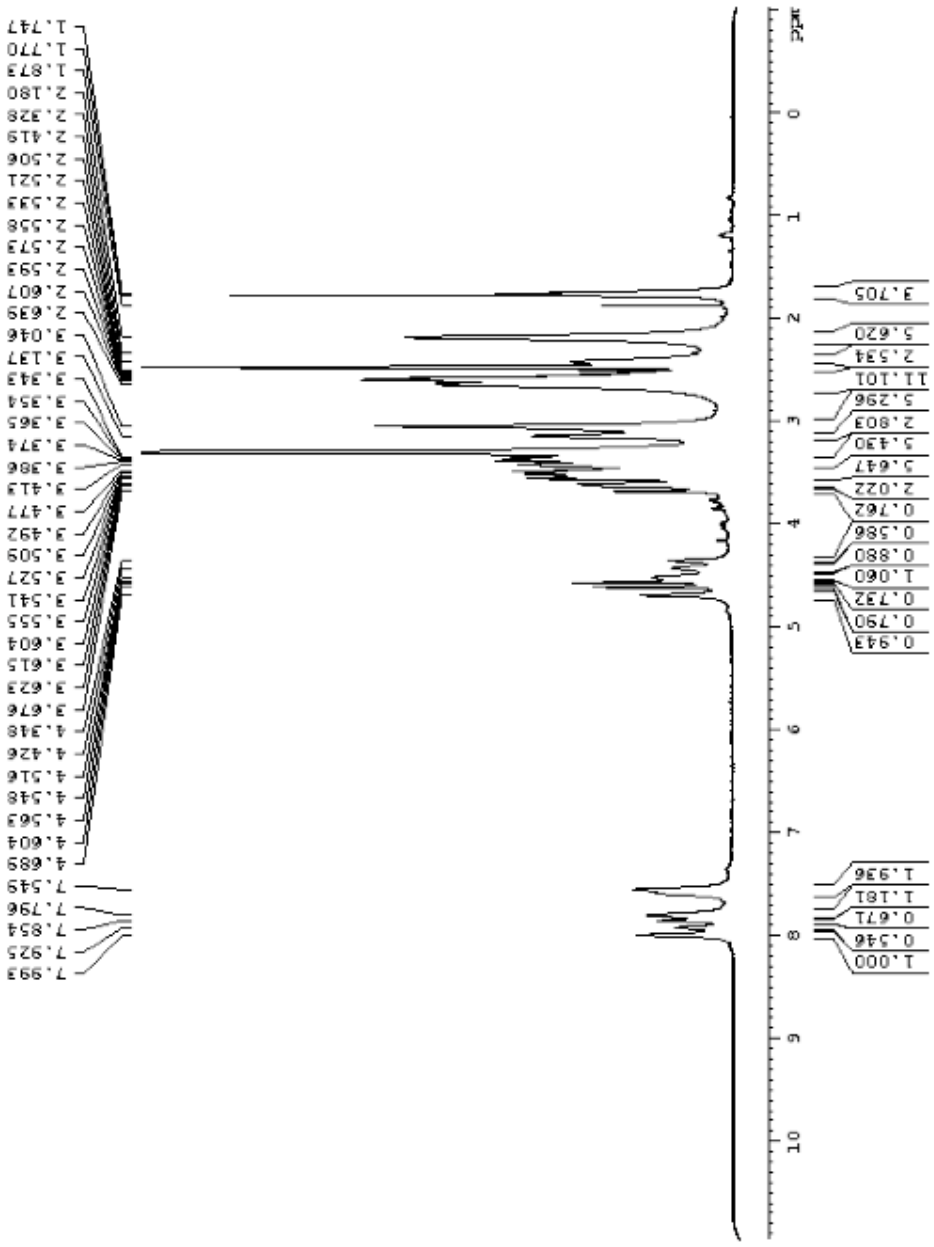

Figure 48 ^{1}H NMR spectrum (500 MHz, d_6-DMSO) of 9m (deacetylated).

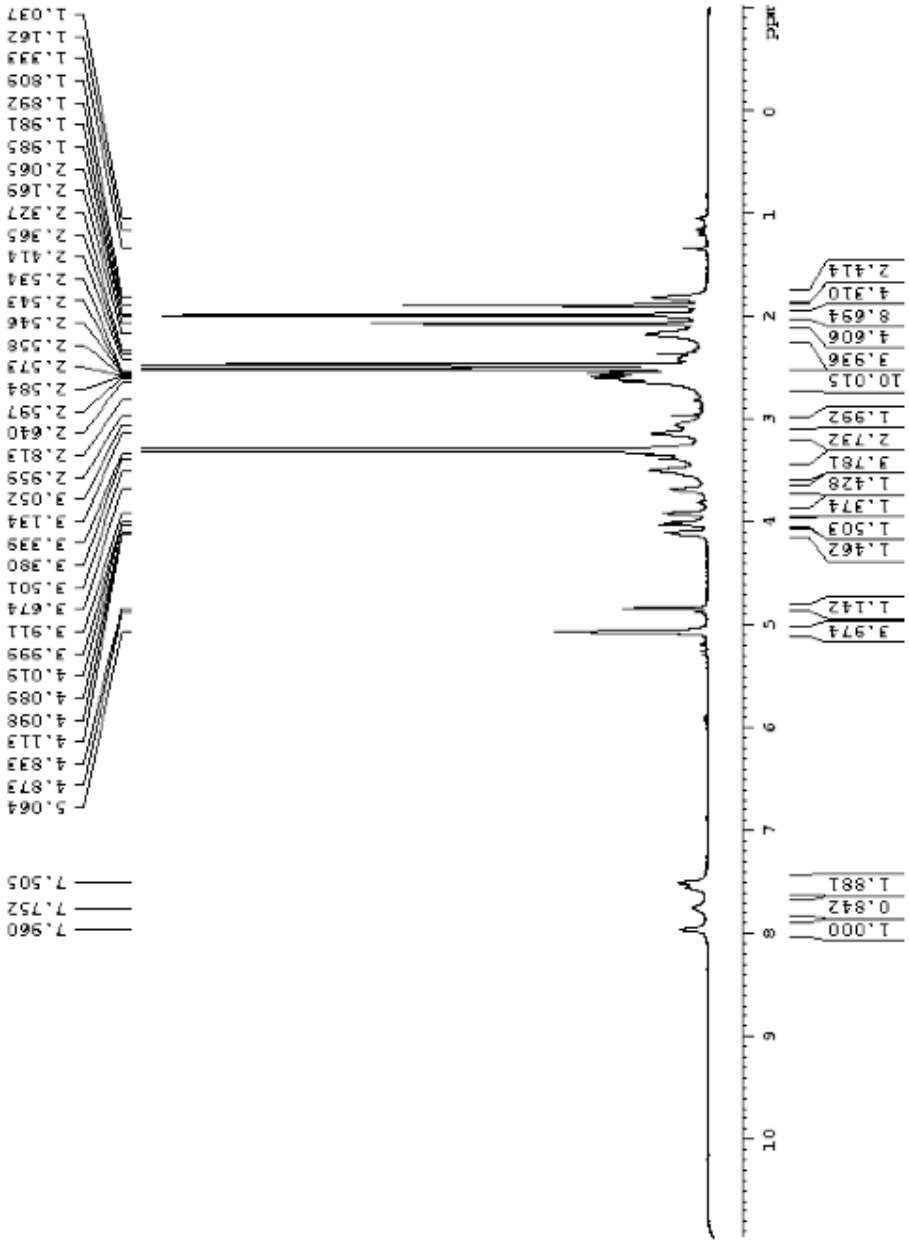

Figure 49 ^{1}H NMR spectrum (500 MHz, d_6-DMSO) of 9i (peracetylated).

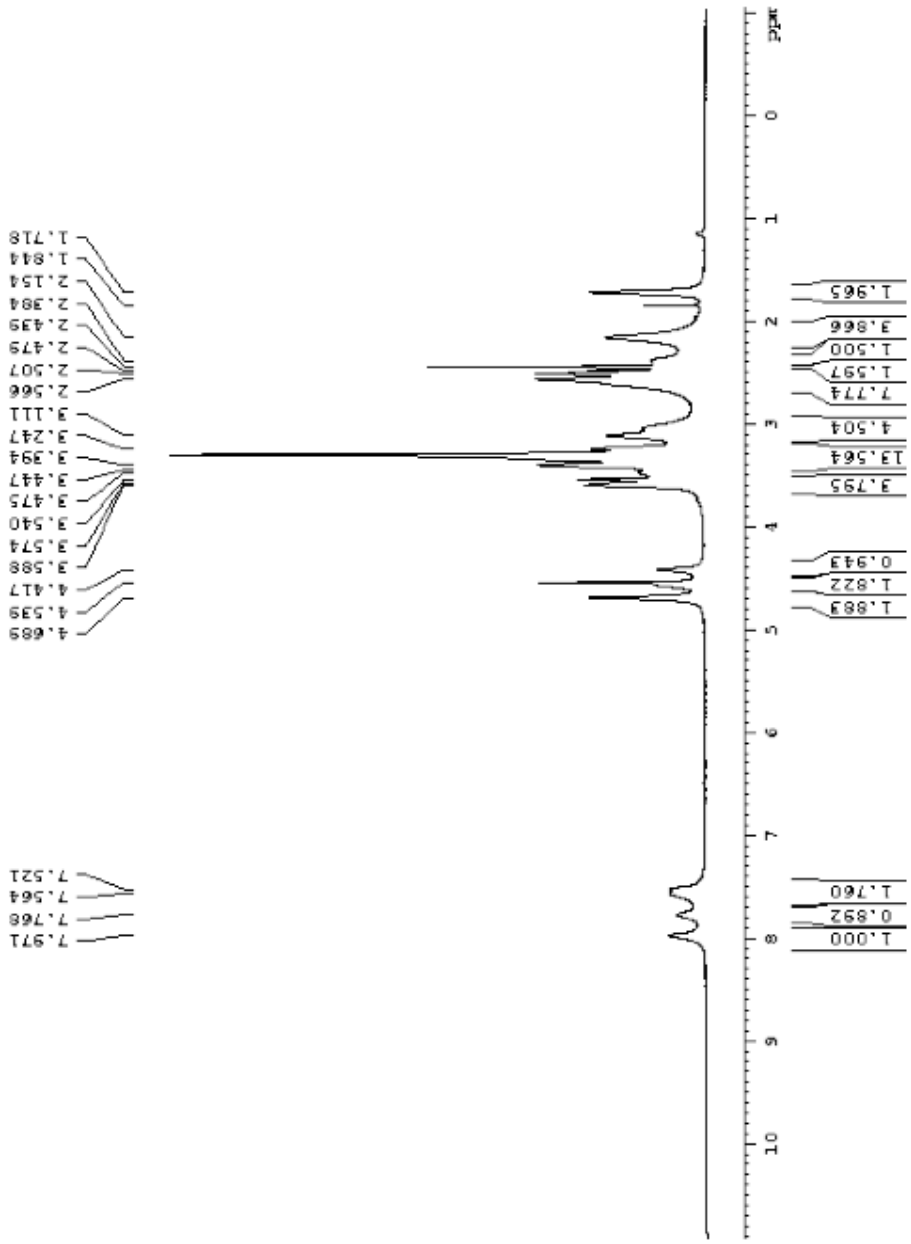

Figure 50 ^{1}H NMR spectrum (500 MHz, d_6-DMSO) of 9i (deacetylated).

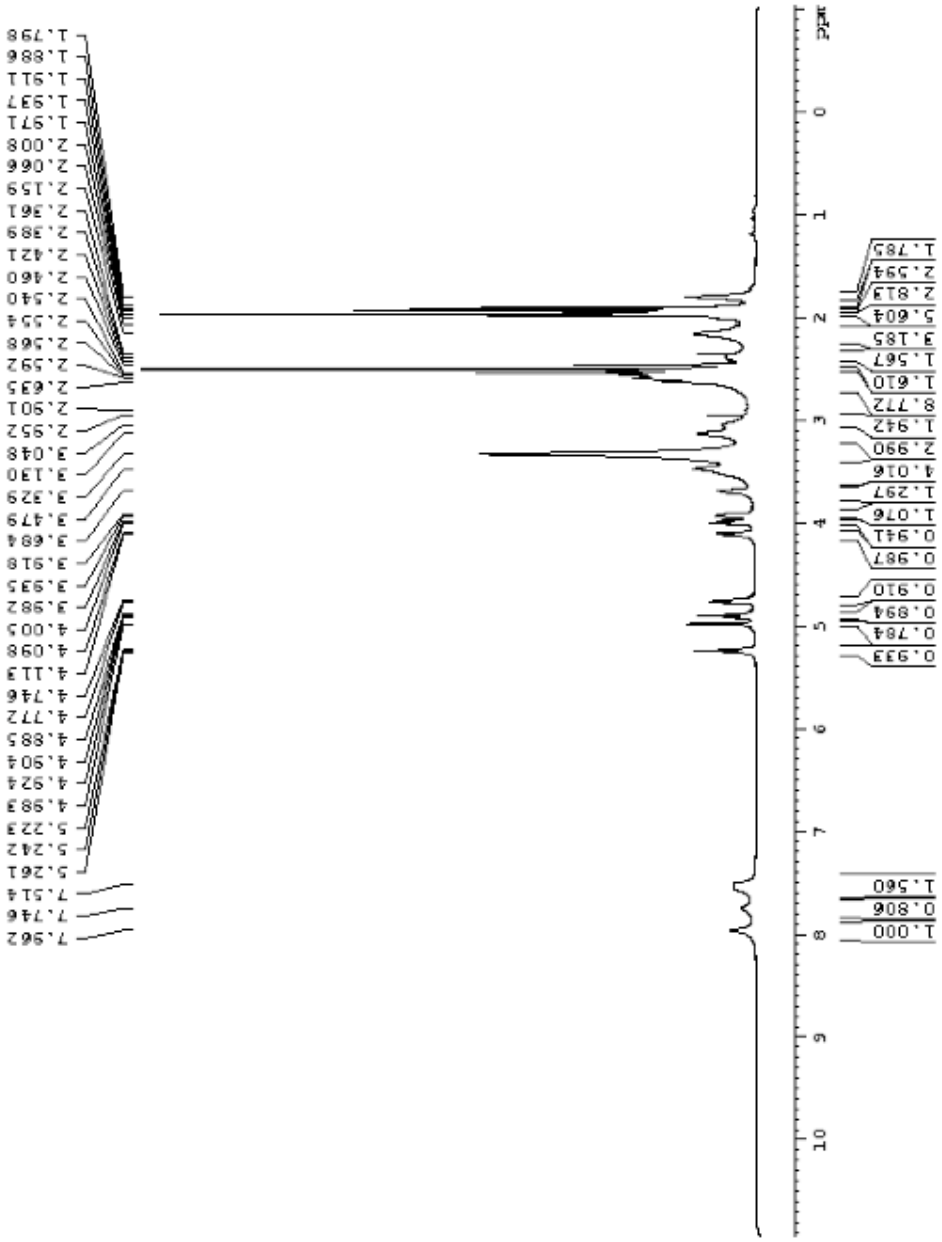

Figure 51 ^{1}H NMR spectrum (500 MHz, d_6-DMSO) of 10e (peracetylated).

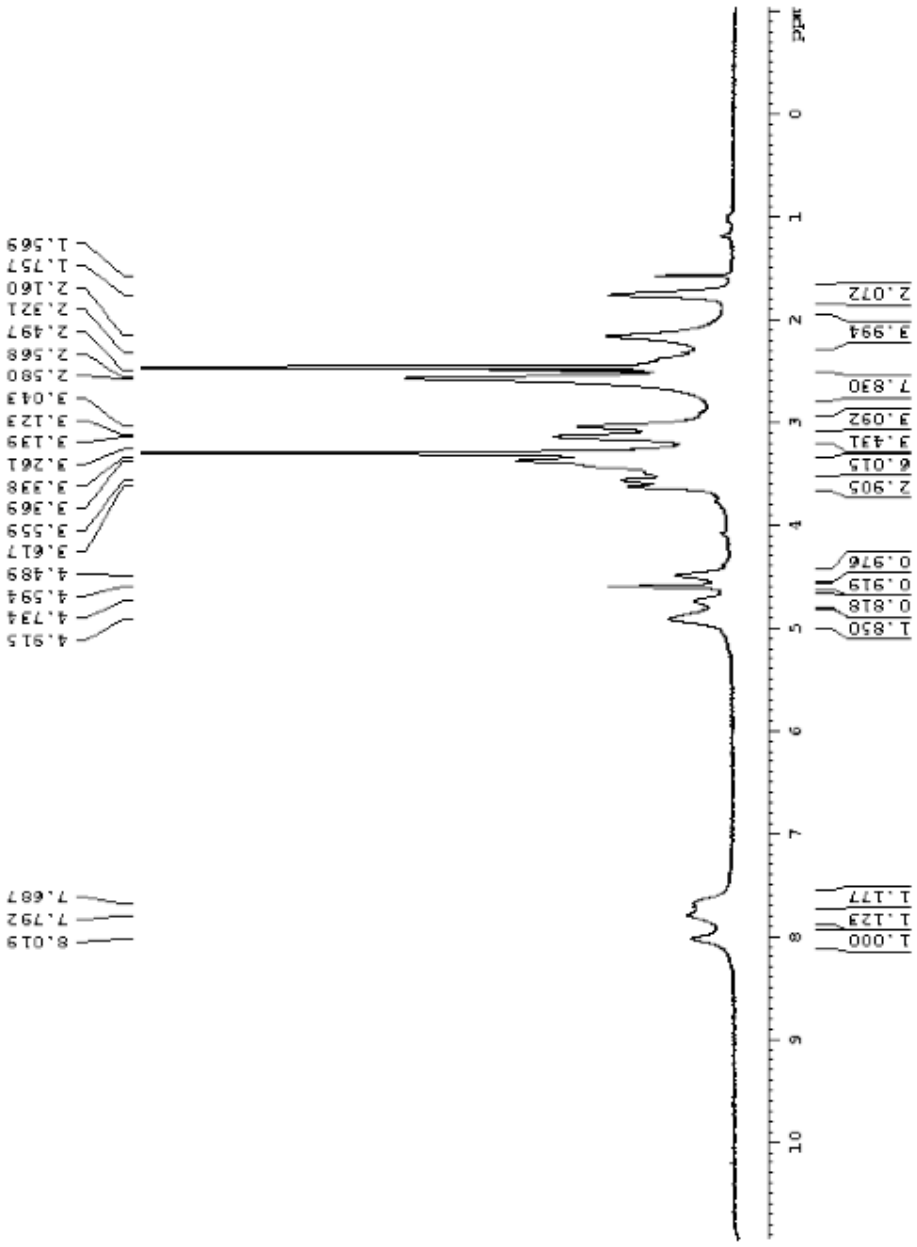

Figure 52 ^{1}H NMR spectrum (500 MHz, d_6-DMSO) of 10e (deacetylated).

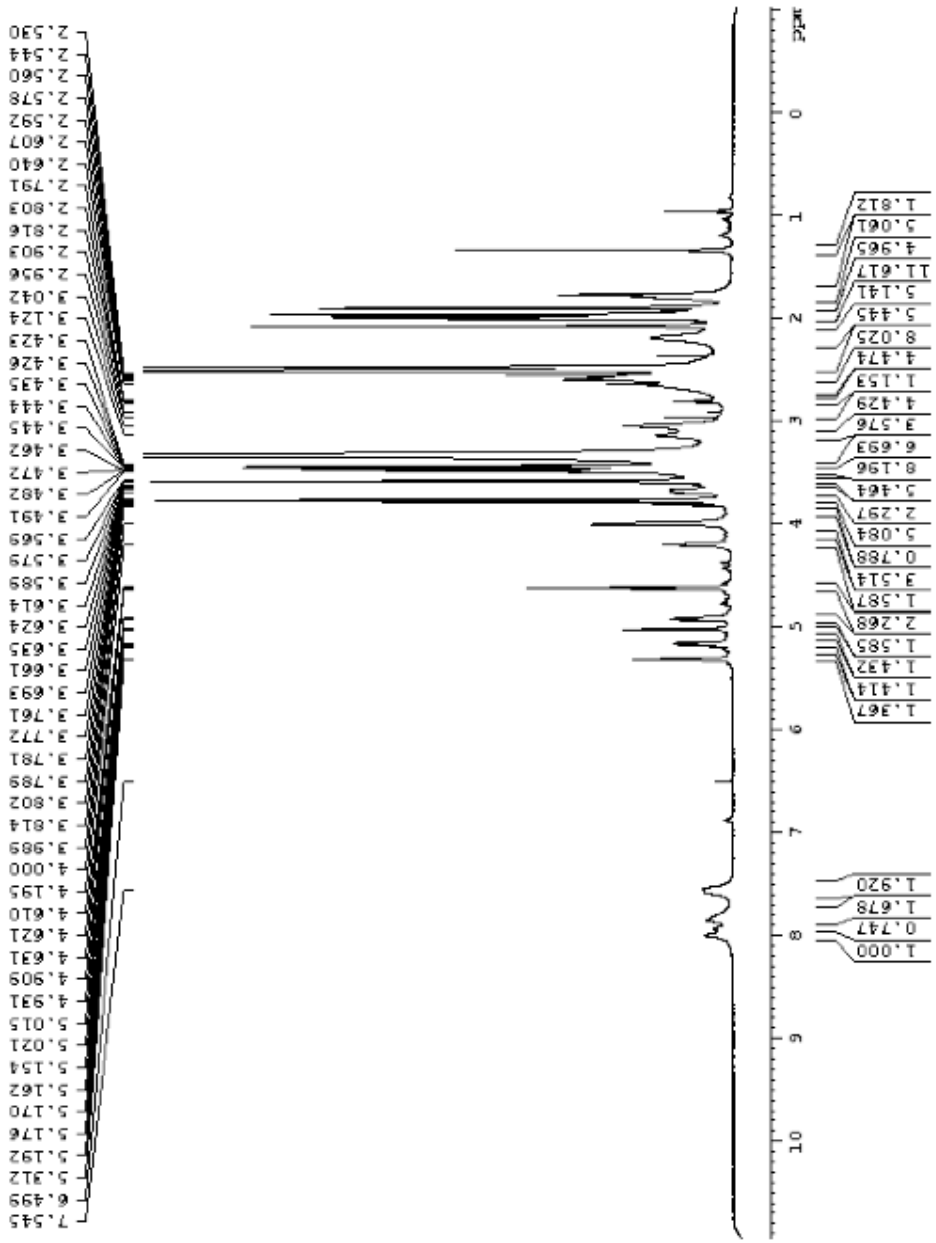

Figure 53 ^{1}H NMR spectrum (500 MHz, d_6-DMSO) of 10i (peracetylated).

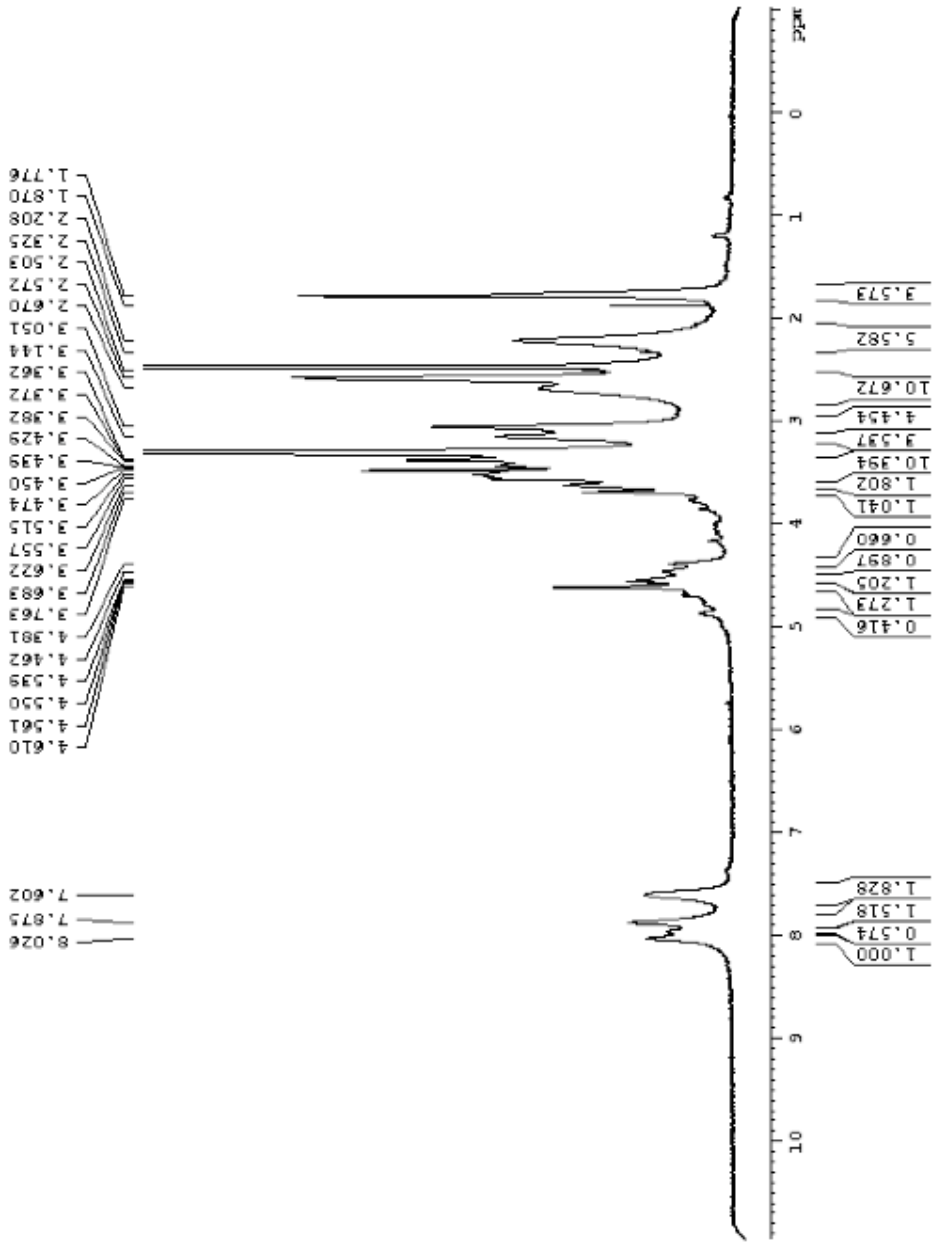

Figure 54 ^{1}H NMR spectrum (500 MHz, d_6-DMSO) of 10i (deacetylated).

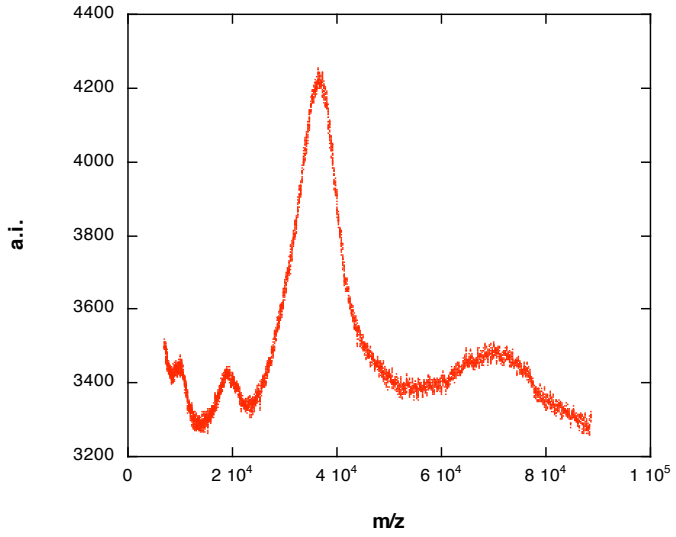

Figure 55 MALDI-TOF spectra for 8d, peracylated, M_W = 36100 g/mol.

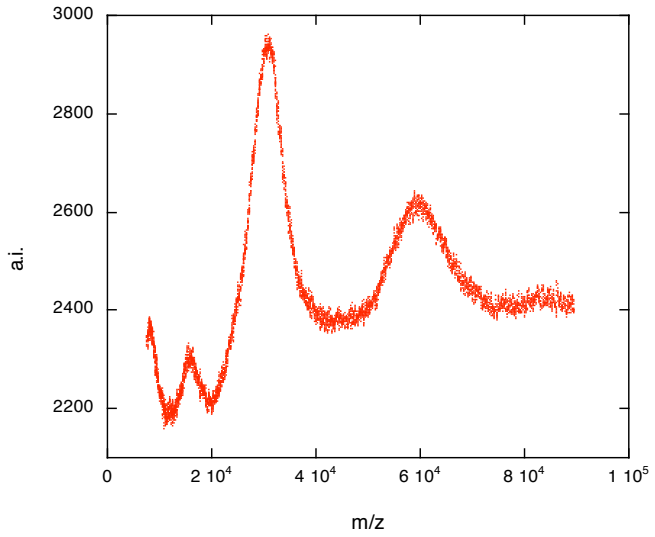

Figure 56 MALDI-TOF spectra for 8d, deacetylated. M_W = 30200 g/mol.

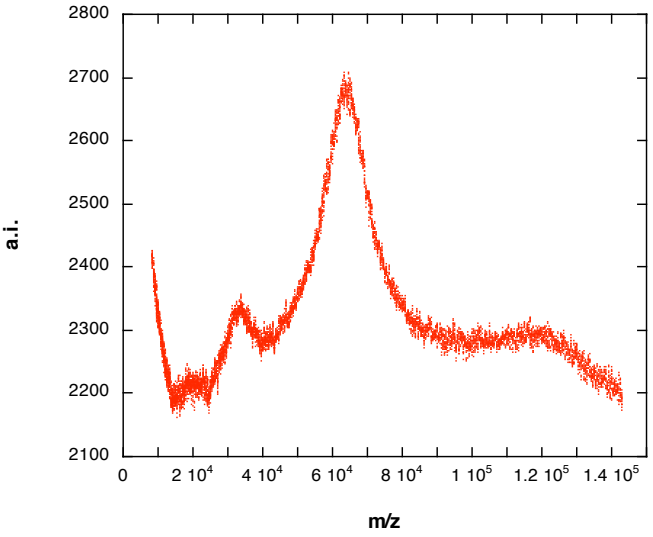

Figure 57 MALDI-TOF spectra for 9b, peracetylated. M_W = 65500 g/mol.

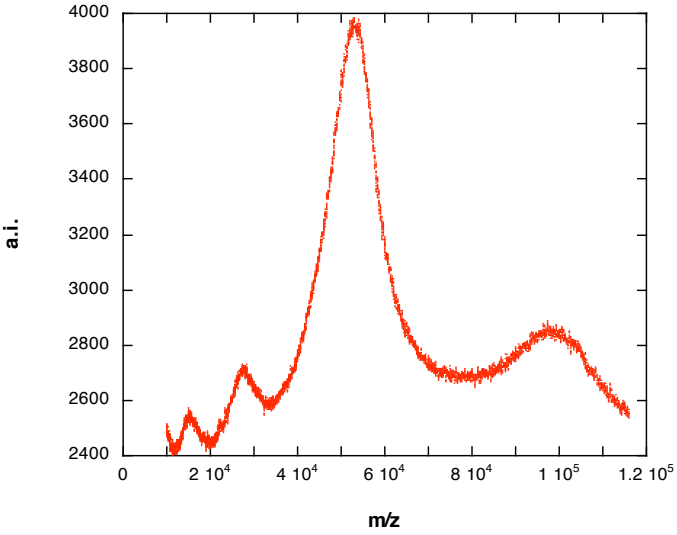

Figure 58 MALDI-TOF spectra for 9b, deacetylated. M_W = 51500 g/mol.

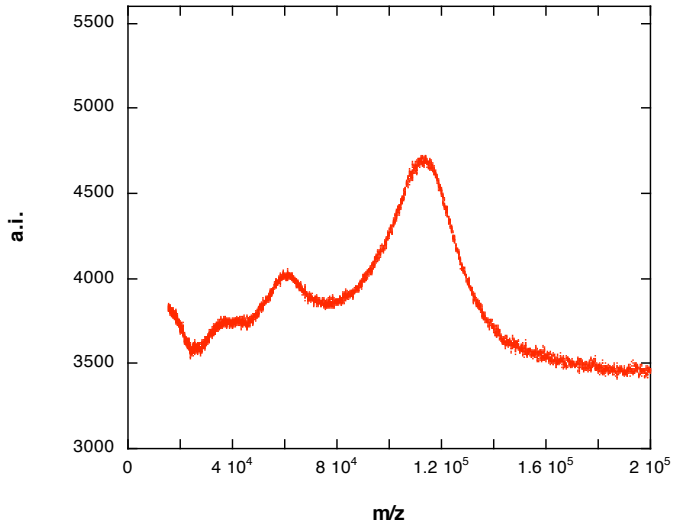

Figure 59 MALDI-TOF spectra for 10c, peracetylated. M_W = 115500 g/mol.

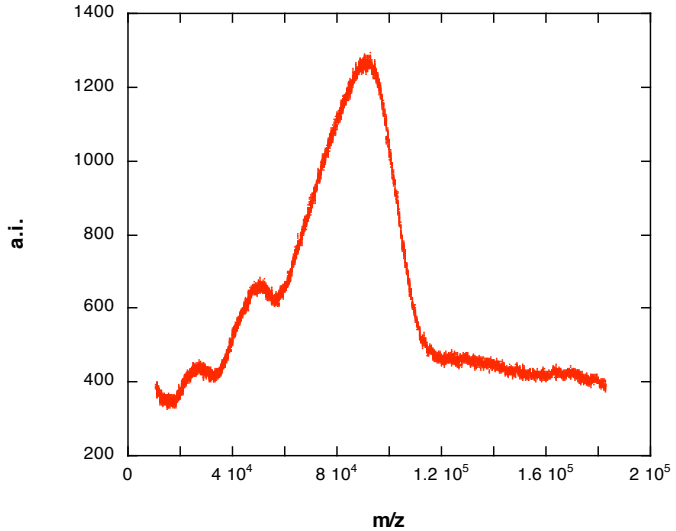

Figure 60 MALDI-TOF spectra for 10c, deacetylated. M_W = 95500 g/mol.

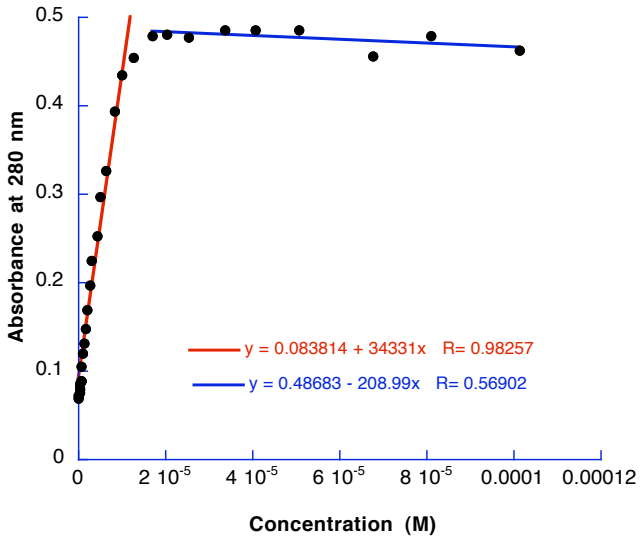

Figure 61 Precipitation Assay Curve for compound 7c.

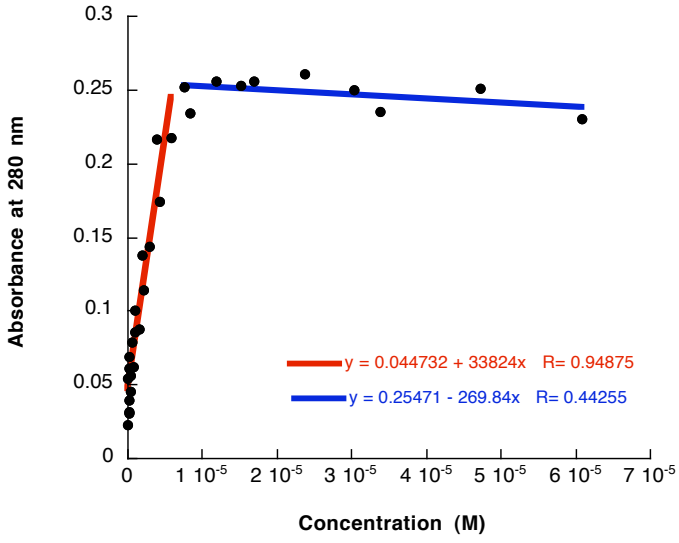

Figure 62 Precipitation Assay Curve for compound 7i.

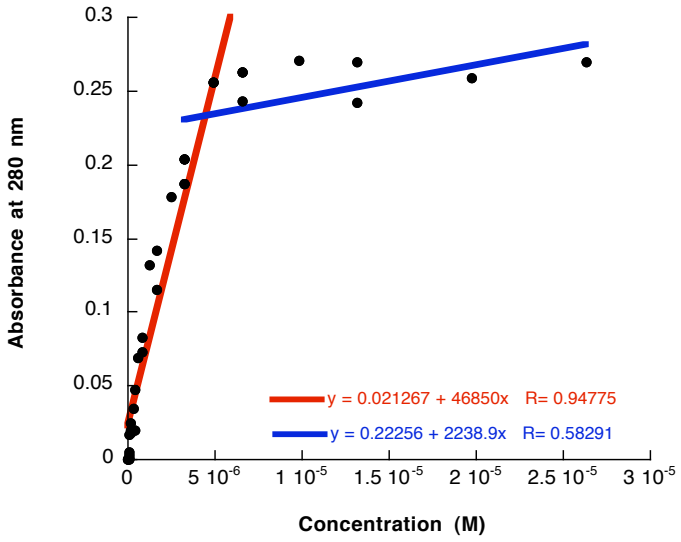

Figure 63 Precipitation Assay Curve for compound 7l.

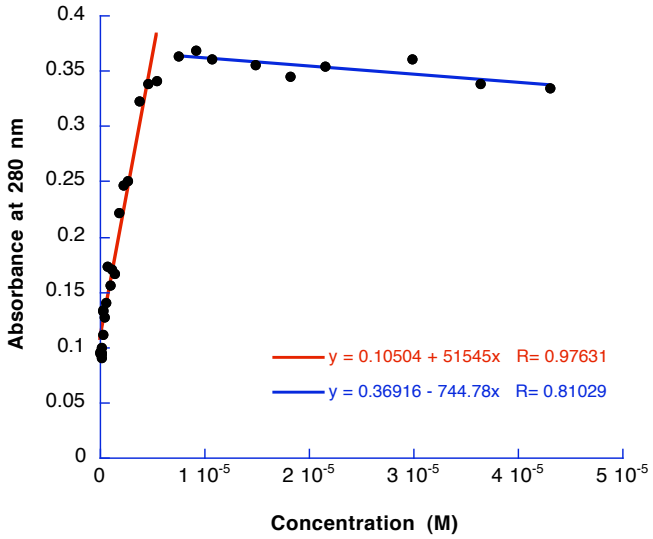

Figure 64 Precipitation Assay Curve for compound 8b.

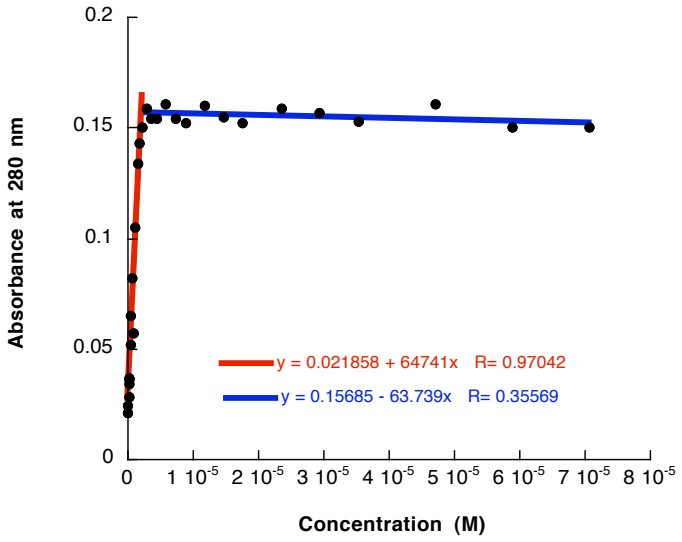

Figure 65 Precipitation Assay Curve for compound 8h.

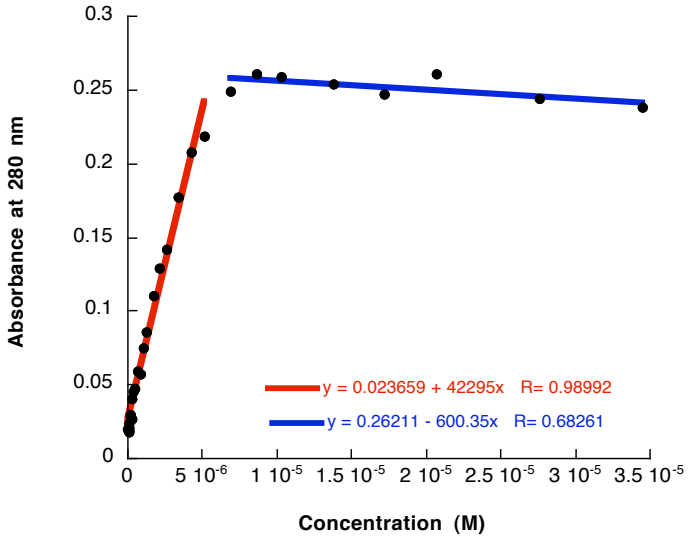

Figure 66 Precipitation Assay Curve for compound 8n.

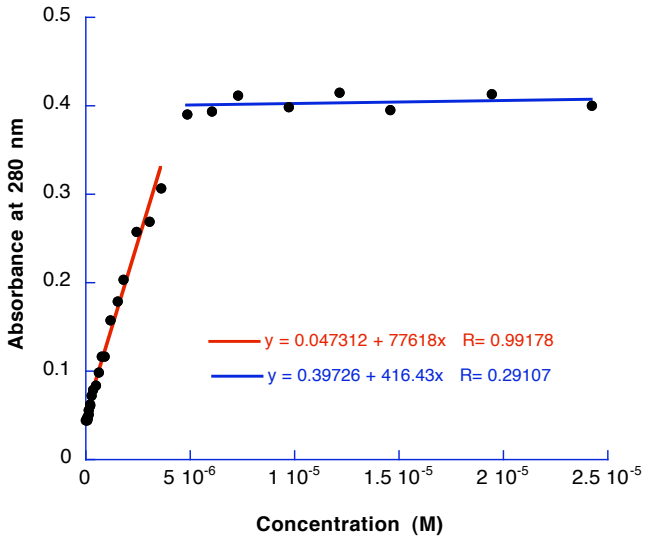

Figure 67 Precipitation Assay Curve for compound 9b.

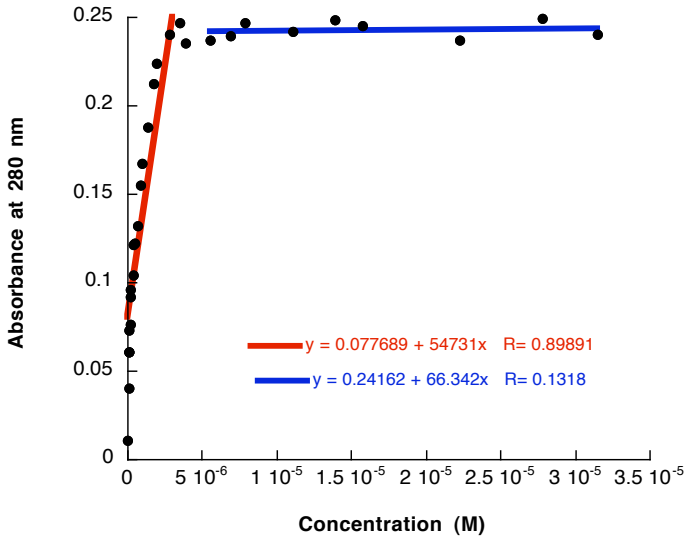

Figure 68 Precipitation Assay Curve for compound 9d.

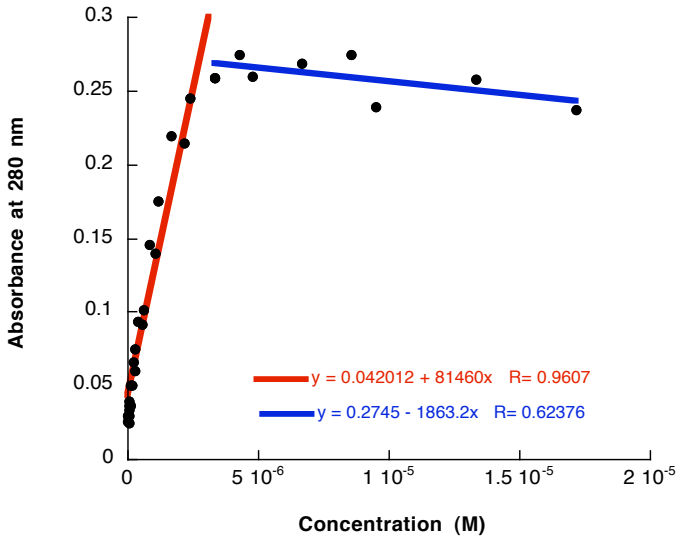

Figure 69 Precipitation Assay Curve for compound 9f.

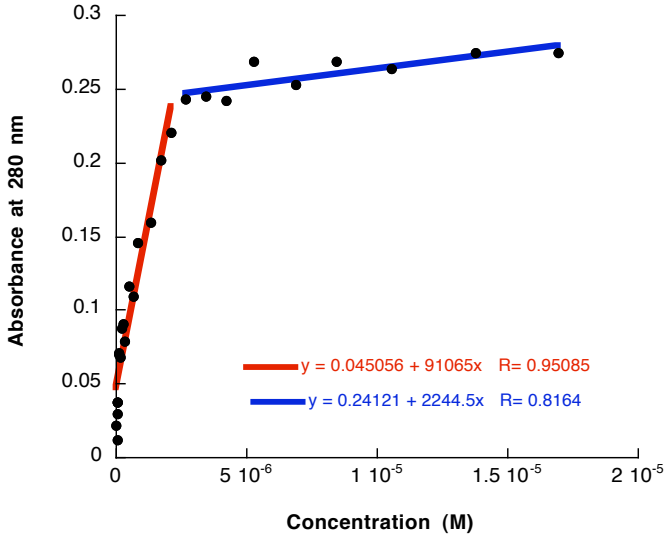

Figure 70 Precipitation Assay Curve for compound 10d.

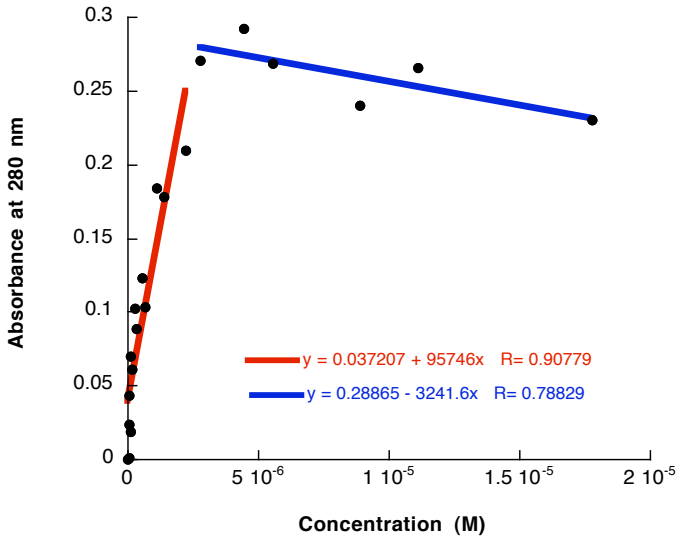

Figure 71 Precipitation Assay Curve for compound 10j.

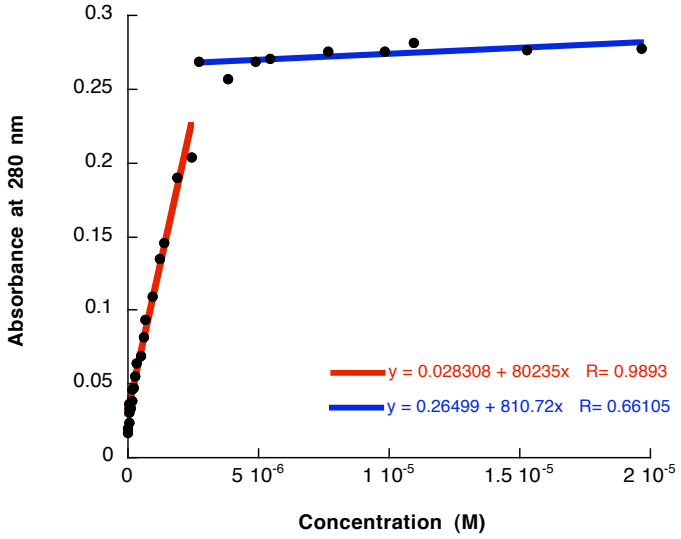

Figure 72 Precipitation Assay Curve for compound 10k.

CHAPTER 4

EXTENDING CARBOHYDRATE BASED MULTIVALENCY INTO MORE COMPLEX SYSTEMS: LOOKING AT GALECTIN-3

Introduction

The role of multivalency in biology is well documented, and examples of this phenomenon abound. In multivalent systems with carbohydrates, the weak individual binding interaction between one carbohydrate and its receptor is enhanced by multiple points of attachment. However the exact effect this has upon biological pathways is unclear. In some cases, cell surface receptor clustering is thought to be important in apoptosis and glycoprotein aggregation, a process that has been implicated in cancer cellular aggregation and tumor formation.

The ability of multivalency to enhance weak interactions has been shown in a variety of protein:carbohydrate systems using a wide variety of scaffolds and sugar moieties. These glycosystems are now being used in numerous applications (see chapter 1 for a review), and applications will no doubt become more widespread as understanding of the roles of carbohydrates in complex biological systems is improved.

Galectins

As research with multivalent glycosystems advances, one important target for potential therapy and understanding is the series of proteins know as galectins. Galectins are a family of proteins that have in common a conserved carbohydrate recognition domain (CRD) that is made up of 130 amino acids that are arranged in a folded beta-sheet structure and have an affinity for β-galactosides [100, 101]. Currently there are 15 galectins that have been characterized and numbered in the order of their discovery, 1 through 15. [102, 103]

The roles of galectins in biological pathways range from regulation of inflammation and immune response to triggering apoptosis and inducing skeletal muscle differentation. Since galectins are implicated in the formation and/or progression in many types cancer, they have generated great interest as potential targets for therapy and understanding of cancer related pathways. Of these, galectin-3 is one of the most studied (along with galectin-1) and is commonly up or down regulated in cancer and is implicated in tumor formation and proliferation, apoptosis, angiogenesis, and B cell activation. Galectin-3 is structurally unique in this protein family, as it has one carbohydrate recognition domain and a collagen like N-terminus tail. This tail, however, was shown to be cleaved and to become truncated, which is thought to have an affect on its function. [104] Galectin-3 has also been reported to form more complex structures: Brewer *et al*. reported findings indicating that a higher order pentameric structure

can be formed, at least at high concentrations of protein. [105] Other reports have indicated that galectin-3 exists as a monomer or as a dimer. [106, 107]

Galectin-3 and Cancer

Galectin-3 has been shown to have variable levels of expression in cancer types, and these expression levels have been linked to cellular proliferation. In gastric and liver cancer, higher levels of galectin-3 have been reported in tumor cells, and metastasis rates in gastric cancer have been shown to increase with increasing amounts of galectin-3.[108, 109] Galectin-3 has been found in high levels in pancreatic metastatic cancer cells and is thought to be aid the invasive potential of these cells.[110] In colon cancer, higher galectin-3 levels up-regulate factors involved in carcinogenesis.[111] Expression of galectin-3 in neo-plastic thyroid tissue was found to be increased,[112] and galectin-3 is not expressed in normal thyroid tissue.[113] In breast cancer studies, galectin-3 was found to be down-regulated, and the reduced level of expression is again correlated with the invasive and metastatic potential.[114-116] A study on adenocarcinoma of the endometrium showed down regulation of galectin-3; however, higher concentrations of galectin-3 were detected in the nucleus and cytoplasm.[117] This down-regulation was also observed in ovarian carcinoma's.[118] In head and neck cancer, galectin-3 was correlated with apoptosis, and the level of expression of galectin-3 was down regulated in these cancer types. An up-regulation of galectin-3 is thought to possibly have a physiological protective effect against the substantial apoptotic features occurring in recurrent cholesteatomas. [119]

Galectin-3 has been reported to be involved in mechanisms that cluster cell surface glycoproteins,[120, 121] cross-link receptors[122] and form lattices and larger aggregates,[123] involved in cellular function. These examples show the inherent complexity as well as the implication of galectin-3 in many types of cancer. They also reveal the potential for targeting and understanding the fundamental attributes of the protein. In particular, galectin-3 is thought to be involved in aggregating processes that lead to tumor proliferation, which make it an interesting target for our multivalent carbohydrate functionalized PAMAM dendrimers.

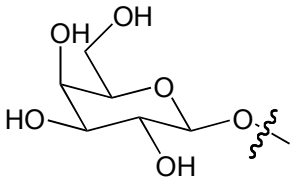

β-galactose

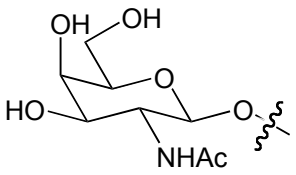

N-Acetyl-β-galactosmine

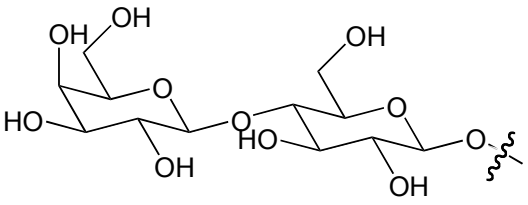

β-lactose

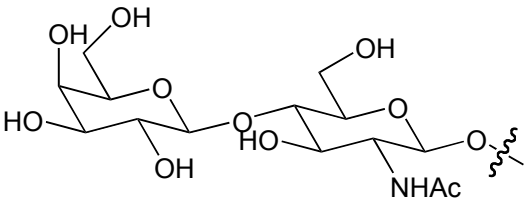

N-Acetyl-β-lactosmine

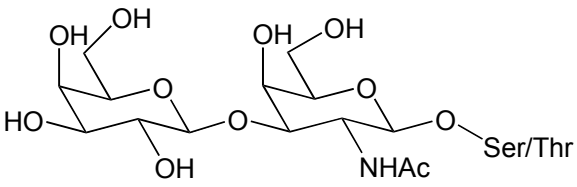

Tf Antigen

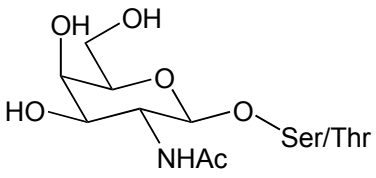

Tn Antigen

Figure 73 Some of the natural galactose based ligands for Galectin-3

Galectin-3 Ligands

Galectins were initially classified as S-type lectins, due to the apparent sufhydryl dependency of the buffers in which the lectin activity could be preserved. In 1994, this S-type lectin subclass was renamed galectins because they all had a conserved carbohydrate recognition domain of 130 amino acids that specifically bound galactose-based carbohydrates. Some of the ligands for galectins are shown in Figure 73. These include galactose, *N*-acetylgalactosamine, lactose, *N*-acetyllactosamine, Tn antigen and Tf antigen, the latter of which is considered to be a natural ligand for galectin-3 and is present on the surface of cancerous cells. In 1998, Barondes *et al*. reported the X-ray crystal structure of the carbohydrate recognition domain of galectin-3 bound to lactose and LacNAc, as shown in Figure 74. [124]

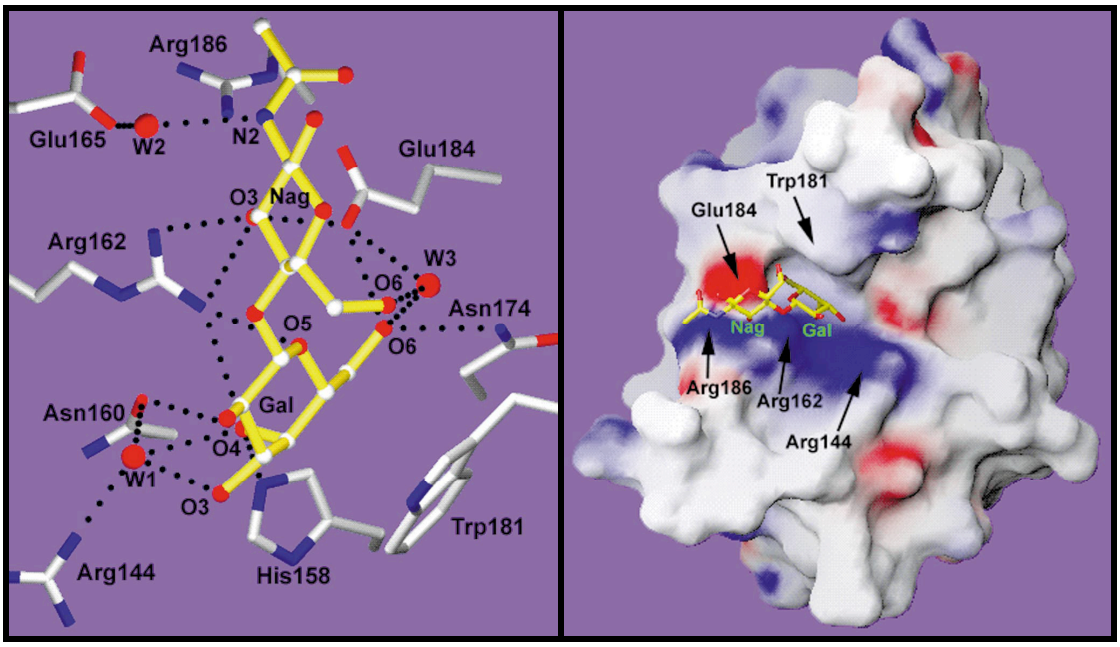

Figure 74 X-ray crystallography structure of the CRD of Galectin-3 with N-acetyl-lactosamine bound.

The important binding interactions from galactose to galectin-3 are the O3-W1-Asn160, O4-Asn160, O5-Arg162 and O6-W3-Glu184 binding. The O2 is not thought to be significantly involved in binding interactions to galectin-3, although altering the C2 moiety has been shown to alter the binding association.

Rationale of Study

Based on the glycodendrimer-lectin model studies that are reported in chapters 2 and 3, transposition of the predictable and tunable aspects of the mannose/glucose:Con A interaction into a more complex system were envisioned. [87, 125] Galectin-3 was chosen as the target of these studies because multiple galactose-based binding ligands have been reported and because multivalent effects are likely to be critically important for this system. Of the reported ligands, galactose, galactoamine lactose, and lactosamine were chosen as initial ligands for dendrimer functionalization, and one major goal of this project was to display these ligands in a variety of mixtures and loadings on a PAMAM dendrimer framework.

The different galectins bind carbohydrates with variations in affinities. Brewer and co workers reported binding studies on galectins 1,3 and 7 with an array of ligands. Through hemagglutination inhibition assays, Brewer *et al*. determined the relative potencies for galectin-7 as follows: lacNAc as 1, lactose as 1.8 and galactose as 66.[126] In studies assessing galectin-3 ligands, Brewer reported the relative inhibitory potencies for lactose as 0.2 and lacNAc as 1.0.[126] Nilsson and co-workers have synthesized various galactose based analogs with

different substituents including benzyl and napthyl groups at the 3 position, which enhanced binding to galectin-3 by over an order of magnitude.[127] For example, Nilsson observed a measured binding constant that was 2-fold higher for a galactose derivative that was sulfated at the 2-position than for galactose. [128] This suggested that there might be a subtle difference in binding between galactose and N-acetyl galactosamine. Although there has been no reported data for binding of galectin-3 to N-acetylgalactosamine, this potentially subtle difference between galactose and galNAc could potentially be enough to be enhanced when multivalent binding occurred, allowing for observations of trends in multivalent binding. Also, the Tn antigen, an N-acetylgalactosamine that is linked to serine at the anomeric position, is a cell surface glycan that is an intriguing target (much like Tf antigen). Capitalizing on the large binding difference between galactose and lactose and on the small difference between galactose and GalNAc, in addition to the range of generations that are readily available for PAMAM dendrimers, the synthess of a library of compounds was designed. The overarching hypothesis for this work was that a series of compounds could be synthesized that would have a large range of binding capabilities with galectin-3 that would allow for attenuation of galectin-3 mediated biological processes.

Results

Tethered Carbohydrate Synthesis

In prior experiments with mannosides and glucosides, synthesis of carbohydrate derivatives that are appropriately functionalized for conjugation to the dendrimer has included generating a trichloroacetimidate prior to glycosylation. During the derivatization of galactose and galNAc, it became apparent that this activation step this was unnecessary. Starting with the penta-acetyl-β-galactopyranoside and using BF_3EtO_2 and 2-(2-isothiocyanatoethoxy)ethanol, the desired β-anomer of the tethered carbohydrate was generated in good yield (see Scheme 4). The β anomer was necessary for all of the carbohydrate derivatives for binding to galectin-3, and this anomer is readily formed for galactosides and glucosides with acetyl groups at the 2-position because of neighboring group participation (Figure 75).

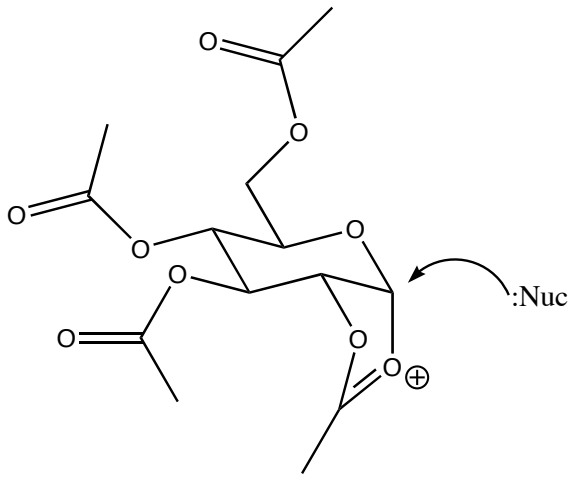

Figure 75 An example of neighboring group participation to generate the β anomer in peracetylated glucose and galactose glycosylations.

The fact that trichloroacetimidate formation was not required was somewhat of a surprise, as previous syntheses required the use of the trichloroacetimidate as the donor. This direct functionalization method also was successful when used with peracetylated β-glucose. However, when this method was used with peracetylated α-mannose, a 60:40 ratio of anomers was obtained, and glycosylation of lactose also afforded a mixture of anomers.

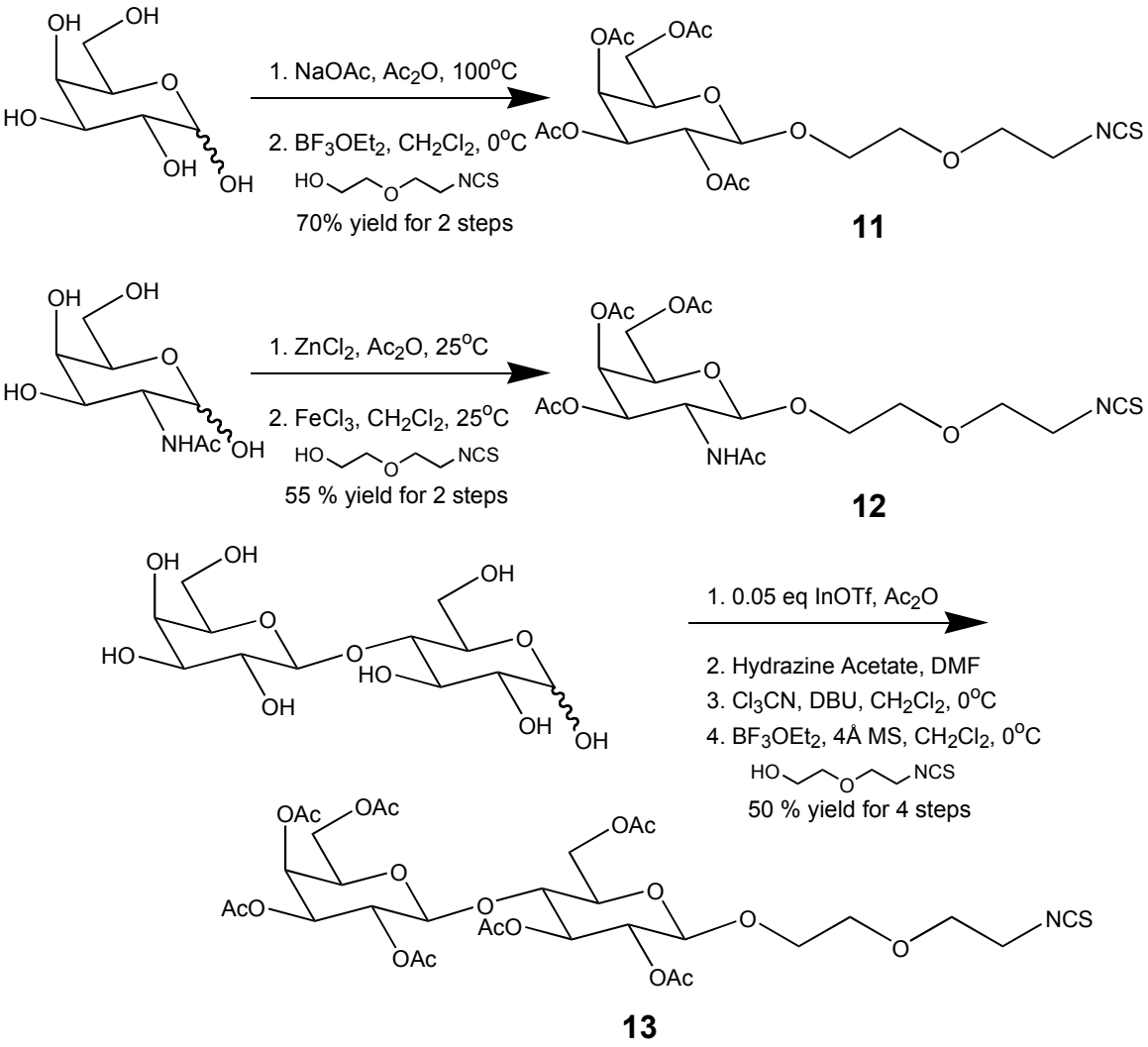

Scheme 4 Synthesis of isothiocyanatoethoxyethanol tethered peracetylated galactose 11, galNAc 12 and lactose 13.

For lactose, the trichloroacetimidate precursor was generated and was treated with 2-(2-isothiocyanatoethoxy)ethanol and BF_3EtO_2 to yield the desired β-anomer of the requisite lactose derivative. With galNAc, a method reported by Anderson using $FeCl_3$ as the Lewis acid with 2-(2-isothiocyanatoethoxy)ethanol to generate the desired β-anomer in reasonable yield (Scheme 4).[129]

Synthesis of Carbohydrate Functionalized PAMAM Dendrimers

Carbohydrate functionalized dendrimers were synthesized by sequentially adding carbohydrates with isothiocyanato tethers. For galactose:galNAc functionalized dendrimers, 12 was added first (Scheme 5), the reaction was monitored via MALDI-TOF, and then 11 was added using MALDI-TOF to monitor the addition. For lactose:galactose functionalized dendrimers 11 was added first (Scheme 6), the reaction was monitored via MALDI-TOF, and then 13 was added using MALDI-TOF to monitor the addition. Initial attempts to make 17-19 a-e were made by adding 13 first, however this blocked further addition of 11. MALDI-TOF MS values are provided in Tables 15 and 16 in the experimental section of this chapter. If the Mw was low, then additional equivalents of 11 were added. However, this rarely altered the Mw, indicating that no more carbohydrates could be added to the dendrimer. Using ^1H NMR the peaks from the varied carbohydrates can be observed (Figure 76), however integration of these peaks does not lead to accurate quantification of the degree of carbohydrate functionalization. Global deacetylation was performed using

Zemplen conditions (NaOMe in MeOH) and was monitored via ^{1}H NMR. NMR monitoring allows for the detection of the disappearance of resonances at ~ 2 ppm that are diagnostic for the methyl groups of the acetyl protecting groups.

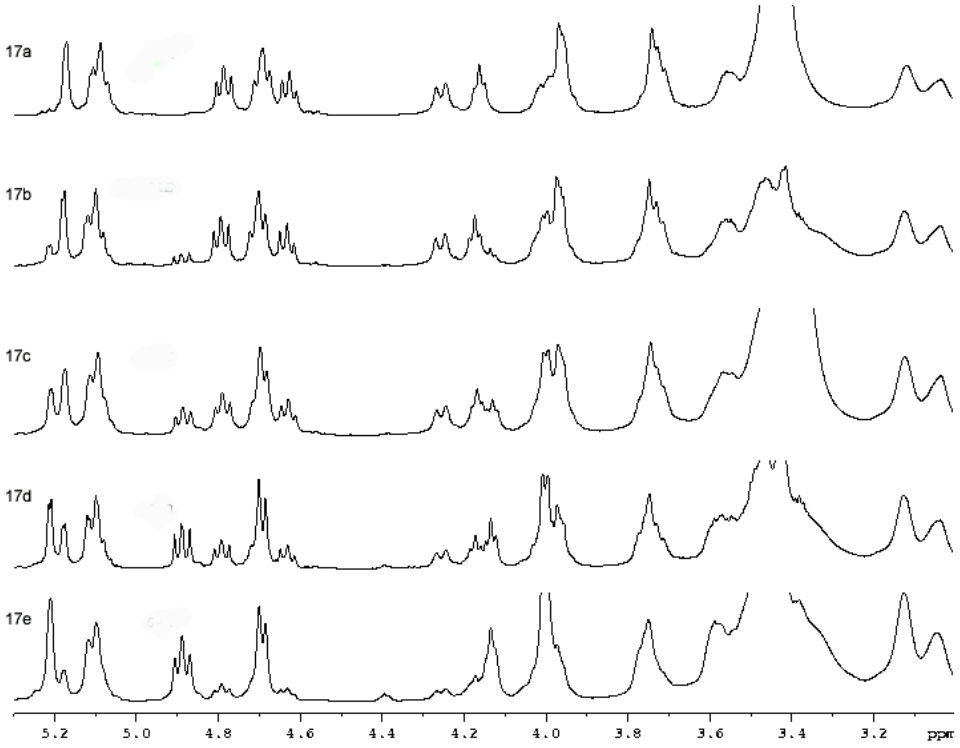

Figure 76 ^{1}H NMR spectra of compounds 17a-e, in the range 3.0-5.3 ppm. Note the increase/decrease of peaks of galactose and lactose with variable loading.

With the galNAc functionalized dendrimers, a peak at ~1.8 ppm remained after treatment with NaOMe/MeOH, which indicated that the *N*-acetyl group was preserved. The deacetylated dendrimers were further characterized via MALDI-TOF MS. Both the change in Mw upon the addition of the protected carbohydrate and the change in Mw upon deacetylation were used to determine the

carbohydrate loading. Results and additional details of the MS characterization procedure are provided in the experimental section.

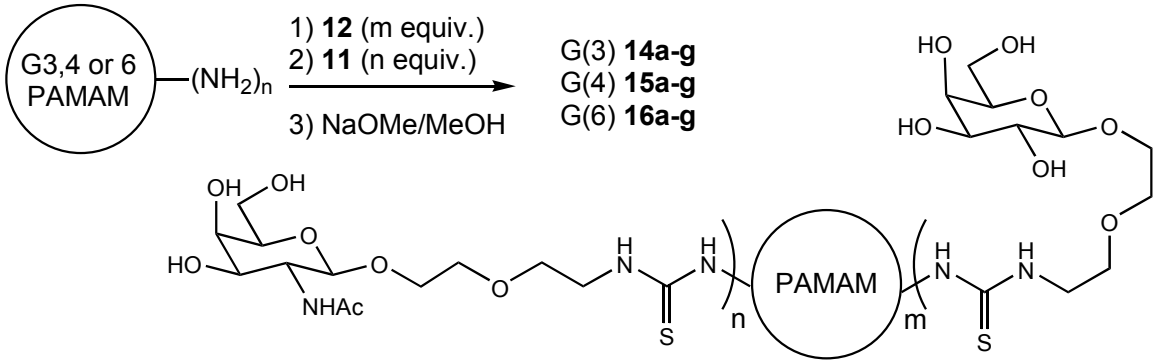

Scheme 5 Synthesis of galNAc:galactose functionalized PAMAM dendrimers.

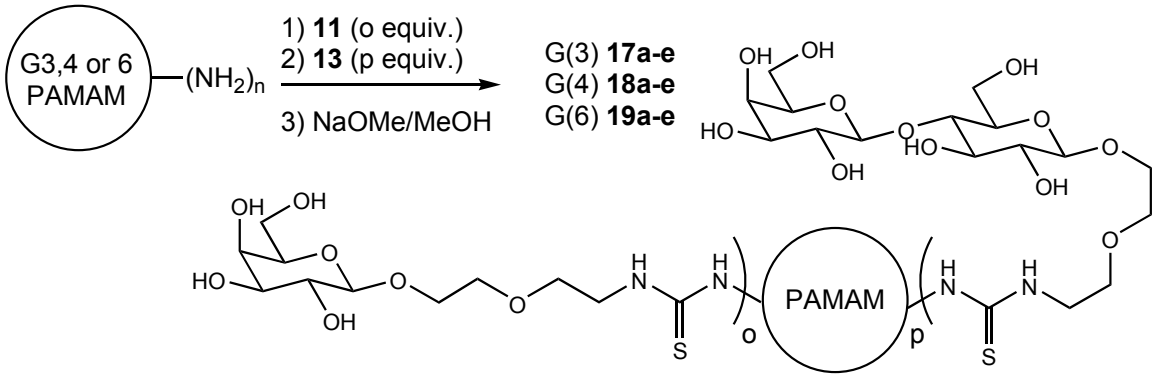

Scheme 6 Synthesis of lactose:galactose functionalized PAMAM dendrimers.

Enzyme Linked Immunosorbent Assays (ELISA)

To evaluate the binding interaction between the carbohydrate functionalized dendrimers and galectin-3, an ELISA based assay was developed. The carbohydrate functionalized dendrimers were bound to a NUNC maxisorp 96

well plate, which was then blocked with a 3% BSA solution of PBS at pH 7.4. After the glycodendrimer-functionalized plate was allowed to dry, a solution of galectin-3 and serially diluted lactose was added. An anti-galectin-3 antibody conjugated to biotin was added, followed by addition of a streptavidin/horse radish peroxidase conjugate. Tetramethylbenzidene oxidation was allowed to occur for 10 minutes at 25°C and stopped with 1M H_3PO_4 and was monitored at 450 nm. The modified ELISA is depicted schematically in Figure 77. Prior to using the modified ELISA shown above, a number of other methods to study the galectin-3/glycodendrimer interaction were attempted, including binding asialofetuin and laminin to the 96 well plate so that competition ELISAs could be performed. Even at high dendrimer concentrations (10 mg/mL), there was no observed reduction of galectin-3 binding to the surface.

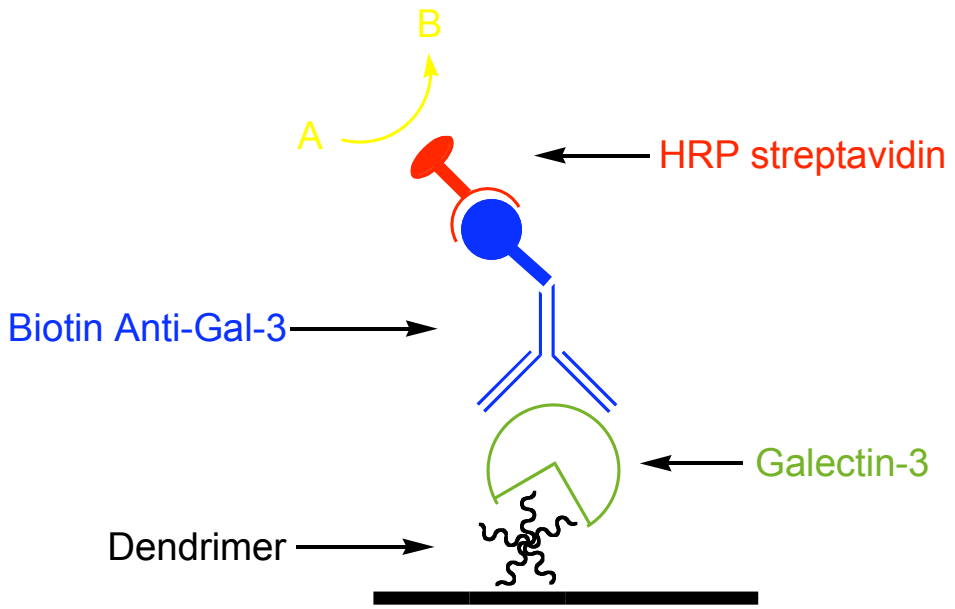

Figure 77 A schematic of the enzyme linked immunosorbent assay used to assess dendrimer:galectin-3 interactions.

These inhibition ELISA's appeared to indicate an aggregative binding effect between the dendrimer, the surface protein, and galectin-3. This assay was repeated using just the carbohydrate recognition domain (CRD) of galectin-3, which appeared to show a slight decrease in galectin-3 binding at higher concentrations of dendrimer. However, even at high dendrimer concentrations, the glycoprotein:galectin-3 interaction was not fully inhibited. Interestingly when lactose was used to inhibit theses competition assays inhibition was observed. A fluorescence assay was performed using fluorescein labeled galectin-3 antibodies as a detection system and appeared to also suggest that a cooperative binding process was occurring. Only assays in which the glycodendrimer was directly bound to the surface afforded data that could be usefully interpreted.

To measure the efficacy of the monomer carbohydrates, the ELISA assay was performed with 17a, 18a and 19a adsorbed to the 96 well plates, and galactose, galNAc, lactose and mannose were used separately as inhibitors. As shown in Figure 78, when compound 17a was adsorbed to the plate surface, lactose had an IC_{50} value of 0.24 mM, galNAc had an IC_{50} value of 26.7 mM, and galactose had an IC_{50} value of 21.7 mM. With compound 18a adsorbed on the surface, the IC_{50} values were: lactose 0.45 mM, galNAc 18.4 mM and galactose 20.9 mM (Figure 79). With compound 19a adsorbed on the surface, the inhibiting concentrations were: lactose 0.24 mM, galNAc 10.0 mM and galactose 12.4 mM (Figure 80).

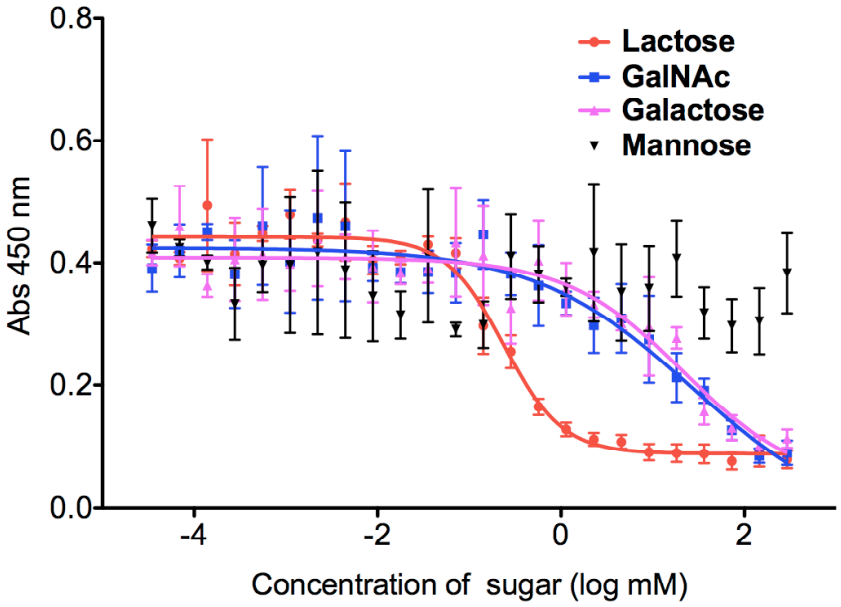

Figure 78 ELISA with 17a bound to the surface and various inhibiting sugars. IC_{50} values are: lactose 0.24 mM, galNAc 26.7 mM, galactose 21.7 mM and mannose showed no inhibition.

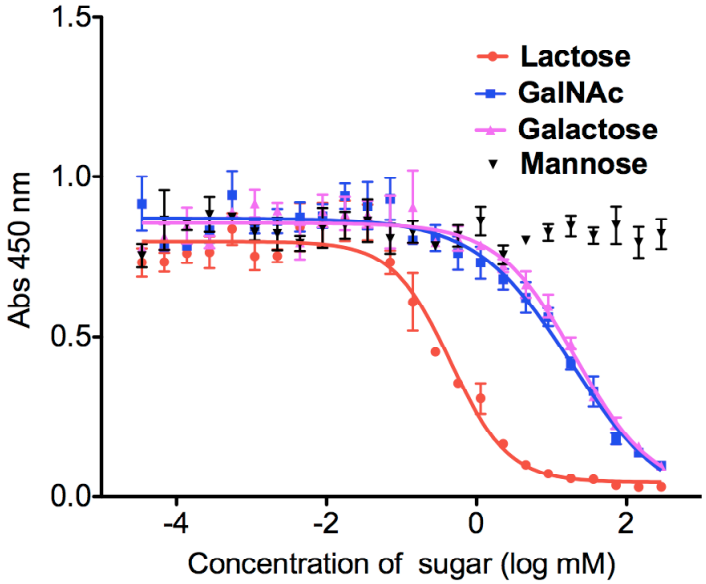

Figure 79 ELISA with 18a bound to the surface and various inhibiting sugars. IC_{50} values are: lactose 0.45 mM, galNAc 18.4 mM, galactose 20.9 mM and Mannose showed no inhibition.

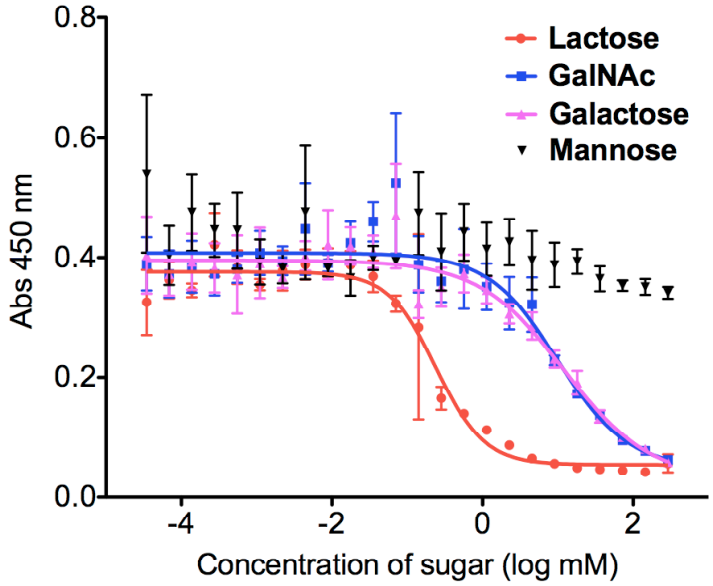

Figure 80 ELISA with 19a bound to the surface and various inhibiting sugars. IC_{50} values are: lactose 0.24 mM, galNAc 10.0 mM, galactose 12.1 mM and Mannose showed no inhibition.

When 18a and 19a were adsorbed to the plate, the lactose monomer inhibited the galectin-3:dendrimer interaction about 50 times more effectively than galactose and galNAc, and with 17a adsorbed lactose was ~100 times more effective than galNAc and galactose. Mannose was used as non-binding control that showed no inhibition, as expected.

The ELISA binding curves for compounds 14a-g are shown in Figure 81, with the lactose inhibiting concentrations shown in Table 13. The IC_{50} values ranged from 0.05 mM for 14a to 0.38 mM for 14e. Except for 14a, all of the measured lactose inhibiting concentrations were very similar, ranging from 0.29 mM to 0.38 mM..

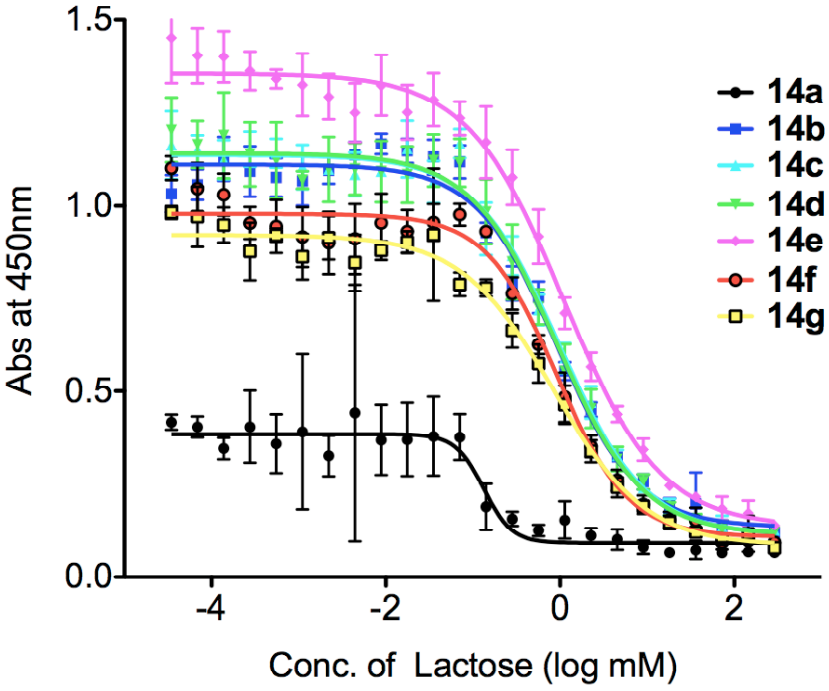

Figure 81 ELISA binding curves for compounds 14a-g.

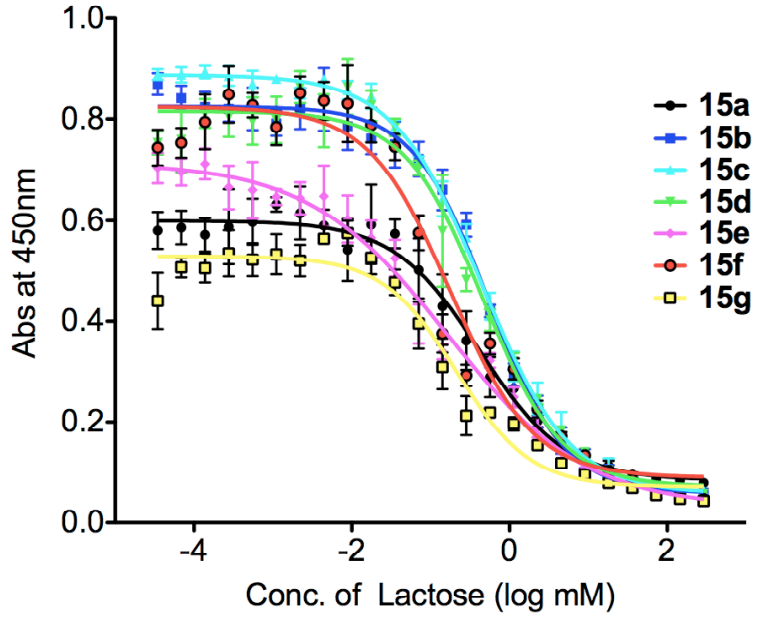

Figure 82 ELISA binding curves for compounds 15a-g.

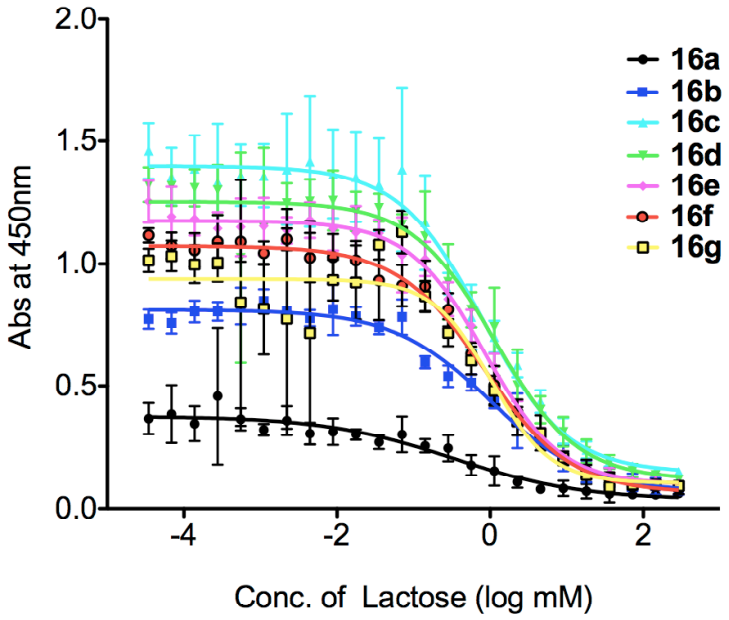

Figure 83 ELISA binding curves for compounds 16a-g.

For compounds 15a-g the ELISA binding curves are shown in Figure 82, and the lactose inhibiting concentrations are reported in Table 13. The IC_{50} values ranged from 0.06 mM for 15e and 15f to 0.19 mM for 15b. Shown in Figure 83 are the ELISA binding curves for compounds 16a-g and the reported lactose inhibiting concentrations are reported in Table 13. The IC_{50} values ranged from 0.11 mM for 16a to 0.40 mM for 16d. Results for ELISA binding curves for compounds 17a-e are shown in Figure 84, and the IC_{50} lactose inhibition values are reported in Table 14. The IC_{50} values ranged from 0.09 mM for 17d to 0.31 mM for 17a. Shown in Figure 85 are the ELISA binding curves for 18a-e, and the reported lactose inhibition values are reported in Table 14. These IC_{50} values ranged from 0.15 mM for 18a to 0.28 mM for 18e. Shown in Figure 86 are the ELISA binding

curves for 19a-e, and the reported lactose IC_{50} values are provided in Table 14. These IC_{50} values ranged from 0.09 mM for 19a to 0.20 mM for 19e.

A trend that is observed in the binding curves of 17a-e, 18a-e, and 19a-e is the increase in maximum signal correlating with the amount of lactose residues on the dendrimer periphery (with 17a being an exception).

Table 13 Carbohydrate loading amounts, ELISA lactose inhibition values, and maximum ELISA absorbance values for compounds 14a-g, 15a-g and 16a-g.

Compound number	PAMAM generation	Number of Galactose Sugars	Number of GalNAc Sugars	Total Number of Sugars	IC_{50} (mM) Lactose	Maximum absorbance value
14a	3	26	0	26	0.05	0.39
14b	3	21	5	26	0.32	1.11
14c	3	115	10	25	0.34	1.14
14d	3	11	15	26	0.32	1.14
14e	3	8	19	27	0.38	1.36
14f	3	2	24	26	0.32	0.98
14g	3	0	28	28	0.29	0.92
15a	4	57	0	57	0.15	0.60
15b	4	46	10	56	0.19	0.82
15c	4	33	22	55	0.15	0.89
15d	4	25	31	56	0.16	0.82
15e	4	12	40	52	0.06	0.71
15f	4	7	49	56	0.06	0.82
15g	4	0	54	54	0.07	0.53
16a	6	145	0	145	0.11	0.38
16b	6	109	32	141	0.35	0.81
16c	6	85	54	139	0.27	1.40
16d	6	56	85	141	0.40	1.25
16e	6	43	105	148	0.29	1.17
16f	6	9	134	143	0.29	1.07
16g	6	0	154	154	0.36	0.94

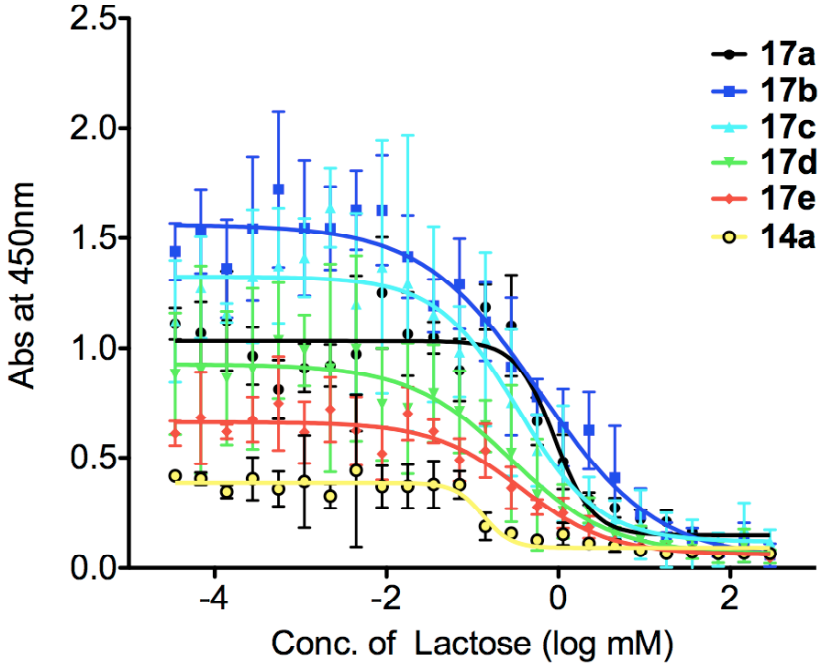

Figure 84 ELISA binding curves for compounds 17a-e and 14a.

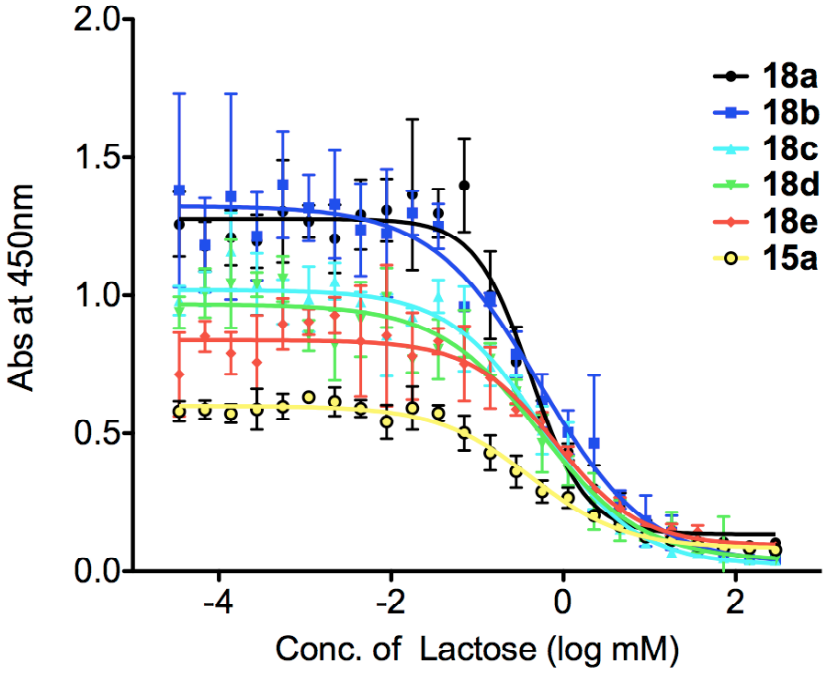

Figure 85 ELISA binding curves for compounds 18a-e and 15a.

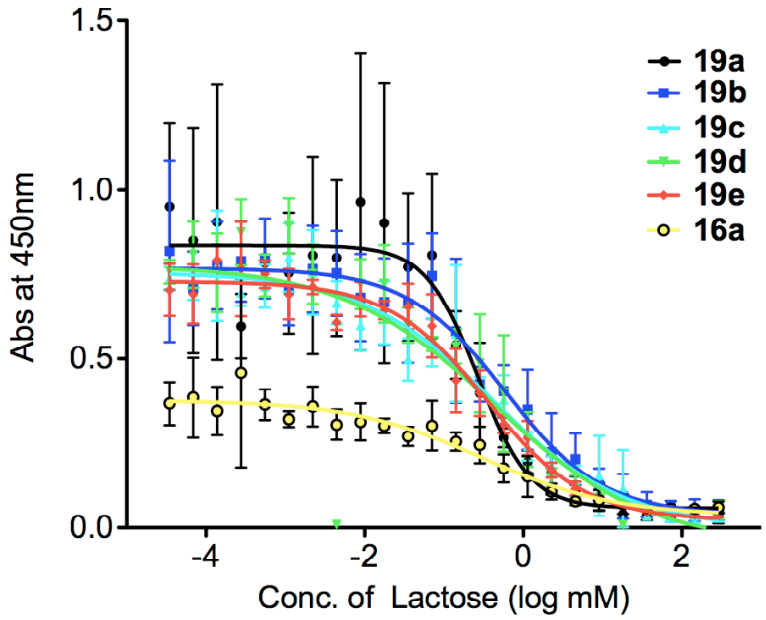

Figure 86 ELISA binding curves for compounds 19a-e and 16a.

The G(3) series trends from a maximum absorption for 14a at 0.39 to a value of 1.56 for 17b. The G(4) series trends from a maximum absorption for 18e at 0.60 to a value of 1.32 for 18b. The G(6) series trends from a maximum absorption for 19e at 0.38 to a value of 0.84 for 19b. This trend is not observed for compounds 14a-g, 15a-g and 16a-g.

Table 14 Carbohydrate loading amounts, ELISA lactose inhibition values, and maximum ELISA absorbance values for compounds 17a-e, 18a-e and 19a-e.

Compound number	PAMAM generation	Number of Galactose Sugars	Number of Lactose Sugars	Total Number of Sugars	IC_{50} (mg/mL) Lactose	Maximum absorbance value
17a	3	0	24	24	0.31	1.03
17b	3	7	20	27	0.21	1.56
17c	3	14	12	26	0.12	1.33
17d	3	19	8	27	0.09	0.93

Table 14 Continued

Compound number	PAMAM generation	Number of Galactose Sugars	Number of Lactose Sugars	Total Number of Sugars	IC_{50} (mg/mL) Lactose	Maximum absorbance value
17e	3	24	3	27	0.12	0.66
18a	4	0	57	57	0.15	1.28
18b	4	17	36	53	0.19	1.32
18c	4	28	25	53	0.20	1.02
18d	4	34	14	48	0.19	0.97
18e	4	44	7	51	0.28	0.84
19a	6	0	130	130	0.09	0.84
19b	6	37	102	139	0.20	0.77
19c	6	59	83	142	0.14	0.75
19d	6	83	55	138	0.15	0.77
19e	6	105	38	142	0.12	0.73

X-ray Photoelectron Spectroscopy

X-ray photoelectron spectroscopy was used to analyze the amount of dendrimer that was adsorbing to the NUNC maxisorp plate surface. Experiments were performed with compounds 14a, 14g, 15a, 15g, 16a, 16g, 17a, 18a, and 19a. This group of dendrimers represented fully functionalized lactose, galactose and galNAc dendrimers of all three of the PAMAM dendrimer generations, G(3), G(4) and G(6) that were studied here. To monitor the amount of dendrimer adsorbed to the plate, the amount of nitrogen was used as a quantitative measurement. Since the NUNC maxisorp plates have oxygen in the surface coating (although made up of polystyrene) to facilitate surface adsorption, a background signal in the oxygen spectrum is always present. The entire nitrogen spectrum, however, is due solely to the dendrimer. The XPS experiments were performed with higher concentrations of dendrimer than the ELISA to increase

the adsorbed dendrimer to the plate surface, hence increasing the signal in the nitrogen spectrum. Experiments with very high amounts of dendrimer in the solution during the adsorption revealed no difference between 5 μmol and 50 μmol solutions, with 5 μmol being the optimal and preferred concentration for XPS experiments.

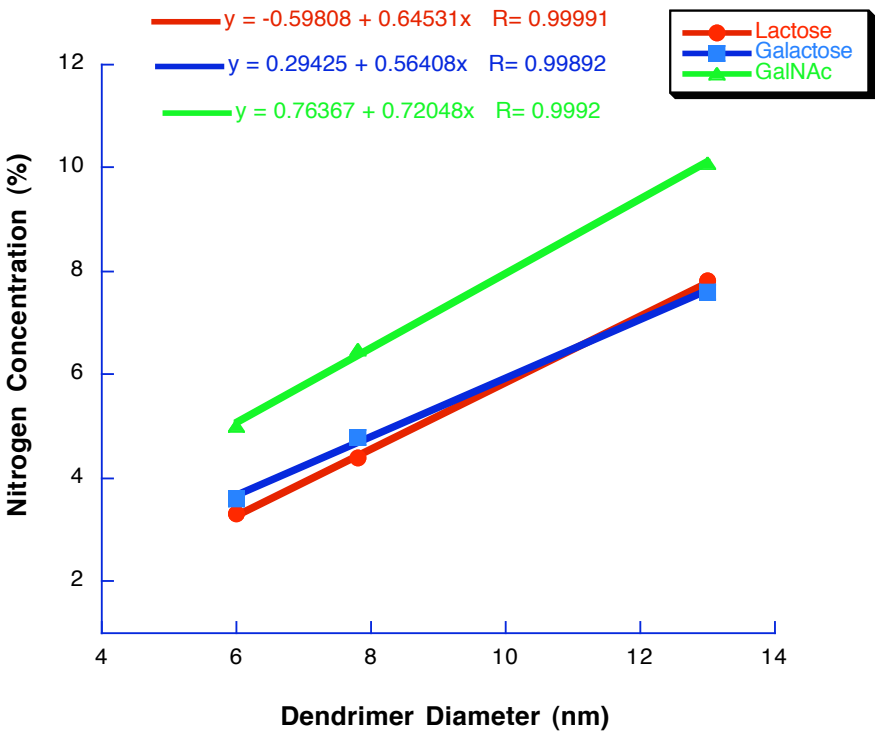

Figure 87 PAMAM dendrimer diameter vs. nitrogen concentration (%), as determined by XPS.

The ELISA assay adsorption concentration was at 250 nmol; at this concentration the same XPS trends were observed although the nitrogen signal was decreased and the sulfur signal was too small to be observable. Shown in Figure 87 is the amount of nitrogen in comparison to the dendrimer diameters as reported previously by this group.[24] The linear relationship between dendrimer

radius and nitrogen content is consistent with R values of 0.9999 for 17a, 18a and 19a, 0.9989 for 14a, 15a and 16a, and 0.9992 for 14g, 15g and 16g. The correlation between the nitrogen concentration and the dendrimer diameter indicate a consistent adsorption, across dendrimer generations, to the surface of the plate. When this experiment was performed at higher concentrations the same results were observed indicating that a maximum adsorption had been reached. If this maximum adsorption were a film of dendrimers, the linear relationship between dendrimer diameter and nitrogen percentage would be very unlikely to be present and plate preparation with higher dendrimer concentrations would yield higher adsorption. As a linear relationship between the generations is present for all the dendrimers, this result is indicative of monolayer formation. The galNAc functionalized dendrimer had an increased amount of nitrogen, which is expected with the amino sugar. However, this increase was larger than anticipated and suggests that galNAc functionalized dendrimers adhere more readily to the surface than lactose and galactose-functionalized dendrimers.

Discussion

Synthesis of Lactose, Galactose and GalNAc Functionalized Dendrimers

In chapters 2 and 3, the synthesis of carbohydrate derivatives with linkers that were incorporated for dendrimer functionalization was reported, and the need to preserve the anomeric integrity of the sugars was discussed. In the synthesis of 11, 12, and 13, β-functionalized carbohydrates were desired so that

the resultant glycodendrimers would bind well to galectin-3. Through Lewis acid facilitated glycosylation and relying on neighboring group participation via the 2-*O*-acetyl or 2-*N*-acetyl protecting groups, the synthesis of 11, 12, and 13 produced the desired anomers in good yields. This synthesis of 2-(2-isothiocyantoethoxy)ethanol-tethered carbohydrates 11 and 12 was shortened because the β-pentaacetates of galactose and galactosamine could be reacted directly with the Lewis acids BF_3OEt_2 and $FeCl_3$, respectively. These routes eliminate the need to generate trichloroacetimidates and reduce the number of purification steps required. However, this method was unsuccessful for the glycosylation of lactose, and synthesis of the trichloroacetimidate was required to gain the desired anomer after glycosylation with 2-(2-isothiocyanatoethoxy)ethanol. The degree of carbohydrate functionalization of the dendrimers was determined by MALDI-TOF MS. As with the dendrimers synthesized in chapters 2 and 3, incomplete functionalization occurred when multiple sugars were used. The amounts of sugars that were incorporated are shown in Tables 13 and 14, and the molecular weights are reported in the experimental procedures section of this chapter. The loadings were determined by both the change in Mw after addition of the carbohydrates and the changes in Mw after deacetylation, enabling a clear picture of how many sugars were added.

Enzyme Linked Immunisorbent Assay (ELISA)

The ELISA that was devised to study the dendrimer:galectin-3 binding interaction is based upon the dendrimer adsorbing to the 96 well plate and

subsequently inhibiting the dendrimer:galectin-3 interaction with varying concentrations of lactose. This method allowed for comparison of the relative binding associations of compounds 14-16 a-g and 17-19 a-e with galectin-3. Other ELISA methods were investigated such as adsorbing glycoproteins, laminin and asialofetuin to the plate and using the sugar coated dendrimers to inhibit the glycoprotein:galectin-3 surface interaction. However, these protocols inevitably resulted in very high galectin-3 binding to the surface. This result is suggestive of a cooperative system that caused galectin-3 to bind to the plate even at very high dendrimer concentrations. Another method of using antibodies and adsorbing galectin-3 to the plate and using dendrimers to perturb the antigal-3:galectin-3 interaction was unsuccessful, indicating that antibody recognition of galectin-3 does not interfere with the carbohydrate recognition domain.

Previous studies have indicated different binding constants for various carbohydrates, both natural and chemically modified, with galectin-3.[126, 130] According to the ELISA inhibition assay (Figure 78) using 17a with various inhibitors and setting the relative IC_{50} value for lactose to 1, galNAc and galactose had relative IC_{50} values of 111 and 90, respectively. Using 18a with various inhibitors (Figure 79) and setting the relative IC_{50} value for lactose to 1, galNAc had a relative inhibitory potency value of 41 and galactose of 46. Using 19a with various inhibitors (Figure 80) and setting the relative IC_{50} value for lactose to 1, galNAc had a relative inhibitory potency value of 40 and galactose of 50. This is in agreement with a report by Brewer *et al*. of a 66 fold increase in

affinity for lactose over galactose using a hemagglutination inhibition assay.[126] Interestingly there appeared to be little or no difference between the relative IC_{50} values for galactose and galNAc. This suggests the *N*-acetyl group on galNAc does not have a significantly different binding interaction than the 2OH group on galactose upon binding to galectin-3. This is not entirely surprising considering the 2'OH position on lactose in X-ray crystallography studies appears to have no major interaction with galectin-3.[101] However, studies with hydrophobic substituents at the 2'OH position have significantly increased binding constants.[131]

The monomeric carbohydrates tested as inhibitors of the glycodendrimer/galectin-3 interaction clearly showed a marked difference (40-fold or higher) between lactose and galactose or galNAc. The results from the ELISA inhibition assays with lactose indicate that there is very little difference in measured binding, both across the varying carbohydrates and the PAMAM dendrimer generations. The IC_{50} values ranged from 0.05 to 0.40 mM of lactose. These results suggest that which carbohydrates were presented on the dendrimers 14-16 a-g and 17-19 a-e did not have a great effect upon the binding affinity of the glycodendrimers toward galectin-3 in a competitive ELISA based assay. In contrast, the amount of galectin-3 that was recruited by the surface bound dendrimer increased significantly with higher lactose loading. For example in Figure 85, the maximum absorbance for 18b is 1.32 and for 15a is 0.60, and other compounds in this series follow an increasing trend in higher maximum

absorbance values with higher lactose loadings. This trend is also apparent in the G(3) series of lactose:galactose functionalized dendrimers (Figure 84), with the exception of 17a. The maximum absorbance value for 17b was 1.56 and was 0.60 for 14a, again with an increasing trend in maximum absorbance value with higher lactose loading. With G(6) dendrimers, it appears that even with lower lactose loading, the galectin-3 recruitment does not change significantly. However, with fully galactose functionalized G(6), 16a, the galectin-3 maximum absorbance is 0.38, which is much lower than the maximum absorbance values of the other G(6) lactose:galactose functionalized dendrimers: absorbance values for 19a-e are 0.84, 0.77, 0.75, 0.77 and 0.73, respectively.

Although the preferred aggregation state of galectin-3 is still unknown, the ELISA results reported here which indicate very similar binding avidity for the all the dendrimers clearly indicates that the interaction between galectin-3 and glycodendrimers is not monomeric. If the glycodendrimer/galectin-3 interaction were monomeric, then the results with glycodendrimers would resemble the results with the monomer inhibitors, and they do not. The trends of increasing galectin-3 recruitment with higher lactose loading suggest that another (not monomeric) process is playing a large role in how these surface bound dendrimers interact with galectin-3. The capacity of the dendrimer to bind galectin-3 was observed to increase when the dendrimers were functionalized with higher affinity carbohydrates compared to results with glycodendrimers bearing lower affinity carbohydrates. This process of multivalently recruiting

varying amounts of galectin-3 by the glycodendrimers could be similar to a cell surface receptor cluster mechanism, The ELISA results indicate that lectin recruitment may have a powerful role in specific receptor clustering.

X-ray Photoelectron Spectroscopy (XPS)

XPS was used to analyze the amount of the glycodendrimer that adsorbs to the NUNC maxisorp 96 well plates that were used in the ELISA's. The plates are made from polystyrene and have a coating to optimize adsorption. Control experiments where XPS measurements were obtained on unfunctionalized plates indicated the presence of oxygen in the NUNC coating, but nitrogen was not detected. Thus, after the dendrimers were adsorbed to the plate, the presence of nitrogen should arise solely from the dendrimer. Compounds 14-16a and 17-19a have the same amount of nitrogen and gave the same amounts of nitrogen signal relative to the dendrimer diameter. Compounds 14-16g have the 2-NHAc group, and this increases the nitrogen signal. Within the G(4) series, 15a and 18a would theoretically contain 303 nitrogen’s and 15g would contain 358 nitrogen’s (assuming perfect PAMAM dendrimers). These values correspond to an 18% increase in nitrogen signal for galNAc over lactose or galactose functionalized dendrimers. However, in the XPS experiments, the increase in the nitrogen signal for 15g was significantly higher than 18%. This was also observed with the G(3) and G(6) series. As shown in Figure 87, the trend for the galNAc functionalized dendrimers is also consistent with dendrimer diameter, but dendrimer adsorption is consistently higher for galNAc functionalized dendrimers

than it is for the galactose and lactose functionalized dendrimers. The amount of galactose functionalized dendrimers 14-16a and lactose functionalized dendrimers 17-19a adsorbed to the surface was shown by XPS to be equal and consistent, indicating formation of a monolayer. The galNAc functionalized dendrimers 14-16g appeared to adsorb somewhat better, but monolayer formation, as shown by the linearity of the relationship between the radius of the dendrimer and the concentration of nitrogen, is still indicated. This increase in adsorption by galNAc functionalized dendrimers does correlate well to the higher maximum absorbance values that were observed in the ELISA's for these compounds. The XPS experiments suggest that the higher galectin-3 recruitment that was observed for glycodendrimers that had higher galNAc loadings when compared to dendrimers with more galactose residues was due to differences in adsorption rather than differences in protein binding affinity.

Interestingly when XPS analysis was performed at the concentrations of the dendrimers that were used to adsorb to the plate for ELISA experiments, lower nitrogen concentrations were observed, indicating less dendrimer was adsorbed. The concentration of dendrimer that was used for surface preparation in the ELISA's, 250 nM, and the concentration that was used for XPS, 50 uM, generated the same absorbance values in control ELISA experiments, showing the maximum absorbance signal had been achieved and indicating that either the same amount of galectin-3 was recruited in both cases, or that the signal was saturated. However if at a 5 uM concentration in the plate preparation (and

higher concentrations) a consistent monolayer is formed, then this suggests that the dendrimers at the lower concentrations that were used for the ELISA assay have a lower dendrimer density on the plate surface. Prior surface adsorption results with glycodendrimers suggest the dendrimers are probably spaced apart in a random distribution.[132] This observation suggests that the dendrimer:galectin-3 interaction that was measured represents a single surface bound dendrimer interacting with galectin-3 proteins.

Conclusions

Syntheses of β-galactoside, β-galNAc, and β-lactoside derivatives that are appropriate for dendrimer functionalization were performed, and carbohydrate functionalized PAMAM dendrimers were synthesized and characterized to generate a library of compounds with a varied sugar presentation on the periphery. A novel ELISA based experiment was developed to further the understanding of how galectin-3 binds to carbohydrates. This assay revealed that galectin-3 interacts with glycodendrimers in a markedly different way than it interacts with the monomer sugars. The binding constants that were determined by this assay for the dendrimers with galectin-3 are all very similar, even with very different sugar epitopes. However, the galectin-3 recruitment increased with higher dendrimer functionalizations with a higher affinity ligand. These results suggest that the binding affinity may play less of a role in the galectin-3 processes than clustering and aggregation mechanisms. Using X-ray

photoelectron spectroscopy, dendrimer adsorption to NUNC maxisorp plates was shown to form a monolayer. Less than maximum dendrimer adsorption was observed at dendrimer concentrations that were used for the ELISA assays, indicating that individual dendrimers were interacting with multiple galectin-3 proteins during the ELISA's. These observations indicate that multivalent architectures will be critical for improving the understanding of galectin-3 behavior in biologically relevant interactions.

Experimental Procedures

General Methods

General reagents were purchased from Acros and Aldrich Chemical Companies. PAMAM dendrimers were purchased from Dendritech. Concanavalin A (Con A) was purchased from Calbiochem. Methylene chloride was purified on basic alumina; other solvents were used as received. 32-63μ “40 micron flash” silica gel for flash column chromatography purification was purchased from Scientific Adsorbants Incorporated.

Matrix Assisted Laser Desorption Ionization MS (MALDI)

See chapter 2 for instrument details. MALDI-TOF MS spectra were obtained after each addition of isothiocyanate, and the change in Mw upon the first addition was divided by the Mw of the isothiocyanato carbohydrate (galNAc 476 g/mol, galactose 477 g/mol) to give a quantity that is denoted here as A

(equation 1). The total number of carbohydrate residues added for the second addition (B in equation 2) was determined by subtracting Mw for unfunctionalized PAMAM from the Mw after each sequential additions of isothiocyanate and then dividing by the Mw of that carbohydrate (galactose - 477 g/mol, galNAc – 476 g/mol, lactose 765 g/mol), and this sum was the total, shown as C (equation 3). The total number of carbohydrate residues was also determined by dividing the change in M_w upon deacylation by 168 (the loss of 4 acetyl groups per galactose), 126 (the loss of 3 acetyl groups per galNAc) or 294 (the loss of 7 acetyl groups per lactose) and this number is denoted as D (equation 4). The total number of carbohydrate residues was determined again by dividing the change in M_w upon deacylation from the PAMAM dendrimer, by the Mw of the deacetylated tethered sugar (309 for galactose, 352 for galNAc and 471 for lactose), denoted by as E (equation 5). These three methods of determining the total sugar loading were then averaged , denoted as F (equation 6). The number of residues of the first sugar was the corrected by dividing A by C times F to give A’ as shown in equation 7, to obtain the most accurate value for how many residues of the first isothiocyanato sugar (and also by difference for how many residues of the second isothiocyanato sugar) were added to the dendrimer. Sample numbers using data from compound 17d are provided in the equations below.

$$A = \frac{M_w \text{ (all galNCS addition)} - M_w \text{ (PAMAM)}}{477} = \frac{15800 - 6800}{477} = 18.9 \qquad \text{(eq. 1)}$$

$$B = \frac{M_w \text{ (all lacNCS additions)} - M_w \text{ (PAMAM)}}{765} = \frac{21800 - 15800}{765} = 7.8 \qquad \text{(eq. 2)}$$

$$C = \text{total \# sugars} = A + B = 18.9 + 7.8 = 26.7 \qquad \text{(eq. 3)}$$

$$D = \frac{M_w \text{ (all RNCS added)} - M_w \text{ (deacetylated)}}{[(A \times 168) + (B \times 294) / C]} = \frac{21800 - 15700}{5469/26.7} = 29.8 \qquad \text{(eq. 4)}$$

$$E = \frac{M_w \text{ (deacetylated)} - M_w \text{ (PAMAM)}}{[(A \times 309) + (B \times 471)] / C)} = \frac{15{,}700 - 6800}{9514 \ / \ 26.7} = 25.0 \qquad \text{(eq. 5)}$$

$$F = \frac{(C + D + E)}{3} = 27.1 \qquad \text{(eq. 6)}$$

$$A' = (A/C) \times F = (18.9 / 26.7) \times 27.1 = 19.2 \qquad \text{(eq. 7)}$$

$$B' = (B/C) \times F = (7.8 / 26.7) \times 27.1 = 7.9 \qquad \text{(eq. 8)}$$

NMR

^{1}H NMR spectra were recorded on Bruker DPX 300 (300 MHz) and Bruker DPX-500 (500 MHz) spectrometers. Chemical shifts are reported in ppm from tetramethylsilane with the residual protic solvent resonance as the internal standard (chloroform: δ 7.25 ppm; dimethyl sulfoxide: δ 2.50 ppm). Data are reported as follows: chemical shift, multiplicity (s = singlet, bs = broad singlet, d = doublet, t = triplet, q = quartet, p = pentet, m = multiplet, app = apparent), integration, coupling constants (in Hz) and assignments. ^{13}C NMR spectra were recorded on a Bruker DPX 500 (125 MHz) spectrometer with complete proton

decoupling. Chemical shifts are reported in ppm from tetramethylsilane with the solvent as the internal standard ($CDCl_3$: δ 77.0 ppm)

X-ray Photoelectron Spectroscopy

Carbohydrate functionalized dendrimers were dissolved in a PBS solution at 1 mg/mL concentration, which required 24 hrs of stirring. These solutions were diluted with PBS buffer to a concentration of 5 μM. 50 μL of this solution was added to a well of a NUNC maxisorp 96 well plate, covered and stored at 5 degrees for 20 h. The well was then washed with PBS twice and washed with nanopure water twice to remove any phosphate buffer that might interfer with the analysis. The bottom of the well plate was removed with scissors and was used for XPS analysis. The analysis was conducted on a Physical Electronics 5600ci XPS system equipped with monochromatized Al KR X-rays. The analysis area of the sample was 0.8 mm in diameter. Electron emissions were collected at 45° to the normal of the surface, and the spherical-sector-analyzer pass energy was selected as 11.75 eV for high-resolution scanning and as 46.95 eV for a survey to achieve optimum energy resolution and count rate. The data acquisition and data analysis were performed using RBD AugerScan 2 software.

Enzyme Linked Immunosorbent Assay

Plate preparation: Dendrimer was dissolved into PBS (pH 7.4, 15 mmol NaCl). The stock solution was commonly prepared at 5 mg/mL, but the concentration of the stock solution was reduced if there were problems with

solubility. The 5mg/mL stock solution was diluted at 1:200 and 50 μL of this solution was added to each well plate. (Nunc maxisorp). The well plate was covered and stored for 24 h at 4 ºC. The solvent was removed from the well plate and 250 μL of 3% BSA solution in PBS (pH 7.4) was added to each well plate to block non-specific interactions. The plate was covered and let stand for 2 h at RT, emptied, and washed once with PBS (pH 7.4). The plate was dried, covered, and stored at 4 ºC or dried and used.

Enzyme linked immunosorbent assay: In a PPI plate, 60 μL of 0.5% BSA in PBS (pH 7.4) was added to each well, except A1, C1, E1 and G1 were filled with 60 μL of 100 mg/mL lactose solution. To A2, C2, E2, and G2, 60 μL of the 100 mg/mL lactose solution were added. Serially dilute for each well was performed so that each well had 60 μL of solution in it and 23 dilutions were performed. From each well, 50 μL were transferred to the corresponding well on the dendrimer coated prepared plate (preparation of the dendrimer coated plate is described above). Galectin-3 was added (50 μL of 10 μg/mL solution, concentration determined using a BCA assay[133]), the plate was covered and placed on an agitator/shaker for 45 minutes.

After 45 minutes, the plate was removed from the shaker and the contents were emptied. Each well was washed 2x with PBS-T (pH 7.4) and 1x with PBS (pH 7.4). Biotinylated anti-galectin-3 was added (50 μL of a 1:100 dilution of 1 mL stock from R and D Systems, Inc.), the plate was covered and placed back on shaker for 45 minutes. After 45 minutes, the plate was removed from the shaker

and the wells were emptied and each well was washed 2x with PBS-T (pH 7.4) and 1x with PBS (pH 7.4). Horseradish peroxidase streptavidin conjugate was added (100 uL of solution that was a 1:200 dilution from the vial that was obtained from BD Biosciences), and the plate was covered and placed on the shaker for 45 min. The plate was removed from the shaker, the wells were emptied and each well was washed 2x with PBS-T (pH 7.4) and 1x with PBS (pH 7.4).

TMB:peroxide solution (100 μL of a 1:1 mix of solutions from kit purchased from BD biosciences) was added and the color change was observed. 100 μL of 1M phosphoric acid was added to stop the reaction. (This can be monitored at 620 nm on a plate reader.) Absorbances were read at 450 nm for each well plate, with the reference at 620 nm.

Making solutions: For *Galectin-3,* a 10 μg/mL solution was prepared in 0.5% BSA in PBS (pH 7.4). The concentration was determined using a BCA assay.[133] Galectin-3 gives the same standard curve as BSA. For each plate, 5 mL of the solution was required.

For *A*nti-Gal-3 biotinylated, 50 μg of antibody conjugate was purchased from R and D Systems, Inc. For each plate, 5 mL of the solution was required.. A solution of (1 mL, pH 7.4) was added to the vial to form a 50 μg/mL solution. For the assay, this solution was diluted 100:1 with 0.5% BSA in PBS (pH 7.4) for the working solution. For each plate, 5 mL of the solution was required.

For HRP streptavidin, the stock solution was purchased from BD Biosciences Inc., then 1:200 dilution was performed with 0.5% BSA in PBS (pH 7.4) to prepare the working assay solution. For each plate, 10 mL of the solution was required.

Color generating solution, The TMB and peroxide were purchased from R and D Systems, Inc. Immediately prior to use, 1 part of each was combine to make a solution. The solution was mixed well, and used: extra solution was discarded.. For each plate, 10 mL of the solution was required.

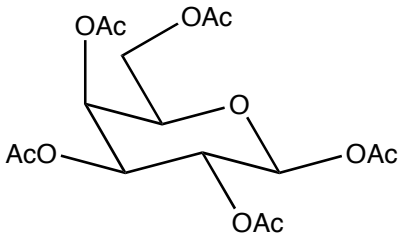

1,2,3,4,6-penta-O-acetyl -β-D-galactopyranoside. 2.0 g of D-galactopyranoside (11 mmol) was added to 30 mL acetic anhydride and 4.1 g sodium acetate (50 mmol) and heated to 100 ^{o}C for 8 h. The mixture was let cool and filtered over celite. Solvent was removed in vacuo. The residue was taken up in CH_2Cl_2 and subjected to decolorizing carbon, filtered and solvent was removed in vacuo. The mixture was recrystallized in hot toluene and minimal hexane to yield grams of 3.9 g (90 % yield) of pure material. ^{1}H NMR (300 MHz $CDCl_3$) δ 5.69 (1H, d, J = 8.7 Hz, H1), 5.41 (1H, d, J = 3.2 Hz, H4), 5.31 (1H, app t, J = 8.7 Hz, H2), 5.06

(1H, dd, J = 3.2, 8.7 Hz, H3), 4.11 (H, m, H5), 3.95 (2H, m, H6), 2.14 (3H, s), 2.10 (3H, s), 2.02 (6H, s), 1.97 (3H, s) ppm. As reported.

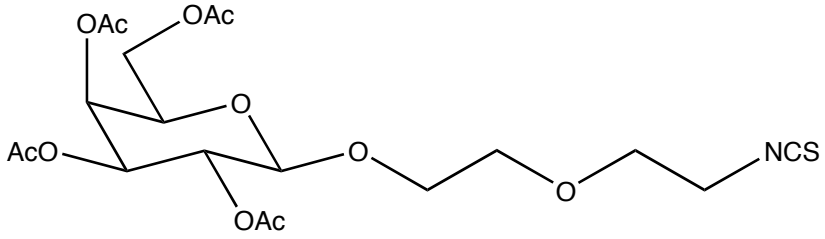

1-O-(5-isothiocyanato-3-oxopentyl)- 2,3,4,6-tetra-O-acetyl -β-D-galactopyranoside (11). 2.0 g of 1,2,3,4,6-penta-O-acetyl-β-D-galactopyranoside (5.1 mmol) was dissolved in 50 mL of methylene chloride with 1.5 g of 2-(2-isothiocyantoethoxy)ethanol (10.2 mmol) and cooled to 0 ^{o}C followed by addition of 1.4 g of BF_3OEt_2 (10.2 mmol) via syringe pump over 30 minutes. The reaction was stirred for 1 h, at which point 1 g of $NaHCO_3$ was added. The mixture was filtered over celite and solvent was removed in vacuo. The residue was purified via column chromatography with a 1:1 ethyl acetate:hexane eluent (Rf 0.25), yielding 1.8 g (76 % yield) of pure material. ^{1}H NMR (300 MHz $CDCl_3$) δ 5.38 (1H, d, J = 2.1 Hz, H4), 5.19 (1H, app t, J = 7.8 Hz, H2), 5.02 (1H, dd, J = 2.1, 10.1 Hz, H3), 4.55 (1H, d, J = 7.8 Hz, H1), 4.11 (2H, m, H5), 3.95 (2H, m, H6), 3.68 (7H, m), 2.19 (3H, s), 2.05 (3H, s), 2.03 (3H, s), 1.96 (3H, s) ppm. As reported[134]

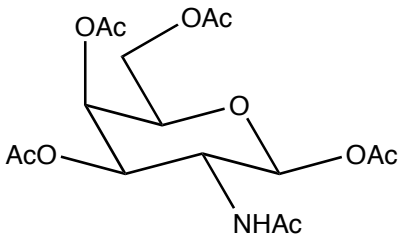

1,3,4,6-penta-O-acetyl -β-D-N-acetyl-galactosaminopyranoside. 1.8 g of galactosaminopyranoside was combined with 0.49 g $ZnCl_2$ (3.6 mmol) in 20 mL acetic anhydride and stirred for 12 h, when a further 0.25 g $ZnCl_2$ was added, and the mixture stirred for 12 h, by which time the solution had become clear. 30 mL of brine solution was added followed by 2 g of $NaHCO_3$. The product was extracted with 4 x 50 mL CH_2Cl_2, dried over $MgSO_4$, filtered and solvent was removed in vacuo, recrystallization was performed with 1:1 CH_2Cl_2:EtOH to yield 3.2 g (78 % yield) of the pure desired anomer. 1H NMR (500MHz d^6 DMSO) δ 7.87 (1H, d, J= 9.2 Hz, N*H*Ac), 5.60 (1H, d, J = 9.5 Hz H1), 5.23 (1H, d, J = 3.0 Hz, H4), 5.02 (1H, dd, J = 3.0, 11.2 Hz, H3), 4.19 (1H, m, H5), 4.06 (1H, app q, J = 9.2, 9.5, 11.2 Hz, H2), 3.96-4.00 (2H, m, H6), 2.18 (3H, s), 2.09 (3H, s), 1.96 (3H, s), 1.86 (3H, s), 1.75 (3H, s) ppm. As reported.[135]

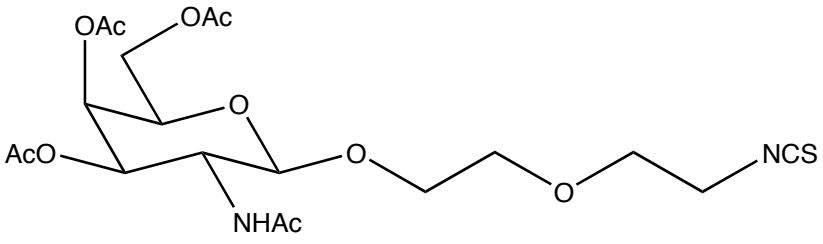

12: 1-O-(5-isothiocyanato-3-oxopentyl)- 2,3,4,6-tetra-O-acetyl -β-D-galactosaminopyranoside. 0.94 g of 1,3,4,6-penta-O-acetyl-β-D-N-acetyl-galactaminopyranoside (2.4 mmol) was dissolved in 15 mL of methylene

chloride, 1.4 g of dririte was added, the slurry stirred for 10 minutes and 1.4 g of $FeCl_3$ (10.2mmol) and 0.83 g of 2-(2-isothiocyantoethoxy)ethanol (5.7 mmol) were added. The reaction was stirred 24 h, then 1 g of $NaHCO_3$ was added. The mixture was filtered over celite and solvent was removed in vacuo. The residue was purified via column chromatography with a 9:1 ethyl acetate:hexane eluant (Rf 0.4), yielding 0.70 grams of pure material. ^{1}H NMR (500MHz d^6 DMSO) δ 7.83 (1H, d, J = 9.2 Hz, N*H*Ac), 5.21 (1H, d, J = 3.0 Hz, H4), 4.97 (1H, dd, J = 3.0, 11.2 Hz, H3), 4.55 (1H, d, J = 9.5 Hz, H1), 4.02 (3H, m, H5, OCH_2CH_2O), 3.87 (1H, app q, J = 9.2 (N*H*Ac), 9.5, 11.2 Hz, H2), 3.80 (2H, t, J = 4.9 Hz, OCH_2CH_2NCS), 3.59 (6H, m, H6, CH_2CH_2OCH_2CH_2), 2.11 (3H, s), 2.04 (3H, s), 1.89 (3H, s), 1.78 (3H, s) ppm. As reported[136]

Galactose:Galactosamine Dendrimers

Representative procedure for the synthesis of heterogeneously functionalized PAMAM-based thiourea-linked 1-O-(5-isothiocyanato-3-oxopentyl)-3,4,6-tetra-O-acetyl -β-D-N-acetyl-galactosaminopyranoside, 1-O-(5-isothiocyanato-3-oxopentyl)- 2,3,4,6-tetra-O-acetyl -β-D-galactopyranoside. (14-16) An aqueous solution of amine terminated Starburst G(4)-PAMAM dendrimer (2.478 g of a 17% w/w solution in water, 421.2 mg, 31.2 μmol) was lyophilized to leave a foamy residue. 7.02 mL of DMSO was then added to this residue to give a 60 mg/mL solution. 0.35 mL of a 300 mM solution of 1-O-(5-isothiocyanato-3-oxopentyl)-3,4,6-tetra-O-acetyl -β-D-N-acetyl-galactosaminopyranoside (12, 85 μmol, 40.2 mg) in DMSO was added to 0.5 mL of a 60 mg/mL G(3) PAMAM

dendrimer (30 mg, 4.40 μmol) solution. The reaction was stirred for 8 h at which point a 75 μL aliquot was removed for MALDI-TOF analysis. After MALDI-TOF analysis indicated reaction completion 0.31 mL of a 300 mM solution of 1-O-(5-isothiocyanato-3-oxopentyl)- 2,3,4,6-tetra-O-acetyl -β-D-galactopyranoside (11, 73 μmol, 35 mg) was added. The solution was then stirred for 8 h. At this time a 75 μL aliquot was removed for MALDI-TOF and NMR analysis.

Acetylated

14a: ^{1}H NMR (500MHz *d*^{6} DMSO) δ 7.95 (1H, bs, amide NH's), 7.74 (1H, bs, amide NH's), 7.46 (2H, bs, CH_2N*H*C(S)N*H*CH_2), 5.21 (1.3H, d, J = 3.2 Hz, H4), 5.11 (1.3H, dd, J = 3.2, 10.3 Hz, H3), 4.89 (1.3H, dd, J = 8.1, 10.3 Hz, H2), 4.69 (1.3H, d, J = 8.1 Hz, H1), 4.12 (1.3H, d, J = 6.1 Hz, OC*H*$_2$$CH_2O$), 4.01 (2.6H, m), 3.76 (1.3H, m), 3.59 (1.3H, m), 3.27-3.52 (12H, m), 3.13 (3H, bs), 3.04 (2.2H, bs), 2.61 (4.8H, m), 2.39 (3.2H, m), 2.16 (4.8H, bs), 2.08 (4H, s), 2.00 (4H, s), 1.96 (4H, s), 1.87 (4H, s) ppm. MALDI-TOF (pos) m/z 19500.

14b: ^{1}H NMR (500MHz *d*^{6} DMSO) δ 7.95 (1H, bs, amide NH's), 7.74-7.79 (1.4H, m, amide NH's, N*H'*Ac), 7.46 (2H, bs, CH_2N*H*C(S)N*H*CH_2), 5.21 (1.2H, d, J = 3.2 Hz, H4), 5.17 (0.2H, s, H4'), 5.11 (1.2H, dd, J = 3.2, 10.3 Hz, H3), 4.92 (0.2H, d, J = 10.3 Hz, H3'), 4.89 (1.2H, t, J = 9.7 Hz, H2), 4.69 (1.2H, d, J = 7.6 Hz, H1), 4.51 (0.2H, d, J = 8.4 Hz, H1'), 4.12 (1.2H, m), 4.01 (3.1H, m), 3.83 (0.2H, app q, J = 8.4, 9.0, 10.3 Hz, H2'), 3.76 (2.0H, m), 3.27-3.59 (14.2H, m), 3.13 (3.1H, bs),

3.04 (2.4H, bs), 2.61 (3.1H, m), 2.16 (4.7H, bs), 2.08 (4H, s), 2.00 (2.8H, s), 1.96 (4.6H, s), 1.87 (3H, s) 1.72 (0.8H, s) ppm. MALDI-TOF (pos) m/z 19100.

14c: ^{1}H NMR (500MHz *d*^{6} DMSO) δ 7.95 (1H, bs, amide NH's), 7.79 (0.7H, d, J = 9.0 Hz, N*H'*Ac), 7.74 (0.9H, bs, amide NH's), 7.46 (2.1H, bs, CH_2N*H*C(S)N*H*CH_2), 5.21 (1.1H, d, J = 3.2 Hz, H4), 5.17 (0.4H, s, H4'), 5.11 (1.1H, dd, J = 3.2, 10.3 Hz, H3), 4.92 (0.4H, d, J = 10.3 Hz, H3'), 4.89 (1.1H, t, J = 9.7 Hz, H2), 4.69 (1.1H, d, J = 7.6 Hz, H1), 4.51 (0.4H, d, J = 8.4 Hz, H1'), 4.12 (1.1H, m), 4.01 (3.7H, m), 3.83 (0.4H, app q, J = 8.4, 9.0, 10.3 Hz, H2'), 3.76 (2.3H, m), 3.27-3.59 (15.9H, m), 3.13 (3.1H, bs), 3.04 (2.6H, bs), 2.61 (5.4H, m), 2.39 (3H, m), 2.16 (4.9H, bs), 2.08 (3H, s), 2.06 (1.5H, s), 1.96 (4.9H, s), 1.87 (2.9H, s), 1.85 (1.4H, s), 1.74 (1.2H, s) ppm. MALDI-TOF (pos) m/z 19000.

14d: ^{1}H NMR (500MHz *d*^{6} DMSO) δ 7.95 (1H, bs, amide NH's), 7.79 (0.8H, d, J = 9.0 Hz, N*H'*Ac), 7.74 (1H, bs, amide NH's), 7.46 (2H, bs, CH_2N*H*C(S)N*H*CH_2), 5.21 (0.8H, d, J = 3.2 Hz, H4), 5.17 (0.7H, s, H4'), 5.11 (0.8H, dd, J = 3.2, 10.3 Hz, H3), 4.92 (0.7H, d, J = 10.3 Hz, H3'), 4.89 (1.3H, t, J = 9.7 Hz, H2), 4.69 (1.3H, d, J = 7.6 Hz, H1), 4.51 (0.7H, d, J = 8.4 Hz, H1'), 4.12 (0.8H, m), 4.01 (3.8H, m), 3.83 (0.7H, app q, J = 8.4, 9.0, 10.3 Hz, H2'), 3.76 (1.9H, m), 3.27-3.59 (15.6H, m), 3.13 (3.2H, bs), 3.04 (2.6H, bs), 2.61 (5.6H, m), 2.39 (3H, m), 2.16 (4.7H, bs), 2.08 (4H, s), 2.00 (4H, s), 1.96 (4H, s), 1.87 (4H, s) ppm. MALDI-TOF (pos) m/z 18900.

14e: ^{1}H NMR (500MHz *d*^{6} DMSO) δ 7.95 (1H, bs, amide NH's), 7.79 (1.1H, d, J = 9.0 Hz, N*H'*Ac), 7.74 (0.9H, bs, amide NH's), 7.46 (2.1H, bs, $CH_2NHC(S)NHCH_2$), 5.21 (0.6H, d, J = 3.2 Hz, H4), 5.17 (0.9H, s, H4'), 5.11 (0.6H, dd, J = 3.2, 10.3 Hz, H3), 4.92 (0.9H, d, J = 10.3 Hz, H3'), 4.89 (0.6H, t, J = 9.7 Hz, H2), 4.69 (0.6H, d, J = 7.6 Hz, H1), 4.51 (0.9H, d, J = 8.4 Hz, H1'), 4.12 (0.6H, m), 4.01 (4.2H, m), 3.83 (0.9H, app q, J = 8.4, 9.0, 10.3 Hz, H2'), 3.76 (2.1H, m), 3.27-3.59 (15.7H, m), 3.13 (3.1H, bs), 3.04 (2.4H, bs), 2.61 (5.2H, m), 2.39 (3.1H, m), 2.16 (4.8H, bs), 2.07 (1.9H, s),2.06 (2.8H, s), 1.98 (0.7H, s), 1.96 (4.9H, s), 1.87 (1.9H, s), 1.85 (2.5H, s), 1.74 (2.5H, s) ppm. MALDI-TOF (pos) m/z 19300.

14f: ^{1}H NMR (500MHz *d*^{6} DMSO) δ 7.95 (1H, bs, amide NH's), 7.79 (1.3H, d, J = 9.0 Hz, N*H'*Ac), 7.74 (0.8H, bs, amide NH's), 7.46 (2.1H, bs, $CH_2NHC(S)NHCH_2$), 5.21 (0.3H, d, J = 3.2 Hz, H4), 5.17 (1.1H, s, H4'), 5.11 (0.3H, dd, J = 3.2, 10.3 Hz, H3), 4.92 (1.1H, d, J = 10.3 Hz, H3'), 4.89 (0.3H, t, J = 9.7 Hz, H2), 4.69 (0.3H, d, J = 7.6 Hz, H1), 4.51 (1.1H, d, J = 8.4 Hz, H1'), 4.12 (0.8H, m), 4.01 (3.8H, m), 3.83 (1.1H, app q, J = 8.4, 9.0, 10.3 Hz, H2'), 3.76 (0.3H, m), 3.27-3.59 (15.3H, m), 3.13 (2.8H, bs), 3.04 (2.2H, bs), 2.61 (4.7H, m), 2.39 (2.7H, m), 2.16 (4.3H, bs), 2.07 (1.4H, s), 2.06 (3.4H, s), 1.95 (5H, s), 1.87 (1H, s), 1.85 (3.5H, s), 1.74 (3.3H, s) ppm. MALDI-TOF (pos) m/z 19000.

14g: ^{1}H NMR (500MHz *d*^{6} DMSO) δ 7.96 (1H, bs, amide NH's), 7.79 (1.3H, d, J = 9.0 Hz, N*H'*Ac), 7.74 (1.1H, bs, amide NH's), 7.46 (2.2H, m, $CH_2NHC(S)NHCH_2$), 5.17 (1.3H, s, H4'), 4.92 (1.3H, dd, J = 3.0, 10.3 Hz, H3'), 4.51 (1.3H, d, J = 8.4 Hz, H1'), 4.01 (4.7H, m), 3.83 (1.3H, app q, J = 8.4, 9.0, 10.3 Hz, H2'), 3.27-3.59 (16.5H, m), 3.13 (3.2H, bs), 3.04 (2.3H, bs), 2.61 (5.1H, m), 2.39 (2.5H, m), 2.16 (4.1H, bs), 2.06 (4.7H, s), 1.95 (4.7H, s), 1.85 (4.2H, s), 1.74 (4.2H, s) ppm. MALDI-TOF (pos) m/z 19900.

15a: ^{1}H NMR (500MHz *d*^{6} DMSO) δ 7.94 (1H, bs, amide NH's), 7.73 (1H, bs, amide NH's), 7.45 (2H, bs, $CH_2NHC(S)NHCH_2$), 5.21 (1.3H, s, H4), 5.11 (1.3H, d, J = 10.3 Hz, H3), 4.89 (1.3H, m, H2), 4.69 (1.3H, m, H1), 4.13 (1.3H, s, OCH_2CH_2O), 4.01 (2.7H, m), 3.76 (1.7H, m), 3.27-3.52 (12H, m), 3.13 (3H, bs), 3.04 (2.0H, bs), 2.61 (4.5H, m), 2.39 (2.7H, m), 2.16 (4.2H, bs), 2.08 (4.1H, s), 2.00 (3.1H, s), 1.96 (4.6H, s), 1.87 (3.7H, s) ppm. MALDI-TOF (pos) m/z 40900.

15b: ^{1}H NMR (500MHz *d*^{6} DMSO) δ 7.95 (1H, bs, amide NH's), 7.74-7.79 (1.4H, m, amide NH's, N*H'*Ac), 7.45 (2.1H, bs, $CH_2NHC(S)NHCH_2$), 5.21 (1.3H, s, H4), 5.17 (0.2H, s, H4'), 5.12 (1.3H, d, 10.5 Hz, H3), 4.92 (0.2H, m, H3'), 4.89 (1.3H, t, J = 9.7 Hz, H2), 4.69 (1.2H, d, J = 7.6 Hz, H1), 4.51 (0.2H, d, J = 8.4 Hz, H1'), 4.12 (1.3H, m), 4.00 (3.3H, m), 3.83 (0.2H, app q, J = 8.4, 9.0, 10.3 Hz, H2'), 3.76 (2.2H, m), 3.27-3.59 (12.7H, m), 3.13 (2.8H, bs), 3.04 (2.4H, bs), 2.61

(5.1H, m), 2.16 (4.8H, bs), 2.08 (4.7H, s), 2.00 (2.5H, s), 1.96 (5.3H, s), 1.87 (3.3H, s) 1.72 (0.8H, s) ppm. MALDI-TOF (pos) m/z 40000.

15c: ^{1}H NMR (500MHz *d*^{6} DMSO) δ 7.95 (1H, bs, amide NH's), 7.79 (0.7H, d, J = 9.0 Hz, N*H'*Ac), 7.74 (1.0H, bs, amide NH's), 7.46 (2.1H, m, CH_2N*H*C(S)N*H*CH_2), 5.21 (1.2H, s, H4), 5.17 (0.5H, s, H4'), 5.11 (1.3H, m, H3), 4.92 (0.5H, d, J = 10.3 Hz, H3'), 4.89 (1.3H, t, J = 9.7 Hz, H2), 4.69 (1.1H, d, J = 7.6 Hz, H1), 4.51 (0.4H, d, J = 8.4 Hz, H1'), 4.12 (1.3H, m), 4.01 (4.1H, m), 3.83 (0.6H, app q, J = 8.4, 9.0, 10.3 Hz, H2'), 3.76 (2.9H, m), 3.27-3.59 (13.8H, m), 3.13 (3.0H, bs), 3.04 (2.6H, bs), 2.61 (4.4H, m), 2.39 (2.7H, m), 2.16 (4.4H, bs), 2.08 (3.6H, s), 2.06 (1.6H, s), 1.96 (5.9H, s), 1.87 (3.2H, s), 1.85 (1.5H, s), 1.74 (1.3H, s) ppm. MALDI-TOF (pos) m/z 39700.

15d: ^{1}H NMR (500MHz *d*^{6} DMSO) δ 7.95 (1H, bs, amide NH's), 7.79 (0.9H, d, J = 9.0 Hz, N*H'*Ac), 7.74 (0.9H, bs, amide NH's), 7.46 (2.1H, bs, CH_2N*H*C(S)N*H*CH_2), 5.21 (0.7H, d, J = 3.2 Hz, H4), 5.17 (0.7H, s, H4'), 5.11 (0.7H, d, J = 10.3 Hz, H3), 4.92 (0.7H, d, J = 10.3 Hz, H3'), 4.89 (0.7H, t, J = 9.7 Hz, H2), 4.69 (0.6H, d, J = 7.6 Hz, H1), 4.51 (0.7H, d, J = 8.4 Hz, H1'), 4.12 (0.8H, m), 4.01 (3.9H, m), 3.83 (0.7H, app q, J = 8.4, 9.0, 10.3 Hz, H2'), 3.76 (1.9H, m), 3.27-3.59 (13.6H, m), 3.13 (2.9H, bs), 3.04 (2.4H, bs), 2.61 (5.3H, m), 2.39 (2.6H, m), 2.16 (4.6H, bs), 2.08 (5H, s), 2.00 (4.8H, s), 1.96 (1.9H, s), 1.87 (2.4H, s) 1.74 (2.1H, s) ppm. MALDI-TOF (pos) m/z 40200.

15e: ^{1}H NMR (500MHz *d*^{6} DMSO) δ 7.95 (1H, bs, amide NH's), 7.80 (1.0H, d, J = 9.0 Hz, N*H'*Ac), 7.79 (0.8H, bs, amide NH's), 7.46 (2.0H, m, $CH_2NHC(S)NHCH_2$), 5.21 (0.5H, s, H4), 5.17 (0.9H, s, H4'), 5.11 (0.4H, d, 10.3 Hz, H3), 4.92 (1H, d, J = 10.3 Hz, H3'), 4.89 (0.4H, t, J = 9.7 Hz, H2), 4.69 (0.4H, d, J = 7.6 Hz, H1), 4.51 (0.9H, d, J = 8.4 Hz, H1'), 4.12 (0.5H, m), 4.01 (4.1H, m), 3.83 (1.1H, app q, J = 8.4, 9.0, 10.3 Hz, H2'), 3.76 (2.0H, m), 3.27-3.59 (13.1H, m), 3.13 (2.7H, bs), 3.04 (2.0H, bs), 2.61 (4.2H, m), 2.39 (2.6H, m), 2.16 (3.8H, bs), 2.07 (1.7H, s), 2.06 (3.9H, s), 1.98 (1H, s), 1.96 (5.3H, s), 1.87 (1.4H, s), 1.85 (2.9H, s), 1.74 (2.8H, s) ppm. MALDI-TOF (pos) m/z 39700.

15f: ^{1}H NMR (500MHz *d*^{6} DMSO) δ 7.95 (1H, bs, amide NH's), 7.79 (1.3H, d, J = 9.0 Hz, N*H'*Ac), 7.74 (0.8H, bs, amide NH's), 7.46 (2.1H, m, $CH_2NHC(S)NHCH_2$), 5.21 (0.3H, d, J = 3.2 Hz, H4), 5.17 (1.2H, s, H4'), 5.11 (0.3H, d, J = 10.3 Hz, H3), 4.92 (1.2H, d, J = 10.3 Hz, H3'), 4.89 (0.3H, t, J = 9.7 Hz, H2), 4.69 (0.2H, d, J = 7.6 Hz, H1), 4.51 (1.2H, d, J = 8.4 Hz, H1'), 4.12 (0.3H, m), 4.01 (3.6H, m), 3.83 (1.3H, app q, J = 8.4, 9.0, 10.3 Hz, H2'), 3.76 (2.2H, m), 3.27-3.59 (15.3H, m), 3.13 (3.0H, bs), 3.04 (2.1H, bs), 2.61 (5.0H, m), 2.39 (2.7H, m), 2.16 (4.4H, bs), 2.07 (1.1H, s), 2.06 (3.4H, s), 1.95 (5.3H, s), 1.87 (1H, s), 1.85 (3.9H, s), 1.74 (3.7H, s) ppm. MALDI-TOF (pos) m/z 40500.

15g: ^{1}H NMR (500MHz *d*^{6} DMSO) δ 7.96 (1H, bs, amide NH's), 7.81 (1.2H, d, J = 9.0 Hz, N*H'*Ac), 7.74 (0.8H, bs, amide NH's), 7.46 (2.0H, m,

$CH_2NHC(S)NHCH_2$), 5.17 (1.3H, s, H4'), 4.92 (1.3H, d, J = 10.3 Hz, H3'), 4.51 (1.4H, d, J = 8.4 Hz, H1'), 4.01 (4.9H, m), 3.83 (1.6H, app q, J = 8.4, 9.0, 10.3 Hz, H2'), 3.27-3.59 (17H, m), 3.13 (2.8H, bs), 3.04 (2.1H, bs), 2.61 (4H, m), 2.39 (2H, m), 2.16 (3.9H, bs), 2.06 (4.7H, s), 1.95 (5H, s), 1.85 (4.5H, s), 1.74 (4.4H, s) ppm. MALDI-TOF (pos) m/z 39300

16a: ^{1}H NMR (500MHz d^6 DMSO) δ 7.95 (1H, bs, amide NH's), 7.74 (0.9H, bs, amide NH's), 7.45 (2H, bs, $CH_2NHC(S)NHCH_2$), 5.21 (1.2H, s, H4), 5.11 (1.3H, d, J = 10.3 Hz, H3), 4.89 (1.3H, m, H2), 4.69 (1.1H, d, J = 8.1 Hz, H1), 4.12 (1.3H, d, J = 6.1 Hz, OCH_2CH_2O), 4.01 (2.7H, m), 3.76 (1.9H, m), 3.27-3.59 (11.8H, m), 3.13 (3H, bs), 3.04 (2.2H, bs), 2.61 (4.5H, m), 2.39 (1.8H, m), 2.16 (3.9H, bs), 2.08 (3.9H, s), 2.00 (8.4H, s), 1.87 (3.6H, s) ppm. MALDI-TOF (pos) m/z 122000.

16b: ^{1}H NMR (500MHz d^6 DMSO) δ 7.95 (1H, bs, amide NH's), 7.74-7.79 (1.3H, m, amide NH's, N*H'*Ac), 7.45 (1.9H, bs, $CH_2NHC(S)NHCH_2$), 5.21 (1H, s, H4), 5.17 (0.2H, s, H4'), 5.11 (1H, d, 10.3 Hz, H3), 4.89 (1H, t, J = 9.7 Hz, H2), 4.69 (1H, d, J = 7.6 Hz, H1), 4.51 (0.2H, d, J = 8.4 Hz, H1'), 4.12 (1H, m), 4.01 (2.6H, m), 3.83 (0.2H, app q, J = 8.4, 9.0, 10.3 Hz, H2'), 3.76 (1.5H, m), 3.27-3.59 (11.4H, m), 3.13 (2.9H, bs), 3.04 (2.3H, bs), 2.61 (4.8H, m), 2.16 (4.1H, bs), 2.08 (4.2H, s), 1.98 (7.6H, s), 1.87 (3.7H, s) 1.72 (0.8H, s) ppm. MALDI-TOF (pos) m/z 119500.

16c: ^{1}H NMR (500MHz *d*^{6} DMSO) δ 7.96 (1H, bs, amide NH's), 7.79 (0.6H, d, J = 9.0 Hz, N*H'*Ac), 7.74 (0.9H, bs, amide NH's), 7.46 (1.9H, bs, $CH_2NHC(S)NHCH_2$), 5.21 (2.1H, d, J = 3.3 Hz, H4), 5.17 (0.4H, s, H4'), 5.11 (2.1H, dd, J = 3.2, 10.3 Hz, H3), 4.92 (0.3H, d, J = 10.3 Hz, H3'), 4.89 (2.1H, t, J = 9.7 Hz, H2), 4.69 (1.9H, d, J = 7.6 Hz, H1), 4.51 (0.2H, d, J = 8.4 Hz, H1'), 4.12 (2.1H, m), 4.01 (5.4H, m), 3.83 (0.3H, app q, J = 8.4, 9.0, 10.3 Hz, H2'), 3.76 (5.4H, m), 3.27-3.59 (17.5H, m), 3.13 (3.2H, bs), 3.04 (2.3H, bs), 2.61 (4.8H, m), 2.39 (2.8H, m), 2.16 (4.4H, bs), 2.08 (7.8H, s), 2.06 (4.6H, s), 1.96 (5.5H, s), 1.85 (1.6H, s), 1.74 (1.4H, s) ppm. MALDI-TOF (pos) m/z 119000.

16d: ^{1}H NMR (500MHz *d*^{6} DMSO) δ 7.95 (1H, bs, amide NH's), 7.81 (0.7H, d, J = 9.0 (H2') Hz, N*H'*Ac), 7.74 (0.9H, bs, amide NH's), 7.46 (2H, bs, $CH_2NHC(S)NHCH_2$), 5.21 (0.7H, d, J = 3.2 Hz, H4), 5.17 (0.6H, s, H4'), 5.11 (0.7H, d, J = 10.3 Hz, H3), 4.92 (0.6H, d, J = 10.3 Hz, H3'), 4.89 (0.7H, t, J = 9.7 Hz, H2), 4.69 (0.6H, d, J = 7.6 Hz, H1), 4.51 (0.5H, d, J = 8.4 Hz, H1'), 4.12 (0.8H, m), 4.01 (3.2H, m), 3.83 (0.7H, app q, J = 8.4, 9.0, 10.3 Hz, H2'), 3.76 (1.7H, m), 3.27-3.59 (12H, m), 3.13 (3H, bs), 3.04 (2.1H, bs), 2.61 (5.4H, m), 2.39 (2H, m), 2.16 (4H, bs), 2.08 (3.7H, s), 2.00 (5.5H, s), 1.96 (1.7H, s), 1.87 (1.6H, s), 1.74 (1.4H, s) ppm. MALDI-TOF (pos) m/z 119000.

16e: ^{1}H NMR (500MHz *d*^{6} DMSO) δ 7.96 (1H, bs, amide NH's), 7.79 (0.8H, d, J = 9.0 Hz, N*H'*Ac), 7.74 (0.7H, bs, amide NH's), 7.46 (1.8H, m,

$CH_2NHC(S)NHCH_2$), 5.21 (0.5H, s, H4), 5.17 (0.6H, s, H4'), 5.11 (0.5H, d, J = 10.3 Hz, H3), 4.92 (0.6H, d, J = 10.3 Hz, H3'), 4.89 (0.5H, t, J = 9.7 Hz, H2), 4.69 (0.4H, d, J = 7.6 Hz, H1), 4.51 (0.6H, d, J = 8.4 Hz, H1'), 4.12 (0.6H, m), 4.01 (3.1H, m), 3.83 (0.8H, app q, J = 8.4, 9.0, 10.3 Hz, H2'), 3.76 (1.5H, m), 3.27-3.59 (10H, m), 3.13 (2.8H, bs), 3.04 (1.7H, bs), 2.61 (4H, m), 2.39 (2.2H, m), 2.16 (3.5H, bs), 2.07 (3.5H, s), 1.98 (0.7H, s), 1.96 (4.4H, s), 1.87 (1.2H, s), 1.85 (2H, s), 1.74 (1.9H, s) ppm. MALDI-TOF (pos) m/z 121500.

16f: ^{1}H NMR (500MHz *d*^{6} DMSO) δ 7.95 (1H, bs, amide NH's), 7.79 (0.8H, d, J = 9.0 Hz, N*H'*Ac), 7.74 (0.7H, bs, amide NH's), 7.46 (1.6H, bs, $CH_2NHC(S)NHCH_2$), 5.21 (0.2H, d, J = 3.2 Hz, H4), 5.17 (0.7H, s, H4'), 5.11 (0.3H, m, Hz, H3), 4.92 (0.7H, d, J = 10.3 Hz, H3'), 4.89 (0.2H, t, J = 9.7 Hz, H2), 4.69 (0.2H, d, J = 7.6 Hz, H1), 4.51 (0.7H, d, J = 8.4 Hz, H1'), 4.12 (0.3H, m), 4.01 (2.9H, m), 3.83 (0.9H, app q, J = 8.4, 9.0, 10.3 Hz, H2'), 3.7 (1.2H, m), 3.27-3.59 (8.6H, m), 3.04-3.13 (2.8H, m), 2.61 (3.2H, m), 2.39 (1.4H, m), 2.16 (2.9H, bs), 2.07 (3.2H, s), 1.95 (3.9H, s), 1.85 (2.9H, s), 1.74 (2.2H, s) ppm. MALDI-TOF (pos) m/z 121500.

16g: ^{1}H NMR (500MHz *d*^{6} DMSO) δ 7.96 (1H, bs, amide NH's), 7.79 (1.1H, d, J = 9.0 Hz, N*H'*Ac), 7.74 (0.8H, bs, amide NH's), 7.46 (2.8H, m, $CH_2NHC(S)NHCH_2$), 5.17 (1.1H, s, H4'), 4.92 (1.1H, d, J = 10.3 Hz, H3'), 4.51 (1.2H, d, J = 8.4 Hz, H1'), 4.01 (4.2H, m), 3.83 (1.2H, app q, J = 8.4, 9.0, 10.3

Hz, H2'), 3.27-3.59 (12.7H, m), 3.04-3.13 (4.2H, m), 2.61 (3.9H, m), 2.16 (3.1H, bs), 2.06 (4.4H, s), 1.95 (4.1H, s), 1.85 (3.7H, s), 1.74 (3.8H, s) ppm. MALDI-TOF (pos) m/z 125000

Deacetylated:

General procedure for deacylation of dendrimers 14-16. To the lyophilized solid product of compounds 14-16 1 mL of 1:1 water:methanol was added, at which point the dendrimer would become a white precipitate solid. To this mixture was added 0.2 equivalents of NaOMe (0.8 M in MeOH) for each peripheral carbohydrate, and let stir for 3 h. If, at this time, the mixture had not become a clear solution a further 0.2 equivalents of NaOMe (0.8 M in MeOH) was added and this step was repeated until the mixture became a clear and colorless solution. $HCl_{(aq)}$ (0.1 M) was then added slowly until the pH was approximately 7. This neutralized solution was placed in a dialysis membrane (Mw cutoff 3500) and dialyzed in 1 L of DI water for 8 h, the water was then changed and let stand for a further 8 h and repeated once more. The remaining liquid in the membrane was frozen and lyophilized to give a white fluffy solid.

14a: ^{1}H NMR (500MHz d^6 DMSO) δ 7.99 (bs, 1H), 7.80 (bs, 1H), 7.50 (bs, 2.1H), 4.96 (bs, 1.0H), 4.73 (m, 1.0H), 4.61 (bs, 1.2H), 4.44 (bs, 1.2H), 4.10 (d, J = 5.2Hz, 1.2H), 3.84 (m, 1.5H), 3.63 (m, 2.4H), 3.38-3.60 (m, 30H), 3.17 (bs, 3.2H), 3.08 (bs, 3.2H), 2.66 (bs, 4.6H), 2.42 (bs, 2.4H), 2.20 (bs, 4.6H) ppm. MALDI-TOF (pos) m/z 15200.

14b: ^{1}H NMR (500MHz *d*^{6} DMSO) δ 8.00 (bs, 1H), 7.81 (bs, 1H), 7.67 (d, J = 8.6 Hz, 0.2H), 7.50 (bs, 2.1H), 4.95 (bs, 0.7H), 4.60-4.70 (m, 1.5H), 4.43 (bs, 0.8H), 4.27 (d, J = 8.3 Hz, 0.2H), 4.11 (d, J = 5.2Hz, 0.8H), 3.84 (m, 1.0H), 3.38-3.65 (m, 27H), 3.17 (bs, 2.8H), 3.08 (bs, 2.6H), 2.66 (bs, 4.0H), 2.42 (bs, 2.3H), 2.20 (bs, 4.3H), 1.80 (m, 0.9H) ppm. MALDI-TOF (pos) m/z 15000.

14c: ^{1}H NMR (500MHz *d*^{6} DMSO) δ 8.00 (bs, 1H), 7.80 (bs, 0.9H), 7.67 (d, J = 8.6 Hz, 0.3H), 7.50 (m, 1.5H), 4.95 (bs, 0.6H), 4.50-4.75 (m, 2.1H), 4.43 (bs, 0.7H), 4.27 (d, J = 8.3 Hz, 0.4H), 4.11 (d, J = 5.2Hz, 0.7H), 3.84 (m, 0.9H), 3.38-3.65 (m, 24H), 3.17 (bs, 2.3H), 3.08 (bs, 1.9H), 2.66 (bs, 3.4H), 2.42 (bs, 1.8H), 2.20 (bs, 3.7H), 1.80 (m, 1.0H) ppm. MALDI-TOF (pos) m/z 15100.

14d: ^{1}H NMR (500MHz *d*^{6} DMSO) δ 8.01 (bs, 1H), 7.83 (bs, 0.9H), 7.67 (d, J = 8.6 Hz, 0.5H), 7.59 (bs, 0.5H), 7.50 (bs, 1.2H), 4.95 (bs, 0.5H), 4.60-4.70 (m, 2.2H), 4.43 (bs, 0.7H), 4.27 (d, J = 8.3 Hz, 0.7H), 4.11 (d, J = 5.2Hz, 0.6H), 3.84 (m, 1.0H), 3.38-3.65 (m, 30H), 3.17 (bs, 3.1H), 3.08 (bs, 2.1H), 2.66 (bs, 4.0H), 2.42 (bs, 1.8H), 2.20 (bs, 3.9H), 1.80 (m, 1.6H) ppm. MALDI-TOF (pos) m/z 14900.

14e: ^{1}H NMR (500MHz *d*^{6} DMSO) δ 8.02 (bs, 1H), 7.83 (bs, 0.8H), 7.67 (d, J = 8.6 Hz, 0.7H), 7.59 (bs, 0.6H), 7.50 (m, 1.1H), 4.95 (bs, 0.4H), 4.60-4.70 (m, 2.4H), 4.43 (bs, 0.5H), 4.27 (d, J = 8.3 Hz, 0.9H), 4.11 (d, J = 5.2Hz, 0.5H), 3.38-

3.65 (m, 30H), 3.17 (bs, 2.9H), 3.08 (bs, 2.0H), 2.66 (bs, 3.9H), 2.42 (bs, 1.9H), 2.20 (bs, 3.9H), 1.80 (m, 2.0H) ppm. MALDI-TOF (pos) m/z 15700.

14f: ^{1}H NMR (500MHz *d*^{6} DMSO) δ 8.01 (bs, 1H), 7.82 (bs, 0.9H), 7.67 (d, J = 8.6 Hz, 0.9H), 7.60 (bs, 0.8H), 7.50 (bs, 0.7H), 4.95 (bs, 0.2H), 4.60-4.70 (m, 2.6H), 4.43 (bs, 0.2H), 4.27 (d, J = 8.3 Hz, 1.0H), 4.11 (d, J = 5.2Hz, 0.3H), 3.38-3.65 (m, 23H), 3.17 (bs, 2.6H), 3.08 (bs, 2.61), 2.66 (bs, 3.9H), 2.42 (bs, 1.7H), 2.20 (bs, 3.7H), 1.80 (m, 2.6H) ppm. MALDI-TOF (pos) m/z 15800.

14g: ^{1}H NMR (500MHz *d*^{6} DMSO) δ 8.01 (bs, 1H), 7.82 (bs, 0.9H), 7.68 (d, J = 8.6 Hz, 1.0H),7.59 (bs, 0.9H), 7.50 (m, 1.0H), 4.60-4.70 (m, 2.8H), 4.27 (d, J = 8.3 Hz, 1.1H), 3.77 (m, 3.3H), 3.38-3.65 (m, 30H), 3.17 (bs, 3.3H), 3.10 (bs, 1.9H), 2.66 (bs, 4.1H), 2.42 (bs, 1.9H), 2.20 (bs, 3.8H), 1.80 (m, 3.0H) ppm. MALDI-TOF (pos) m/z 16400.

15a: ^{1}H NMR (500MHz *d*^{6} DMSO) δ 7.97 (bs, 1H), 7.78 (bs, 0.9H), 7.44 (bs, 2.0H), 4.97 (bs, 0.8H), 4.75 (m, 0.9H), 4.65 (bs, 1.2H), 4.44 (bs, 1.2H), 4.08 (m, 1.2H), 3.80 (m, 1.5H), 3.38-3.65 (m, 30H), 3.13 (bs, 2.9H), 3.05 (bs, 2.3H), 2.62 (bs, 4.3H), 2.46 (bs, 2.1H), 2.17 (bs, 3.9H) ppm. MALDI-TOF (pos) m/z 31500.

15b: ^{1}H NMR (500MHz *d*^{6} DMSO) δ 8.01 (bs, 1H), 7.81 (bs, 1H), 7.67 (m, 0.2H), 7.50 (bs, 1.8H), 4.95 (bs, 0.6H), 4.60-4.70 (m, 2.0H), 4.43 (bs, 0.9H), 4.27 (m,

0.2H), 4.11 (m, 0.8H), 3.84 (m, 1.0H), 3.38-3.65 (m, 30H), 3.17 (bs, 2.5H), 3.08 (bs, 2.6H), 2.66 (bs, 3.9H), 2.42 (bs, 2.1H), 2.20 (bs, 4.1H), 1.80 (m, 0.7H) ppm. 31200.

15c: ^{1}H NMR (500MHz *d*^{6} DMSO) δ 8.03 (bs, 1H), 7.85 (bs, 0.9H), 7.73 (d, J = 8.6 Hz, 0.4H), 7.50 (m, 1.6H), 4.95 (bs, 0.4H), 4.50-4.90 (m, 2.3H), 4.52 (bs, 0.6H), 4.27 (d, J = 8.3 Hz, 0.5H), 4.12 (s, 0.9H), 3.38-3.70 (m, 30H), 3.17 (bs, 2.7H), 3.08 (bs, 2.1H), 2.66 (bs, 3.8H), 2.42 (bs, 1.8H), 2.20 (bs, 3.9H), 1.80 (m, 1.2H) ppm. MALDI-TOF (pos) m/z 31700.

15d: ^{1}H NMR (500MHz *d*^{6} DMSO) δ 8.02 (bs, 1H), 7.83 (bs, 0.9H), 7.71 (m, 0.5H), 7.58 (bs, 0.6H), 7.50 (bs, 1.0H), 4.95 (bs, 0.3H), 4.60-4.70 (m, 1.7H), 4.58 (bs, 0.5H), 4.48 (bs, 0.5H), 4.27 (d, J = 8.3 Hz, 0.5H), 4.11 (m, 0.4H), 3.84 (m, 1.6H), 3.38-3.65 (m, 30H), 3.17 (bs, 2.4H), 3.08 (bs, 2.1H), 2.66 (bs, 3.8H), 2.42 (bs, 1.7H), 2.20 (bs, 4.0H), 1.80 (m, 1.8H) ppm. MALDI-TOF (pos) m/z 33000.

15e: ^{1}H NMR (500MHz *d*^{6} DMSO) δ 8.02 (bs, 1H), 7.83 (bs, 0.8H), 7.67 (d, J = 8.6 Hz, 0.8H), 7.58 (bs, 0.7H), 7.43 (m, 0.9H), 4.95 (bs, 0.1H), 4.69 (bs, 1.7H),4.58 (bs, 0.8H), 4.43 (bs, 0.2H), 4.27 (d, J = 8.3 Hz, 0.8H), 4.11 (m, 0.1H), 3.38-3.65 (m, 30H), 3.17 (bs, 2.5H), 3.08 (bs, 1.8H), 2.66 (bs, 4.1H), 2.42 (bs, 1.8H), 2.21 (bs, 3.8H), 1.80 (m, 2.2H) ppm. MALDI-TOF (pos) m/z 34300.

15f: ^{1}H NMR (500MHz *d*^{6} DMSO) δ 8.02 (bs, 1H), 7.83 (bs, 0.8H), 7.67 (d, J = 8.6 Hz, 0.9H), 7.58 (bs, 0.8H), 7.44 (bs, 0.8H), 4.68 (m, 1.5H), 4.58 (1.0H), 4.27 (d, J = 8.3 Hz, 0.9H), 3.38-3.65 (m, 23H), 3.17 (bs, 2.4H), 3.08 (bs, 1.9H), 2.66 (bs, 3.8H), 2.42 (bs, 1.6H), 2.20 (bs, 3.8H), 1.80 (m, 2.8H) ppm. MALDI-TOF (pos) m/z 34300.

15g: ^{1}H NMR (500MHz *d*^{6} DMSO) δ 8.02 (bs, 1H), 7.83 (bs, 0.8H), 7.69 (d, J = 8.6 Hz, 0.8H),7.58 (bs, 0.8H), 7.43 (m, 0.9H), 4.67 (m, 1.6H), 4.58 (bs, 0.8H), 4.27 (d, J = 8.3 Hz, 0.8H), 3.38-3.65 (m, 30H), 3.10-3.17 (m, 4.6H), 2.66 (bs, 3.7H), 2.42 (bs, 1.6H), 2.20 (bs, 3.6H), 1.80 (m, 2.4H) ppm. MALDI-TOF (pos) m/z 33300.

16a: ^{1}H NMR (500MHz *d*^{6} DMSO) δ 8.00 (bs, 1H), 7.80 (bs, 0.9H), 7.48 (bs, 1.6H), 4.99 (bs, 0.7H), 4.80 (m, 0.7H), 4.63 (bs, 0.9H), 4.48 (bs, 0.8H), 4.12 (s, 0.8H), 3.80 (m, 0.9H), 3.38-3.65 (m, 14H), 3.18 (bs, 2.4H), 3.09 (bs, 1.7H), 2.62 (bs, 3.3H), 2.46 (bs, 1.5H), 2.17 (bs, 4.0H) ppm. MALDI-TOF (pos) m/z 101000.

16b: ^{1}H NMR (500MHz *d*^{6} DMSO) δ 8.01 (bs, 1H), 7.83 (bs, 0.7H), 7.67 (m, 0.2H), 7.48 (bs, 1.5H), 5.04 (bs, 0.7H), 4.60-4.70 (m, 1.7H), 4.43 (bs, 0.8H), 4.28 (m, 0.2H), 4.11 (s, 1.0H), 3.84 (m, 2.0H), 3.38-3.65 (m, 30H), 3.17 (bs, 2.1H), 3.08 (bs, 1.7H), 2.65 (bs, 3.2H), 2.42 (bs, 1.4H), 2.20 (bs, 3.5H), 1.80 (m, 0.6H) ppm. MALDI-TOF (pos) m/z 100000.

16c: ^{1}H NMR (500MHz *d*^{6} DMSO) δ 8.03 (bs, 1H), 7.85 (bs, 0.7H), 7.73 (s, 0.3H), 7.47 (m, 1.4H), 5.07 (bs, 0.5H), 4.68-4.90 (m, 1.7H), 4.63 (bs, 0.4H), 4.54 (bs, 0.6H), 4.27 (s, 0.4H), 4.12 (s, 0.9H), 3.38-3.70 (m, 30H), 3.17 (bs, 2.2H), 3.08 (bs, 1.6H), 2.66 (bs, 2.8H), 2.20 (bs, 3.4H), 1.80 (m, 1.2H) ppm. MALDI-TOF (pos) m/z 101000

16d: ^{1}H NMR (500MHz *d*^{6} DMSO) δ 8.02 (bs, 1H), 7.84 (bs, 0.7H), 7.72 (s, 0.5H), 7.58 (bs, 0.5H), 7.44 (bs, 0.9H), 5.04 (bs, 0.3H), 4.72 (m, 1.7H), 4.61 (bs, 0.8H), 4.28 (s, 0.6H), 4.13 (m, 0.4H), 3.38-3.80 (m, 30H), 3.10-3.17 (m, 3.5H), 2.66 (bs, 3.0H), 2.42 (bs, 1.0H), 2.20 (bs, 3.4H), 1.80 (m, 1.5H) ppm. MALDI-TOF (pos) m/z 101500

16e: ^{1}H NMR (500MHz *d*^{6} DMSO) δ 8.02 (bs, 1H), 7.84 (bs, 0.8H), 7.72 (s, 0.4H), 7.57 (bs, 0.5H), 7.48 (m, 0.9H), 5.05 (bs, 0.4H), 4.69 (bs, 1.6H),4.58 (bs, 0.5H), 4.43 (bs, 0.2H), 4.27 (s, 0.5H), 4.13 (m, 0.5H), 3.38-3.65 (m, 30H), 3.10-3.17 (bs, 3.6H), 2.66 (bs, 3.0H), 2.42 (bs, 1.3H), 2.21 (bs, 3.3H), 1.82 (m, 1.4H) ppm. MALDI-TOF (pos) m/z 102000

16f: ^{1}H NMR (500MHz *d*^{6} DMSO) δ 8.02 (bs, 1H), 7.82 (bs, 0.7H), 7.67 (s, 0.7H), 7.58 (bs, 0.7H), 7.44 (bs, 0.8H), 5.05 (bs, 0.2H), 4.68 (m, 1.7H), 4.60 (0.7H), 4.28 (s, 0.7H), 3.38-3.65 (m, 23H), 3.10-3.17 (m, 3.6H), 2.66 (bs, 2.9H), 2.42 (bs, 0.8H), 2.21 (bs, 3.2H), 1.80 (m, 1.8H) ppm. MALDI-TOF (pos) m/z 106500

16g: ^{1}H NMR (500MHz *d*^{6} DMSO) δ 8.03 (bs, 1H), 7.84 (bs, 0.7H), 7.72 (s, 0.8H), 7.58 (bs, 0.7H), 7.43 (m, 0.9H), 4.73 (m, 1.6H), 4.62 (bs, 0.9H), 4.27 (s, 0.8H), 3.38-3.65 (m, 30H), 3.10-3.17 (m, 3.8H), 2.66 (bs, 3.0H), 2.42 (bs, 1.2H), 2.21 (bs, 3.5H), 1.80 (m, 2.2H) ppm. MALDI-TOF (pos) m/z 107500.

Table 15 MALDI-TOF data for heterogeneously functionalized dendrimers 14-16 a-g.

Compound number	M_w after Galactose addition	M_w after Galactosamine addition	M_w after deacylation
14a	19500	6800	15200
14b	19100	8950	15000
14c	19000	11700	15100
14d	18900	13900	14900
14e	19300	15700	15700
14f	19000	18200	15800
14g	n/a	20000	16400
15a	40900	13500	31500
15b	40000	18200	31200
15c	39700	23900	31700
15d	40200	28300	33000
15e	39700	33500	34300
15f	40500	37200	34300
15g	n/a	39300	33300
16a	122000	51000	101000
16b	119500	66500	100000
16c	119000	77500	101000
16d	119000	92000	101500
16e	121500	101000	102000
16f	121500	117000	106500
16g	n/a	125000	107500

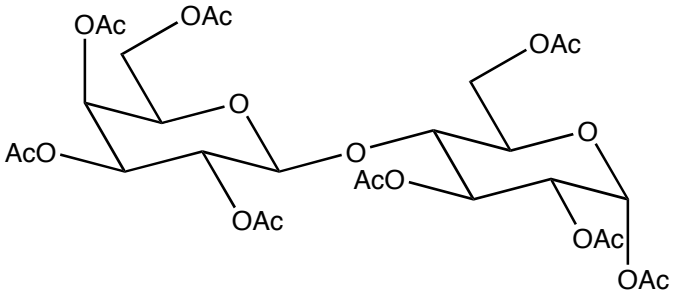

2,3,4,6-tetra-O-acetyl-β-galactopyranose [1→4] 1,2,3,6-tetra-O-acetyl-β-glucopyranose. 1.0 g (2.76 mmol) of lactose was added to acetic anhydride (7.9 mL, 30 equiv.), and the solution was cooled to 0 °C. $In(OTf)_3$ (79.5 mg, 141 μmol, 0.05 equiv.) was added, and the reaction was allowed to warm to room temperature while stirring for 1 h. EtOAc (100 mL) and 10% aqueous Na_2CO_3 solution (150 mL) were added, and the mixture was stirred for 1 h. Isolation of the organic layer, washing with water (3 x 50 mL) and brine (3 x 50 mL), and dried over $MgSO_4$ yielded 1.88 g of product (97% yield). ^1H NMR ($CDCl_3$, 300 MHz, ppm) δ ^1H NMR ($CDCl_3$, 300 MHz, ppm) δ 6.23 (1H, d, J = 3.1 Hz, H1), 5.45 (1H, app t, J = 9.6 Hz, H3), 5.34 (1H, d, J = 3.0 Hz, H4'), 5.12 (1H, dd, J = 8.1, 10.1 Hz, H2'), 4.97 (2H, m), 4.46 (2H, m), 4.09 (5H, m), 3.83 (2H, m), 2.16 (3H, s), 2.14 (3H, s), 2.11 (3H, s), 2.04 (9H, m), 1.99 (3H, s), 1.95 (3H, s). As reported[35]

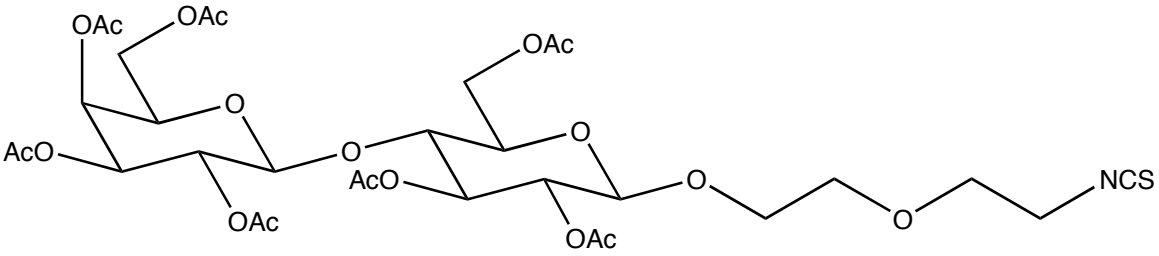

13: 1-O-(5-isothiocyanato-3-oxopentyl)- 2,3,4,6-tetra-O-acetyl-β-galactopyranose [1→4] 2,3,6-tetra-O-acetyl-β-glucopyranose. 4.4 g of 2,3,4,6-tetra-O-acetyl-β-galactopyranose [1→4] 1,2,3,6-tetra-O-acetyl-β-glucopyranose. (6.4 mmol) was dissolved in dry DMF (20 mL) and 0.77 g of hydrazine acetate (8.4 mmol) was added and the reaction mixture was heated to 55^{o}C for 1 h. The mixture was then dissolved in 20 mL methylene chloride and washed with brine (2 x 10 mL) and water (2 x 10 mL), dried with $MgSO_4$, filtered and solvent removed en vacuo. The product was added to 20 mL methylene chloride and 2.3 mL trichloroacetonitrile (3.34 g, 23.1 mmol) and cooled in an ice bath, 60 mg of DBU (0.32 mmol) was added dropwise and the reaction was stirred for 3 h. The reaction mixture was dissolved in 30 mL CH_2Cl_2,, washed with brine (2 x 10mL) and water (2 x 10mL), dried with $MgSO_4$, filtered and solvent removed in vacuo. The product was taken up in 50 mL CH_2Cl_2 with 0.6 g of 6 (4 mmol) and 4 A molecular sieves and cooled to 0 ^{o}C. 0.6 g BF_3OEt_2 (4 mmol) was added over 30 min, let stir and warmed to RT over 2 h. Solvent was removed and the resulting residue was taken up in 50 mL ethyl acetate, washed with sat. aqueous $NaHCO_3$ solution (2 x 20 mL), brine (2 x 20 mL), and water (1 x 20 mL), dried over $MgSO_4$, filtered and solvent removed en vacuo. The oily reside was then purified via

column chromatography, with a 60:40 ethyl acetate:hexanes eluant, followed by a 20:1 ethyl acetate:MeOH eluant to yield 2.6 g of pure material. ^{1}H NMR (300 MHz $CDCl_3$) δ 5.33 (1H, d, J = 3.1 Hz, H4'), 5.20 (1H, app t, J = 9.3 Hz, H3), 5.09 (1H, dd, J = 8.1, 10.1 Hz, H2'), 4.93 (2H, m, H2, H3') 4.50 (3H, m, H1, H1', H6), 4.06 (4H, m,), 3.89 (6H, m), 3.78 (3H, m), 3.63 (6H, m), 2.13 (3H, s), 2.10 (3H, s), 2.04 (3H, s), 2.02 (9H, m), 1.95 (3H, s) ppm. As reported.[35]

Galactose:Lactose Dendrimers

Acetylated:

Representative procedure for the synthesis of heterogeneously functionalized PAMAM-based thiourea-linked 1-O-(5-isothiocyanato-3-oxopentyl)-2,3,6,2',3',4',6'-per-O-acetyl -β-D-lactose, 1-O-(5-isothiocyanato-3-oxopentyl)-2,3,4,6-tetra-O-acetyl -β-D-galactopyranoside. (17-19). An aqueous solution of amine terminated Starburst G(4)-PAMAM dendrimer (2.478 g of a 17% w/w solution in water, 421.2 mg, 31.2 μmol) was lyophilized to leave a foamy residue. 7.02 mL of DMSO was added to this residue to give a 60 mg/mL solution. 0.35 mL of a 300 mM solution of 1-O-(5-isothiocyanato-3-oxopentyl)- 2,3,6,2',3',4',6'-per-O-acetyl -β-D-lactopyranoside (13, 85 μmol, 40.2 mg) in DMSO was added to 0.5 mL of a 60 mg/mL G(3) PAMAM dendrimer (30 mg, 4.40 μmol) solution. The reaction was stirred for 8 h at which point a 75 μL aliquot was removed for MALDI-TOF analysis. After MALDI-TOF analysis indicated reaction completion, 0.31 mL of a 300 mM solution of 1-O-(5-isothiocyanato-3-oxopentyl)- 2,3,4,6-

tetra-O-acetyl -β-D-galactopyranoside (11, 73 μmol, 35 mg) was added. The solution was then stirred for 8 h. At this time a 75 μL aliquot was removed for MALDI-TOF and NMR analysis.

17a: ^{1}H NMR (500MHz *d*^{6} DMSO) δ 7.97 (1H, bs), 7.78 (0.9H, bs), 7.47 (1.5H, bs), 5.17 (1.3H, s), 5.11 (2.4H, m), 4.79 (1.5H, app t, J = 9.0 Hz), 4.69 (2.2H, m), 4.62 (1.1H, J = 9.0Hz), 4.25 (1.2H, d, J = 11.3Hz), 4.16 (1.4H, m), 3.97 (4.3H, m), 3.74 (3.7H, m), 3.56 (2.5H, bs), 3.12 (2.7H, bs), 3.04 (2.0H, bs), 2.64 (5.7H, bs), 2.16 (4.4H, bs), 2.04 (4.3H, s), 2.02 (4.8H, s), 1.95 (8.9H, s), 1.92 (7.3H, s), 1.84 (3.9H, s) ppm. . MALDI-TOF (pos) m/z 24400.

17b: ^{1}H NMR (500MHz *d*^{6} DMSO) δ 7.95 (1H, bs), 7.75 (1.1H, bs), 7.47 (2H, bs), 5.21 (0.4H, s), 5.17 (1.3H, s), 5.12 (2.6H, m), 4.89 (0.4H, m), 4.79 (1.5H, app t, J = 9.0 Hz), 4.69 (2.4H, m), 4.62 (1.1H, J = 9.0Hz), 4.25 (1.2H, d, J = 11.3Hz), 4.16 (1.7H, m), 3.98 (4.8H, m), 3.74 (4.1H, m), 3.40-3.56 (16H, m), 3.13 (3.2H, bs), 3.04 (2.3H, bs), 2.64 (5.9H, bs), 2.16 (4.2H, bs), 2.07 (1.2H, s), 2.05 (3.6H, s), 2.03 (3.1H, s), 1.96 (10.2H, s), 1.92 (6.2H, s), 1.87 (1.2H, s), 1.84 (3.9H, s) ppm. . MALDI-TOF (pos) m/z 24600.

17c: ^{1}H NMR (500MHz *d*^{6} DMSO) δ 7.96 (1H, bs), 7.75 (1.1H, bs), 7.47 (1.9H, bs), 5.21 (0.6H, s), 5.17 (0.9H, s), 5.12 (1.8H, m), 4.89 (0.6H, app t, J = 9.1Hz), 4.79 (0.9H, app t, J = 9.0 Hz), 4.69 (1.8H, m), 4.62 (0.6H, J = 9.0Hz), 4.25 (0.7H,

d, J = 11.3Hz), 4.17 (1.5H, m), 3.98 (3.8H, m), 3.74 (3.2H, m), 3.40-3.56 (20H, m), 3.13 (2.7H, bs), 3.04 (2.3H, bs), 2.64 (4.4H, bs), 2.37 (2.9H, bs), 2.16 (4.1H, bs), 2.07 (1.9H, s), 2.05 (2.1H, s), 2.03 (2.5H, s), 1.95 (8.4H, s), 1.92 (4.6H, s), 1.87 (1.5H, s), 1.85 (2.3H, s) ppm. . MALDI-TOF (pos) m/z 22200.

17d: ^{1}H NMR (500MHz *d*^{6} DMSO) δ 7.96 (1H, bs), 7.75 (0.9H, bs), 7.47 (1.7H, bs), 5.21 (0.7H, d, J = 3.1Hz), 5.17 (0.5H, s), 5.12 (1.5H, m), 4.89 (0.7H, app t, J = 9.1Hz), 4.79 (0.5H, app t, J = 9.0 Hz), 4.69 (1.3H, m), 4.62 (0.4H, J = 9.0Hz), 4.25 (0.4H, d, J = 11.3Hz), 4.17 (1.2H, m), 3.98 (3H, m), 3.74 (2.3H, m), 3.40-3.56 (13H, m), 3.13 (2.5H, bs), 3.04 (1.8H, bs), 2.64 (3.8H, bs), 2.37 (2.1H, bs), 2.16 (3.5H, bs), 2.07 (2.2H, s), 2.05 (1.2H, s), 2.03 (2.3H, s), 1.95 (4.9H, s), 1.92 (2.2H, s), 1.87 (1.6H, s), 1.85 (1.3H, s) ppm. MALDI-TOF (pos) m/z 21800.

17e: ^{1}H NMR (500MHz *d*^{6} DMSO) δ 7.96 (1H, bs), 7.75 (0.9H, bs), 7.47 (1.7H, bs), 5.21 (0.9H, s), 5.17 (0.2H, s), 5.12 (1.3H, m), 4.89 (0.9H, app t, J = 9.1Hz), 4.79 (0.2H, app t, J = 9.0 Hz), 4.69 (1.1H, m), 4.62 (0.2H, J = 9.0Hz), 4.25 (0.2H, d, J = 11.3Hz), 4.17 (1.2H, m), 3.98 (2.6H, m), 3.74 (1.9H, m), 3.40-3.56 (13H, m), 3.13 (2.7H, bs), 3.04 (1.7H, bs), 2.64 (5H, bs), 2.37 (3H, bs), 2.16 (3.6H, bs), 2.07 (2.7H, s), 2.05 (0.7H, s), 2.03 (0.6H, s), 1.95 (6.9H, s), 1.92 (1.4H, s), 1.87 (3H, s) ppm. MALDI-TOF (pos) m/z 20500.

18a: ^{1}H NMR (500MHz *d*^{6} DMSO) δ 7.95 (1H, bs), 7.78 (0.8H, bs), 7.47 (1.9H, bs), 5.17 (1.7H, s), 5.11 (2.8H, m), 4.79 (1.7H, app t, J = 9.0 Hz), 4.69 (2.5H, m), 4.62 (1.2H, J = 9.0Hz), 4.25 (1.4H, d, J = 10.8Hz), 4.16 (1.6H, m), 3.97 (4.9H, m), 3.74 (4.4H, m), 3.40-3.56 (10H, m), 3.12 (2.7H, bs), 3.04 (1.4H, bs), 2.64 (4.9H, bs), 2.16 (3.8H, bs), 2.04 (5.2H, s), 2.02 (4.7H, s), 1.95 (10.5H, s), 1.92 (7.4H, s), 1.84 (4.6H, s) ppm. . MALDI-TOF (pos) m/z 54500.

18b: ^{1}H NMR (500MHz *d*^{6} DMSO) δ 7.95 (1H, bs), 7.75 (1H, bs), 7.47 (1.7H, bs), 5.21 (0.3H, s), 5.17 (1.1H, s), 5.12 (2.1H, m), 4.89 (0.3H, m), 4.79 (1.1H, app t, J = 9.0 Hz), 4.69 (1.9H, m), 4.62 (0.8H, J = 9.0Hz), 4.25 (1H, d, J = 11.3Hz), 4.16 (1.3H, m), 3.98 (3.8H, m), 3.74 (3.2H, m), 3.40-3.56 (10H, m), 3.13 (2.7H, bs), 3.04 (2.1H, bs), 2.64 (5.7H, bs), 2.16 (3.9H, bs), 2.07 (1.1H, s), 2.05 (2.7H, s), 2.03 (3H, s), 1.96 (8.2H, s), 1.92 (4.5H, s), 1.87 (1H, s), 1.84 (2.5H, s) ppm. . MALDI-TOF (pos) m/z 48000.

18c: ^{1}H NMR (500MHz *d*^{6} DMSO) δ 7.96 (1H, bs), 7.75 (1H, bs), 7.46 (1.7H, bs), 5.21 (0.5H, s), 5.17 (0.8H, s), 5.12 (1.8H, m), 4.89 (0.5H, app t, J = 9.1Hz), 4.79 (0.8H, app t, J = 9.0 Hz), 4.69 (1.6H, m), 4.62 (0.6H, J = 9.0Hz), 4.25 (0.7H, d, J = 11.3Hz), 4.17 (1.3H, m), 3.98 (3.5H, m), 3.74 (2.8H, m), 3.40-3.56 (10H, m), 3.13 (2.5H, bs), 3.04 (2H, bs), 2.64 (4.9H, bs), 2.37 (2.3H, bs), 2.16 (4H, bs), 2.07 (1.6H, s), 2.05 (2.2H, s), 2.03 (1.8H, s), 1.95 (7.8H, s), 1.92 (3.5H, s), 1.87 (1.4H, s), 1.85 (1.8H, s) ppm. . MALDI-TOF (pos) m/z 45500.

18d: ^{1}H NMR (500MHz *d*^{6} DMSO) δ 7.96 (1H, bs), 7.75 (0.9H, bs), 7.47 (1.9H, bs), 5.21 (0.8H, d, J = 3.1Hz), 5.17 (0.6H, s), 5.12 (1.7H, m), 4.89 (0.7H, app t, J = 9.1Hz), 4.79 (0.5H, app t, J = 9.0 Hz), 4.69 (1.5H, m), 4.62 (0.4H, J = 9.0Hz), 4.25 (0.4H, d, J = 11.3Hz), 4.17 (1.4H, m), 3.98 (3.2H, m), 3.74 (2.6H, m), 3.40-3.56 (10H, m), 3.13 (2.6H, bs), 3.04 (2.1H, bs), 2.64 (6.2H, bs), 2.37 (3H, bs), 2.16 (3.9H, bs), 2.07 (2.2H, s), 2.05 (1.4H, s), 2.03 (1.2H, s), 1.95 (8.3H, s), 1.92 (2.5H, s), 1.87 (1.9H, s), 1.85 (1.5H, s) ppm. MALDI-TOF (pos) m/z 41500.

18e: ^{1}H NMR (500MHz *d*^{6} DMSO) δ 7.96 (1H, bs), 7.75 (0.9H, bs), 7.47 (2H, bs), 5.21 (1H, s), 5.17 (0.3H, s), 5.12 (1.5H, m), 4.89 (1H, app t, J = 9.1Hz), 4.79 (0.2H, app t, J = 9.0 Hz), 4.69 (1H, m), 4.62 (0.2H, J = 9.0Hz), 4.25 (0.3H, d, J = 11.3Hz), 4.17 (1H, m), 3.98 (2.9H, m), 3.74 (2.1H, m), 3.40-3.56 (12H, m), 3.13 (2.7H, bs), 3.04 (1.9H, bs), 2.64 (5.2H, bs), 2.37 (2.8H, bs), 2.16 (4.3H, bs), 2.07 (2.8H, s), 2.05 (1H, s), 2.03 (0.9H, s), 1.95 (8.8H, s), 1.92 (1.5H, s), 1.87 (2.5H, s) ppm. MALDI-TOF (pos) m/z 41000.

19a: ^{1}H NMR (500MHz *d*^{6} DMSO) δ 7.96 (1H, bs), 7.76 (0.7H, bs), 7.47 (1.5H, bs), 5.17 (1H, s), 5.11 (1.8H, m), 4.79 (1.2H, m), 4.69 (1.5H, m), 4.62 (0.9H, m), 4.25 (0.9H, m), 4.16 (1H, m), 3.97 (3.2H, m), 3.74 (2.9H, m), 3.56 (1.6H, bs), 3.04-3.12 (3.8H, m), 2.64 (2.4H, bs), 2.16 (3.3H, bs), 2.04 (3H, s), 2.02 (3.4H, s), 1.95 (7.1H, s), 1.92 (4.9H, s), 1.84 (3.1H, s) ppm. . MALDI-TOF (pos) m/z 147000.

19b: ^{1}H NMR (500MHz d^{6} DMSO) δ 7.95 (1H, bs), 7.75 (0.8H, bs), 7.47 (1.6H, bs), 5.21 (0.3H, s), 5.17 (0.8H, s), 5.12 (1.8H, m), 4.89 (0.2H, m), 4.79 (1.2H, m), 4.69 (1.6H, m), 4.62 (0.8H, m), 4.25 (0.8H, m), 4.16 (1.2H, m), 3.98 (3.4H, m), 3.74 (2.8H, m), 3.40-3.56 (15H, m), 3.13 (2.6H, bs), 3.04 (1.6H, bs), 2.16 (3.6H, bs), 2.05 (4.3H, s), 2.03 (3.5H, s), 1.96 (8H, s), 1.92 (4.8H, s), 1.84 (3.8H, s) ppm. . MALDI-TOF (pos) m/z 144000.

19c: ^{1}H NMR (500MHz d^{6} DMSO) δ 7.96 (1H, bs), 7.75 (0.8H, bs), 7.47 (1.4H, bs), 5.21 (0.4H, s), 5.17 (0.6H, s), 5.12 (1.4H, m), 4.89 (0.3H, m), 4.79 (0.7H, m), 4.69 (1.2H, m), 4.62 (0.5H, m), 4.25 (0.5H, m), 4.17 (1H, m), 3.98 (2.6H, m), 3.74 (2H, m), 3.40-3.56 (8H, m), 3.13 (2H, bs), 3.04 (1.6H, bs), 2.64 (3.9H, bs), 2.37 (2.3H, bs), 2.16 (2.9H, bs), 2.07 (1.2H, s), 2.05 (1.6H, s), 2.03 (2.3H, s), 1.95 (6.1H, s), 1.92 (3.1H, s), 1.87 (1H, s), 1.85 (1.9H, s) ppm. . MALDI-TOF (pos) m/z 140500.

19d: ^{1}H NMR (500MHz d^{6} DMSO) δ 7.96 (1H, bs), 7.75 (0.8H, bs), 7.47 (1.6H, bs), 5.21 (0.6H, m), 5.17 (0.4H, s), 5.12 (1.3H, m), 4.89 (0.5H, m), 4.79 (0.5H, m), 4.69 (1.1H, m), 4.62 (0.4H, m), 4.25 (0.4H, m), 4.17 (1H, m), 3.98 (2.4H, m), 3.74 (1.8H, m), 3.40-3.56 (8.6H, m), 3.13 (2.4H, bs), 3.04 (1.6H, bs), 2.64 (4.1H, bs), 2.37 (1.9H, bs), 2.16 (3.1H, bs), 2.07 (1.7H, s), 2.05 (1.2H, s), 2.03 (1.6H, s), 1.95 (6H, s), 1.92 (2.3H, s), 1.87 (1.3H, s), 1.85 (1.1H, s) ppm. MALDI-TOF (pos) m/z 132500.

19e: ^{1}H NMR (500MHz *d*^{6} DMSO) δ 7.96 (1H, bs), 7.75 (0.8H, bs), 7.47 (1.6H, bs), 5.21 (0.8H, s), 5.17 (0.3H, s), 5.12 (1.2H, m), 4.89 (0.7H, m), 4.79 (0.3H, m), 4.69 (1.1H, m), 4.62 (0.2H, m), 4.25 (0.2H, m), 4.17 (1.1H, m), 3.98 (2.5H, m), 3.74 (1.5H, m), 3.40-3.56 (9H, m), 3.13 (2.4H, bs), 3.04 (1.7H, bs), 2.64 (4.8H, bs), 2.37 (2.9H, bs), 2.16 (3.2H, bs), 2.07 (2.3H, s), 2.05 (0.8H, s), 2.03 (1.3H, s), 1.95 (6.8H, s), 1.92 (1.7H, s), 1.87 (2.1H, s), 1.85 (1H, s) ppm. MALDI-TOF (pos) m/z 131500.

Deacetylated:

General procedure for deacylation of dendrimers 17-19. To the lyophilized solid product of compounds 17-19, 1 mL of 1:1 water:methanol was added, at which point the dendrimer became a white precipitate. To this mixture was added 0.2 equivalents of NaOMe (0.8 M in MeOH) for each peripheral carbohydrate, and let stir for 3 h. If, at this time, the mixture had not become a clear solution a further 0.2 equivalents of NaOMe (0.8 M in MeOH) was added and this step was repeated until the mixture became a clear and colorless solution. Aqueous HCl solution (0.1 M) was then added slowly until the pH was ~ 7. This neutralized solution was placed in a dialysis membrane (Mw cutoff 3500) and dialyzed in 1 L of DI water for 8 h. The water was changed and let stand for a further 8 h twice more. The remaining liquid in the membrane was frozen and lyophilized to give a white fluffy solid.

17a: ^{1}H NMR (500MHz *d*^{6} DMSO) δ 8.02 (bs, 1H), 7.82 (bs 0.9H), 7.54 (bs, 1.4H), 5.12 (bm, 1.8H), 4.64 (m, 3.7H), 4.33 (m, 2.1H), 3.87 (d, J = 4.8Hz, 1.4H), 3.74 (m, 1.7H), 3.47-3.62 (m, 18H), 3.17 (bs, 2.6H), 3.08 (bs, 1.7H), 3.03 (m, 1.3H), 2.66 (bs, 3.7H), 2.43 (bs, 1.9H), 2.20 (bs, 3.6H), 1.89 (s, 0.4H), 1.80 (s, 0.2H) ppm. MALDI-TOF (pos) m/z 15000.

17b: ^{1}H NMR (500MHz *d*^{6} DMSO) δ 8.04 (bs, 1H), 7.51 (bs 0.8H), 5.08 (bm, 0.8H), 4.53-4.70 (m, 2.6H), 4.20 (m, 1.0H), 4.09 (s, 0.2H), 3.83 (bs, 0.9H), 3.77 (m, 1.0H), 3.43-3.58 (m, 13H), 3.14 (bs, 2.0H), 3.05 (bs, 0.6H), 2.62 (bs, 1.8H), 2.39 (bs, 1.9H), 2.26 (bs, 1.6H), 1.85 (s, 0.1H), 1.76 (s, 0.2H) ppm MALDI-TOF (pos) m/z 15100.

17c: ^{1}H NMR (500MHz *d*^{6} DMSO) δ 8.03 (bs, 1H), 7.51 (bs 0.8H), 5.08 (bm, 0.6H), 4.53-4.70 (m, 2.1H), 4.20 (m, 0.6H), 4.09 (s, 0.3H), 3.82 (bs, 0.7H), 3.72 (m, 0.7H), 3.43-3.58 (m, 14H), 3.14 (bs, 1.8H), 2.99 (bs, 0.7H), 2.73 (bs, 1.8H), 2.24 (bs, 1.8H), 1.85 (s, 0.1H), 1.76 (s, 0.3H) ppm. MALDI-TOF (pos) m/z 14900.

17d: ^{1}H NMR (500MHz *d*^{6} DMSO) δ 8.10 (bs, 1H), 7.55 (bs 0.9H), 5.08 (bm, 0.5H), 4.53-4.70 (m, 2.2H), 4.23 (m, 0.6H), 4.12 (s, 0.6H), 3.85 (bs, 1.2H), 3.72 (m, 0.7H), 3.43-3.58 (m, 15H), 3.14 (bs, 1.8H), 2.84 (bs, 1.9H), 2.64 (bs, 1.0H), 2.32 (bs, 1.9H), 1.85 (s, 0.1H), 1.76 (s, 0.1H) ppm. MALDI-TOF (pos) m/z 15700.

17e: ^{1}H NMR (500MHz *d*^{6} DMSO) δ 8.08 (bs, 1H), 7.51 (bs 0.9H), 4.33-5.30 (m, 2.5H), 4.22 (m, 0.4H), 4.12 (s, 0.9H), 3.82 (bs, 1.5H), 3.43-3.65 (m, 20H), 3.14 (bs, 2.3H), 2.82 (bs, 2.2H), 2.62 (bs, 0.8H), 2.24 (bs, 2.0H) ppm. MALDI-TOF (pos) m/z 15800.

18a: ^{1}H NMR (500MHz *d*^{6} DMSO) δ 8.03 (bs, 1H), 7.86 (bs 0.8H), 7.52 (bs, 1.7H), 5.22 (bs, 1.0H), 5.12 (bm, 1.1H), 4.82 (bs 1.1H), 4.72 (m, 2.1H), 4.55 (m, 1.9H), 4.22 (m, 2.1H), 3.87 (d, 1.4H), 3.74 (m, 1.8H), 3.47-3.62 (m, 34H), 3.17 (bs, 2.2H), 3.03 (bs, 1.2H), 2.70 (bs, 3.1H), 2.23 (bs, 3.2H) ppm. MALDI-TOF (pos) m/z 31200.

18b: ^{1}H NMR (500MHz *d*^{6} DMSO) δ 8.11 (bs, 1H), 7.57 (bs 0.9H), 5.13 (bm, 0.9H), 4.53-4.70 (m, 2.3H), 4.22 (m, 0.9H), 4.11 (s, 0.2H), 3.86 (bs, 0.9H), 3.76 (m, 0.8H), 3.43-3.58 (m, 18H), 3.14 (bs, 1.7H), 3.05 (bs, 0.8H), 2.85 (bs, 1.6H), 2.39 (bs, 1.5H) ppm. MALDI-TOF (pos) m/z 31700.

18c: ^{1}H NMR (500MHz *d*^{6} DMSO) δ 8.06 (bs, 1H), 7.95 (bs, 0.7H), 7.54 (bs 1.3H), 5.11 (bs, 0.9H), 4.53-4.70 (m, 3.2H), 4.20 (m, 1.0H), 4.09 (s, 0.4H), 3.82 (bs, 1.1H), 3.72 (m, 0.9H), 3.43-3.58 (m, 29H), 3.14 (bs, 3.3H), 3.03 (bs, 0.9H), 2.77 (bs, 3.0H), 2.24 (bs, 3.1H) ppm. MALDI-TOF (pos) m/z 33000.

18d: ^{1}H NMR (500MHz *d*^{6} DMSO) δ 8.06 (bs, 1H), 7.95 (bs, 0.7H), 7.55 (bs 1.3H), 4.53-5.30 (m, 4.0H), 4.22 (m, 0.8H), 4.12 (s, 0.8H), 3.85 (bs, 1.4H), 3.72 (m, 0.7H), 3.43-3.58 (m, 21H), 3.14 (bs, 3.5H), 2.84 (bs, 3.2H), 2.64 (bs, 0.8H), 2.32 (bs, 2.7H) ppm. MALDI-TOF (pos) m/z 34300

18e: ^{1}H NMR (500MHz *d*^{6} DMSO) δ 8.02 (bs, 1H), 7.86 (bs, 0.9H), 7.51 (bs, 1.7H), 4.33-5.30 (m, 4.0H), 4.22 (m, 0.3H), 4.12 (s, 1.0H), 3.85 (bs, 1.3H), 3.43-3.65 (m, 29H), 3.18 (bs, 4,4H), 2.70 (bs, 3.8H), 2.23 (bs, 3.7H) ppm. MALDI-TOF (pos) m/z 34300

19a: ^{1}H NMR (500MHz *d*^{6} DMSO) δ 8.02 (bs, 1H), 7.81 (bs 0.9H), 7.53 (bs, 1.3H), 5.22 (bs, 0.8H), 5.12 (bs, 0.8H), 4.64 (m, 3.7H), 4.22 (m, 1.7H), 3.87 (m, 1.2H), 3.74 (bs, 1.4H), 3.47-3.62 (m, 28H), 3.17 (bs, 1.8H), 3.08 (bs, 2.4H), 2.66 (bs, 2.7H), 2.43 (bs, 1.3H), 2.20 (bs, 3.0H) ppm. MALDI-TOF (pos) m/z 100000

19b: ^{1}H NMR (500MHz *d*^{6} DMSO) δ 8.08 (bs, 1H), 7.57 (bs 0.8H), 5.15 (bm, 0.9H), 4.53-4.79 (m, 2.3H), 4.23 (m, 0.9H), 4.10 (s, 0.2H), 3.83 (bs, 0.9H), 3.77 (m, 1.0H), 3.43-3.58 (m, 16H), 3.18 (bs, 1.0H), 3.03 (bs, 0.9H), 2.77 (bs, 1.2H), 2.29 (bs, 1.0H) ppm. MALDI-TOF (pos) m/z 101000

19c: ^{1}H NMR (500MHz *d*^{6} DMSO) δ 8.06 (bs, 1H),7.83 (bs, 0.6H), 7.55 (bs 1.2H), 5.13 (m 1.2H), 4.53-4.70 (m, 3.1H), 4.23 (m, 1.0H), 4.12 (s, 0.4H), 3.86

(bs, 1.4H), 3.72 (m, 1.0H), 3.43-3.58 (m, 21H), 3.18 (bs, 1.8H), 3.03 (bs, 0.8H), 2.73 (bs, 2.6H), 2.25 (bs, 2.3H) ppm. MALDI-TOF (pos) m/z 101500

19d: ^{1}H NMR (500MHz *d*^{6} DMSO) δ 8.03 (bs, 1H), 7.89 (bs, 0.9H), 7.55 (bs, 1.5H), 5.13 (m, 0.9H), 4.53-4.70 (m, 3.1H), 4.23 (m, 0.8H), 4.12 (s, 0.7H), 3.85 (bs, 1.2H), 3.72 (m, 0.4H), 3.43-3.58 (m, 23H), 3.14 (bs, 4.5H), 2.70 (bs, 3.5H), 2.23 (bs, 3.5H) ppm. MALDI-TOF (pos) m/z 102000

19e: ^{1}H NMR (500MHz *d*^{6} DMSO) δ 8.06 (bs, 1H), 7.55 (bs 0.8H), 4.33-5.30 (m, 2.2H), 4.22 (m, 0.4H), 4.12 (s, 0.5H), 3.82 (bs, 0.8H), 3.43-3.65 (m, 12H), 3.14 (bs, 2.2H), 2.77 (bs, 1.7H), 2.28 (bs, 1.8H) ppm. MALDI-TOF (pos) m/z 106500

Table 16 MALDI-TOF data for heterogeneously functionalized dendrimers 17-19 a-e.

Compound number	M_w after Galactose addition	M_w after Lactose addition	M_w after deacylation
17a	6800	24400	15000
17b	10200	24600	15100
17c	13300	22200	14900
17d	15800	21800	15700
17e	18400	20500	15800
18a	13500	54500	31200
18b	21200	48000	31700
18c	26700	45400	33000
18d	30500	41700	34300
18e	35500	41000	34300
19a	51000	147000	100000
19b	68000	144000	101000
19c	78500	140500	101500
19d	90500	132500	102000
19e	102000	131500	106500

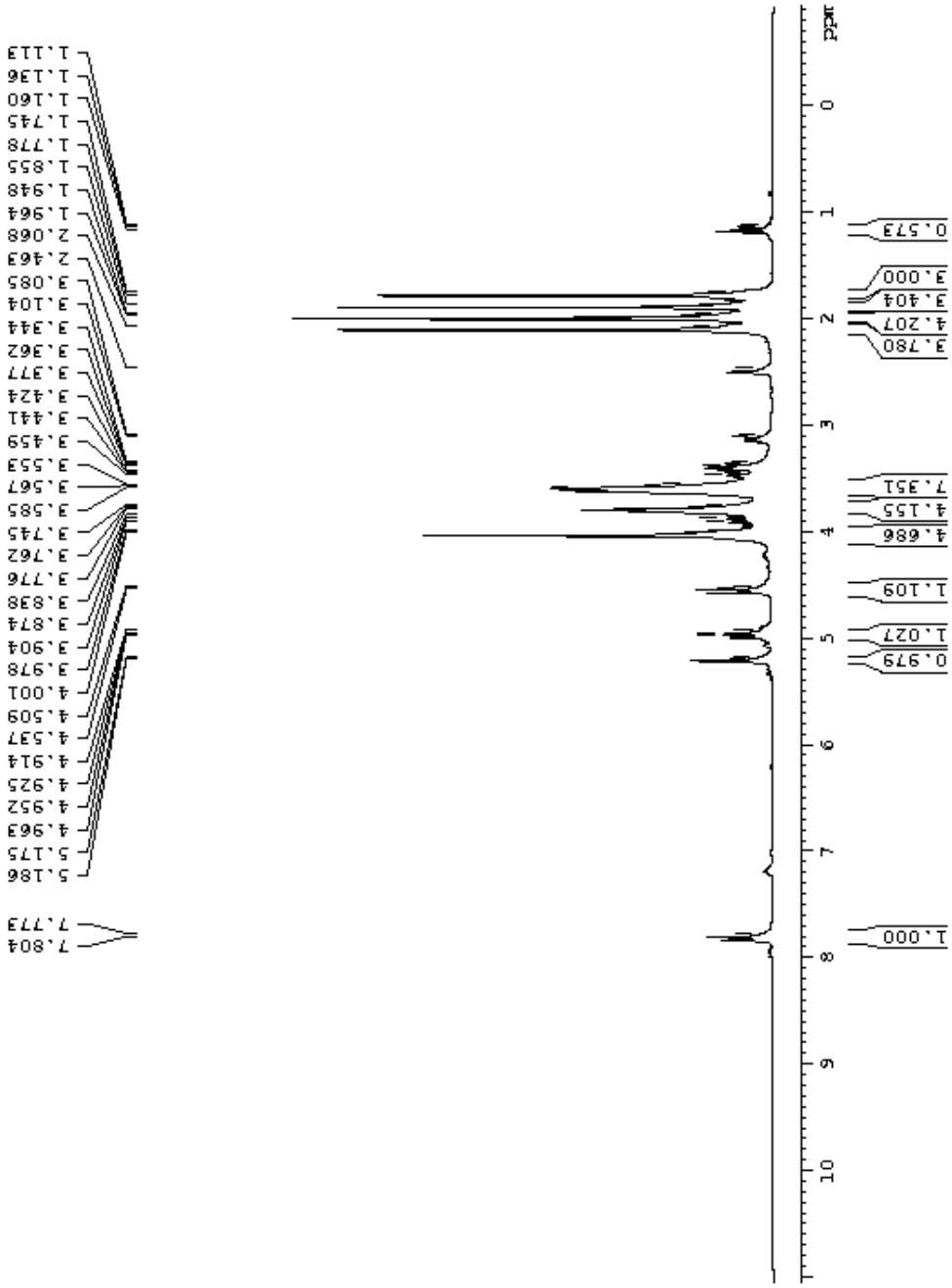

Figure 88 ^{1}H NMR spectrum (300 MHz, d_6-DMSO) of 12.

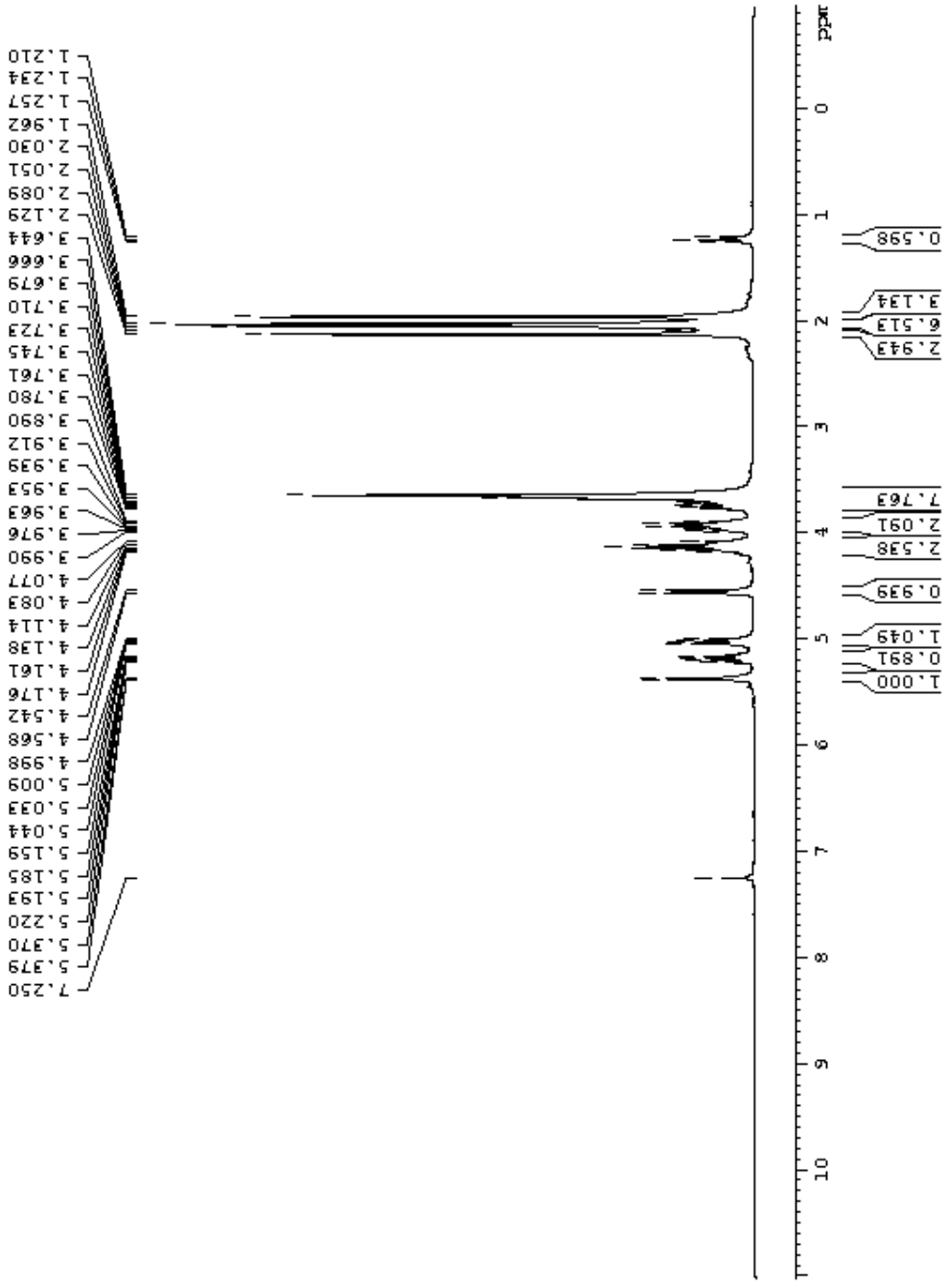

Figure 89 ^{1}H NMR spectrum (300 MHz, $CDCl_3$) of 11.

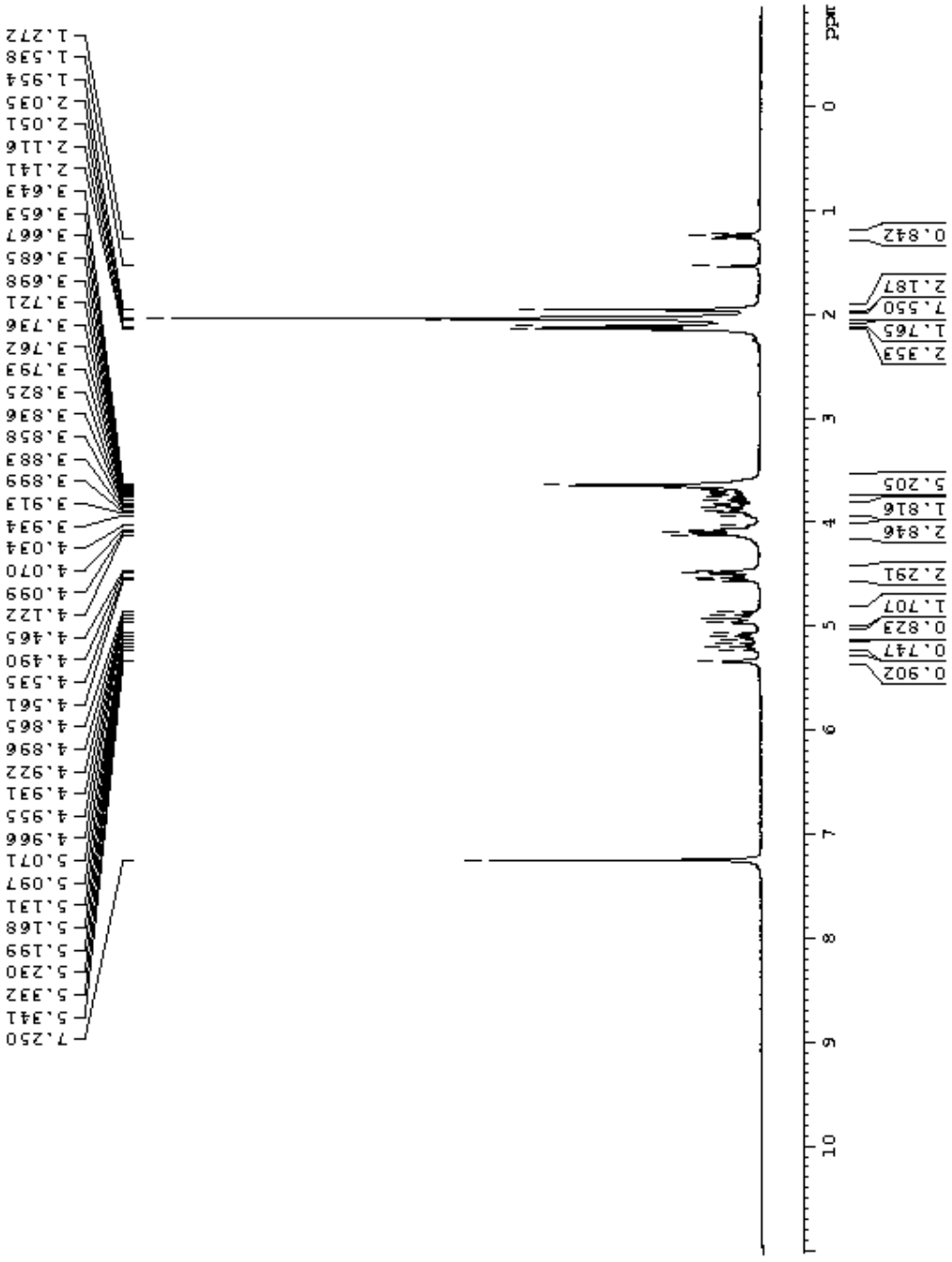

Figure 90 ^{1}H NMR spectrum (300 MHz, $CDCl_3$) of 13.

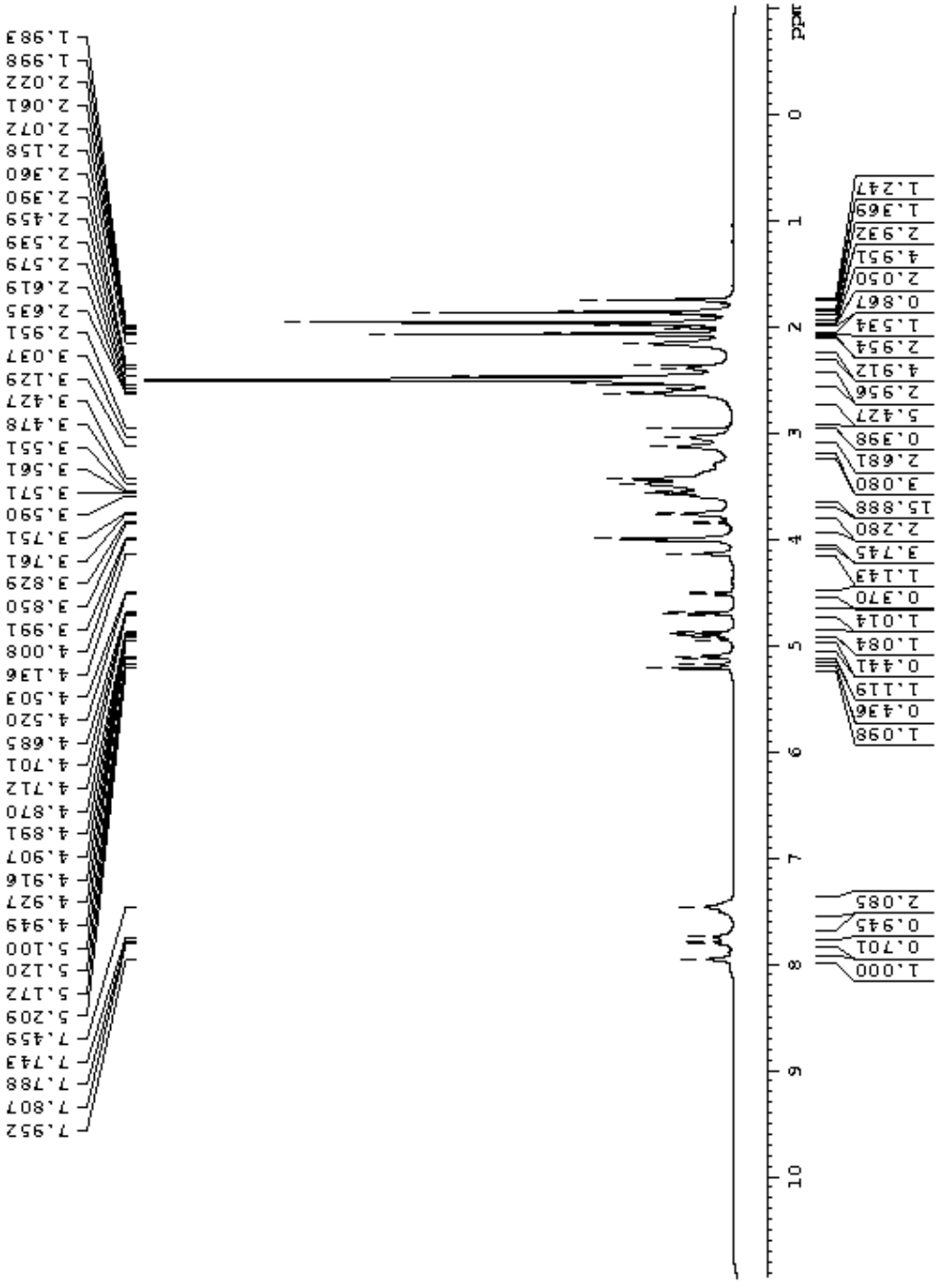

Figure 91 ^{1}H NMR spectrum (500 MHz, d_6-DMSO) of 14c. (acetylated)

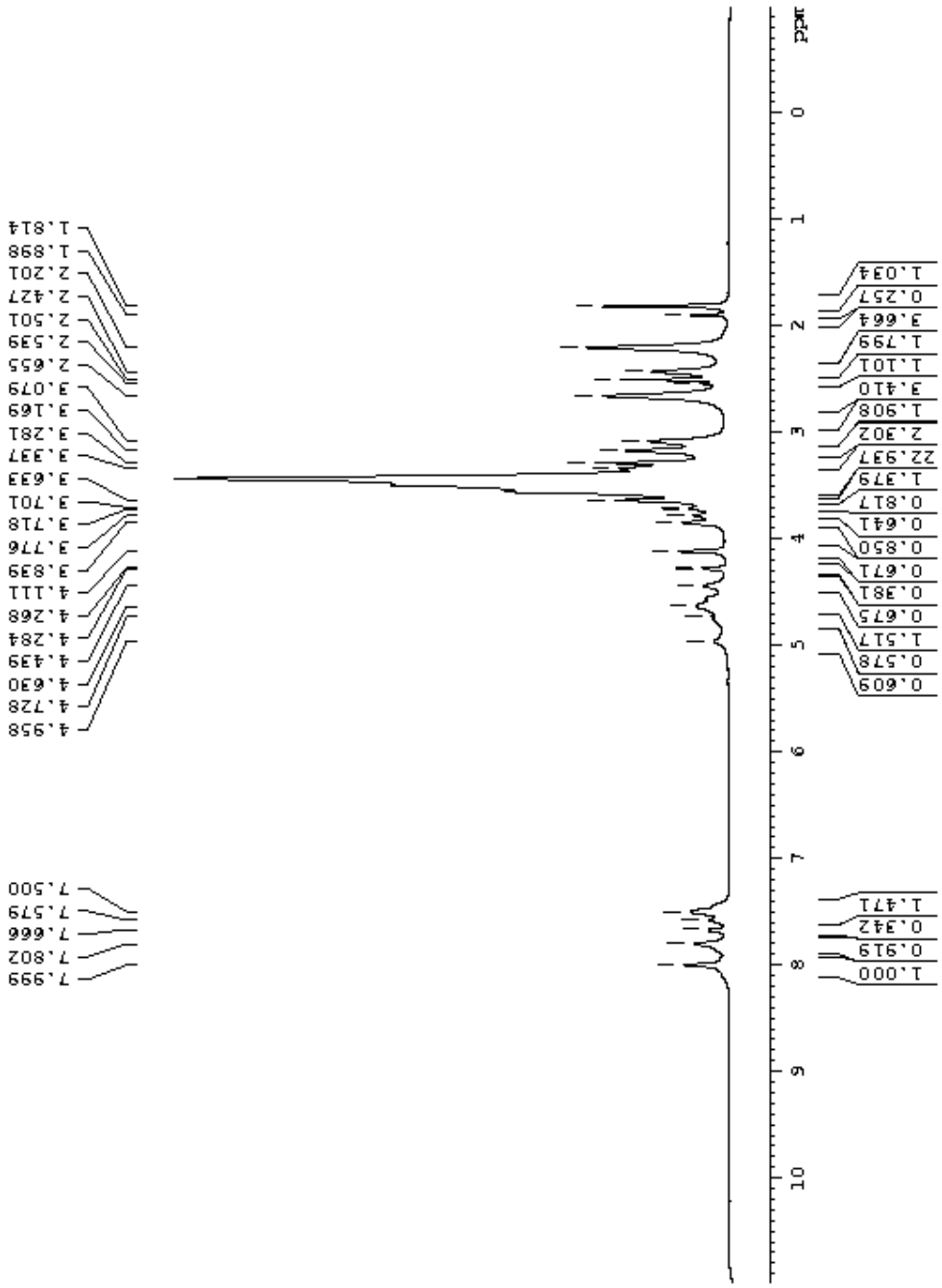

Figure 92 ^{1}H NMR spectrum (500 MHz, d_6-DMSO) of 14c. (deacetylated)

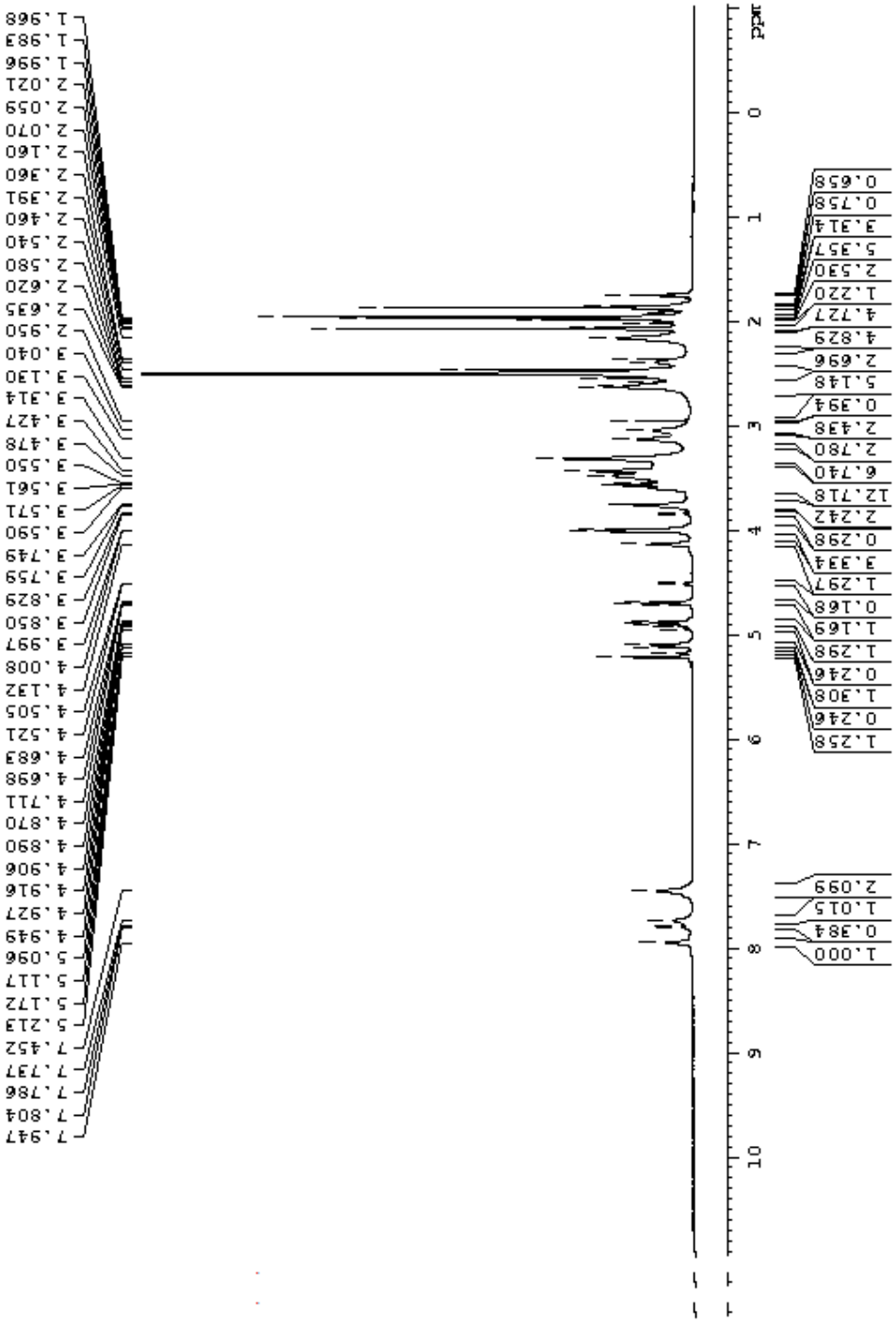

Figure 93 ^{1}H NMR spectrum (500 MHz, d_6-DMSO) of 15b (acetylated).

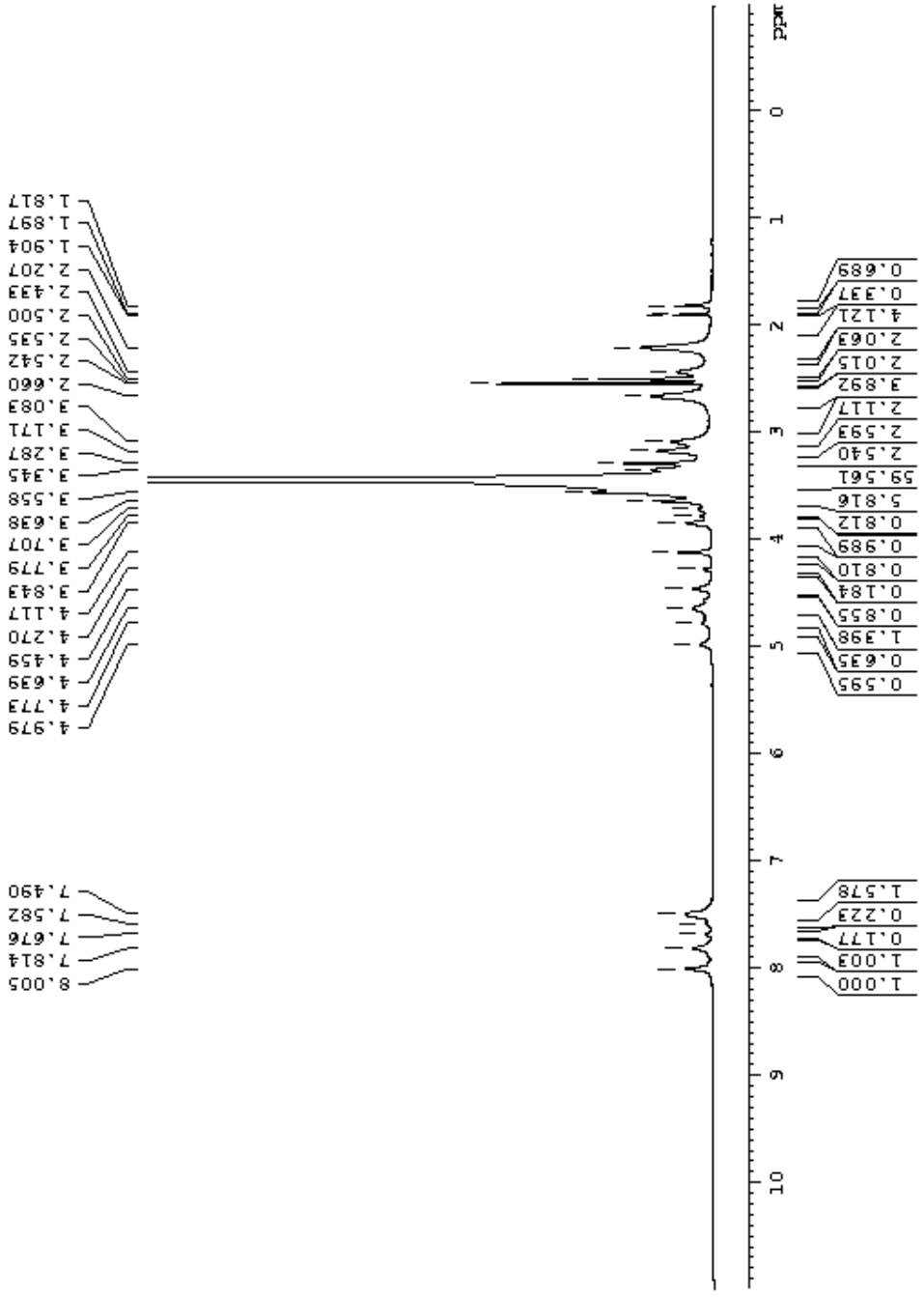

Figure 94 ^{1}H NMR spectrum (500 MHz, d_6-DMSO) of 15b. (deacetylated)

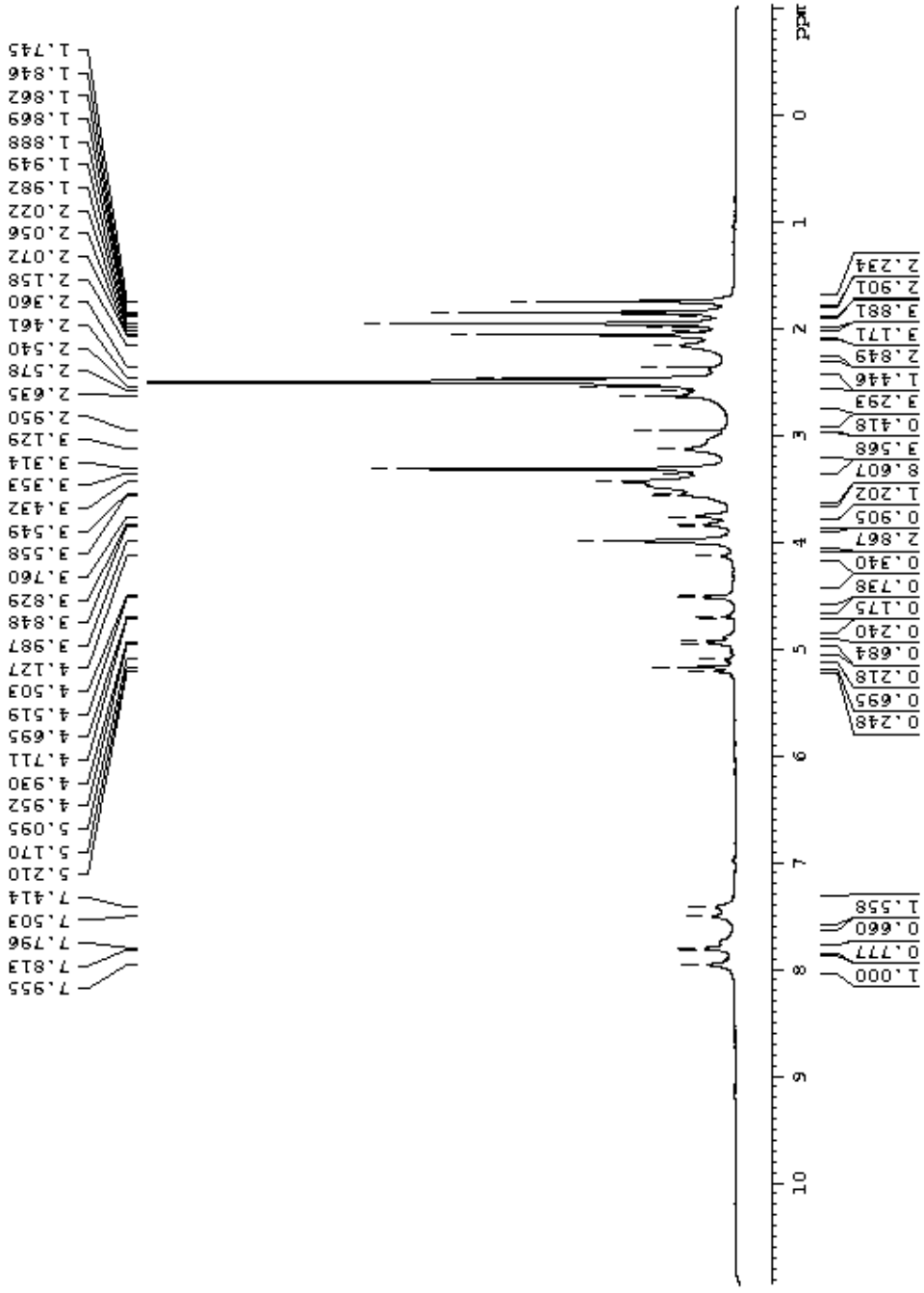

Figure 95 ^{1}H NMR spectrum (500 MHz, d_6-DMSO) of 16f. (acetylated)

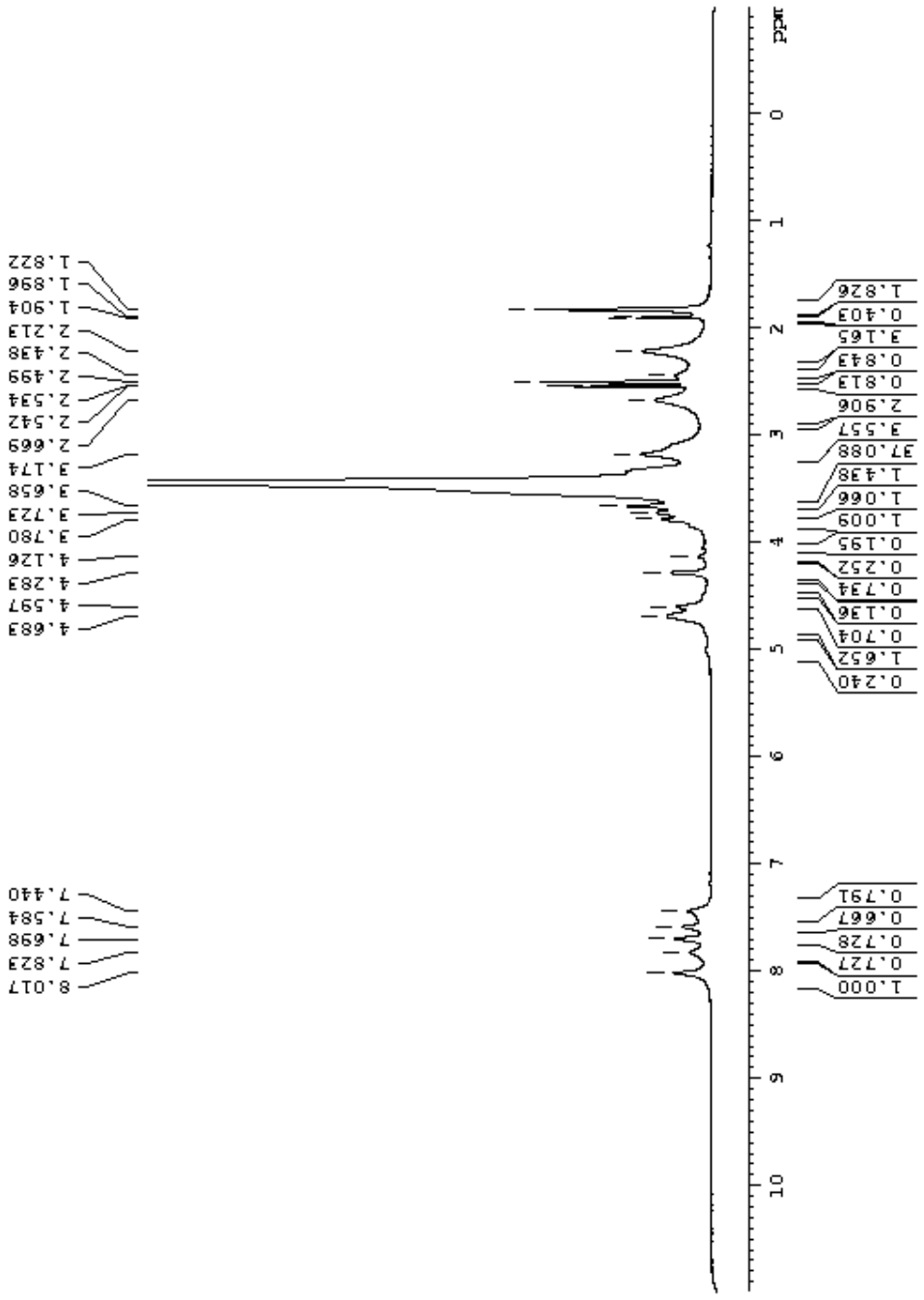

Figure 96 ^{1}H NMR spectrum (500 MHz, d_6-DMSO) of 16f. (deacetylated)

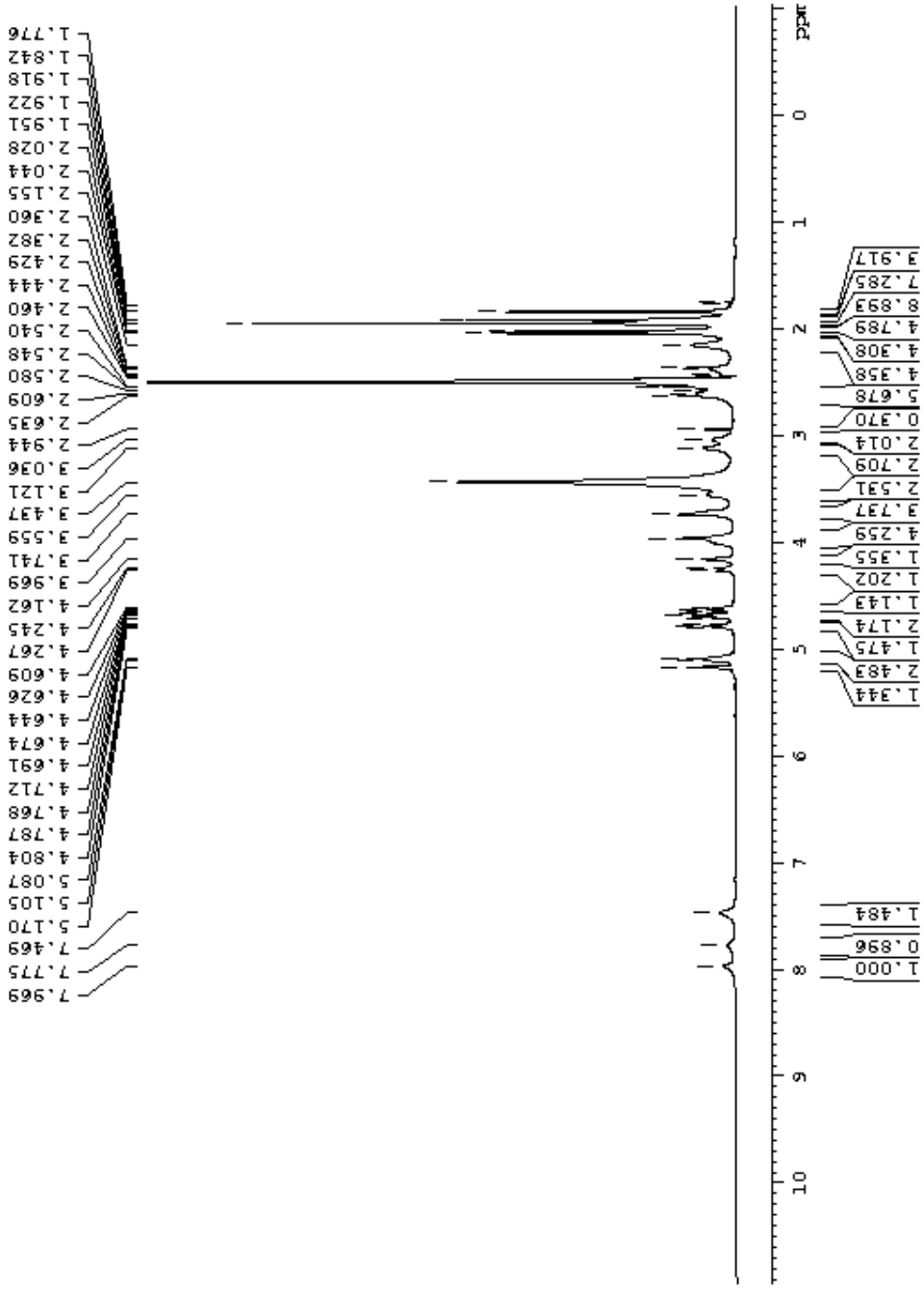

Figure 97 ^{1}H NMR spectrum (500 MHz, d_6-DMSO) of 17a. (acetylated)

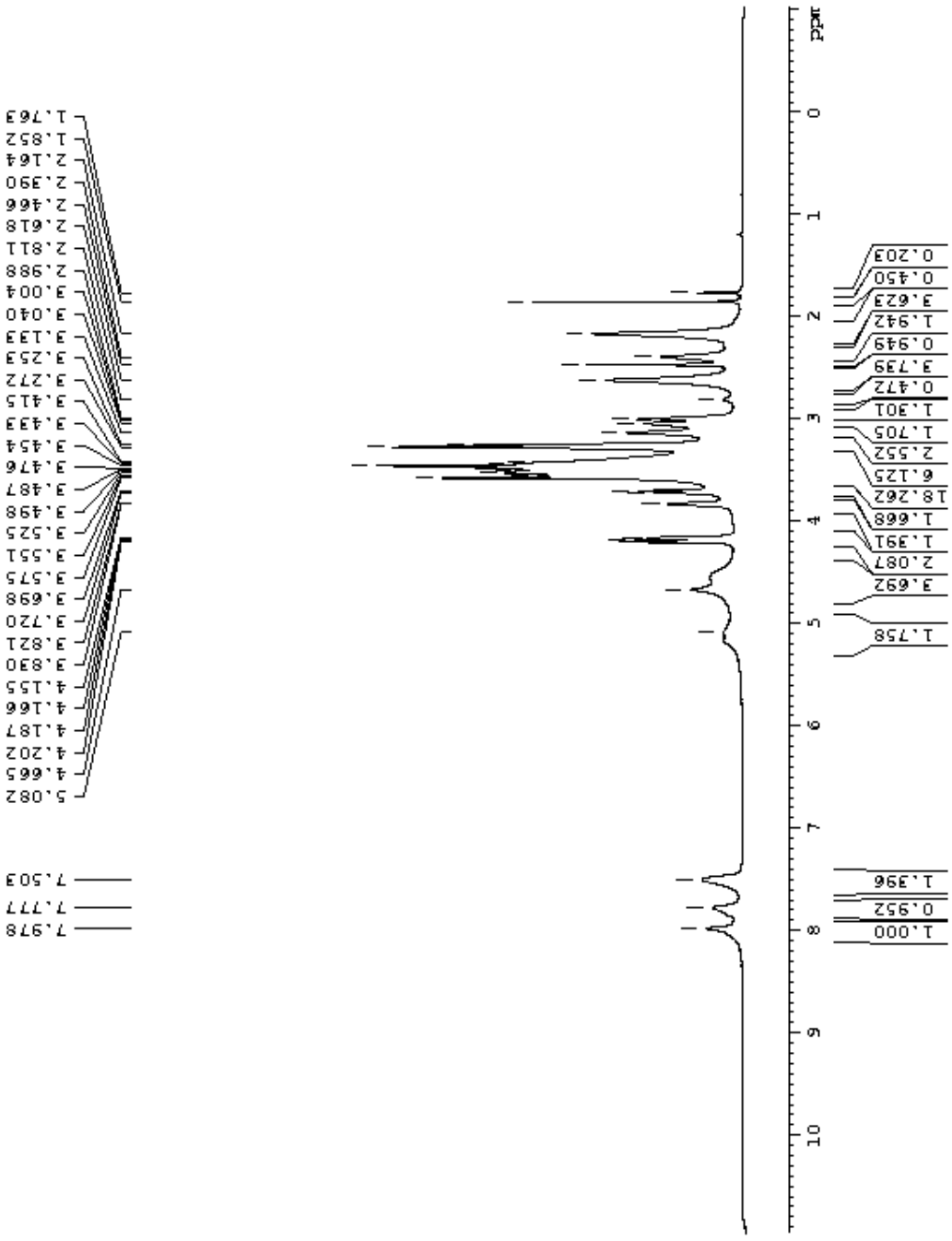

Figure 98 ^{1}H NMR spectrum (500 MHz, d_6-DMSO) of 17a. (deacetylated)

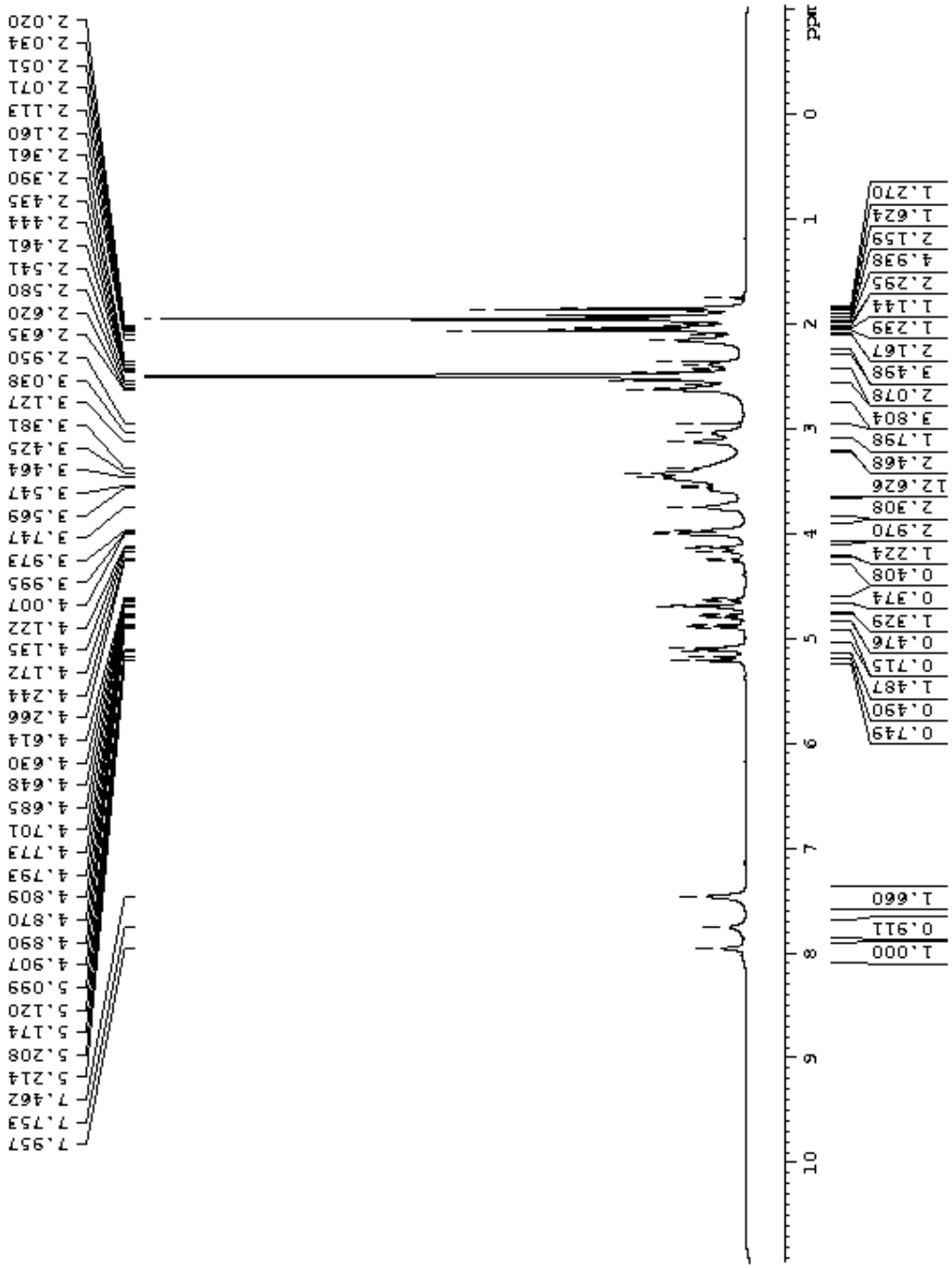

Figure 99 ^{1}H NMR spectrum (500 MHz, d_6-DMSO) of 17d. (acetylated)

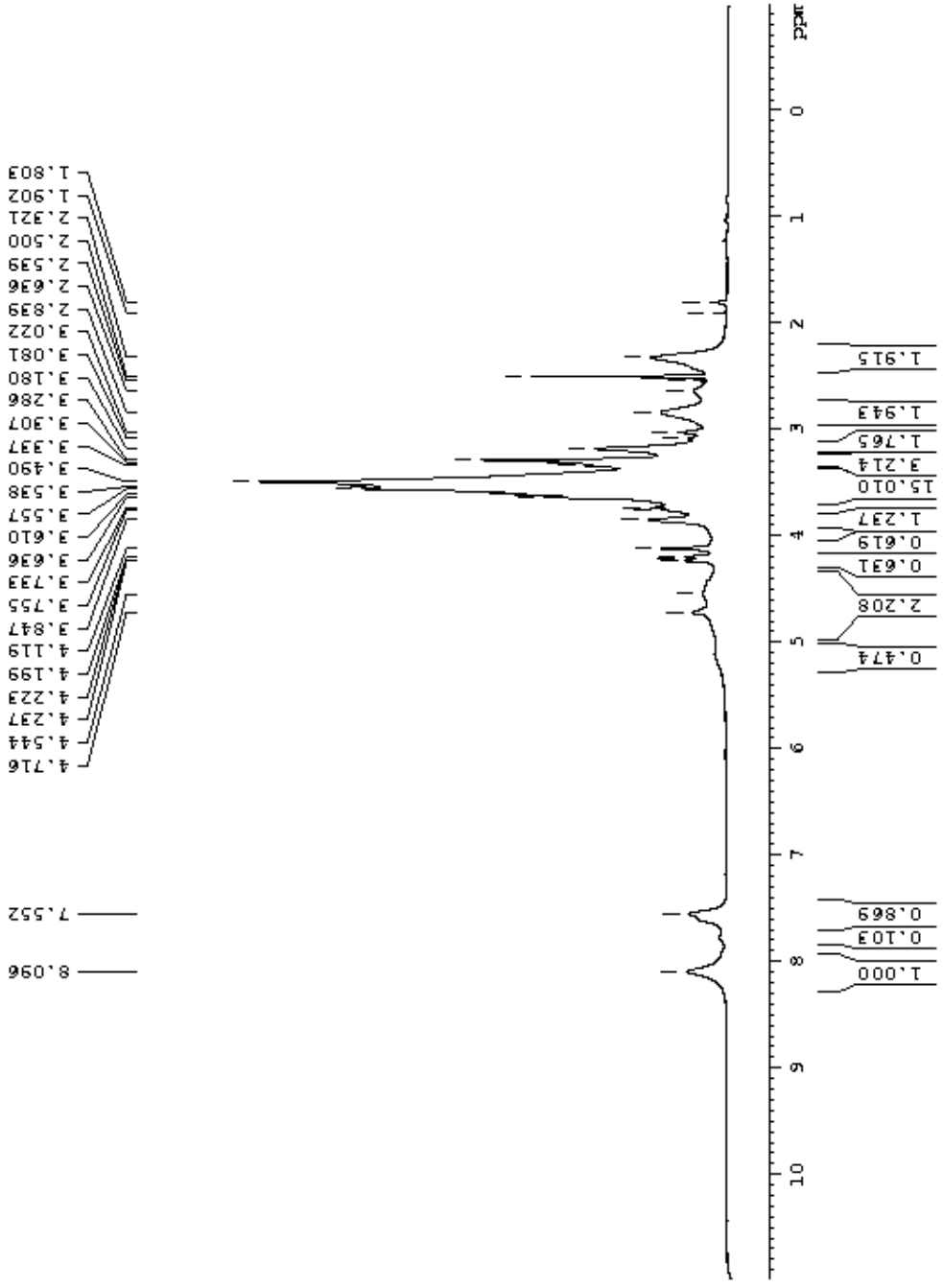

Figure 100 ^{1}H NMR spectrum (500 MHz, d_6-DMSO) of 17d. (deacetylated)

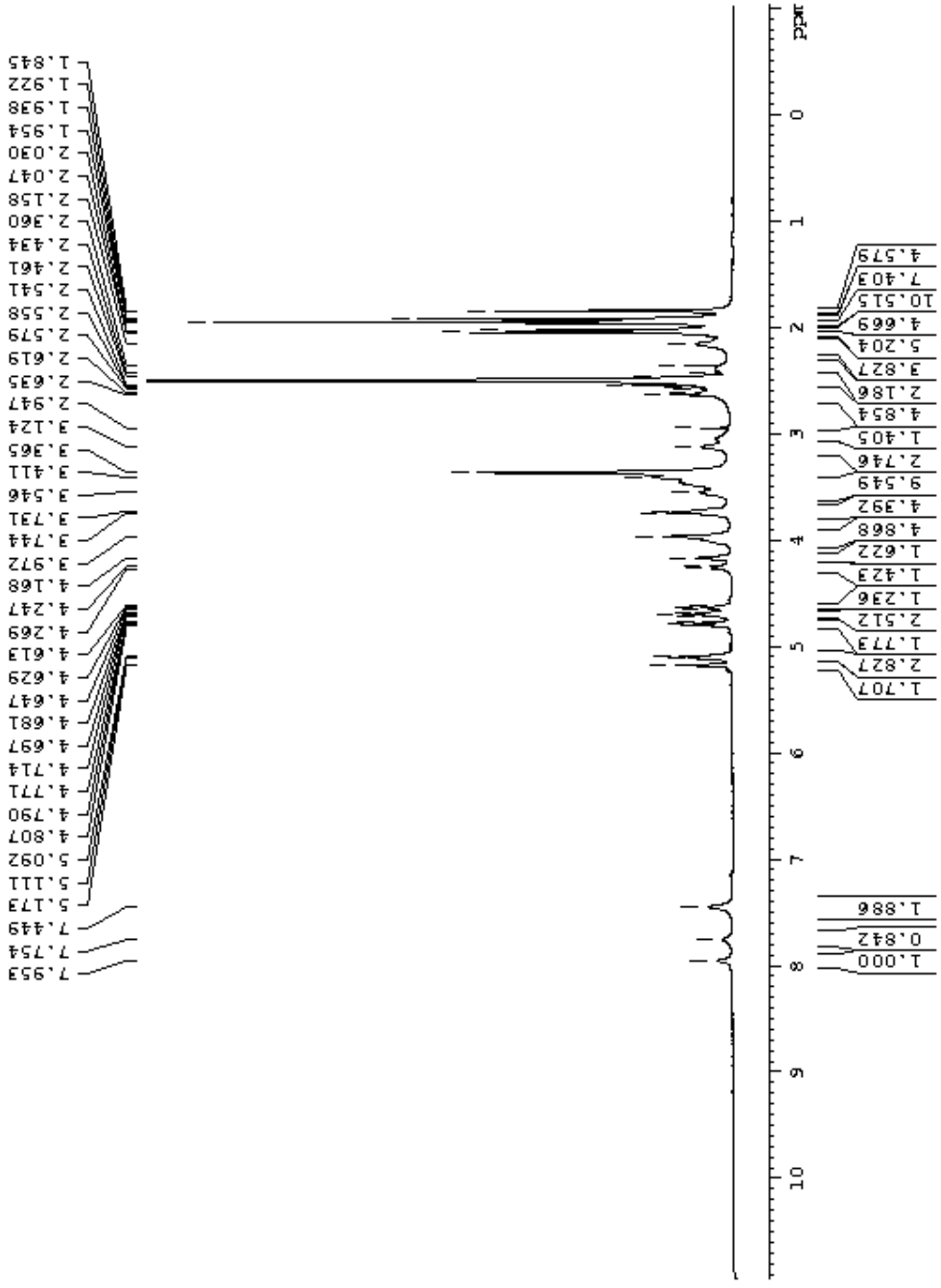

Figure 101 ^{1}H NMR spectrum (500 MHz, d_6-DMSO) of 18a. (acetylated)

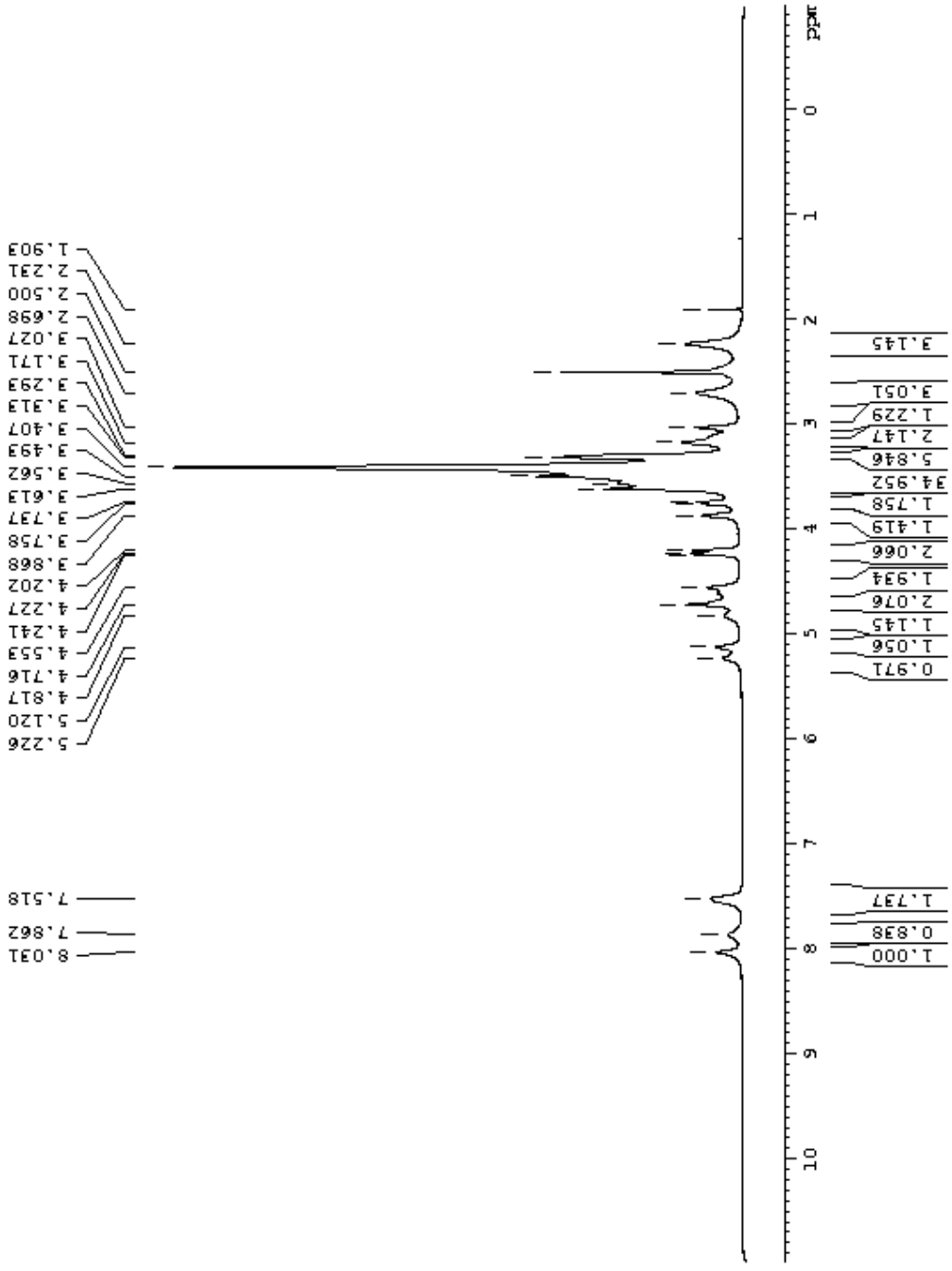

Figure 102 ^{1}H NMR spectrum (500 MHz, d_6-DMSO) of 18a. (deacetylated)

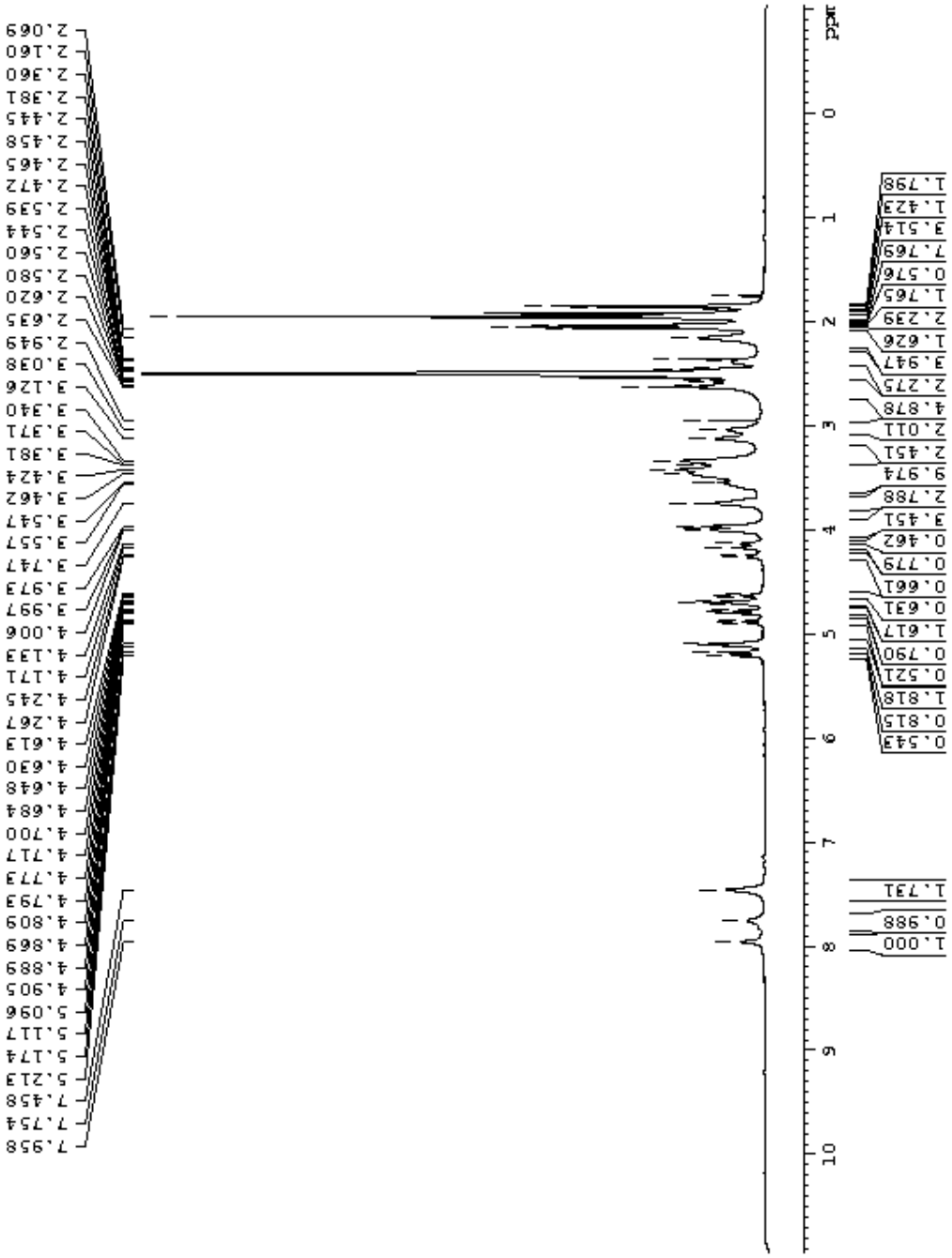

Figure 103 ^{1}H NMR spectrum (500 MHz, d_6-DMSO) of 18c. (acetylated)

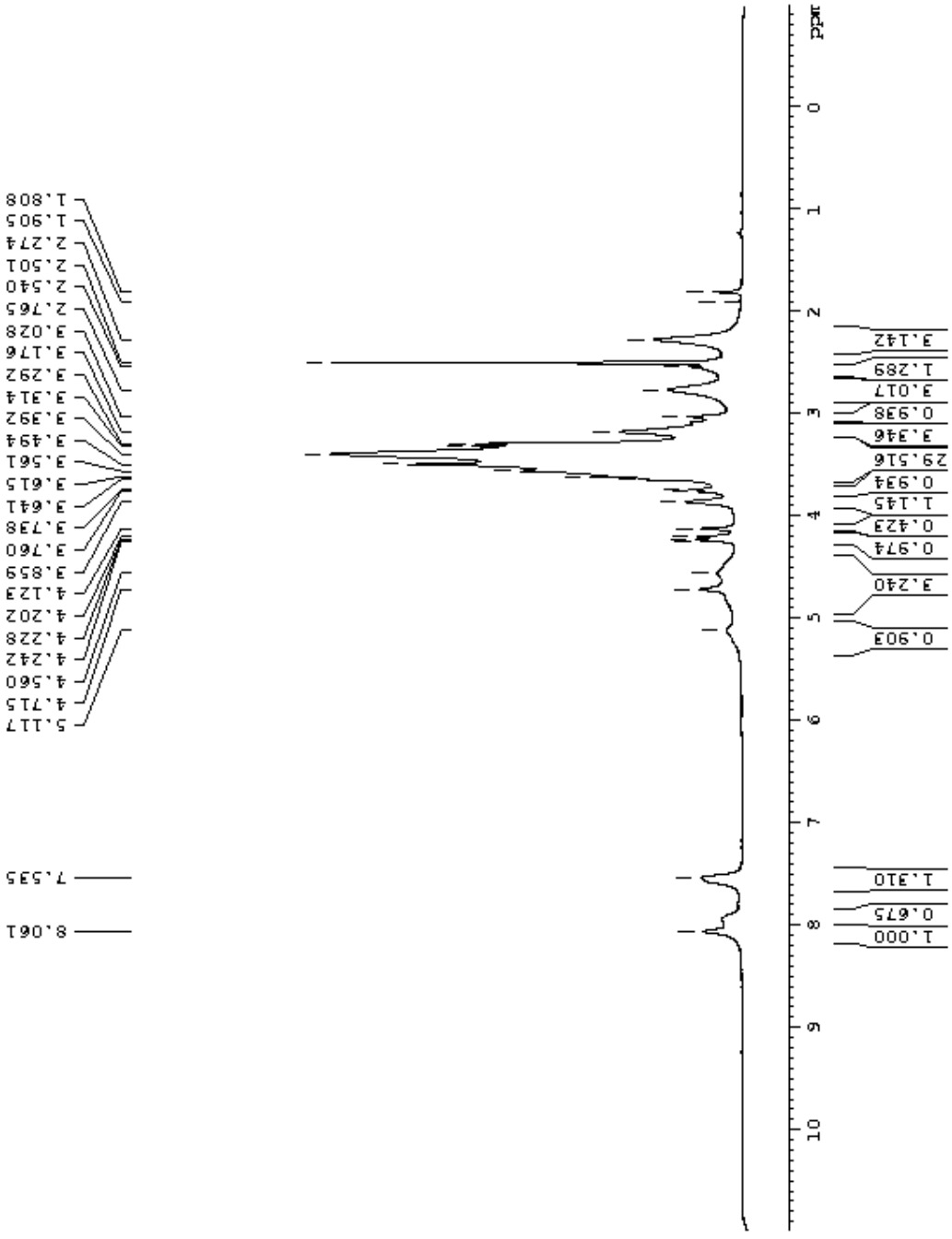

Figure 104 ^{1}H NMR spectrum (500 MHz, d_6-DMSO) of 18c. (deacetylated)

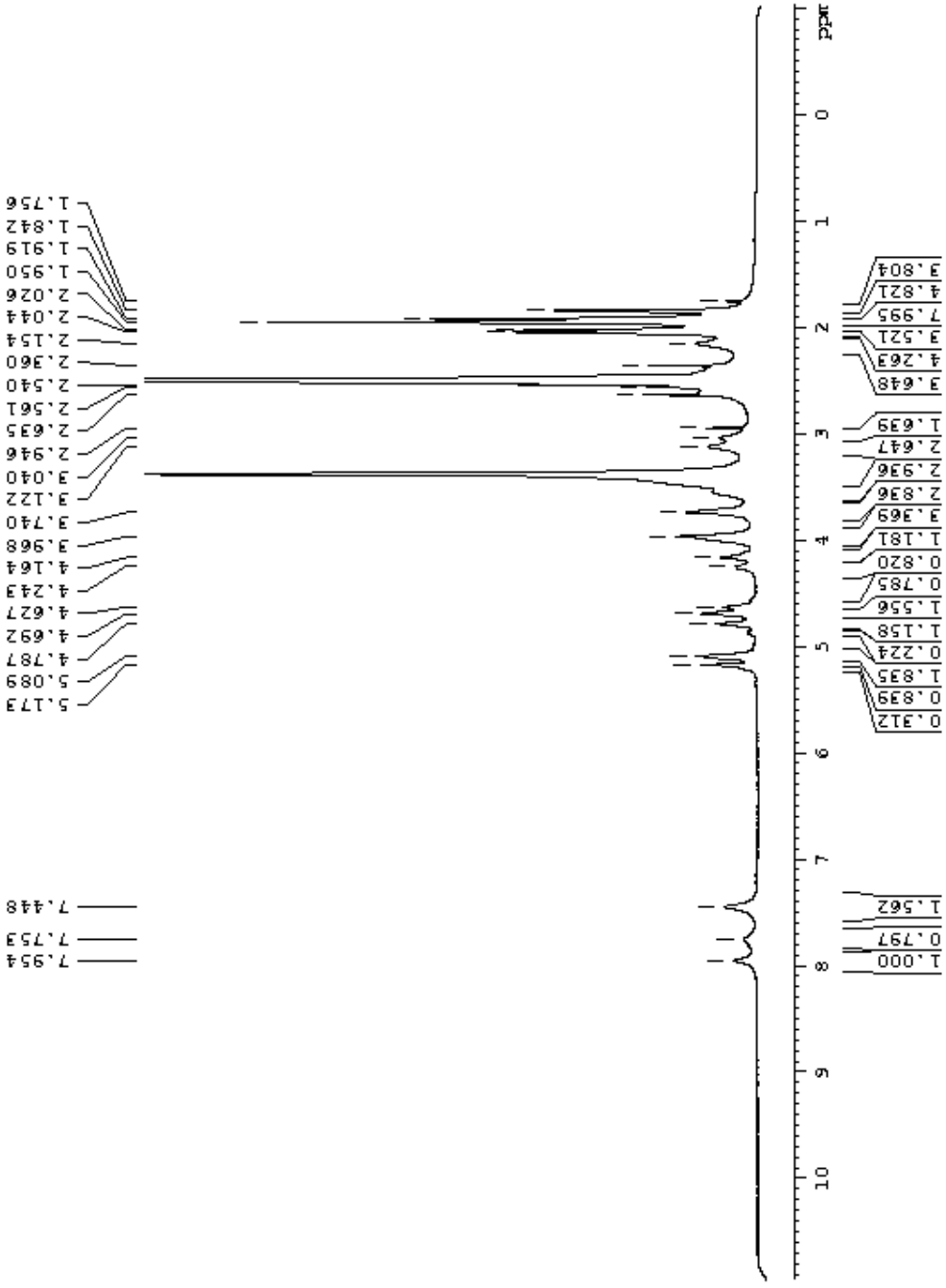

Figure 105 ^{1}H NMR spectrum (500 MHz, d_6-DMSO) of 19b. (acetylated)

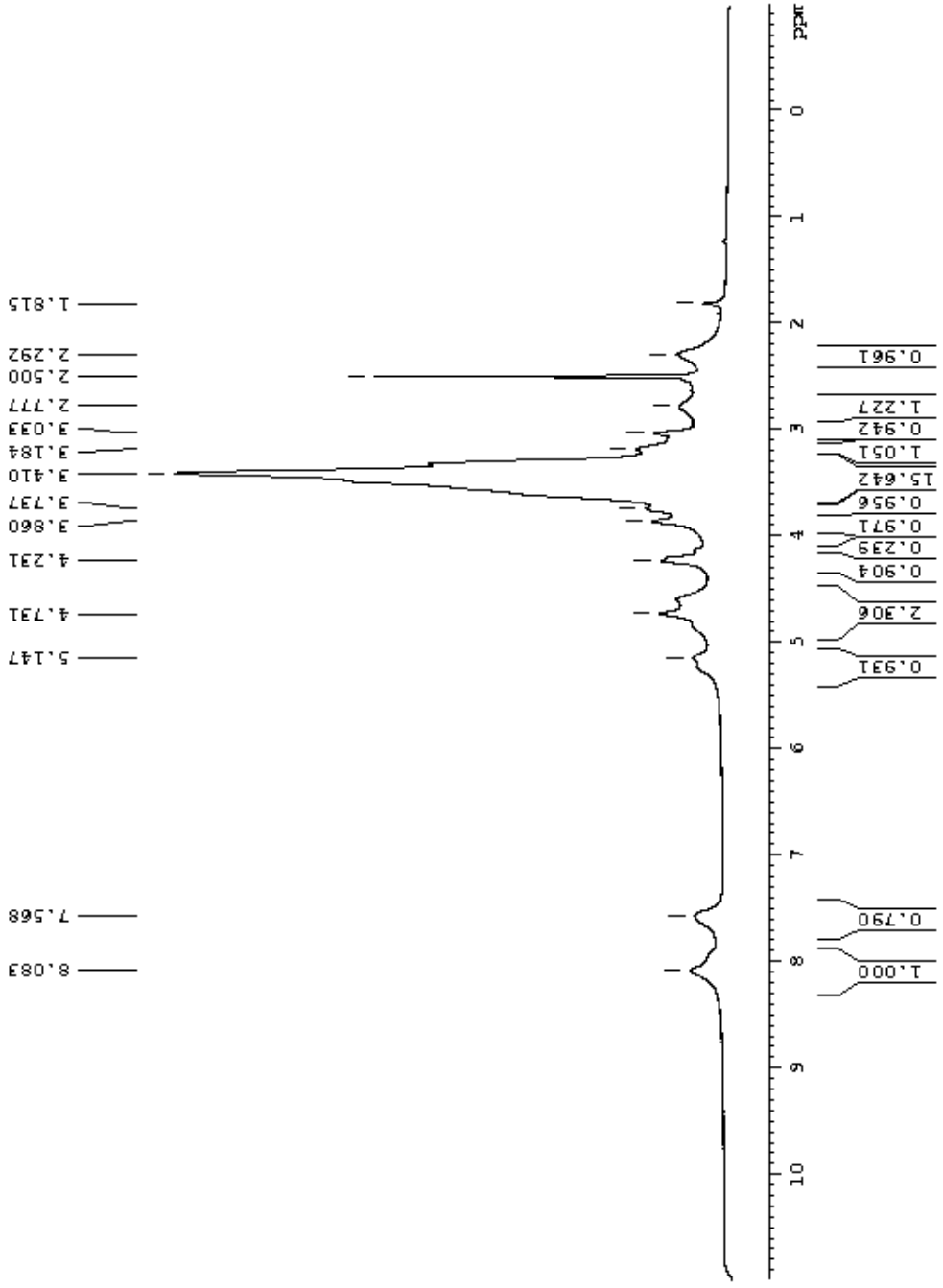

Figure 106 ^{1}H NMR spectrum (500 MHz, d_6-DMSO) of 19b. (deacetylated)

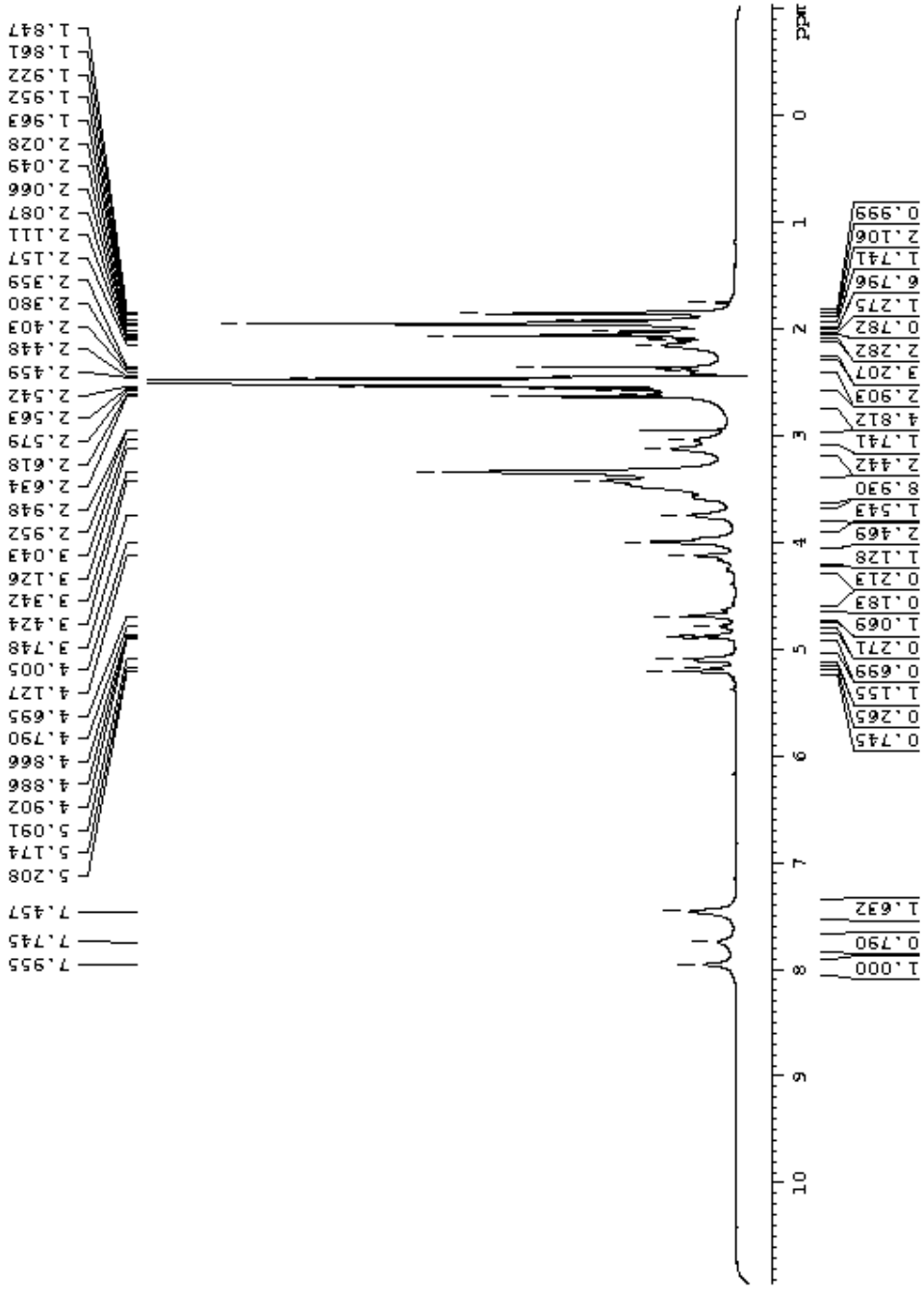

Figure 107 ^{1}H NMR spectrum (500 MHz, d_6-DMSO) of 19e. (acetylated)

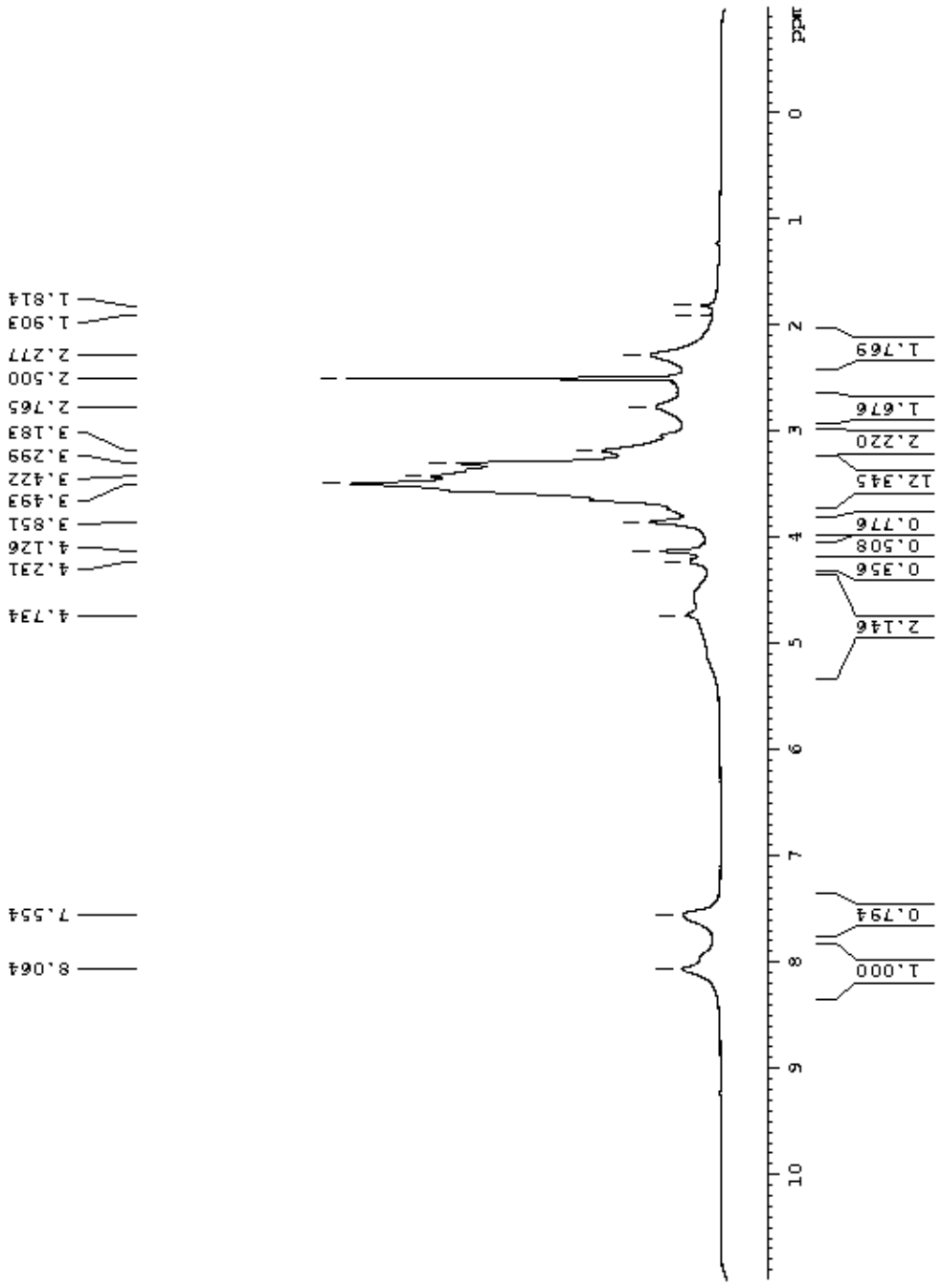

Figure 108 ^{1}H NMR spectrum (500 MHz, d_6-DMSO) of 19e. (deacetylated)

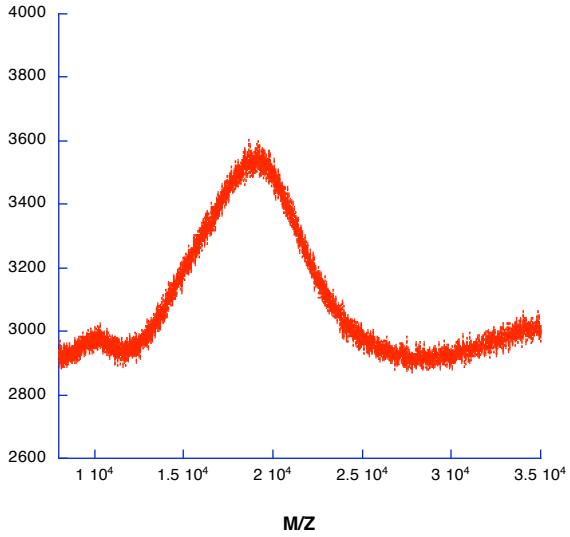

Figure 109 MALDI-TOF spectra for 14b after second addition. M_W = 19100 g/mol.

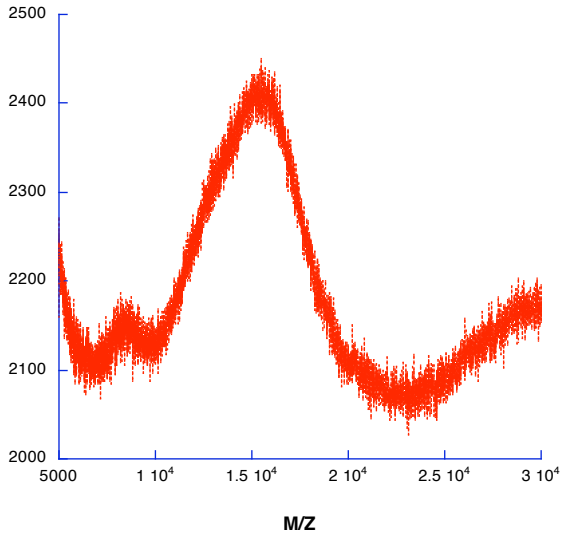

Figure 110 MALDI-TOF spectra for 14b after deacetylation. M_W = 15000 g/mol.

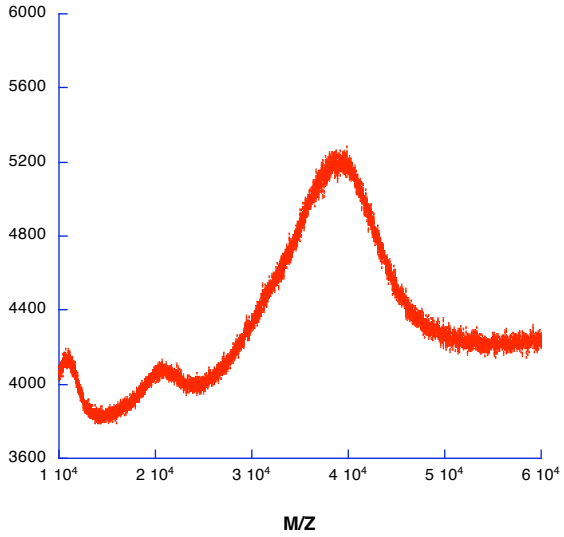

Figure 111 MALDI-TOF spectra for 15c after second addition. M_W = 39700 g/mol.

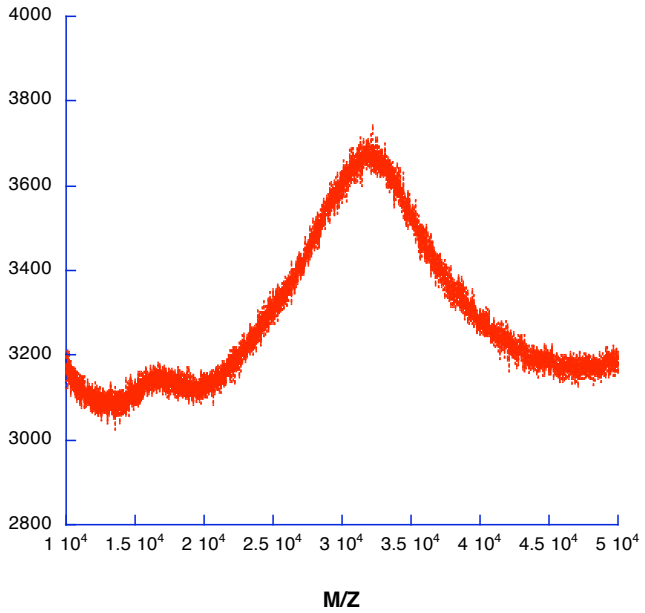

Figure 112 MALDI-TOF spectra for 15c after deacetylation. M_W = 31700 g/mol.

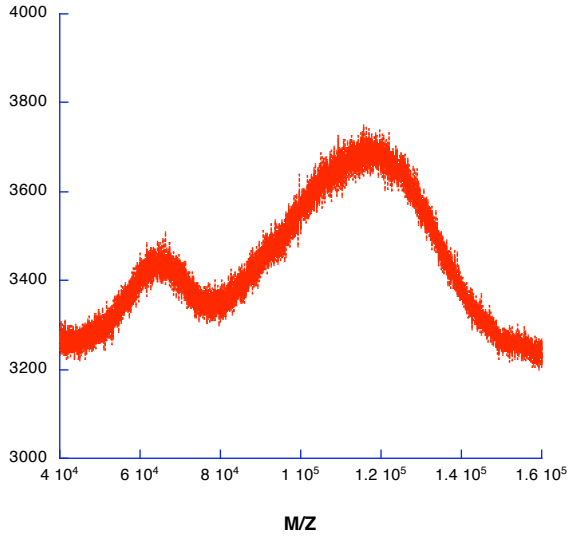

Figure 113 MALDI-TOF spectra for 16e after second addition. M_W = 121500 g/mol.

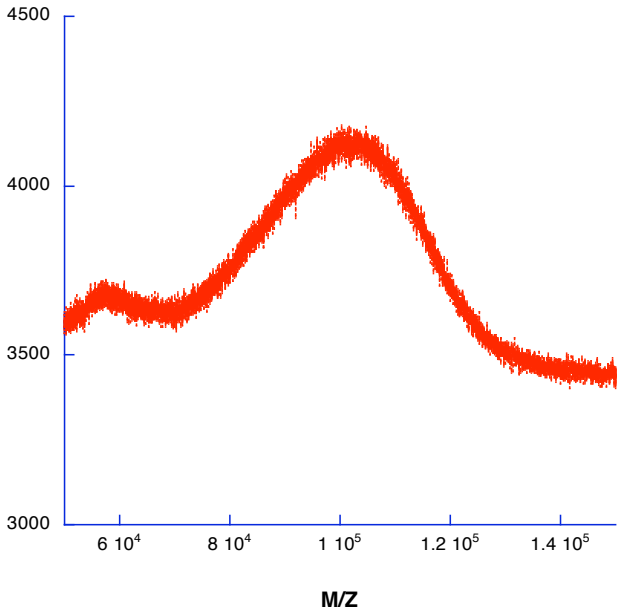

Figure 114 MALDI-TOF spectra for 16e after deacetylation. M_W = 102000 g/mol.

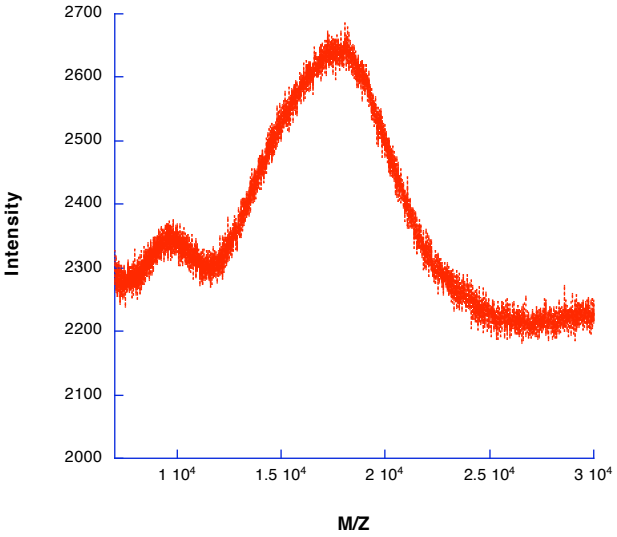

Figure 115 MALDI-TOF spectra for 17e after first addition. M_W = 18400 g/mol.

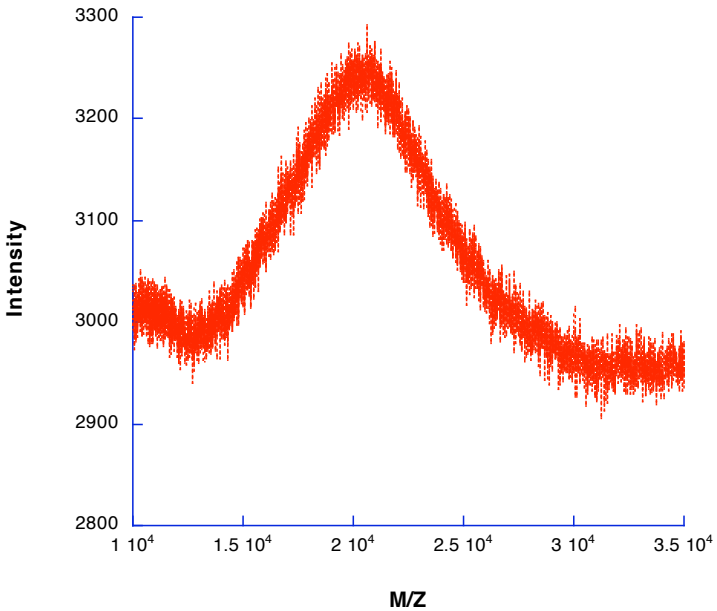

Figure 116 MALDI-TOF spectra for 17e after second addition. M_W = 20500 g/mol.

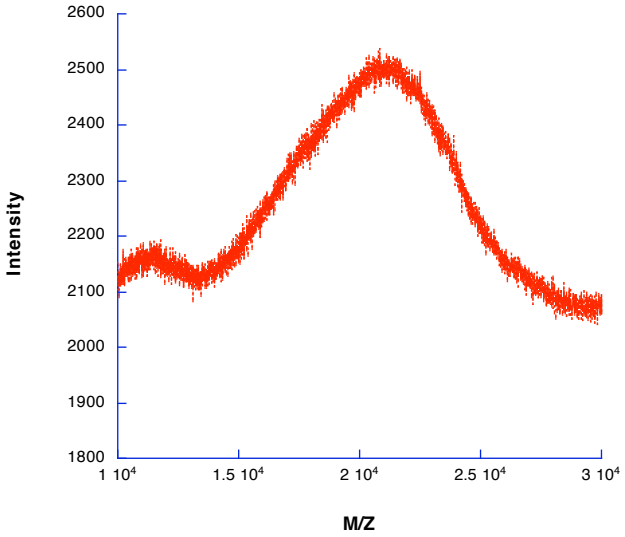

Figure 117 MALDI-TOF spectra for 18b after first addition. M_W = 21200 g/mol.

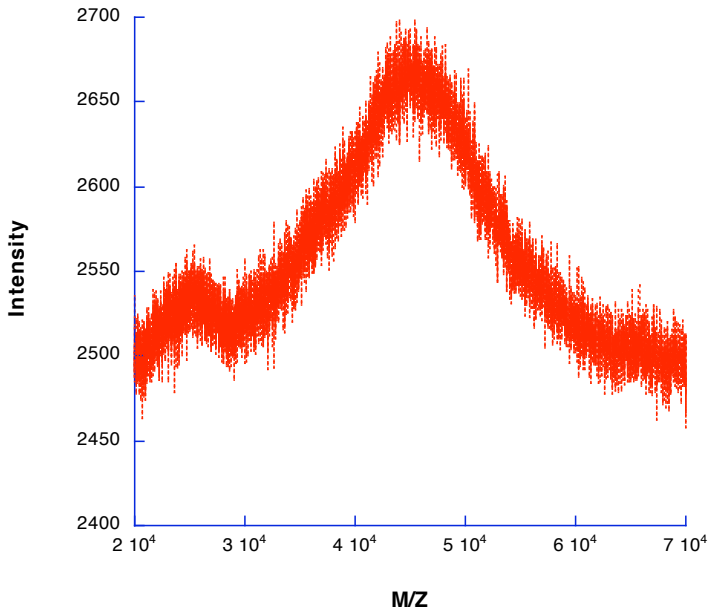

Figure 118 MALDI-TOF spectra for 18b after second addition. M_W = 41700 g/mol.

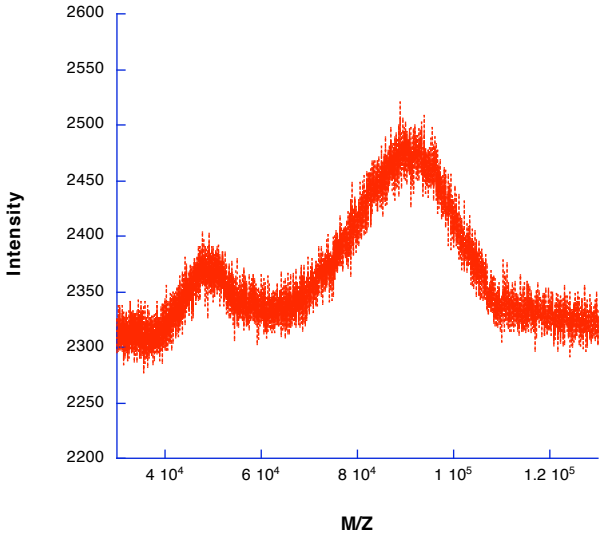

Figure 119 MALDI-TOF spectra for 19d after first addition. M_W = 90500 g/mol.

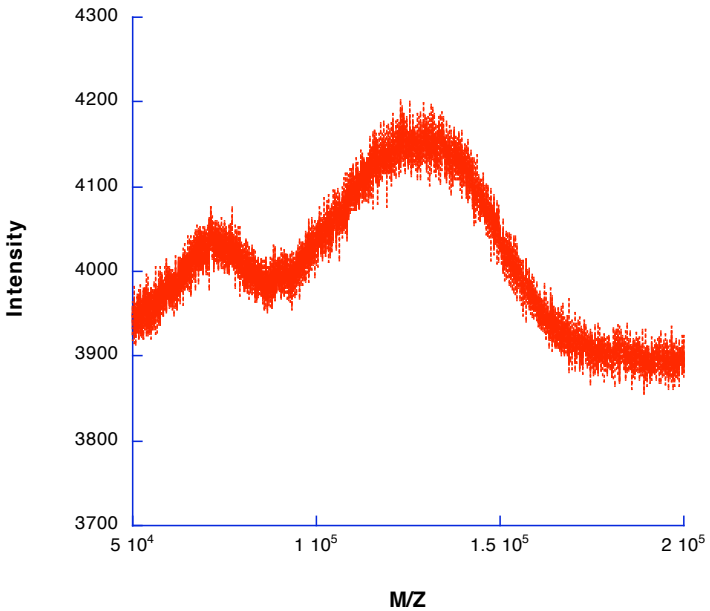

Figure 120 MALDI-TOF spectra for 19d after second addition. M_W = 132500 g/mol.

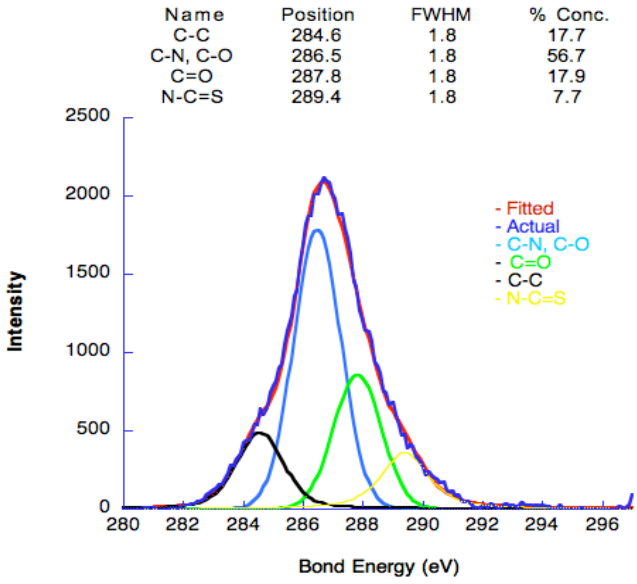

Figure 121 XPS carbon spectrum for compound 19a.

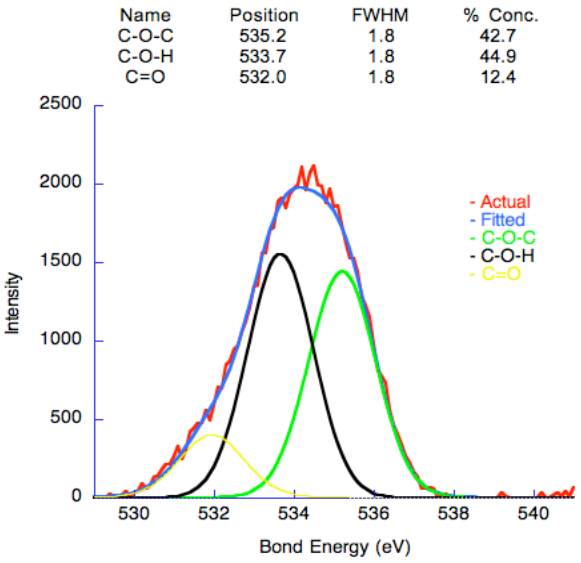

Figure 122 XPS oxygen spectrum for compound 19a.

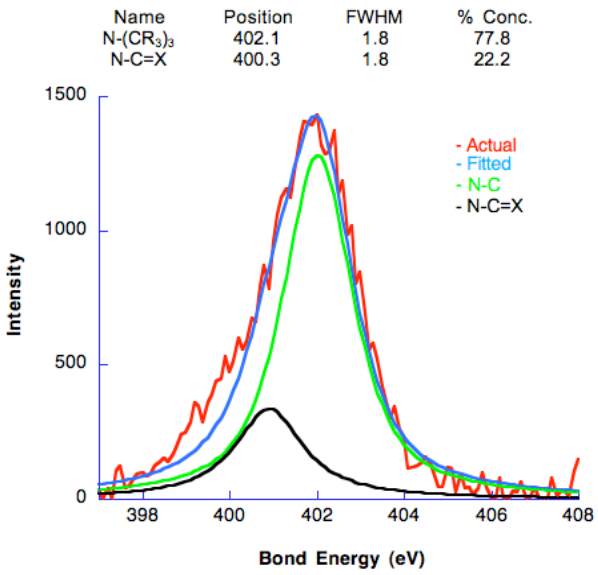

Figure 123 XPS nitrogen spectrum for compound 19a.

Note: XPS analysis of carbon, oxygen and nitrogen peaks is provided, however for the purpose of analyzing the dendrimer adsorption only nitrogen percentage was utilized and this more extensive peak analysis is for data representation only and not used in the discussion of this manuscript.

CHAPTER 5

CONCLUDING REMARKS

Until recent advances in analytical tools, complex carbohydrates have been notoriously challenging to work with: in synthesis, characterization and study in biological systems. Nature, in carbohydrates, has created a structure that contains huge amounts of information, with multiple points for conjugation, subtle stereochemical changes and complex expression on cellular surfaces. These facets make understanding carbohydrate interactions very complicated, never mind how nature has made a system to make up for rather weak interactions, by having many events depending on multiple points of attachment for recognition. This is where knowledge of the characteristics of multivalent interactions has become critical to the understanding of biological systems where lectin : carbohydrate binding is involved.

The work performed here was started by creating a multivalent carbohydrate display upon a highly dynamic and flexible scaffold in PAMAM dendrimers that has evolved into researching multivalent effects at the cellular level. Initially this group used a robust system with the well characterized jackbean lectin Concanavalin A; and studied it’s binding with mannose functionalized dendrimers. This lead to observing a highly optimized system with ideal dendrimer loading amounts at fifty percent. From this work, we synthesized mannose and glucose functionalized dendrimers and studied their binding with

Con A, that proved to be tunable and predictable in a model set out previously by another group. This predictable binding however had little effect upon the clustering ability of the lectin binding dendrimers. The separation of these two modes of interactions was quite remarkable and gave thought to perhaps there is a delicate interplay of binding modes that dictate how these events take place.

With the knowledge gained by the glucose/mannose functionalized PAMAM dendrimers interacting with Con A, we turned our attention to a more complicated system, that of Galectins. This series of galactose binding lectins are ubiquitous in nature and found in the cellular nucleus and cytoplasm as well as the extracellular matrix and there is strong indication of roles in multiple diseases and involvement in cellular lifetimes. There is most likely a subtle interplay within the family of galectins and understanding their relationship to each other is important. However, first we need to have a better understanding of the individual components and how they interact in these events that appear to be causal in tumor formation and proliferation. We started with galectin-3 and future experiments will be aimed at the other members of this lectin family. The results described in this manuscript indicate galectin-3 functions in a multivalent manner, and the specific strength of association of the larger multivalent molecules may play a lesser role than the ability to cluster, or aggregate receptors together. This was evident in an assay developed to further the techniques available to observe lectin : carbohydrate interactions that allowed us to both assess specific monomeric binding and surface bound multivalent binding. Efforts to develop

methods to understand this exciting series of lectins will no doubt shed more light on the binding intricacies involved, and how they affect cellular behavior.

The field of multivalency is no doubt burgeoning and a fast growing number of researchers are lending their efforts toward it's understanding. This work has been invigorating, sometimes confounding and often lead to unexpected results that require complex evaluation. The results from these studies will certainly lead to insights into diseases and ways to subtly effect some of the more challenging health related problems we are currently facing.

REFERENCES CITED

1. Lis, H.; Sharon, N., Lectins: Carbohydrate-specific proteins that mediate cellular recognition. *Chemical Reviews* 1998, *98* (2), 637-674.

2. Bovin, N. V.; Gabius, H. J., Polymer-immobilized carbohydrate ligands: Versatile chemical tools for biochemistry and medical sciences. *Chemical Society Reviews* 1995, *24* (6), 413-428.

3. Gestwicki, J. E.; Cairo, C. W.; Strong, L. E.; Oetjen, K. A.; Kiessling, L. L., Influencing receptor-ligand binding mechanisms with multivalent ligand architecture. *Journal of the American Chemical Society* 2002, *124* (50), 14922-14933.

4. Mammen, M.; Choi, S. K.; Whitesides, G. M., Polyvalent interactions in biological systems: Implications for design and use of multivalent ligands and inhibitors. *Angewandte Chemie-International Edition* 1998, *37* (20), 2755-2794.

5. Lee, Y. C.; Townsend, R. R.; Hardy, M. R.; Lonngren, J.; Arnarp, J.; Haraldsson, M.; Lonn, H., Binding of Synthetic Oligosaccharides to the Hepatic Gal Galnac Lectin - Dependence on Fine-Structural Features. *Journal of Biological Chemistry* 1983, *258* (1), 199-202.

6. Lee, Y. C.; Lee, R. T., Carbohydrate-Protein Interactions - Basis of Glycobiology. *Accounts of Chemical Research* 1995, *28* (8), 321-327.

7. Jencks, W. P., On the Attribution and Additivity of Binding-Energies. *Proceedings of the National Academy of Sciences of the United States of America-Biological Sciences* 1981, *78* (7), 4046-4050.

8. Barclay, G. R.; Flewett, T. H.; Keller, E.; Halsall, H. B.; Spragg, S. P., Effect of Polymerized Orosomucoid on Some Strains of Influenza Virus. *Biochemical Journal* 1969, *111* (3), 353-&.

9. Lees, W. J.; Spaltenstein, A.; Kingerywood, J. E.; Whitesides, G. M., Polyacrylamides Bearing Pendant Alpha-Sialoside Groups Strongly Inhibit Agglutination of Erythrocytes by Influenza-a Virus - Multivalency and Steric Stabilization of Particulate Biological-Systems. *Journal of Medicinal Chemistry* 1994, *37* (20), 3419-3433.

10. Roy, R.; Pon, R. A.; Tropper, F. D.; Andersson, F. O., Michael Addition of Poly-L-Lysine to N-Acryloylated Sialosides - Syntheses of Influenza-a Virus Hemagglutinin Inhibitor and Group-B Meningococcal Polysaccharide Vaccines. *Journal of the Chemical Society-Chemical Communications* 1993, (3), 264-265.

11. Manning, D. D.; Hu, X.; Beck, P.; Kiessling, L. L., Synthesis of sulfated neoglycopolymers: Selective P-selectin inhibitors. *Journal of the American Chemical Society* 1997, *119* (13), 3161-3162.

12. Rojo, J.; Diaz, V.; de la Fuente, J. M.; Segura, I.; Barrientos, A. G.; Riese, H. H.; Bernade, A.; Penades, S., Gold glyconanoparticles as new tools in antiadhesive therapy. *Chembiochem* 2004, *5* (3), 291-297.

13. Sundgren, A.; Barchi, J. J., Varied presentation of the Thomsen-Friedenreich disaccharide tumor-associated carbohydrate antigen on gold nanoparticles. *Carbohydrate Research* 2008, *343* (10-11), 1594-1604.

14. Gamblin, D. P.; Scanlan, E. M.; Davis, B. G., Glycoprotein Synthesis: An Update. *Chemical Reviews* 2009, *109* (1), 131-163.

15. Polizzotti, B. D.; Maheshwari, R.; Vinkenborg, J.; Kiick, K. L., Effects of saccharide spacing and chain extension on toxin inhibition by glycopolypeptides of well-defined architecture. *Macromolecules* 2007, *40* (20), 7103-7110.

16. Manimala, J. C.; Li, Z. T.; Jain, A.; VedBrat, S.; Gildersleeve, J. C., Carbohydrate array analysis of anti-Tn antibodies and lectins reveals unexpected specificities: Implications for diagnostic and vaccine development. *Chembiochem* 2005, *6* (12), 2229-2241.

17. Manimala, J. C.; Roach, T. A.; Li, Z. T.; Gildersleeve, J. C., High-throughput carbohydrate microarray analysis of 24 lectins. *Angewandte Chemie-International Edition* 2006, *45* (22), 3607-3610.

18. Geng, J.; Mantovani, G.; Tao, L.; Nicolas, J.; Chen, G. J.; Wallis, R.; Mitchell, D. A.; Johnson, B. R. G.; Evans, S. D.; Haddleton, D. M., Site-directed conjugation of "Clicked" glycopolymers to form glycoprotein mimics: Binding to mammalian lectin and induction of immunological function. *Journal of the American Chemical Society* 2007, *129* (49), 15156-15163.

19. Rendle, P. M.; Seger, A.; Rodrigues, J.; Oldham, N. J.; Bott, R. R.; Jones, J. B.; Cowan, M. M.; Davis, B. G., Glycodendriproteins: A synthetic glycoprotein mimic enzyme with branched sugar-display potently inhibits bacterial aggregation. *Journal of the American Chemical Society* 2004, *126* (15), 4750-4751.

20. Nelson, A.; Belitsky, J. M.; Vidal, S.; Joiner, C. S.; Baum, L. G.; Stoddart, J. F., A self-assembled multivalent pseudopolyrotaxane for binding galectin-1. *Journal of the American Chemical Society* 2004, *126* (38), 11914-11922.

21. Marra, A.; Moni, L.; Pazzi, D.; Corallini, A.; Bridi, D.; Dondoni, A., Synthesis of sialoclusters appended to calix[4]arene platforms via multiple azide-

alkyne cycloaddition. New inhibitors of hemagglutination and cytopathic effect mediated by BK and influenza A viruses. *Organic & Biomolecular Chemistry* 2008, *6* (8), 1396-1409.

22. Chabre, Y. M.; Roy, R., Recent trends in glycodendrimer syntheses and applications. *Current Topics in Medicinal Chemistry* 2008, *8* (14), 1237-1285.

23. Bezouska, K., Design, functional evaluation and biomedical applications of carbohydrate dendrimers. *reviews in molecular biotechnology* 2002, (90), 269-290.

24. Woller, E. K.; Walter, E. D.; Morgan, J. R.; Singel, D. J.; Cloninger, M. J., Altering the strength of lectin binding interactions and controlling the amount of lectin clustering using mannose/hydroxyl-functionalized dendrimers. *Journal of the American Chemical Society* 2003, *125* (29), 8820-8826.

25. Wang, S. K.; Liang, P. H.; Astronomo, R. D.; Hsu, T. L.; Hsieh, S. L.; Burton, D. R.; Wong, C. H., Targeting the carbohydrates on HIV-1: Interaction of oligomannose dendrons with human monoclonal antibody 2G12 and DC-SIGN. *Proceedings of the National Academy of Sciences of the United States of America* 2008, *105* (10), 3690-3695.

26. Kaltgrad, E.; Sen Gupta, S.; Punna, S.; Huang, C. Y.; Chang, A.; Wong, C. H.; Finn, M. G.; Blixt, O., Anti-carbohydrate antibodies elicited by polyvalent display on a viral scaffold. *Chembiochem* 2007, *8* (12), 1455-1462.

27. Kim, B. S.; Hong, D. J.; Bae, J.; Lee, M., Controlled self-assembly of carbohydrate conjugate rod-coil amphiphiles for supramolecular multivalent ligands. *Journal of the American Chemical Society* 2005, *127* (46), 16333-16337.

28. Thoma, G.; Streiff, M. B.; Katopodis, A. G.; Duthaler, R. O.; Voelcker, N. H.; Ehrhardt, C.; Masson, C., Non-covalent polyvalent ligands by self-assembly of small glycodendrimers: A novel concept for the inhibition of polyvalent carbohydrate-protein interactions in vitro and in vivo. *Chemistry-a European Journal* 2006, *12* (1), 99-117.

29. Bruehl, R. E.; Dasgupta, F.; Katsumoto, T. R.; Tan, J. H.; Bertozzi, C. R.; Spevak, W.; Ahn, D. J.; Rosen, S. D.; Nagy, J. O., Polymerized liposome assemblies: Bifunctional macromolecular selectin inhibitors mimicking physiological selectin ligands. *Biochemistry* 2001, *40* (20), 5964-5974.

30. Kitov, P. I.; Sadowska, J. M.; Mulvey, G.; Armstrong, G. D.; Ling, H.; Pannu, N. S.; Read, R. J.; Bundle, D. R., Shiga-like toxins are neutralized by tailored multivalent carbohydrate ligands. *Nature* 2000, *403* (6770), 669-672.

31. Buskas, T.; Ingale, S.; Boons, G. J., Towards a fully synthetic carbohydrate-based anticancer vaccine: Synthesis and immunological evaluation of a lipidated glycopeptide containing the tumor-associated Tn antigen. *Angewandte Chemie-International Edition* 2005, *44* (37), 5985-5988.

32. Penades, S., *Host-Guest Chemistry: Mimetic Approaches to Study Carbohydrate Recognition* 1ed.; springer-verlag, LLC: New York, 2001; p 241.

33. de la Fuente, J. M.; Barrientos, A. G.; Rojas, T. C.; Rojo, J.; Canada, J.; Fernandez, A.; Penades, S., Gold glyconanoparticles as water-soluble polyvalent models to study carbohydrate interactions. *Angewandte Chemie-International Edition* 2001, *40* (12), 2258-+.

34. Wang, H. F.; Gu, L. R.; Lin, Y.; Lu, F. S.; Meziani, M. J.; Luo, P. G. J.; Wang, W.; Cao, L.; Sun, Y. P., Unique aggregation of anthrax (Bacillus anthracis) spores by sugar-coated single-walled carbon nanotubes. *Journal of the American Chemical Society* 2006, *128* (41), 13364-13365.

35. Seah, N.; Santacroce, P. V.; Basu, A., Probing the Lactose center dot GM3 Carbohydrate-Carbohydrate Interaction with Glycodendrimers. *Organic Letters* 2009, *11* (3), 559-562.

36. Yoon, S. J.; Nakayama, K. I.; Hikita, T.; Handa, K.; Hakomori, S. I., Epidermal growth factor receptor tyrosine kinase is modulated by GM3 interaction with N-linked GlcNAc termini of the receptor. *Proceedings of the National Academy of Sciences of the United States of America* 2006, *103* (50), 18987-18991.

37. Verez-Bencomo, V.; Fernandez-Santana, V.; Hardy, E.; Toledo, M. E.; Rodriguez, M. C.; Heynngnezz, L.; Rodriguez, A.; Baly, A.; Herrera, L.; Izquierdo, M.; Villar, A.; Valdes, Y.; Cosme, K.; Deler, M. L.; Montane, M.; Garcia, E.; Ramos, A.; Aguilar, A.; Medina, E.; Torano, G.; Sosa, I.; Hernandez, I.; Martinez, R.; Muzachio, A.; Carmenates, A.; Costa, L.; Cardoso, F.; Campa, C.; Diaz, M.; Roy, R., A synthetic conjugate polysaccharide vaccine against Haemophilus influenzae type b. *Science* 2004, *305* (5683), 522-525.

38. Johansson, S. M. C.; Arnberg, N.; Elofsson, M.; Wadell, G.; Kihlberg, J., Multivalent HSA conjugates of 3 '-siallyllactose are potent inhibitors of adenoviral cell attachment and infection. *Chembiochem* 2005, *6* (2), 358-364.

39. Disney, M. D.; Zheng, J.; Swager, T. M.; Seeberger, P. H., Detection of bacteria with carbohydrate-functionalized fluorescent polymers. *Journal of the American Chemical Society* 2004, *126* (41), 13343-13346.

40. Carlson, C. B.; Mowery, P.; Owen, R. M.; Dykhuizen, E. C.; Kiessling, L. L., Selective tumor cell targeting using low-affinity, multivalent interactions. *Acs Chemical Biology* 2007, *2* (2), 119-127.

41. van Kasteren, S. I.; Campbell, S. J.; Serres, S.; Anthony, D. C.; Sibson, N. R.; Davis, B. G., Glyconanoparticles allow pre-symptomatic in vivo imaging of brain disease (vol 106, pg 18, 2008). *Proceedings of the National Academy of Sciences of the United States of America* 2009, *106* (10), 4061-4061.

42. Osawa, T., Matsumoto, I., Gorse (Ulex europeus) phytohemagglutinins. *Methods Enzymol.* 1972, (28), 323-327.

43. Gestwicki, J. E.; Cairo, C. W.; Mann, D. A.; Owen, R. M.; Kiessling, L. L., Selective immobilization of multivalent ligands for surface plasmon resonance and fluorescence microscopy. *Analytical Biochemistry* 2002, *305* (2), 149-155.

44. Brewer, C. F.; Ahmad, N.; Dam, T. K.; Gabius, H. J.; Oscarson, S., Comparative studies of the carbohydrate binding and physical properties of galectin-1 and galectin-3. *Glycobiology* 2000, *10* (10), 1077-1077.

45. Ragupathi, G.; Coltart, D. M.; Williams, L. J.; Koide, F.; Kagan, E.; Allen, J.; Harris, C.; Glunz, P. W.; Livingston, P. O.; Danishefsky, S. J., On the power of chemical synthesis: Immunological evaluation of models for multiantigenic carbohydrate-based cancer vaccines. *Proceedings of the National Academy of Sciences of the United States of America* 2002, *99* (21), 13699-13704.

46. Roy, R.; Page, D.; Perez, S. F.; Bencomo, V. V., Effect of shape, size, and valency of multivalent mannosides on their binding properties to phytohemagglutinins. *Glycoconjugate Journal* 1998, *15* (3), 251-263.

47. Khan, M. I.; Mandal, D. K.; Brewer, C. F., Interactions of Concanavalin-a with Glycoproteins - a Quantitative Precipitation Study of Concanavalin-a with the Soybean Agglutinin. *Carbohydrate Research* 1991, *213*, 69-77.

48. Kaltgrad, E.; O'Reilly, M. K.; Liao, L. A.; Han, S. F.; Paulson, J. C.; Finn, M. G., On-virus construction of polyvalent glycan ligands for cell-surface receptors. *Journal of the American Chemical Society* 2008, *130* (14), 4578-+.

49. Gour, N.; Verma, S., Synthesis and AFM studies of lectin-carbohydrate self-assemblies. *Tetrahedron* 2008, *64* (30-31), 7331-7337.

50. Kussrow, A., Kaltgrad, E., Wolfenden, M.L., Cloninger, M.J., Finn, M. G., Bornhop, D.J., Measurement of Monovalent and Polyvalent Carbohydrate−Lectin Binding by Back-Scattering Interferometry. *Anal. Chem.* 2009, *81* (12), 4889-4897.

51. Wilczewski, M.; Van der Heyden, A.; Renaudet, O.; Dumy, P.; Coche-Guerente, L.; Labbe, P., Promotion of sugar-lectin recognition through the multiple sugar presentation offered by regioselectively addressable functionalized templates (RAFT): a QCM-D and SPR study. *Organic & Biomolecular Chemistry* 2008, *6* (6), 1114-1122.

52. Lundquist, J. J.; Toone, E. J., The cluster glycoside effect. *Chemical Reviews* 2002, *102* (2), 555-578.

53. Dwek, R. A., Glycobiology: Toward Understanding the Function of Sugars. *Chem Rev* 1996, *96* (2), 683-720.

54. Mann, D. A., and Kiessling, L. L. The chemistry and biology of multivalent saccharide displays. In (2001) Glycochemistry: Principles, Synthesis, and Applications, (Wang, G., Bertozzi, C. R., Eds.) pp 221-275, P. Marcel Dekker, New York.

55. Gabius, H. J.; Siebert, H. C.; Andre, S.; Jimenez-Barbero, J.; Rudiger, H., Chemical biology of the sugar code. *Chembiochem* 2004, *5* (6), 740-64.

56. For many examples, see: Choi, S.-K. Synthetic MultiValent Molecules Wiley-VCH: New York, 2004.

57. Mowery, P.; Yang, Z. Q.; Gordon, E. J.; Dwir, O.; Spencer, A. G.; Alon, R.; Kiessling, L. L., Synthetic glycoprotein mimics inhibit L-selectin-mediated rolling and promote L-selectin shedding. *Chem Biol* 2004, *11* (5), 725-32.

58. Sigal, G. B.; Mammen, M.; Dahmann, G.; Whitesides, G. M., Polyacrylamides bearing pendant alpha-sialoside groups strongly inhibit agglutination of erythrocytes by influenza virus: The strong inhibition reflects enhanced binding through cooperative polyvalent interactions. *Journal of the American Chemical Society* 1996, *118* (16), 3789-3800.

59. Sen Gupta, S.; Kuzelka, J.; Singh, P.; Lewis, W. G.; Manchester, M.; Finn, M. G., Accelerated bioorthogonal conjugation: a practical method for the ligation of diverse functional molecules to a polyvalent virus scaffold. *Bioconjug Chem* 2005, *16* (6), 1572-9.

60. Andre, S.; Kaltner, H.; Furuike, T.; Nishimura, S.; Gabius, H. J., Persubstituted cyclodextrin-based glycoclusters as inhibitors of protein-carbohydrate recognition using purified plant and mammalian lectins and wild-type and lectin-gene-transfected tumor cells as targets. *Bioconjug Chem* 2004, *15* (1), 87-98.

61. Dong, C. M.; Chaikof, E. L., Self-assembled nanostructures of a biomimetic glycopolymer-polypeptide triblock copolymer. *Colloid and Polymer Science* 2005, *283* (12), 1366-1370.

62. Wang, Y.; Kiick, K. L., Monodisperse protein-based glycopolymers via a combined biosynthetic and chemical approach. *J Am Chem Soc* 2005, *127* (47), 16392-3.

63. Thayer, D. A.; Yu, H. N.; Galan, M. C.; Wong, C. H., A general strategy toward S-linked glycopeptides. *Angew Chem Int Ed Engl* 2005, *44* (29), 4596-9.

64. Kanda, V.; Kitov, P.; Bundle, D. R.; McDermott, M. T., Surface plasmon resonance imaging measurements of the inhibition of Shiga-like toxin by synthetic multivalent inhibitors. *Analytical Chemistry* 2005, *77* (23), 7497-7504.

65. Roy, R., A decade of glycodendrimer chemistry. *Trends in Glycoscience and Glycotechnology* 2003, *15* (85), 291-310.

66. Arnusch, C. J.; Andre, S.; Valentini, P.; Lensch, M.; Russwurm, R.; Siebert, H. C.; Fischer, M. J.; Gabius, H. J.; Pieters, R. J., Interference of the galactose-dependent binding of lectins by novel pentapeptide ligands. *Bioorg Med Chem Lett* 2004, *14* (6), 1437-40.

67. Benito, J. M.; Gomez-Garcia, M.; Ortiz Mellet, C.; Baussanne, I.; Defaye, J.; Garcia Fernandez, J. M., Optimizing saccharide-directed molecular delivery to biological receptors: design, synthesis, and biological evaluation of glycodendrimer-cyclodextrin conjugates. *J Am Chem Soc* 2004, *126* (33), 10355-63.

68. Kalovidouris, S. A.; Blixt, O.; Nelson, A.; Vidal, S.; Turnbull, W. B.; Paulson, J. C.; Stoddart, J. F., Chemically defined sialoside scaffolds for investigation of multivalent interactions with sialic acid binding proteins. *J Org Chem* 2003, *68* (22), 8485-93.

69. Vrasidas, I.; Andre, S.; Valentini, P.; Bock, C.; Lensch, M.; Kaltner, H.; Liskamp, R. M.; Gabius, H. J.; Pieters, R. J., Rigidified multivalent lactose molecules and their interactions with mammalian galectins: a route to selective inhibitors. *Org Biomol Chem* 2003, *1* (5), 803-10.

70. Page, D.; Roy, R., Synthesis and biological properties of mannosylated starburst poly(amidoamine) dendrimers. *Bioconjug Chem* 1997, *8* (5), 714-23.

71. Hayes, W.; Osborn, H. M. I.; Osborne, S. D.; Rastall, R. A.; Romagnoli, B., One-pot synthesis of multivalent arrays of mannose mono- and disaccharides. *Tetrahedron* 2003, *59* (40), 7983-7996.

72. Dimick, S. M.; Powell, S. C.; McMahon, S. A.; Moothoo, D. N.; Naismith, J. H.; Toone, E. J., On the meaning of affinity: Cluster glycoside effects and concanavalin A. *Journal of the American Chemical Society* 1999, *121* (44), 10286-10296.

73. Tsvetkov, D. E.; Cheshev, P. E.; Tuzikov, A. B.; Chinarev, A. A.; Pazynina, G. V.; Sablina, M. A.; Gambarian, A. S.; Bovin, N. V.; Rieben, R.; Shashkov, A. S., [Neoglycoconjugates based on dendrimeric poly(aminoamides)]. *Bioorg Khim* 2002, *28* (6), 518-34.

74. Lee, N. Y.; Jang, W. J.; Yu, S. H.; Im, J.; Chung, S. K., Syntheses of glycodendrimers having scyllo-inositol as the scaffold. *Tetrahedron Letters* 2005, *46* (36), 6063-6066.

75. Srinivas, O.; Radhika, S.; Bandaru, N. M.; Nadimpalli, S. K.; Jayaraman, N., Synthesis and biological evaluation of mannose-6-phosphate-coated multivalent dendritic cluster glycosides. *Organic & Biomolecular Chemistry* 2005, *3* (23), 4252-4257.

76. Rele, S. M.; Cui, W.; Wang, L.; Hou, S.; Barr-Zarse, G.; Tatton, D.; Gnanou, Y.; Esko, J. D.; Chaikof, E. L., Dendrimer-like PEO glycopolymers exhibit anti-inflammatory properties. *J Am Chem Soc* 2005, *127* (29), 10132-3.

77. Kensinger, R. D.; Yowler, B. C.; Benesi, A. J.; Schengrund, C. L., Synthesis of novel, multivalent glycodendrimers as ligands for HIV-1 gp120. *Bioconjug Chem* 2004, *15* (2), 349-58.

78. Van Damme, E. J. M.; Peumans, W. J.; Barre, A.; Rouge, P., Plant lectins: A composite of several distinct families of structurally and evolutionary related proteins with diverse biological roles. *Critical Reviews in Plant Sciences* 1998, *17* (6), 575-692.

79. Mortell, K. H.; Weatherman, R. V.; Kiessling, L. L., Recognition specificity of neoglycopolymers prepared by ring-opening metathesis polymerization. *Journal of the American Chemical Society* 1996, *118* (9), 2297-2298.

80. Kanai, M.; Mortell, K. H.; Kiessling, L. L., Varying the size of multivalent ligands: The dependence of concanavalin a binding on neoglycopolymer length. *Journal of the American Chemical Society* 1997, *119* (41), 9931-9932.

81. Andre, S.; Ortega, P. J. C.; Perez, M. A.; Roy, R.; Gabius, H. J., Lactose-containing starburst dendrimers: influence of dendrimer generation and binding-site orientation of receptors (plant/animal lectins and immunoglobulins) on binding properties. *Glycobiology* 1999, *9* (11), 1253-1261.

82. Lee, R. T.; Lee, Y. C., Affinity enhancement by multivalent lectin-carbohydrate interaction. *Glycoconj J* 2000, *17* (7-9), 543-51.

83. Quesenberry, M. S.; Lee, R. T.; Lee, Y. C., Difference in the binding mode of two mannose-binding proteins: demonstration of a selective minicluster effect. *Biochemistry* 1997, *36* (9), 2724-32.

84. Page, M. I.; Jencks, W. P., Entropic Contributions to Rate Accelerations in Enzymic and Intramolecular Reactions and Chelate Effect. *Proceedings of the National Academy of Sciences of the United States of America* 1971, *68* (8), 1678-&.

85. Gargano, J. M.; Ngo, T.; Kim, J. Y.; Acheson, D. W. K.; Lees, W. J., Multivalent inhibition of AB(5) toxins. *Journal of the American Chemical Society* 2001, *123* (51), 12909-12910.

86. Mulder, A.; Huskens, J.; Reinhoudt, D. N., Multivalency in supramolecular chemistry and nanofabrication. *Org Biomol Chem* 2004, *2* (23), 3409-24.

87. Wolfenden, M. L.; Cloninger, M. J., Mannose/glucose-functionalized dendrimers to investigate the predictable tunability of multivalent interactions. *Journal of the American Chemical Society* 2005, *127* (35), 12168-12169.

88. Naismith, J. H.; Emmerich, C.; Habash, J.; Harrop, S. J.; Helliwell, J. R.; Hunter, W. N.; Raftery, J.; Kalb, A. J.; Yariv, J., Refined structure of concanavalin A complexed with methyl alpha-D-mannopyranoside at 2.0 A resolution and comparison with the saccharide-free structure. *Acta Crystallogr D Biol Crystallogr* 1994, *50* (Pt 6), 847-58.

89. Lee, R. T.; Lee, Y. C., Synthesis of 3-(2-aminoethylthio)propyl glycosides. *Carbohydr Res* 1974, *37* (1), 193-201.

90. Acetylation and BOC protection are not required but facilitate purification and characterization.

91. Statistical/proximity enhancements are discussed in: Lee, R. T.; Lee, Y. C. *Glycoconjugate J.* 2000, 17, 543-551.

92. Schlick, K. H.; Udelhoven, R. A.; Strohmeyer, G. C.; Cloninger, M. J., Binding of mannose-functionalized dendrimers with pea (Pisum sativum) lectin. *Mol Pharm* 2005, *2* (4), 295-301.

93. This method has been shown to give equal loading amounts. Newkome, G. R., Wies, C. D., Moorefield, C. N., Baker, G. R., Childs, B. J., and Epperson, J. (1998) Isocyanate-based dendritic building blocks: Combinatorial tier construction and macromolecular-

property modification. Angew. Chem., Int. Ed. 37, 307-310.

94. Newkome, G. R., Moorefield, C. N., and Vo¨gtle, F., *Dendrimers and Dendrons: Concepts, Syntheses.* . Wiley-VCH: Weinheim, Germany, 2001.

95. Mandal, D. K.; Kishore, N.; Brewer, C. F., Thermodynamics of lectin-carbohydrate interactions. Titration microcalorimetry measurements of the binding of N-linked carbohydrates and ovalbumin to concanavalin A. *Biochemistry* 1994, *33* (5), 1149-56.

96. Corbell, J. B.; Lundquist, J. J.; Toone, E. J., A comparison of biological and calorimetric analyses of multivalent glycodendrimer ligands for concanavalin A. *Tetrahedron-Asymmetry* 2000, *11* (1), 95-111.

97. Schlick, K. H.; Udelhoven, R. A.; Strohniever, G. C.; Cloninger, M. J., Binding of mannose-functionalized dendrimers with pea (Pisum sativum) lectin. *Molecular Pharmaceutics* 2005, *2* (4), 295-301.

98. See ref 44 for an example of precipitation assays where monovalent associations between dendrimers and lectins are occurring.

99. See the experimentals for a more complete discussion on this point.

100. Barondes, S. H.; Castronovo, V.; Cooper, D. N. W.; Cummings, R. D.; Drickamer, K.; Feizi, T.; Gitt, M. A.; Hirabayashi, J.; Hughes, C.; Kasai, K.; Leffler, H.; Liu, F. T.; Lotan, R.; Mercurio, A. M.; Monsigny, M.; Pillai, S.; Poirer, F.; Raz, A.; Rigby, P. W. J.; Rini, J. M.; Wang, J. L., Galectins - a Family of Animal Beta-Galactoside-Binding Lectins. *Cell* 1994, *76* (4), 597-598.

101. Barondes, S. H.; Cooper, D. N. W.; Gitt, M. A.; Leffler, H., Galectins - Structure and Function of a Large Family of Animal Lectins. *Journal of Biological Chemistry* 1994, *269* (33), 20807-20810.

102. Gray, C. A.; Adelson, D. L.; Bazer, F. W.; Burghardt, R. C.; Meeusen, E. N. T.; Spencer, T. E., Discovery and characterization of an epithelial-specific galectin in the endometrium that forms crystals in the trophectoderm. *Proceedings of the National Academy of Sciences of the United States of America* 2004, *101* (21), 7982-7987.

103. Kasai, K.; Hirabayashi, J., Galectins: A family of animal lectins that decipher glycocodes. *Journal of Biochemistry* 1996, *119* (1), 1-8.

104. Nangia-Makker, P.; Raz, T.; Tait, L.; Hogan, V.; Fridman, R.; Raz, A., Galectin-3 cleavage: a novel surrogate marker for matrix metalloproteinase activity in growing breast cancers. *Cancer Res* 2007, *67* (24), 11760-8.

105. Ahmad, N.; Gabius, H. J.; Andre, S.; Kaltner, H.; Sabesan, S.; Roy, R.; Liu, B. C.; Macaluso, F.; Brewer, C. F., Galectin-3 precipitates as a pentamer with synthetic multivalent carbohydrates and forms heterogeneous cross-linked complexes. *Journal of Biological Chemistry* 2004, *279* (12), 10841-10847.

106. Ochieng, J.; Platt, D.; Tait, L.; Hogan, V.; Raz, T.; Carmi, P.; Raz, A., Structure-function relationship of a recombinant human galactoside-binding protein. *Biochemistry* 1993, *32* (16), 4455-60.

107. Kuklinski, S.; Probstmeier, R., Homophilic binding properties of galectin-3: involvement of the carbohydrate recognition domain. *J Neurochem* 1998, *70* (2), 814-23.

108. Hsu, D. K.; Dowling, C. A.; Jeng, K. C. G.; Chen, J. T.; Yang, R. Y.; Liu, F. T., Galectin-3 expression is induced in cirrhotic liver and hepatocellular carcinoma. *International Journal of Cancer* 1999, *81* (4), 519-526.

109. Lotan, R.; Ito, H.; Yasui, W.; Yokozaki, H.; Lotan, D.; Tahara, E., Expression of a 31-Kda Lactoside-Binding Lectin in Normal Human Gastric-Mucosa and in Primary and Metastatic Gastric Carcinomas. *International Journal of Cancer* 1994, *56* (4), 474-480.

110. Berberat, P. O.; Friess, H.; Wang, L.; Zhu, Z. W.; Bley, T.; Frigeri, L.; Zimmermann, A.; Buchler, M. W., Comparative analysis of galectins in primary tumors and tumor metastasis in human pancreatic cancer. *Journal of Histochemistry & Cytochemistry* 2001, *49* (4), 539-549.

111. Song, S. M.; Mazurek, N. M.; Liu, C. M.; Sun, Y. J.; Ding, Q. Q.; Liu, K. F.; Hung, M. C.; Bresalier, R. S., Galectin-3 Mediates Nuclear beta-Catenin Accumulation and Wnt Signaling in Human Colon Cancer Cells by Regulation of Glycogen Synthase Kinase-3 beta Activity. *Cancer Research* 2009, *69* (4), 1343-1349.

112. Xu, X. C.; Elnaggar, A. K.; Lotan, R., Differential Expression of Galectin-1 and Galectin-3 in Thyroid-Tumors - Potential Diagnostic Implications. *American Journal of Pathology* 1995, *147* (3), 815-822.

113. Kawachi, K.; Matsushita, Y.; Yonezawa, S.; Nakano, S.; Shirao, K.; Natsugoe, S.; Sueyoshi, K.; Alkou, T.; Sato, E., Galectin-3 expression in various thyroid neoplasms and its possible role in metastasis formation. *Human Pathology* 2000, *31* (4), 428-433.

114. Castronovo, V.; vandenBrule, F. A.; Jackers, P.; Clausse, N.; Liu, F. T.; Gillet, C.; Sobel, M. E., Decreased expression of galectin-3 is associated with progression of human breast cancer. *Journal of Pathology* 1996, *179* (1), 43-48.

115. Idikio, H., Galectin-3 expression in human breast carcinoma: correlation with cancer histologic grade. *International Journal of Oncology* 1998, *12* (6), 1287-1290.

116. Kim, H. R. C.; Lin, H. M.; Biliran, H.; Raz, A., Cell cycle arrest and inhibition of anoikis by galectin-3 in human breast epithelial cells. *Cancer Research* 1999, *59* (16), 4148-4154.

117. VandenBrule, F. A.; Buicu, C.; Berchuck, A.; Bast, R. C.; Deprez, M.; Liu, F. T.; Cooper, D. N. W.; Pieters, C.; Sobel, M. E.; Castronovo, V., Expression of the 67-kD laminin receptor, galectin-1, and galectin-3 in advanced human uterine adenocarcinoma. *Human Pathology* 1996, *27* (11), 1185-1191.

118. Vandenbrule, F. A.; Berchuck, A.; Bast, R. C.; Liu, F. T.; Gillet, C.; Sobel, M. E.; Castronovo, V., Differential Expression of the 67-Kd Laminin Receptor and 31-Kd Human Laminin-Binding Protein in Human Ovarian Carcinomas. *European Journal of Cancer* 1994, *30A* (8), 1096-1099.

119. Danguy, A.; Rorive, S.; Decaestecker, C.; Bronckart, Y.; Kaltner, H.; Hadari, Y. R.; Goren, R.; Zich, Y.; Petein, M.; Salmon, I.; Gabius, H. J.; Kiss, R., Immunohistochemical profile of galectin-8 expression in benign and malignant tumors of epithelial, mesenchymatous and adipous origins, and of the nervous system. *Histology and Histopathology* 2001, *16* (3), 861-868.

120. Friedrichs, J.; Manninen, A.; Muller, D. J.; Helenius, J., Galectin-3 regulates integrin alpha2beta1-mediated adhesion to collagen-I and -IV. *J Biol Chem* 2008, *283* (47), 32264-72.

121. Stillman, B. N.; Hsu, D. K.; Pang, M.; Brewer, C. F.; Johnson, P.; Liu, F. T.; Baum, L. G., Galectin-3 and galectin-1 bind distinct cell surface glycoprotein receptors to induce T cell death. *J Immunol* 2006, *176* (2), 778-89.

122. Delacour, D.; Greb, C.; Koch, A.; Salomonsson, E.; Leffler, H.; Le Bivic, A.; Jacob, R., Apical sorting by galectin-3-dependent glycoprotein clustering. *Traffic* 2007, *8* (4), 379-88.

123. Nieminen, J.; Kuno, A.; Hirabayashi, J.; Sato, S., Visualization of galectin-3 oligomerization on the surface of neutrophils and endothelial cells using fluorescence resonance energy transfer. *J Biol Chem* 2007, *282* (2), 1374-83.

124. Seetharaman, J.; Kanigsberg, A.; Slaaby, R.; Leffler, H.; Barondes, S. H.; Rini, J. M., X-ray crystal structure of the human galectin-3 carbohydrate recognition domain at 2.1-A resolution. *J Biol Chem* 1998, *273* (21), 13047-52.

125. Wolfenden, M. L.; Cloninger, M. J., Carbohydrate-functionalized dendrimers to investigate the predictable tunability of multivalent interactions. *Bioconjugate Chemistry* 2006, *17* (4), 958-966.

126. Ahmad, N.; Gabius, H. J.; Kaltner, H.; Andre, S.; Kuwabara, I.; Liu, F. T.; Oscarson, S.; Norberg, T.; Brewer, C. F., Thermodynamic binding studies of cell surface carbohydrate epitopes to galectins-1,-3, and-7: Evidence for differential binding specificities. *Canadian Journal of Chemistry-Revue Canadienne De Chimie* 2002, *80* (8), 1096-1104.

127. Cumpstey, I.; Sundin, A.; Leffler, H.; Nilsson, U. J., C-2-symmetrical thiodigalactoside bis-benzamido derivatives as high-affinity inhibitors of galectin-3: efficient lectin inhibition through double arginine-arene interactions. *Angewandte Chemie-International Edition* 2005, *44* (32), 5110-5112.

128. Oberg, C. T.; Leffler, H.; Nilsson, U. J., Arginine binding motifs: Design and synthesis of galactose-derived arginine tweezers as galectin-3 inhibitors. *Journal of Medicinal Chemistry* 2008, *51* (7), 2297-2301.

129. Kiso, M.; Anderson, L., Ferric Chloride-Catalyzed Glycosylation of Alcohols by 2-Acylamido-2-Deoxy-Beta-D-Glucopyranose 1-Acetates. *Carbohydrate Research* 1979, *72* (JUL), C12-C14.

130. Cumpstey, I.; Salomonsson, E.; Sundin, A.; Leffler, H.; Nilsson, U. J., Studies of arginine-arene interactions through synthesis and evaluation of a series of galectin-binding aromatic lactose esters. *Chembiochem* 2007, *8* (12), 1389-1398.

131. Cumpstey, I.; Salomonsson, E.; Sundin, A.; Leffler, H.; Nilsson, U. J., Double affinity amplification of galectin-ligand interactions through arginine-arene interactions: Synthetic, thermodynamic, and computational studies with aromatic diamido thiodigalactosides. *Chemistry-a European Journal* 2008, *14* (14), 4233-4245.

132. prior work from this group showed mannose functionalized dendrimers and Concanavalin A not clumping on a surface. See ref 24.

133. Smith, P. K.; Krohn, R. I.; Hermanson, G. T.; Mallia, A. K.; Gartner, F. H.; Provenzano, M. D.; Fujimoto, E. K.; Goeke, N. M.; Olson, B. J.; Klenk, D. C., Measurement of Protein Using Bicinchoninic Acid. *Analytical Biochemistry* 1985, *150* (1), 76-85.

134. For full characterization see Eric Wollers thesis, page 248.

135. For full characterization of compound 12 see page 128 of Joel Morgans thesis.

136. For full characterization of compound 12 see page 128 of Joel Morgans thesis.